

University of Denver

Digital Commons @ DU

Electronic Theses and Dissertations

Graduate Studies

1-1-2019

Photoassisted Synthesis of Complex Polyheterocycles via ES IPT-Driven Dearomative Intramolecular Cycloadditions

Dmitry Kuznetsov
University of Denver

Follow this and additional works at: <https://digitalcommons.du.edu/etd>



Part of the [Chemicals and Drugs Commons](#), [Chemistry Commons](#), and the [Life Sciences Commons](#)

Recommended Citation

Kuznetsov, Dmitry, "Photoassisted Synthesis of Complex Polyheterocycles via ES IPT-Driven Dearomative Intramolecular Cycloadditions" (2019). *Electronic Theses and Dissertations*. 1670.
<https://digitalcommons.du.edu/etd/1670>

This Dissertation is brought to you for free and open access by the Graduate Studies at Digital Commons @ DU. It has been accepted for inclusion in Electronic Theses and Dissertations by an authorized administrator of Digital Commons @ DU. For more information, please contact jennifer.cox@du.edu, dig-commons@du.edu.

Photoassisted Synthesis of Complex Polyheterocycles via ESIPT-Driven Dearomative Intramolecular Cycloadditions

Abstract

This research is focused on the development of novel photoassisted synthetic methodologies that provide straightforward access to complex and diverse libraries of polyheterocycles from modularly assembled precursors. All methods are based on the dearomative cycloadditions between two components: (i) *o*-azaxylylenes, generated by the excited-state intramolecular proton transfer, and (ii) tethered arene groups.

We have demonstrated the synthetic utility of four new photoinduced processes that yield complex products amenable for post-photochemical modifications:

- *[4+4] Cycloaddition of o-azaxylylenes to 1,3,4-oxadiazoles with subsequent dinitrogen extrusion.* This reaction furnishes compounds outfitted with epoxide fragments, which undergo ring-openings with various nucleophiles; furthermore, the oxidized products rearrange into triazocanoindolinones under Schmidt reaction conditions.
- *[4+2] Reaction between amino-o-azaxylylenes and tethered pyrroles.* The primary pyrroline photoproducts are converted into stable polyheterocycles by 1,3-dipolar cycloaddition with tosyl azide and an intramolecular Friedel-Crafts reaction.
- *Photodearomatization of benzenoid arenes via [2+4] reactions with o-azaxylylenes.* This process transforms readily available benzene units into 1,3-cyclohexadienes, which are reactive in acid-catalyzed modifications and thermal [4+2] cycloadditions.
- *Photocascade reaction involving [2+4] photocycloaddition of tethered anilines to o-azaxylylenes followed by secondary cyclization enabled by the oxalyl linker.* This transformation permits strategic installation of specific functionalities into the photoproducts, with the purpose of further ring-forming modifications.

Document Type

Dissertation

Degree Name

Ph.D.

Department

Chemistry and Biochemistry

First Advisor

Andrei Kutateladze, Ph.D.

Keywords

Azaxylylenes, Cascade reaction, Dearomatization, ESIPT, Photochemistry, Polyheterocycles, Excited state intramolecular proton transfer

Subject Categories

Chemicals and Drugs | Chemistry | Life Sciences

Publication Statement

Copyright is held by the author. User is responsible for all copyright compliance.

Photoassisted Synthesis of Complex Polyheterocycles via ESIPT-Driven
Dearomative Intramolecular Cycloadditions

A Dissertation
Presented to
the Faculty of Natural Sciences and Mathematics
University of Denver

In Partial Fulfillment
of the Requirements for the Degree
Doctor of Philosophy

by
Dmitry Kuznetsov
August 2019
Advisor: Andrei G. Kutateladze

Author: Dmitry Kuznetsov
Title: Photoassisted Synthesis of Complex Polyheterocycles via ESIPT-Driven Dearomative Intramolecular Cycloadditions
Advisor: Andrei G. Kutateladze
Degree Date: August 2019

Abstract

This research is focused on the development of novel photoassisted synthetic methodologies that provide straightforward access to complex and diverse libraries of polyheterocycles from modularly assembled precursors. All methods are based on the dearomative cycloadditions between two components: (i) *o*-azaxylylenes, generated by the excited-state intramolecular proton transfer, and (ii) tethered arene groups.

We have demonstrated the synthetic utility of four new photoinduced processes that yield complex products amenable for post-photochemical modifications:

- *[4+4] Cycloaddition of o-azaxylylenes to 1,3,4-oxadiazoles with subsequent dinitrogen extrusion.* This reaction furnishes compounds outfitted with epoxide fragments, which undergo ring-openings with various nucleophiles; furthermore, the oxidized products rearrange into triazocanoindolinones under Schmidt reaction conditions.
- *[4+2] Reaction between amino-o-azaxylylenes and tethered pyrroles.* The primary pyrroline photoproducts are converted into stable polyheterocycles by 1,3-dipolar cycloaddition with tosyl azide and an intramolecular Friedel–Crafts reaction.
- *Photodearomatization of benzenoid arenes via [2+4] reactions with o-azaxylylenes.* This process transforms readily available benzene units into

1,3-cyclohexadienes, which are reactive in acid-catalyzed modifications and thermal [4+2] cycloadditions.

- *Photocascade reaction involving [2+4] photocycloaddition of tethered anilines to o-azaxylylenes followed by secondary cyclization enabled by the oxalyl linker.* This transformation permits strategic installation of specific functionalities into the photoproducts, with the purpose of further ring-forming modifications.

Acknowledgements

Most importantly, I would like to thank my PhD advisor, Dr. Andrei Kutateladze, for providing me with an opportunity to work on multiple exciting and high-impact projects, and for being an excellent mentor. His guidance has made a vital contribution into my professional growth as a scientist.

I am also grateful to all “kgroup” members, former and present, for their constant support and willingness to help. Particularly, I want to thank Drs. Bhuvan Kumar and Olga Mukhina, who were supervising me during my first years of the graduate school, for teaching me numerous skills that are essential for a successful synthetic chemist. Besides, I am thankful to Tina Holt who proofread a significant portion of this dissertation and helped me to identify and correct some flaws in my writing.

Table of Contents

Chapter One : Introduction and General Background	1
Chapter Two : Literature Review	6
Excited-State Intramolecular Proton Transfer: a Photophysical Overview	6
Excited-State Intramolecular Proton Transfer: Synthetic Applications	17
Synthetic Utility of Dearomative Photocycloadditions to Selected Arenes	39
Chapter Three : Results and Discussion	54
Project 1: Photogenerated Diketopiperazine-Spiro-Oxiranes as Versatile Synthons for Accessing Diverse Polyheterocyclic Scaffolds [108]	54
Project 2: Synthesis of Complex Enantiopure Polyheterocycles by Cycloadditions of Amino- <i>o</i> -Azaxylylenes to Pyrroles [119]	61
Project 3: Dearomatization of Benzenoid Arenes with <i>o</i> -Azaxylylenes via an Unprecedented [2+4] Reaction Topology [121]	66
Project 4: Access to Complex Polyheterocyclic Architectures by Photoinduced Dearomatization Cascade Reactions of Oxalyl Anilides [130]	78
Chapter Four : Experimental Section.....	100
General Methods.....	100
Experimental Section for Project 1	101
Synthesis of Photoprecursors	101
Photochemical Reactions	106
Post-Photochemical Modifications	107
Experimental Section for Project 2.....	113
Synthesis of Photoprecursors	113
Photochemical Reactions Followed by Post-Photochemical Modifications	117
Experimental Section for Project 3.....	119
Synthesis of Photoprecursors	119
Photochemical Reactions and Acid-Catalyzed Post-Photochemical Modifications	133
Post-Photochemical Hetero-Diels–Alder Reactions and Further Transformations	149
Experimental Section for Project 4.....	155
Synthesis of Photoprecursors.....	155

Photochemical Reactions	182
Post-Photochemical Modifications	196
Kinetic Isotope Effect Measurements	206
Experiment 1	206
Experiment 2	209
Chapter Five : Conclusions	213
References	218
Appendix A: X-Ray Structures	228
Appendix B: List of Abbreviations and Acronyms	235
Appendix C: List of Publications Based on this Dissertation	240

List of Figures

Figure 1.1	1
Figure 1.2	2
Figure 2.1	7
Figure 2.2	7
Figure 2.3	9
Figure 2.4	11
Figure 2.5	12
Figure 2.6	13
Figure 2.7	14
Figure 2.8	14
Figure 2.9	16
Figure 2.10	26
Figure 2.11	29
Figure 2.12	38
Figure 2.13	38
Figure 3.1	85
Figure 3.2	86
Figure 4.1	208
Figure 4.2	208
Figure 4.3	210
Figure 4.4	211
Figure 5.1	215
Figure 5.2	216

List of Schemes

Scheme 1.1	3
Scheme 1.2	4
Scheme 2.1	6
Scheme 2.2	15
Scheme 2.3	17
Scheme 2.4	18
Scheme 2.5	18
Scheme 2.6	19
Scheme 2.7	20
Scheme 2.8	20
Scheme 2.9	21
Scheme 2.10	21
Scheme 2.11	22
Scheme 2.12	22
Scheme 2.13	23
Scheme 2.14	24
Scheme 2.15	25
Scheme 2.16	27
Scheme 2.17	28
Scheme 2.18	30
Scheme 2.19	31
Scheme 2.20	33
Scheme 2.21	34
Scheme 2.22	35
Scheme 2.23	35
Scheme 2.24	36
Scheme 2.25	39
Scheme 2.26	40
Scheme 2.27	40
Scheme 2.28	42
Scheme 2.29	43
Scheme 2.30	44
Scheme 2.31	45
Scheme 2.32	45
Scheme 2.33	46
Scheme 2.34	47
Scheme 2.35	48
Scheme 2.36	48
Scheme 2.37	49
Scheme 2.38	50
Scheme 2.39	51

Scheme 2.40.....	52
Scheme 2.41.....	52
Scheme 2.42.....	53
Scheme 3.1.....	54
Scheme 3.2.....	55
Scheme 3.3.....	56
Scheme 3.4.....	57
Scheme 3.5.....	58
Scheme 3.6.....	58
Scheme 3.7.....	59
Scheme 3.8.....	60
Scheme 3.9.....	61
Scheme 3.10.....	62
Scheme 3.11.....	63
Scheme 3.12.....	64
Scheme 3.13.....	65
Scheme 3.14.....	66
Scheme 3.15.....	67
Scheme 3.16.....	68
Scheme 3.17.....	69
Scheme 3.18.....	71
Scheme 3.19.....	73
Scheme 3.20.....	74
Scheme 3.21.....	75
Scheme 3.22.....	76
Scheme 3.23.....	77
Scheme 3.24.....	78
Scheme 3.25.....	80
Scheme 3.26.....	80
Scheme 3.27.....	82
Scheme 3.28.....	83
Scheme 3.29.....	87
Scheme 3.30.....	89
Scheme 3.31.....	90
Scheme 3.32.....	91
Scheme 3.33.....	92
Scheme 3.34.....	93
Scheme 3.35.....	94
Scheme 3.36.....	95
Scheme 3.37.....	96
Scheme 3.38.....	97
Scheme 3.39.....	98
Scheme 3.40.....	99

List of Tables

Table 2.1	10
Table 2.2	16
Table 2.3	37
Table 2.4	41
Table 4.1	134
Table 4.2	183
Table 5.1	216

Chapter One: Introduction and General Background

Progress in the field of drug discovery is seemingly never-ending, as illustrated by the fact that, every year since 1990, the U.S. Food and Drug Administration (FDA) has been steadily approving at least 17 new molecular entities for use as therapeutics [1] (**Figure 1.1**). Recent growth in the number of approvals is especially impressive: in 2018, the FDA has hit a new record by permitting 59 new drugs to enter the U.S. market [1, 2]. The majority of these novel therapies (38, or 64%) are small molecules, such as Pfizer's Lorlatinib (**1.1**), designed to treat a certain type of lung cancer, and an anti-influenza agent Xofluza (**1.2**) developed by Shionogi and Genentech (**Figure 1.2**). All these observations indicate that the demand in new small-molecule drugs is persisting and will most likely keep growing.

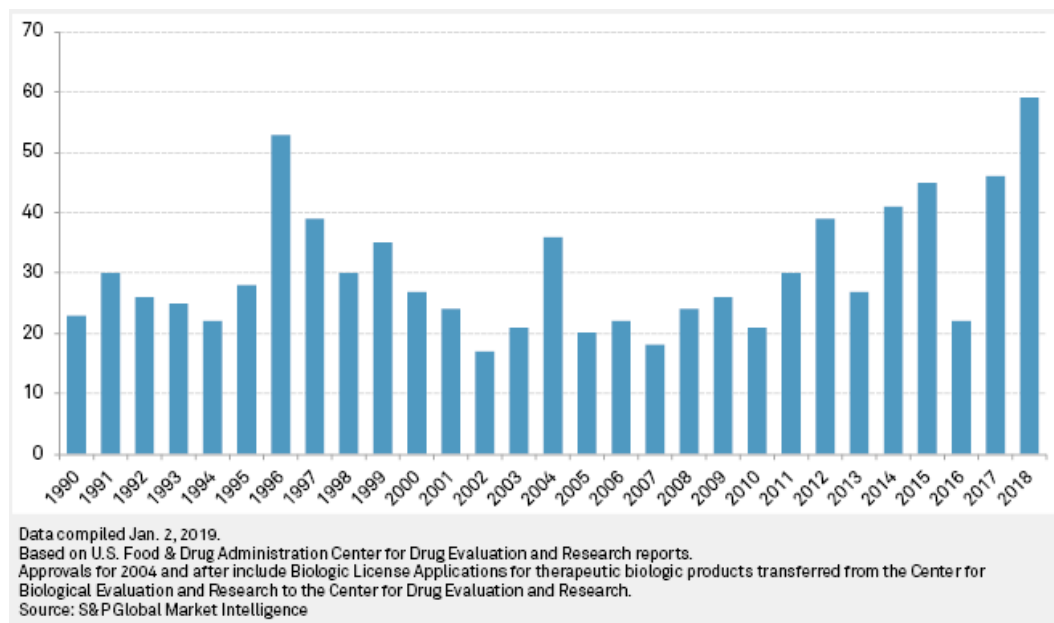


Figure 1.1: Annual FDA drug approvals for the 1990–2018 period [2].

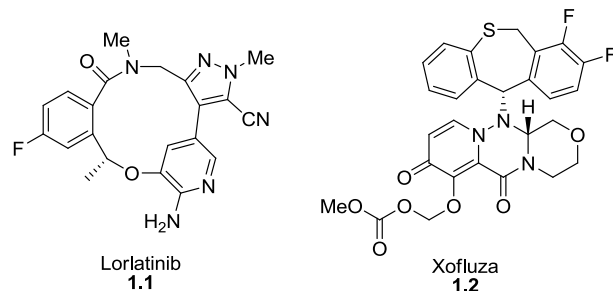
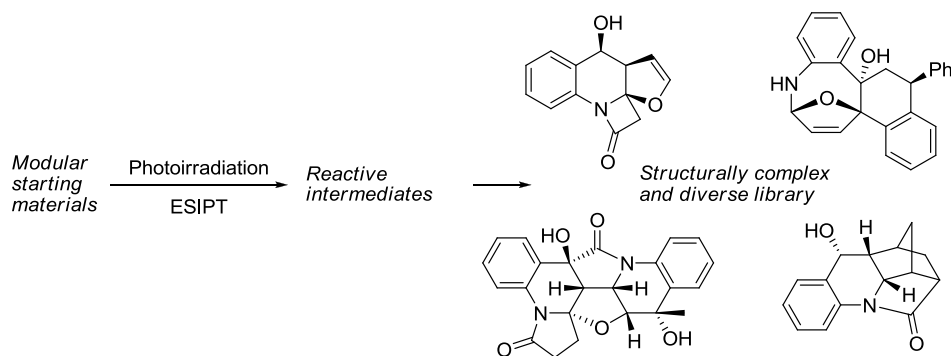


Figure 1.2: Examples of drugs approved by FDA in 2018 [1].

The process of drug discovery involves extensive screening of compound libraries. Biological evaluations required for the identification of a new therapeutic can be performed either on a *focused library*, which consists of drug candidates sharing common structural features that are known to facilitate binding to a specific target, or on a *structurally complex and diverse library* of molecules that are tested for their ability to perturbate a disease-related pathway without consideration of any particular target [3]. While the first approach relies on retrosynthetic analysis that allows efficient planning of routes towards specific compounds, the second strategy is implemented with the help of *diversity-oriented synthesis (DOS)* designed to probe a wide area of *chemical space*. This term is used to denote the imaginable multi-dimensional space encompassing all possible carbon-based small molecules, where the distance between each two points is directly proportional to the degree of dissimilarity between the molecules located at these points [4, 5]. An important feature of the DOS methodology is that it increases the chance of encountering *unexplored regions of biologically relevant chemical space*. In other words, it facilitates discovery of previously unknown structural elements responsible for the specific binding interactions between small molecules and biological targets, such as proteins, RNA and DNA. Therefore, the strategy of generating diverse libraries serves as

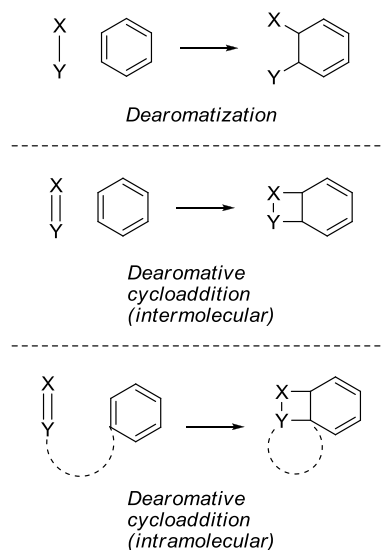
a powerful tool for the identification of new drug candidates, effectively complementing the target-oriented approach.

Photochemical synthetic methods have not been widely utilized by modern medicinal chemists actively searching for novel therapeutics; however, recent “boom” in the discovery of powerful photoredox-based reactions seems to have started changing this situation [6]. At the same time, traditional metal-free photochemistry has an immense potential for applications in DOS, because it is capable of converting modularly assembled and easily diversifiable starting materials into reactive intermediates that can be involved in transformations leading to various complex molecular scaffolds (**Scheme 1.1**). An illustrative example is the recently developed methodology that takes advantage of transient species generated by the *excited-state intramolecular proton transfer* (ESIPT) [7-10] – a photoinduced process that has been well-studied by photophysicists but has long been overlooked by synthetic chemists. All relevant reactions will be discussed in detail in the Literature Review; a representative set of small molecules produced by the diversity-oriented ESIPT-based photochemistry is depicted in **Scheme 1.1**.



Scheme 1.1: Utility of the photochemical ESIPT-based synthetic methodology [7-10] for DOS applications.

An important class of molecular transformations that can be achieved photochemically and are suitable for DOS is *dearomatization* reactions [11]. These processes enable quick conversion of ubiquitous aromatic moieties, found in many feedstock chemicals, into complex scaffolds enriched with sp^3 -hybridized carbons. Lovering and co-workers have shown that compounds with a greater degree of three-dimensional complexity, which is quantified as a fraction of saturated carbons in the molecule, are more likely to become successful drug candidates [12]; therefore, dearomatized products are especially attractive from the medicinal chemistry standpoint. Even more complex structures, which would cover a larger region of chemical space, can be accessed through *dearomative cycloadditions* that produce polycyclic architectures with a high content of sp^3 carbons. Furthermore, if this reaction is performed in *intramolecular* fashion, the tether linking two reactive components together transforms into an additional cycle in the product molecule (**Scheme 1.2**).



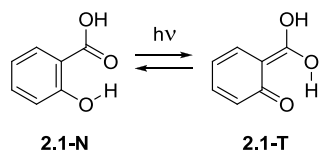
Scheme 1.2: Hypothetical dearomatization reactions of various topologies.

The present work is aimed at the development of new synthetic methods based on *intramolecular dearomative cycloadditions driven by ESIPT*. Through the straightforward modular assembly of the starting materials, as well as structural diversity and complexity of the products, we intend to demonstrate that these novel strategies conform to the criteria of *diversity-oriented synthesis* – a powerful approach utilized to discover new small-molecule drugs demanded by modern society.

Chapter Two: Literature Review

Excited-State Intramolecular Proton Transfer: a Photophysical Overview

Excited-state intramolecular proton transfer (ESIPT) is a photoinduced relocation of a proton from an acidic site to a basic group within the same molecule [13]. Since the discovery of this phenomenon by Weller in the 1950s for salicylic acid (**Scheme 2.1**) [14], it has found a variety of applications, such as, fluorescent imaging probes utilized for the selective detection of biologically and environmentally important species [15], and in synthetic organic photochemistry, which is the focus of the present work.



Scheme 2.1: ESIPT process in salicylic acid (simplified representation).

ESIPT is feasible in the molecules where acidic and basic functionalities are situated in a close proximity to each other, so that an intramolecular hydrogen bond can be formed between two sites [13]. Typical proton donors are hydroxyl [13, 15-17] and amide groups [15-18], whereas proton acceptors are usually heterocyclic [13, 15, 17, 18] and imine nitrogen atoms [13, 15], as well as carbonyl oxygen [15-18]. Representative examples of the systems capable of ESIPT are shown in **Figure 2.1**.

Energetics of a typical ESIPT and related processes are illustrated in the diagram for 2-(2'-hydroxyphenyl)-benzothiazole (**2.2-N**; **Figure 2.2**) [17]. Photoexcitation promotes the molecule in its initial form, often referred to as *normal* or *enol*, from the ground state

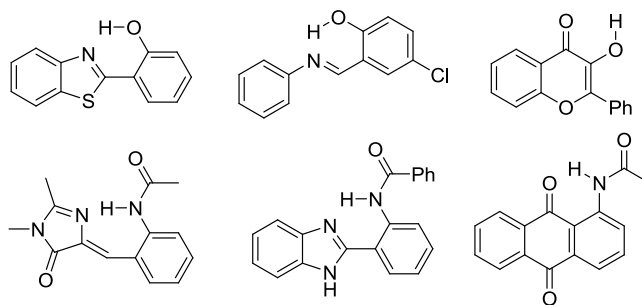


Figure 2.1: Structures of selected ESIPT-reactive compounds.

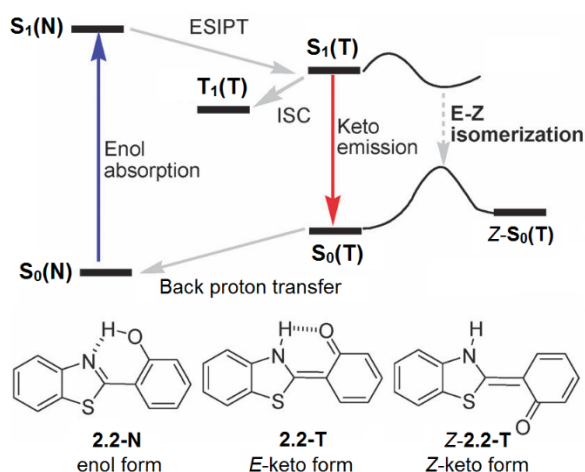


Figure 2.2: Energetic diagram of ESIPT for 2-(2'-hydroxyphenyl)benzothiazole (**2.2**). Republished with permission of Royal Society of Chemistry, from ref. [17]; permission conveyed through Copyright Clearance Center, Inc.

$S_0(N)$ to its first singlet excited state $S_1(N)$, which then converts into a lower energy *tautomeric* or *keto* excited state $S_1(T)$ through ESIPT. The resulting proton-transferred singlet has three main deactivation routes:

- Changing the spin state by intersystem crossing (ISC) into $T_1(T)$;
- Isomerization from *E*- to *Z*-form, where proton donor and acceptor are located on opposite sides of a newly formed double bond;
- Relaxation to the ground state $S_0(T)$ that is subject to barrierless back proton transfer (BPT) to $S_0(N)$.

$S_0(T) \rightarrow S_0(N)$ transition process is radiative, i.e. accompanied by the emission of a photon, and therefore provides the opportunity to detect the presence of tautomerized species by fluorescence spectroscopy and to investigate the influence of various factors on the photophysical properties of ESIPT.

Among numerous molecules where ESIPT is feasible, 1-(acylamino)anthraquinones constitute an instructive example, for which photophysics are well studied [19-21]. Furthermore, these compounds contain the same ESIPT-reactive *o*-amidoketone moieties that are present in all systems examined in this work (see “Results and Discussion” chapter).

In their seminal work, Smith, Barbara and co-workers performed comprehensive photophysical investigations of the ESIPT mechanism in a series of four 1-(acylamino)anthraquinones, where electron-withdrawing properties of *N*-acyl group were successively increased (heptanoyl, chloroacetyl, dichloroacetyl and trifluoroacetyl derivatives, abbreviated as HPAQ, CAAQ, DCAQ and TFAQ, respectively; **Figure 2.3a**) [19]. Fluorescence spectroscopy studies revealed characteristic dual emission of these compounds (**Figure 2.3b, c**) consisting of:

- Short-wavelength emission (SWE; ca. 510 nm) decreasing when moving from the most electron-rich HPAQ to the most electron-poor TFAQ;
- Long-wavelength emission (LWE; ca. 635 nm) that experiences the opposite trend, increasing with the electron-withdrawing ability of an amide group.

SWE is in the mirror-image relationship with absorption peak (**Figure 2.3c**), indicating the emission from the $S_1(N)$ state. The substantially Stokes-shifted LWE was

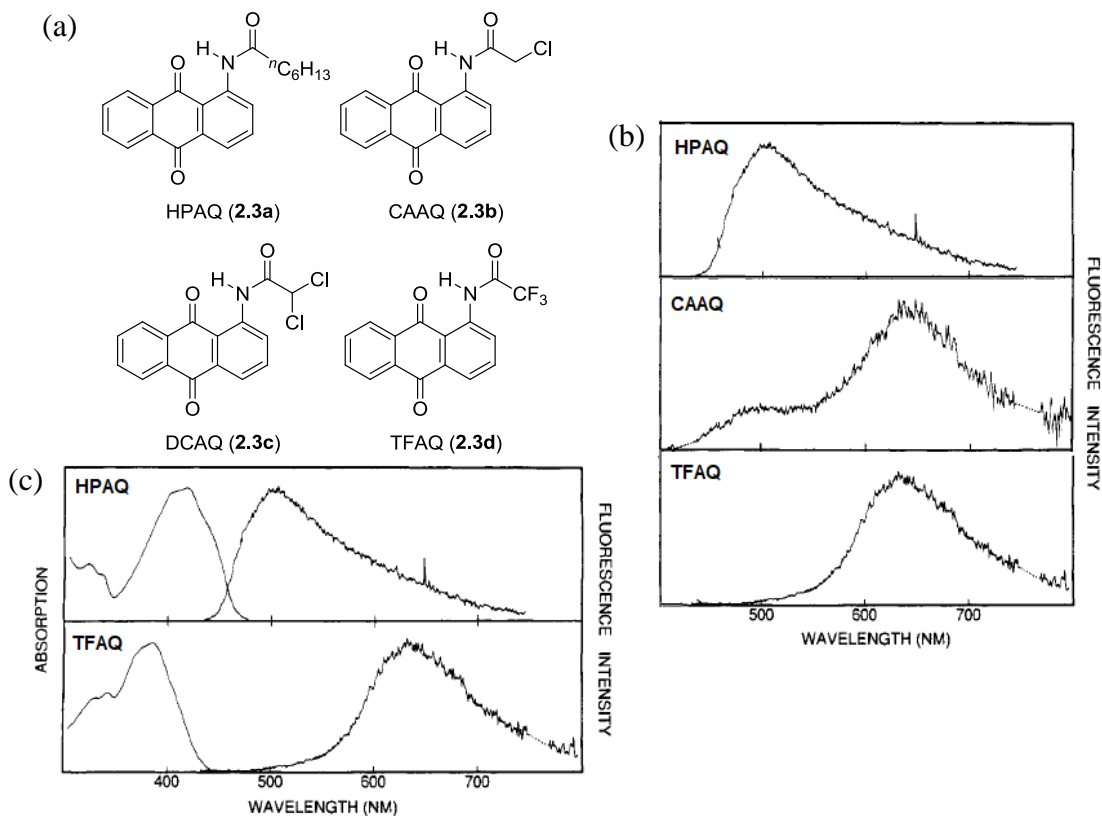


Figure 2.3: (a) Structures of studied 1-(acylamino)anthraquinones; (b) Emission spectra for cyclohexane solutions of HPAQ, CAAQ and TFAQ; (c) Absorption and emission spectra for cyclohexane solutions of HPAQ and TFAQ. Adapted with permission from ref. [19]. Copyright © 1991, American Chemical Society.

assigned to the $S_1(T) \rightarrow S_0(T)$ transition, thus serving as experimental evidence for the ESIPT process in 1-(acylamino)anthraquinones.

Authors noted that, in theory, there could be other possible explanations for the observed dual emission. For instance, twisted internal charge transfer (TICT) state is known to produce a similar effect [22]; however, TICT emission band is expected to undergo a red shift with the increase of solvent polarity, whereas the opposite trend was detected for LWE of aminoanthraquinone derivatives. Besides, photoionization of the $S_1(N)$ molecule could produce an excited-state anion responsible for LWE, although this emission would become weaker in less polar solvents and diminish in the presence of a

strong acid, which is in disagreement with the experimental results. Another feasible rationale for the dual fluorescence could be emissions from two S_1 states that are produced by exciting two different ground-state species, such as free analyte molecule and its complex with solvent. This possibility was ruled out by the fact that two excitation spectra, one with monitoring SWE and another with monitoring LWE, are identical and look similar to the absorption spectrum. Such crucial observation supports the ESIPT mechanism, where both SWE and LWE are derived from a common excited state $S_1(N)$: one is the direct $S_1(N)$ emission and the other is the emission from $S_1(T)$ produced by tautomerization of $S_1(N)$.

By examination of the dual emission pattern, they established the influence of several internal and external factors on the ESIPT in 1-(acylamino)anthraquinones. As it was noted earlier, the LWE/SWE ratio increases with the electron-withdrawing character of an acyl substituent (**Table 2.1**), suggesting that enhancing NH acidity has a positive impact on ESIPT. The opposite trend (LWE/SWE decline) was observed in the series of

Table 2.1: LWE/SWE Ratios^a for 1-(Acylamino)anthraquinones in Cyclohexane [19]

Compound	LWE/SWE Ratio
HPAQ	0.34
CAAQ	3.3
DCAQ	14
TFAQ	27

^aDefined as the emission intensity at 635 nm divided by the emission intensity at 510 nm.

spectra recorded in different solvents, going from less polar to more polar: cyclohexane → dichloromethane → acetonitrile (**Figure 2.4**); this result indicates a stabilization of $S_1(N)$ relative to $S_1(T)$ in a more polar medium.

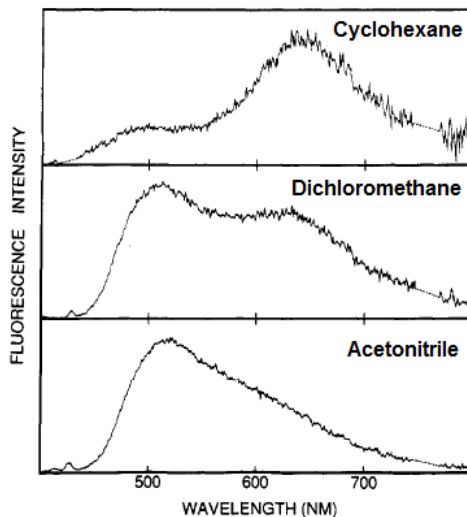


Figure 2.4: Corrected fluorescence emission spectra for CAAQ in various solvents. Adapted with permission from ref. [19]. Copyright © 1991, American Chemical Society.

While static fluorescence spectroscopy allows for detecting the existence of singlet excited tautomeric species and to study the influence of various factors on the extent of ESIPT, time-resolved emission experiments (performed by methods such as time-correlated single-photon counting, TCSPC) provide the information about the dynamics of the process. For instance, by monitoring the rise in mostly tautomer-produced fluorescence at 593 nm of DCAQ with subpicosecond resolution, it was concluded that ESIPT process is extremely fast and is complete within 3 ps (**Figure 2.5a**). In addition, plotting the decay of emission at the same wavelength and performing exponential fitting (**Figure 2.5b**) gave the value for the lifetime of emitting $S_1(T)$ species, which is 82 ps in this case.

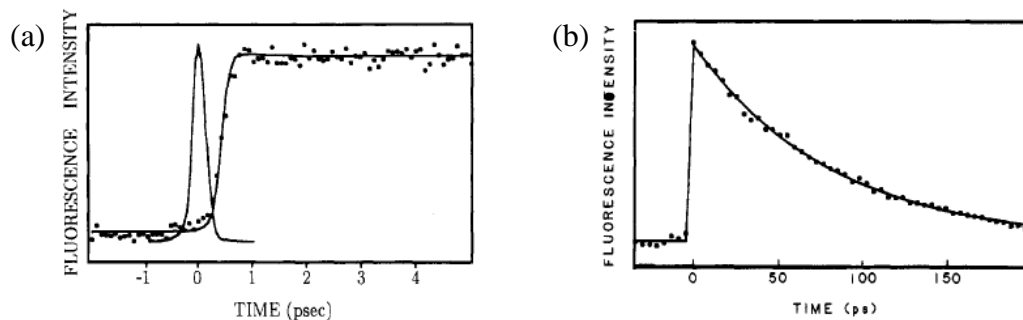


Figure 2.5: Time-resolved fluorescence emission of DCAQ in acetone monitored at 593 nm: (a) Rise in emission, together with the instrument response function (arbitrary zero of time); (b) Emission decay curve monitored over longer period. Adapted with permission from ref. [19]. Copyright © 1991, American Chemical Society.

Importantly, the ESIPT process in 1-(acylamino)anthraquinones can also occur in the triplet manifold, as suggested by Nagaoka et al. who probed the T_1 states of the same series of compounds (**Figure 2.3a**) by transient absorption spectroscopy [20]. Given that the data was obtained at 2 μ s after photoexcitation (six orders of magnitude longer than the typical singlet lifetime), and that the spectra were quenched by oxygen, the authors concluded that observed absorption was produced by triplet species. In most cases, two bands were detected: short-wavelength absorption (SWA; ca. 450 nm) and long-wavelength absorption (LWA; ca. 480 nm), which were ascribed to $T_1(N)$ and $T_1(T)$ respectively. Assignments were made based on the same trends reported for singlet states: namely, decrease in the amount of tautomerized species in more polar solvents and for compounds with less electron-withdrawing acyl groups (**Figure 2.6**). The authors concluded that both ESIPT and back proton transfer take place in the triplet state, due to the following observations:

- The absorption spectrum of TFAQ obtained after triplet photosensitization with benzophenone, which is supposed to produce $T_1(N)$ exclusively¹, contains both SWA and LWA, indicating the formation of $T_1(T)$;
- Spectrum of TFAQ in acetonitrile has only SWA arising from the untautomerized form; given the high propensity of this compound for singlet ESIPT [19], it was proposed that back proton transfer predominates in the triplet state.

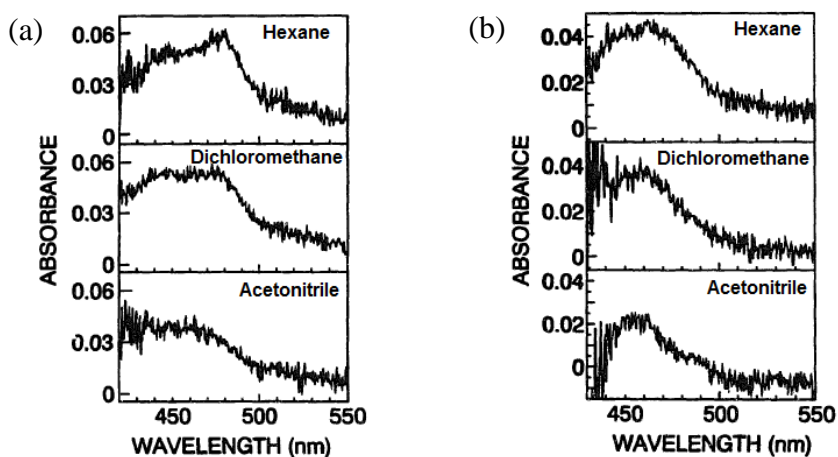


Figure 2.6: Transient absorption spectra of TFAQ (a) and CAAQ (b) obtained in various solvents at room temperature. Reprinted from ref. [20], Copyright © 1997, with permission from Elsevier.

In addition to amidoanthraquinones, a number of other systems deserve brief discussion, because they allowed revelation of several crucial trends in ESIPT reactivity.

Chou and co-workers investigated thermodynamics and kinetics of ESIPT in a series of 2-(2'-aminophenyl)benzothiazole (ABT) derivatives by fluorescence spectroscopy and

¹ It is, however, challenging to induce selective photoexcitation of benzophenone in presence of TFAQ, since both compounds absorb in the same region (250–300 nm) [19, 23]. If TFAQ gets excited to $S_1(N)$, then the formation of $T_1(T)$ is possible via singlet ESIPT followed by ISC.

DFT calculations [24]. They found that stronger acidic character of NH proton correlates not only with greater exergonicity of the proton transfer, but also with a smaller energy barrier for the process (**Figure 2.7**). At the same time, in the case of 2-(imidazo[1,2-*a*]pyridin-2-yl)aniline-based (IPA) compounds, the effect of NH acidity on the ESIPT rate was almost the opposite, with trifluoroacetyl derivative being the slowest (**Figure 2.8**) [25]. This apparent abnormality was rationalized by proposing a highly charge-separated non-planar transition state **2.6** leading to the formation of zwitter-ionic

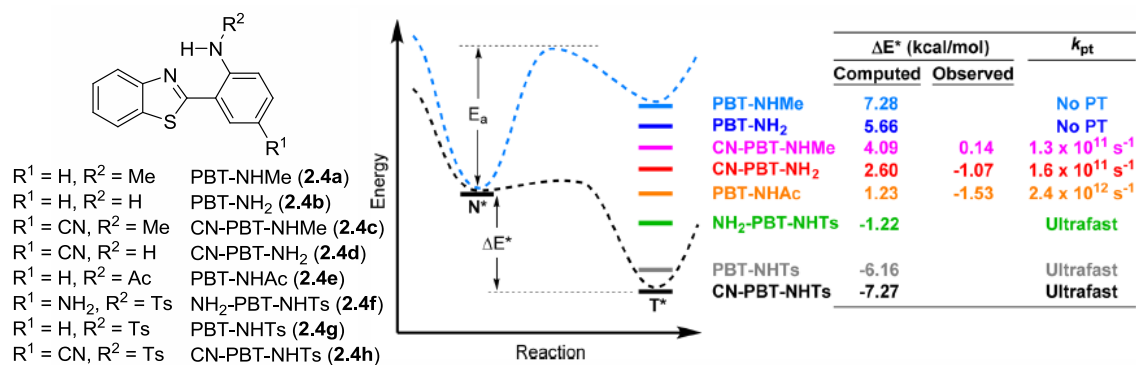


Figure 2.7: Thermodynamic and kinetic correlations for ESIPT in the series of ABT compounds **2.4a–h**. k_{pt} is the proton-transfer rate constant. The potential energy curves (dashed lines) are qualitative. Adapted with permission from ref. [24]. Copyright © 2015, American Chemical Society.

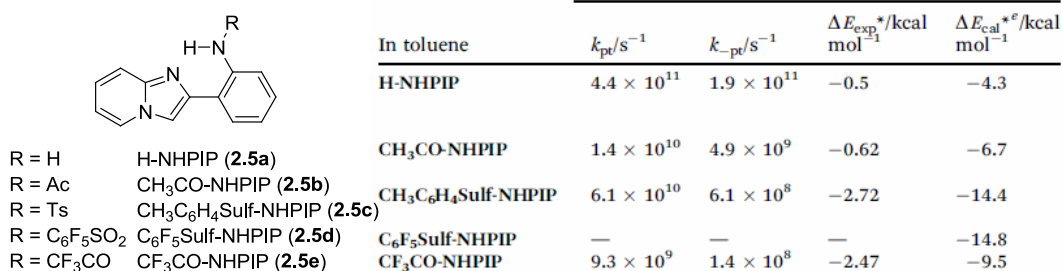
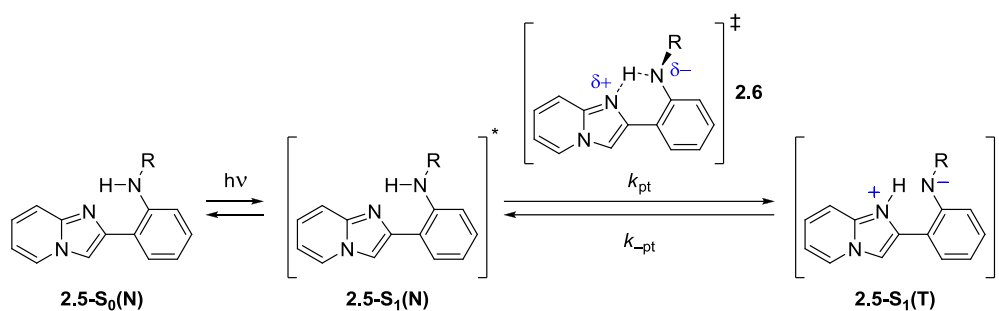


Figure 2.8: Thermodynamic and kinetic correlations for ESIPT in the series of IPA compounds **2.5a–e**. k_{pt} and k_{-pt} are the proton-transfer and back proton-transfer rate constants respectively. ΔE_{exp}^* and ΔE_{cal}^* are experimental and calculated energy differences between the normal form and tautomer form species in S₁ excited states. Republished with permission of Royal Society of Chemistry, from ref. [25]; permission conveyed through Copyright Clearance Center, Inc.



Scheme 2.2: ES IPT of IPA system via a plausible non-planar transition state [25].

tautomer **2.5-S₁(T)** (**Scheme 2.2**), as opposed to ABT systems where ES IPT proceeds through flat semi- π -conjugated structure. Presumably, increase in the electron-withdrawing character of R group provides stronger stabilization of a negative charge on the amide nitrogen, forcing it to adopt non-planar geometry. This distortion destabilizes the transition state **2.6** by reducing the amount of π -conjugation in it, and therefore results in a slower ES IPT.

For 2-(2'-benzamido-phenyl)benzimidazole (2-BAPBI; **Figure 2.9**), effect of the solvent on the singlet tautomer lifetime was studied (**Table 2.2**) [26]. In less polar cyclohexane and dioxane, monoexponential decays were observed and gave lifetimes around 2 ns. In contrast, fitting the data measured in more polar media (acetonitrile, methanol and water) produced biexponential decays, suggesting the presence of two different emitting species in these solvents. The authors proposed that the major short-lived species is a “closed” tautomer with intramolecular hydrogen bond **2.7-T**, whereas the minor long-lived fluorescence, which was detected exclusively in polar solvents, was assigned to an “open” tautomer bound to a solvent molecule **2.7-T'**. Lifetime of the “closed” species decreases with the solvent polarity; however, this trend is broken in

water, so it was suggested that this emission component belongs to an untautomerized form **2.7-N'**. At the same time, a stronger hydrogen bonding capacity of the solvent results in greater stabilization of the “open” tautomer **2.7-T'**, increasing its proportion and extending its lifetime.

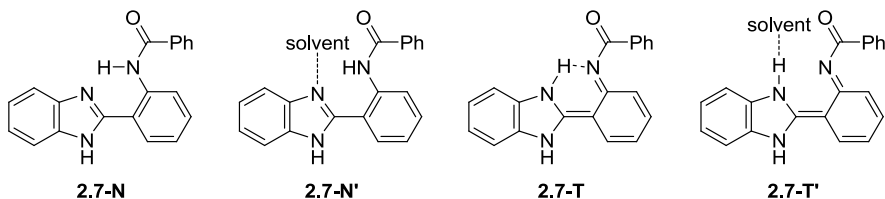


Figure 2.9: 2-BAPBI and derived species detected by time-resolved fluorescence [26].

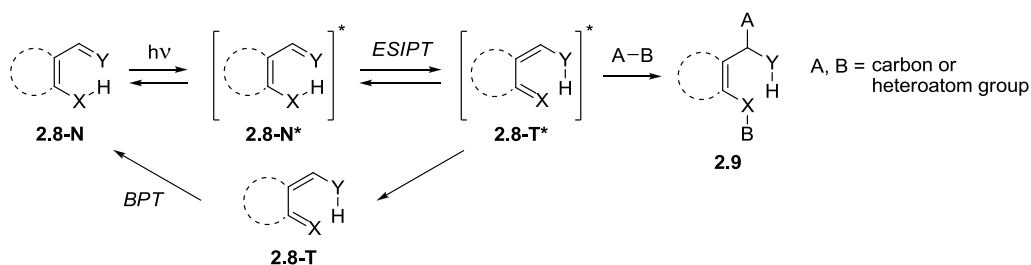
Table 2.2: Fluorescence Lifetimes (τ , ns) for 2-BAPBI in Different Solvents (Reprinted from ref. [26], Copyright © 1999, with permission from Elsevier)

Solvent	Fit 1 (single exp. decay)		Fit 2 (double exp. decay)		
	τ	χ^2 ^a	τ_1	τ_2	χ^2
Cyclohexane	2.1	1.2			
Dioxane	2.0	1.2			
Acetonitrile	0.28	1.6	0.28 (96.2 ^b)	7.2 (3.8)	1.2
Methanol	3.6	2.5	0.21 (84.7)	5.4 (15.3)	1.3
Water	4.6	4.2	1.8 (52.1)	9.1 (47.9)	1.1

^a χ^2 is the measure of goodness of fit. ^bNumbers in parentheses are amplitudes which represent relative proportions of species decaying with the corresponding lifetimes.

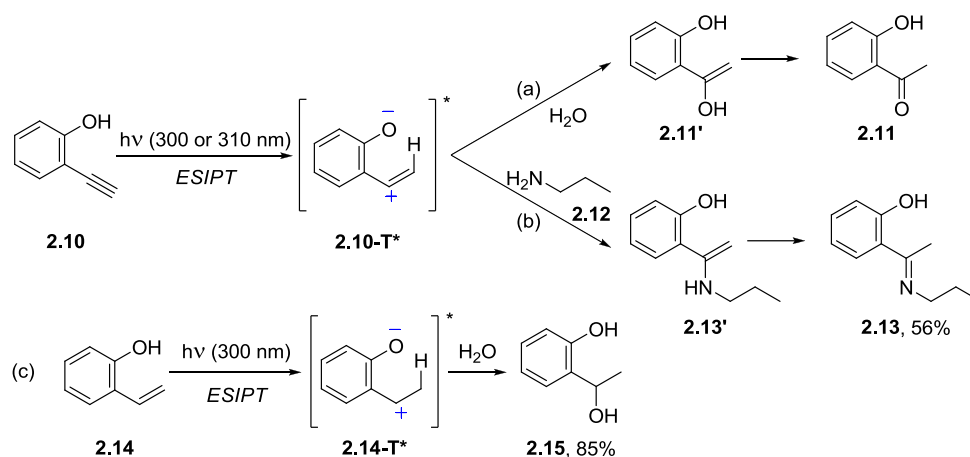
Excited-State Intramolecular Proton Transfer: Synthetic Applications

Short-lived tautomers produced by ESIPT are highly energetic, and therefore are expected to be very reactive. One can envision taking advantage of their reactivity and engaging them in chemical transformations that would create new C–C and/or C–heteroatom bonds. However, the number of synthetic methods employing ESIPT has been limited, presumably due to short lifetimes of photogenerated excited tautomers that suffer from a multitude of fast decay pathways, such as back proton transfer (BPT; **Scheme 2.3**).



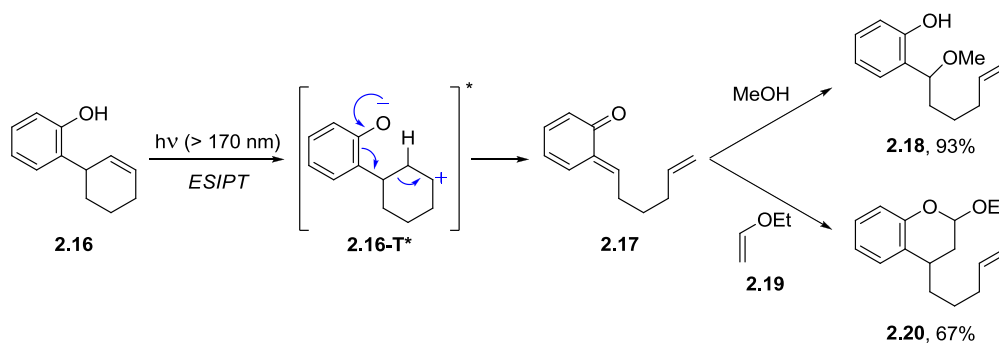
Scheme 2.3: Hypothetical “trapping” reaction of ESIPT-generated tautomer.

One of the earliest examples of an ESIPT-based transformation that irreversibly leads to a new compound is the alkyne photohydration in *o*-hydroxy-substituted phenylethylene **2.10** discovered by Yates in 1984 (**Scheme 2.4**, reaction a); yield of the resulting acetophenone **2.11** was not reported [27]. It was suggested that the OH group protonates a triple bond in the excited state species **2.10-N***, and subsequent nucleophilic addition of water to the carbocation **2.10-T*** leads to the ketone product **2.11**. The newer study shows that utilizing the primary amine **2.12**, as a trapping agent in this reaction, provides access to imine **2.13** in 56% yield (**Scheme 2.4**, reaction b) [28]. A similar process is also feasible for alkene substrates: photohydration of *o*-hydroxystyrene **2.14** affords benzyl alcohol **2.15** (**Scheme 2.4**, reaction c) [29].



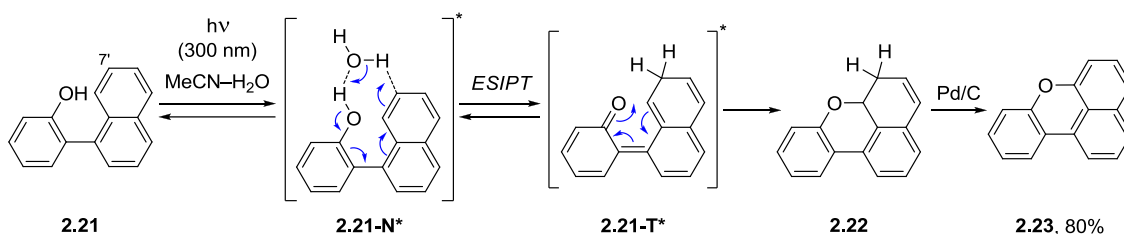
Scheme 2.4

In addition, some systems with a more distant location of the double bond are ES IPT-reactive as well [30, 31]. For example, formation of products **2.18** and **2.20** from 2-(2'-cyclohexenyl)phenol **2.16** was rationalized by proposing transfer of a proton to the proximal olefinic carbon, followed by ring opening of the secondary cyclohexyl carbocation forming the key *o*-quinone methide intermediate **2.17** (Scheme 2.5) [30]. Subsequent trapping of this species by nucleophilic addition of methanol and by Diels–Alder reaction with ethyl vinyl ether **2.19** yields methoxy-adduct **2.18** and dihydrobenzopyran **2.20**, respectively.



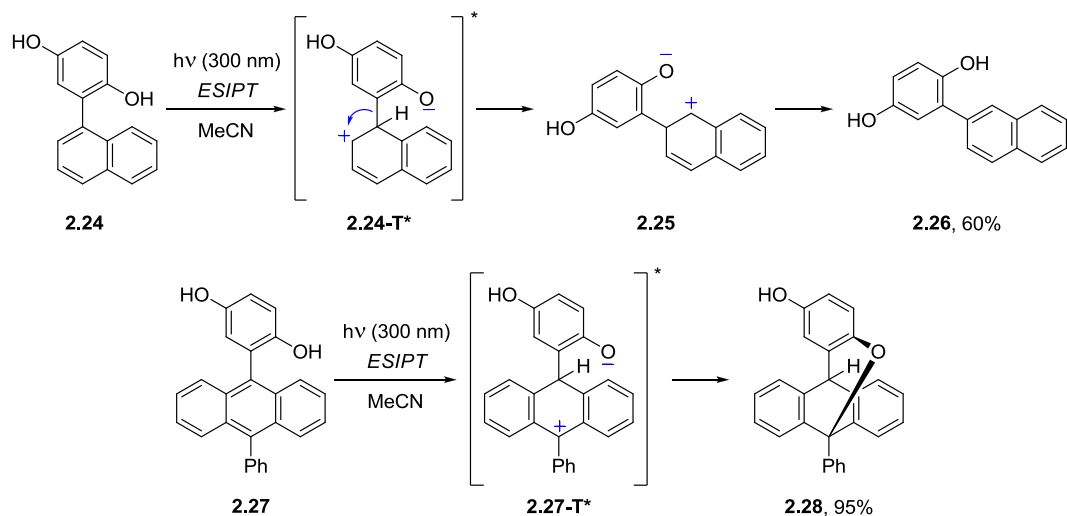
Scheme 2.5

Wan and co-workers extended the applicability of ESIPT to a carbon atom onto the systems where a proton is transferred to a polyaromatic moiety. Irradiation of the naphthyl-substituted phenol **2.21** triggered ESIPT to the 7'-position, followed by 6π -electrocyclization of the quinone methide **2.21-T*** yielding product **20**, which was readily oxidized to the stable 1,9-benzoxanthene **2.23** (**Scheme 2.6**) [32]. Since no reaction was observed in neat acetonitrile, the authors concluded that ESIPT to a distant carbon atom in this system is water-mediated.

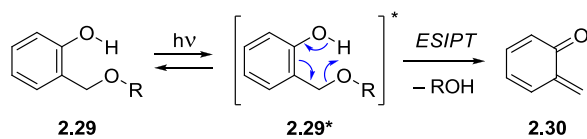


Scheme 2.6

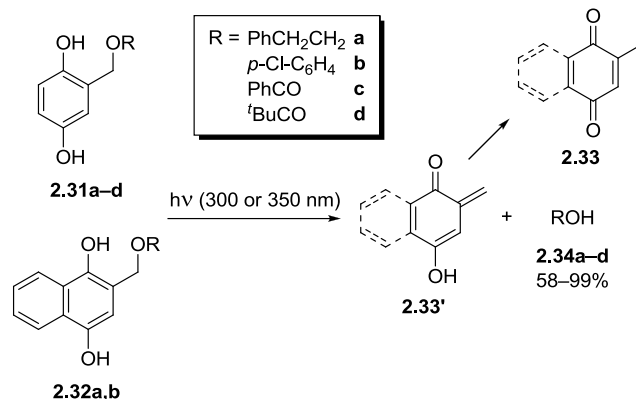
Interestingly, introduction of a second OH group into the *para*-position to phenol forced the proton transfer to occur under anhydrous conditions (**Scheme 2.7**) [33]. In this case, *ipso*-carbon of the naphthalene ring in **2.24** undergoes direct protonation, and the resulting zwitterionic intermediate **2.24-T*** rearranges to the more stable benzylic carbocation **2.25** via 1,2-shift of phenyl group; reverse proton transfer gives the product **2.26**. Photolysis of the phenylanthracene analogue **2.27** in neat acetonitrile induces the same ESIPT; however, the produced carbocation **2.27-T*** is stabilized by three adjacent phenyl rings, and instead of rearranging, it cyclizes to the ether **2.28**.



It has been found that there is a much larger number of synthetic applications in ES IPT-reactive compounds where the oxygen acts as a proton acceptor. One important class of transformations involving these systems is based on the formation of *o*-quinone methide intermediate **2.30** produced by elimination of water or alcohol, which presumably takes place simultaneously with the ES IPT (**Scheme 2.8**).

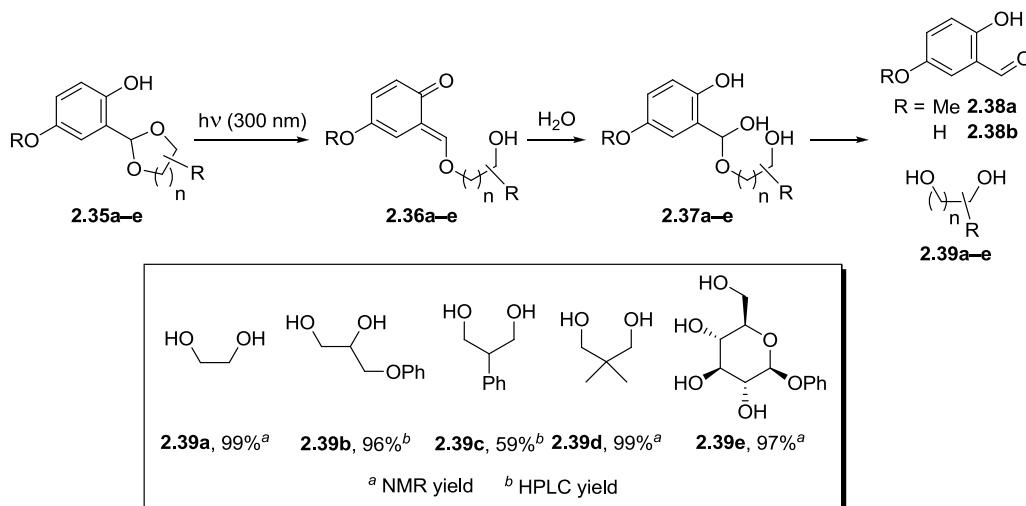


Kostikov and Popik took advantage of this process for the development of photolabile protecting groups [34, 35]. Irradiation of 2,5-dihydroxybenzyl ethers **2.31** and their naphthalene analogues **2.32** induces ES IPT accompanied by clean elimination of alcohol substrates **2.34** (**Scheme 2.9**) [34].



Scheme 2.9

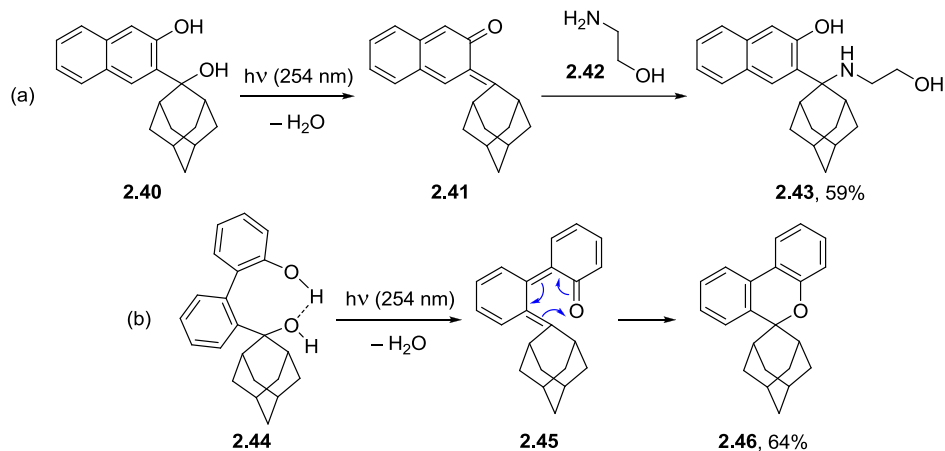
In another example, the same mechanism enables traceless photorelease of various diols **2.39** from corresponding acetals of 5-methoxy- or 5-hydroxysalicylaldehydes **2.35**: transfer of a proton to the acetal oxygen concurrent with the departure of alcohol leads to **2.37** that hydrolyzes to aldehyde **2.38** and diol **2.39** (Scheme 2.10) [35].



Scheme 2.10

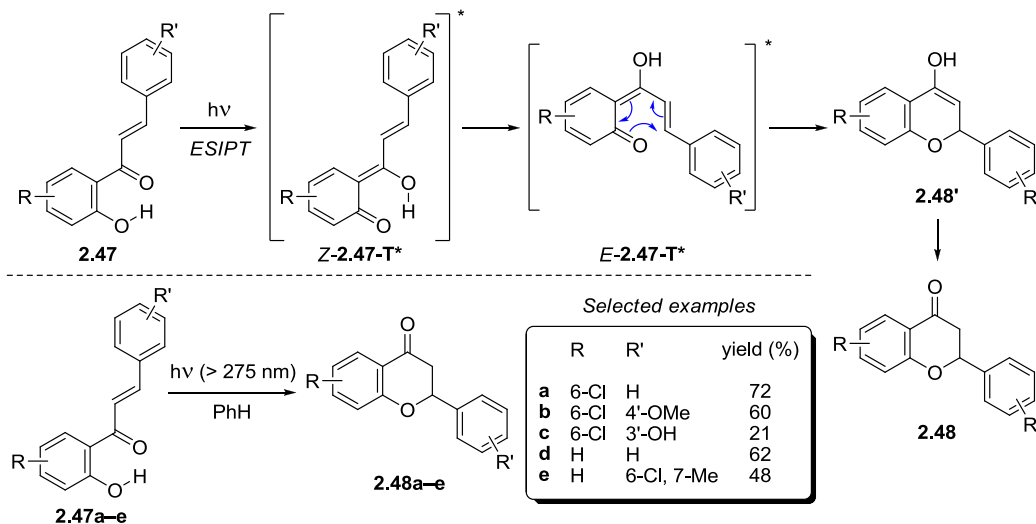
A group of researchers led by Basarić studied a number of ESIPT-driven quinone methide formations in hydroxyadamantyl-substituted phenols and naphthols [36, 37]. For instance, photolysis of alcohol **2.40** gives rise to the intermediate **2.41** which is trapped by ethanolamine **2.42** (Scheme 2.11, reaction a) [37]. A different reactivity was observed

for the biphenyl alcohol **2.44**, where two hydroxyl groups are separated with a longer bridge: the resulting quinone methide **2.45** contains an additional double bond, which makes the system perfectly arranged for the 6π -electrocyclic ring closure delivering chromane **2.46** (Scheme 2.11, reaction b) [36].



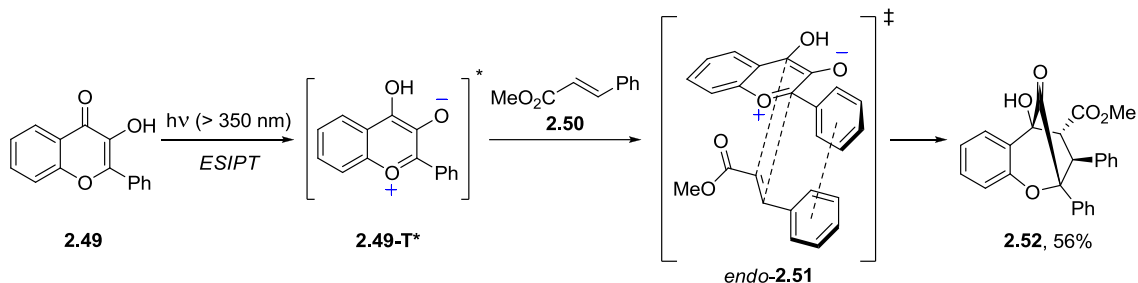
Scheme 2.11

2-Hydroxychalcones are also amenable for ES IPT/electrocyclization cascade [38]. In this case, transfer of a proton to the carbonyl oxygen in substrate **2.47** directly provides quinone methide *Z*-**2.47-T***, which after *Z-E* isomerization of the exocyclic double bond undergoes pericyclic reaction that furnishes flavanone **2.48** (Scheme 2.12).



Scheme 2.12

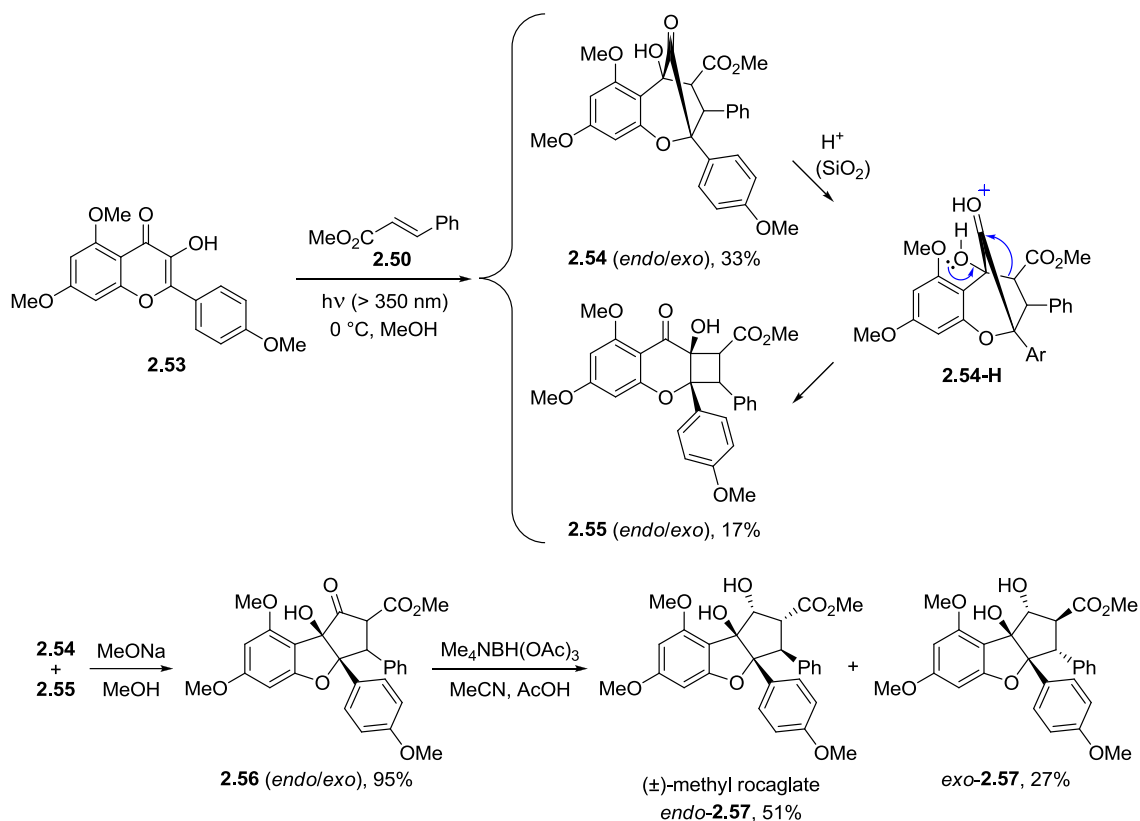
A prominent example of a synthetically useful system where ES IPT to oxygen plays a central role in its reactivity is 3-hydroxyflavone; its photochemistry has been thoroughly studied in Porco's lab [39-43]. They discovered that the zwitterionic 3-oxidopyryllium species **2.49-T***, which is produced as a result of a proton transfer in this photoactive core (**2.49**) can be efficiently engaged in 1,3-dipolar cycloaddition with an alkene, such as methyl cinnamate **2.50** (**Scheme 2.13**) – the process that conceivably takes place in the biosynthesis of numerous cyclopenta[bc]benzopyran derivatives occurring in *Aglaia* plants [44, 45]. Remarkably, this one-pot ES IPT/cycloaddition sequence proceeds with high regioselectivity and good *endo/exo* diastereoselectivity, which was rationalized by plausible π -stacking interactions between aryl groups in the dipolarophile and 3-oxidopyryllium in the proposed transition state *endo-2.51* [42].



Scheme 2.13

The novel transformation enabled exceptionally concise biomimetic synthesis of the natural product (\pm)-methyl rocaglate *endo-2.57* (**Scheme 2.14**) [39]. After irradiation of the 3-hydroxyflavone **2.53**, two compounds were isolated: the major adduct **2.54** and the product of the acid-catalyzed α -ketol shift **2.55** that formed during silica gel purification. Treatment of the resulting mixture with base induced 1,2-shift of dimethoxyphenyl group in **2.54** and expansion of cyclobutane ring in **2.55**, yielding the single tetrahydro-

benzofuran **2.56**. Subsequent hydroxy-directed reduction of α -ketol afforded the desired (\pm)-methyl rocaglate *endo*-**2.57**, as well as its stereoisomer *exo*-**2.57**.

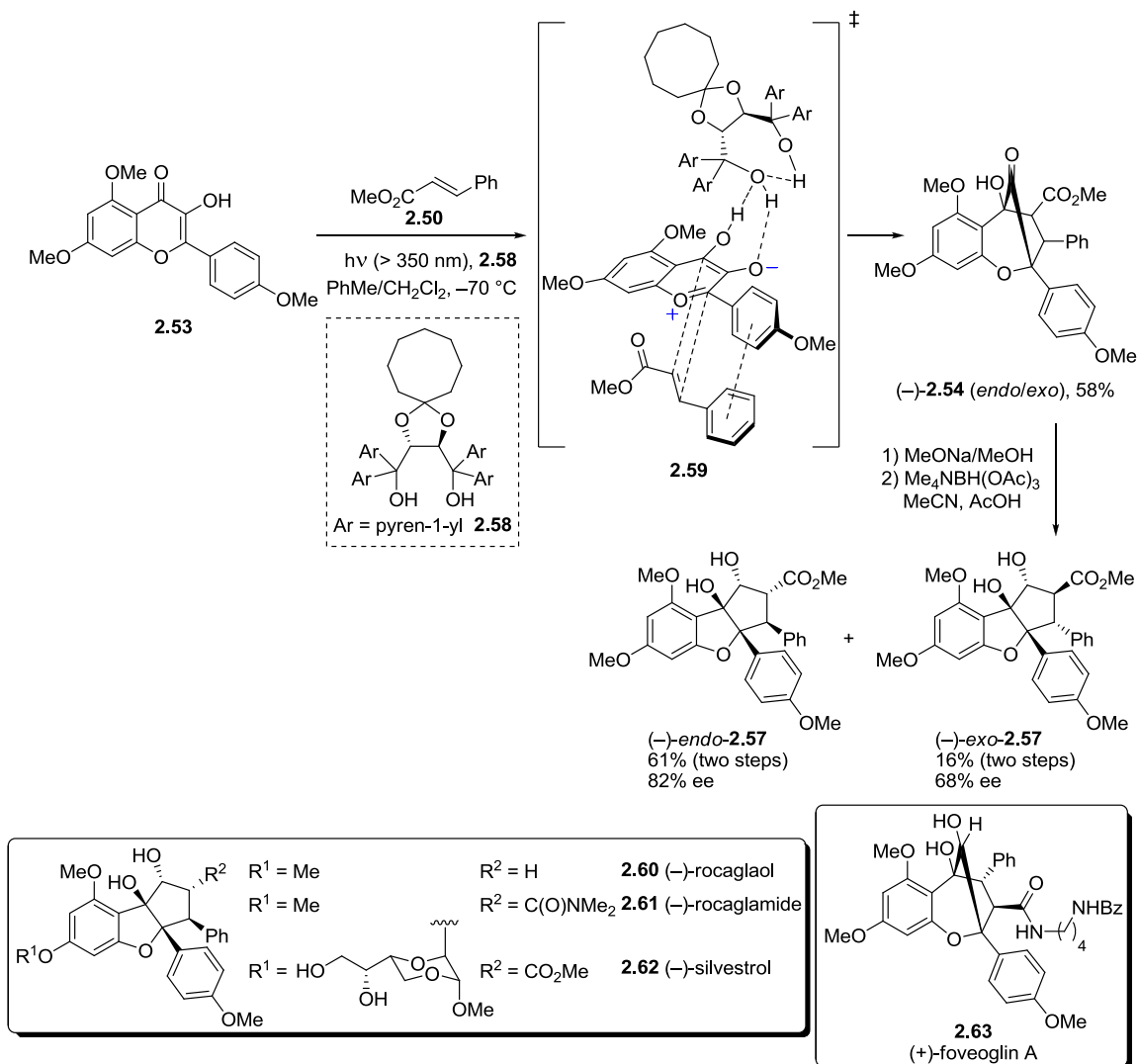


Scheme 2.14

Furthermore, extending the scope of the process on a wide range of dipolarophiles (predominantly β -aryl and β -hetaryl-substituted acrylates and acrylamides) allowed for generating a library of 16 rocaglate derivatives used for *in vitro* and *in vivo* biological evaluations [42].

Importantly, Porco's group developed an enantioselective version of the transformation, utilizing chiral TADDOL-based reagents and applied this approach for the asymmetric total syntheses of (–)-rocaglaol **2.60** and (–)-rocaglamide **2.61** [40], as well as (–)-silvestrol **2.62** [41] and (+)-foveoglin A **2.63** [43] (**Scheme 2.15**). The high

degree of enantiocontrol (up to 96% ee for the final product) is presumably achieved through the hydrogen bonding of the chiral mediator **2.58** to 3-oxidopyryllium; this stereospecific interaction effectively blocks one stereoface from the attack of the dipolarophile (transition state **2.59**).



Scheme 2.15

Certain mechanistic aspects of the photoinduced cycloaddition in 3-hydroxyflavone systems were also investigated [42, 43]. The importance of the ES IPT process in the mechanism of the transformation was emphasized by the fact that protic solvents (e.g.

methanol) and additives (e.g. trifluoroethanol) improve the product yield and enhance the intensity of long-wavelength fluorescence emission attributed to the tautomerized species **2.53-T*** (Figure 2.10). Based on these observations, it was proposed that protic compounds facilitate ESIPT through the formation of hydrogen-bonded complexes and acting as “proton shuttles.” Besides the ESIPT pathway, the authors did not exclude the possibility of the excited-state charge transfer (ESICT) form **2.53-N*** participating in the cycloaddition: in the fluorescence spectra of 3-hydroxyflavone **2.53**, a short-wavelength shoulder band around 440 nm was detected; given that a similar peak was observed in the spectrum of ESIPT-inactive 3-methoxyflavone **2.64**, this emission was assigned to the ESICT species **2.53-N***.

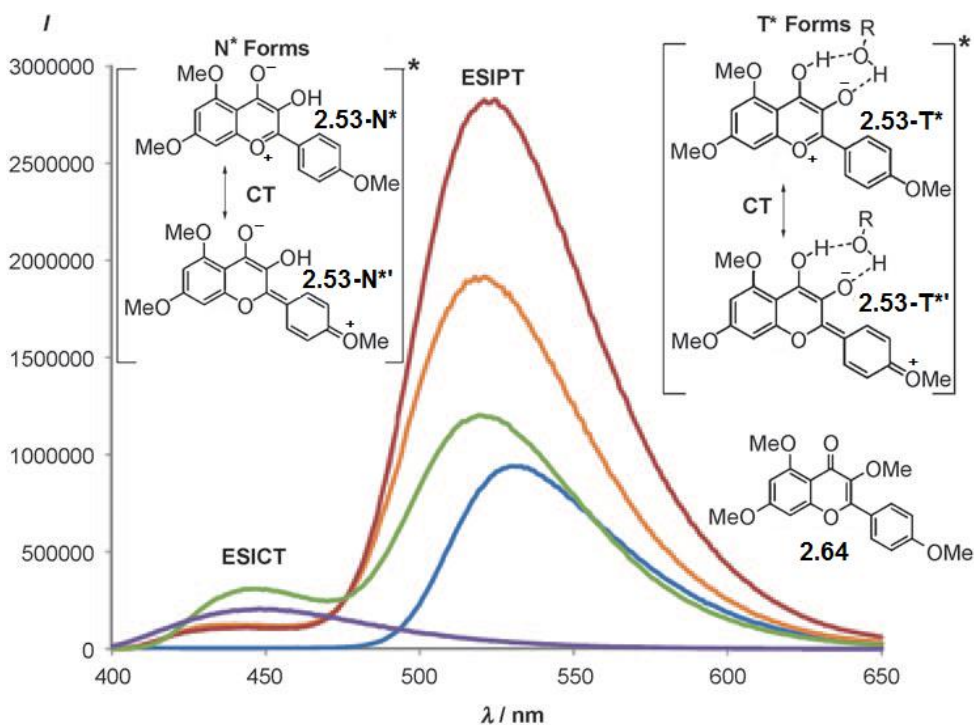
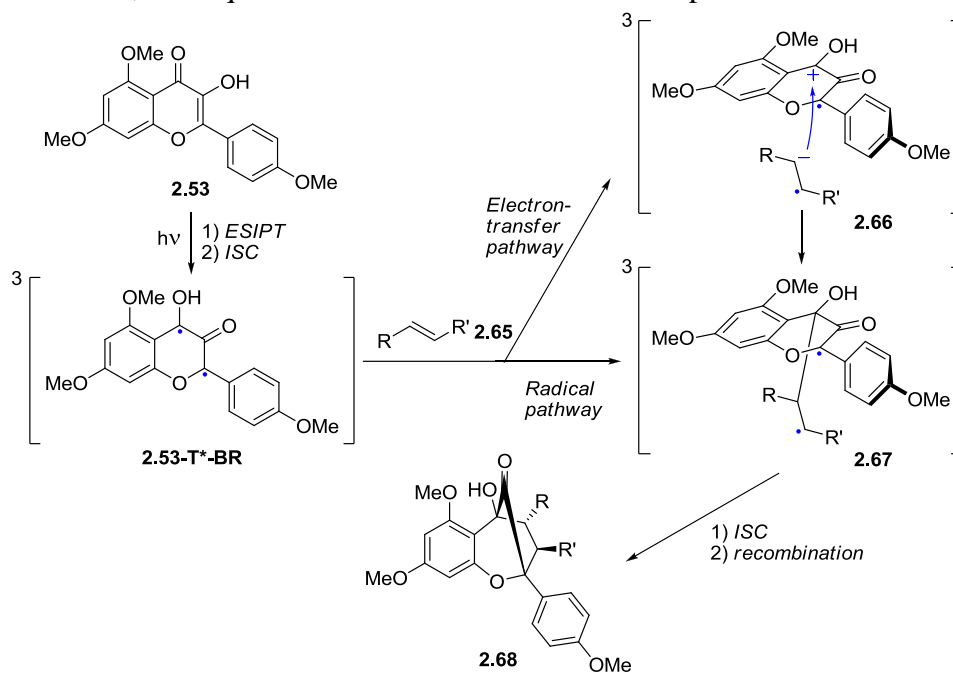


Figure 2.10: Fluorescence emission of 3-hydroxyflavone **2.53** and 3-methoxyflavone **2.64** indicating both ESICT and ESIPT processes with presumed charge transfer (CT) in both excited states from phototautomers **2.53-N***/**2.53-N***' and **2.53-T***/**2.53-T***'. Light blue: **2.53** in CHCl₃; orange: **2.53** in CHCl₃/TFE (95:5); red: **2.53** in CHCl₃/TFE (70:30); green: **2.53** in TFE; purple: **2.64** in TFE. Adapted from ref. [42], Copyright © 2010, with permission from John Wiley and Sons, Inc.

With regard to the spin multiplicity of excited-state intermediates involved in the ESIPT/cycloaddition process, several results support the participation of triplet biradicaloids [43]:

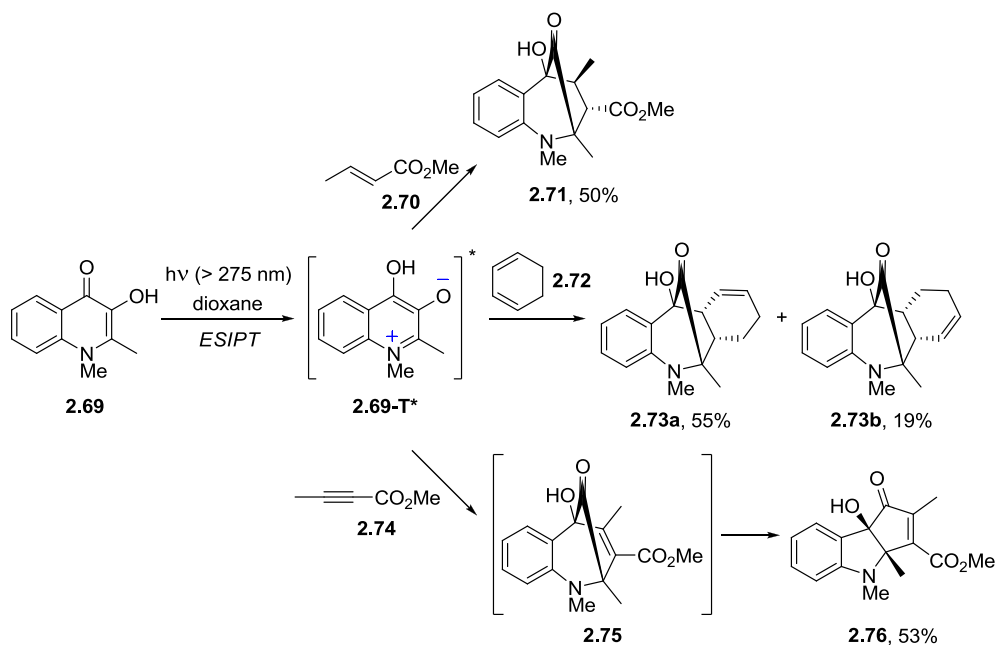
- Addition of the triplet quencher 9,10-dibromoanthracene completely suppressed the reaction;
- Running the irradiation in presence of the triplet sensitizer benzophenone lead to increase in the product yield (from 40 to 56%).

In view of these observations, the authors slightly revised the mechanism and proposed a stepwise cycloaddition pathway, where proton-transferred 3-oxidopyryllium is represented as a triplet biradical resonance form **2.53-T*-BR** (Scheme 2.16). This species reacts with dipolarophile **2.65** either through the direct radical addition, or via photoinduced electron transfer (PET) that forms radical ion pair **2.66** collapsing into the semi-adduct **2.67**; subsequent ISC and recombination afford product **2.68**.



Scheme 2.16

In addition to 3-hydroxyflavones, Porco's group engaged their aza-analogues, 3-hydroxyquinolinones, into the same ESIPT-driven transformation [46, 47]. Fluorescence studies performed on the simplest derivative **2.69** revealed that $S_1(T)$ species **2.69-T*** (Scheme 2.17), which produces largely Stokes-shifted emission band around 475 nm (Figure 2.11), is formed with a high quantum yield and has a relatively long lifetime: for instance, the values obtained in dioxane are 0.65 and 16.8 ns, respectively. Therefore, it was envisioned that the excited-state tautomer **2.69-T*** can be efficiently captured with various dipolarophiles, and this hypothesis found experimental verification: irradiating quinolinone **2.69** with various unsaturated compounds (e.g. **2.70**, **2.72**, **2.74**) afforded expected cycloadducts in good yields (Scheme 2.17) [46]. Interestingly, the product of the alkyne addition **2.75** spontaneously converted into the indolino-cyclopentenone **2.76** by α -ketol shift.



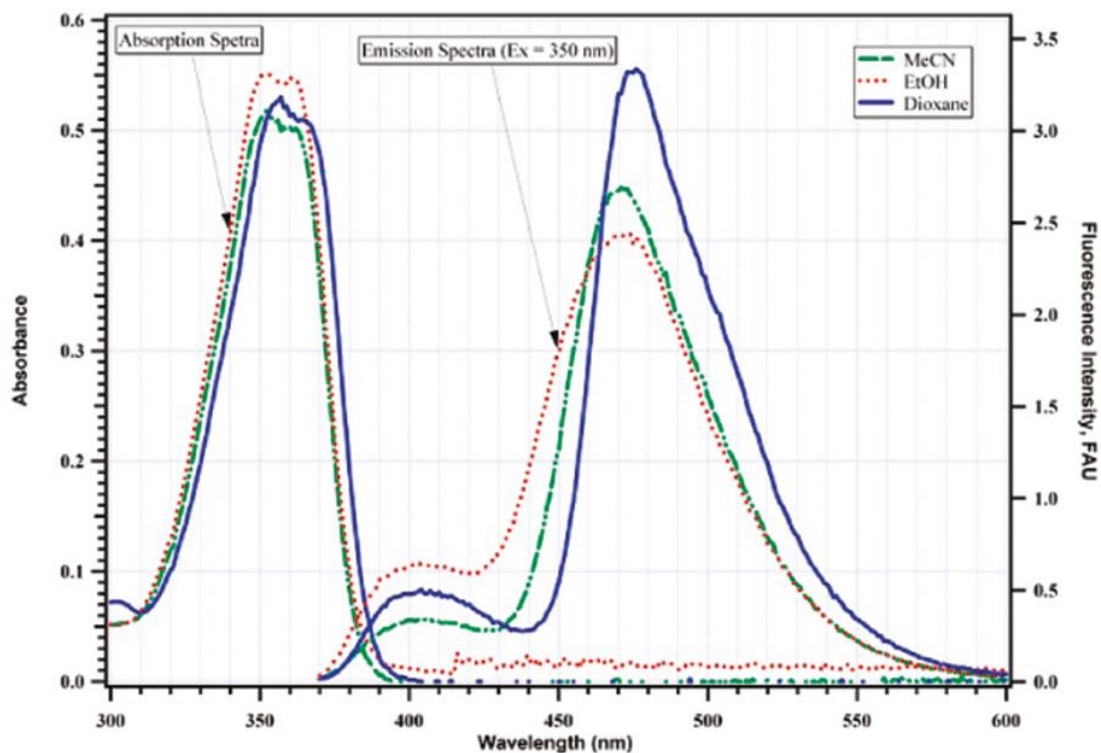
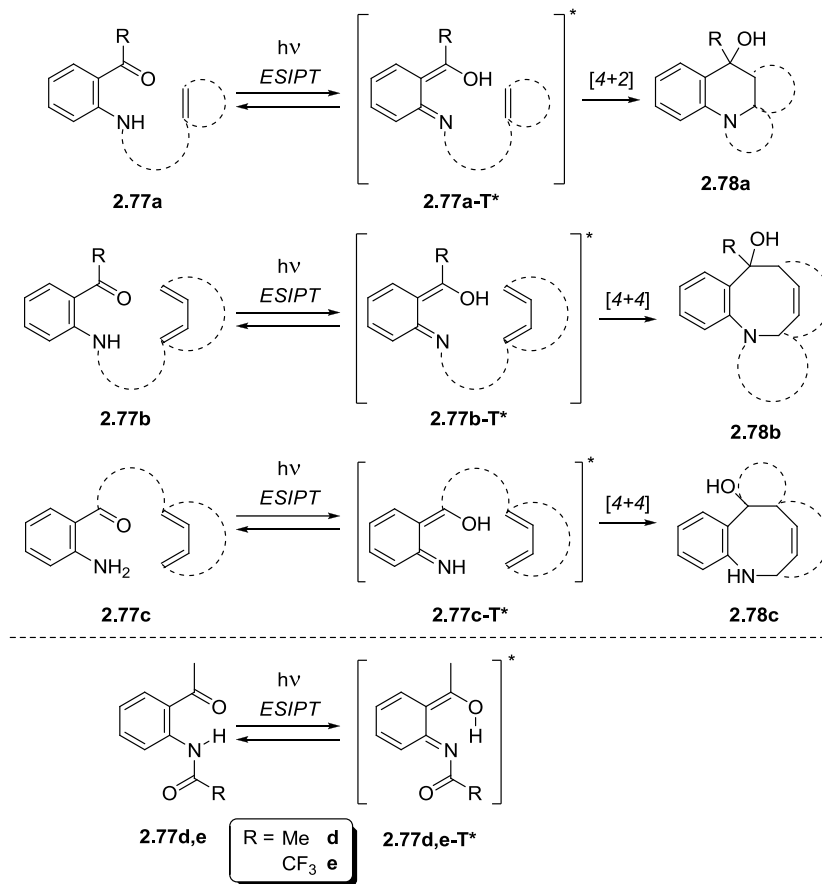


Figure 2.11: Absorption and normalized fluorescence spectra of **2.69**. Reprinted with permission from ref. [46]. Copyright © 2011, American Chemical Society.

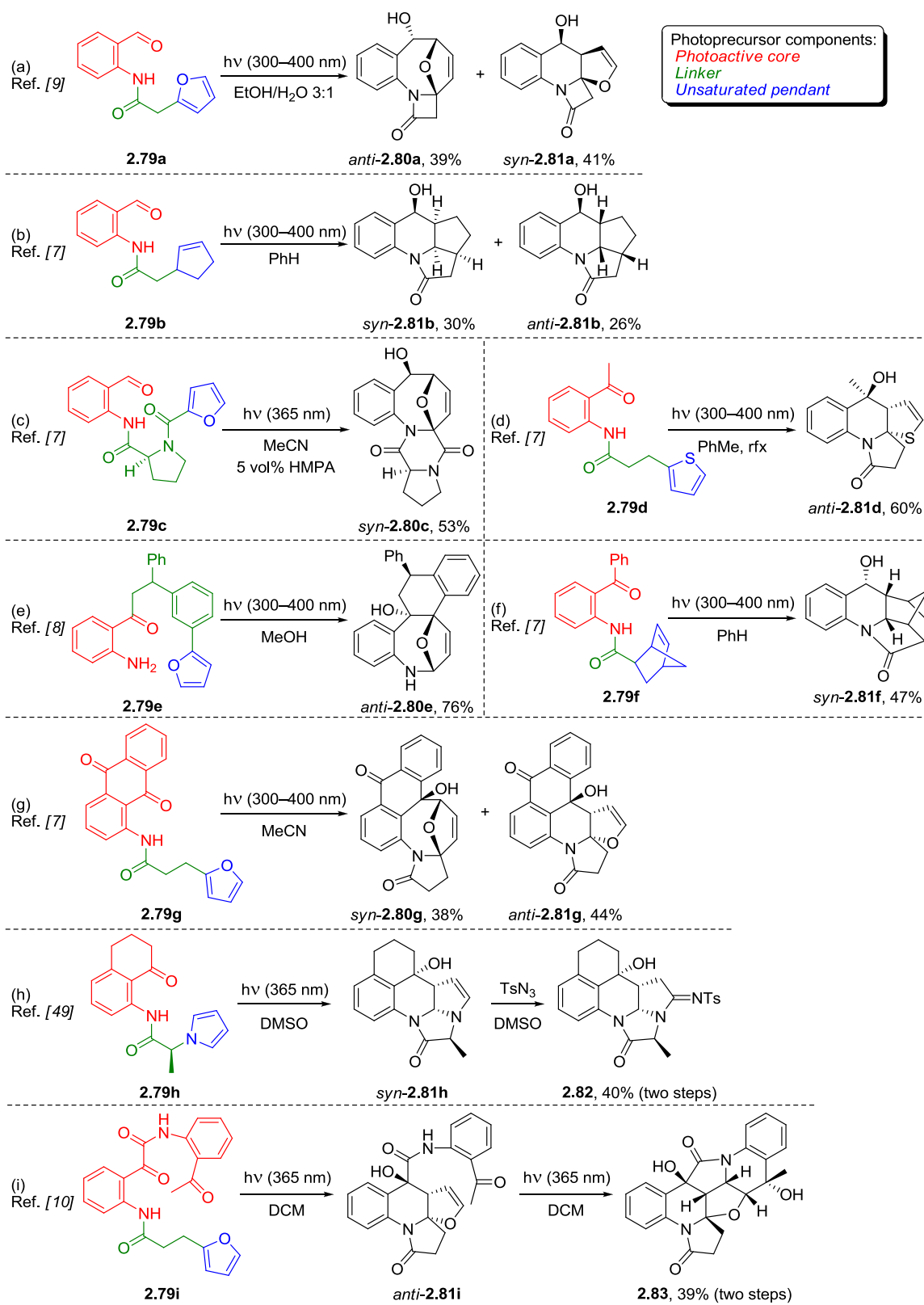
The strategy of utilizing ESIPT-generated species for cycloaddition reactions, which are especially appealing from the complexity building standpoint, was successfully implemented by Kutateladze's group for *o*-carbonyl-functionalized anilides (**2.77a,b**, **Scheme 2.18**) and anilines (**2.77c**) [7-10, 48-50]. The main challenge associated with these systems is that their excited-state tautomers (called *o*-azaxylenes, **2.77a-c-T***) are extremely short-lived: for instance, fluorescence lifetimes measured for LWE in *N*-acetyl- and *N*-trifluoroacetyl-substituted *o*-aminoacetophenones **2.77d,e** are only 45 and 409 ps, respectively [51] – at least 1000 times less than the values obtained for previously discussed 3-hydroxyquinolinones [46]. This apparent obstacle, however, was surmounted by tying two cycloaddition components together in one molecule:

intramolecular processes, such as [4+4] and [4+2] reactions with the attached heterocyclic moieties, turned out to be fast enough to effectively compete with the decay of the *o*-azaxylylene species.



Scheme 2.18

Even though the intramolecular aspect of the photocycloaddition required additional synthetic manipulations in order to make the precursor molecules, the assembly of the substrates was achieved through simple and high-yielding methods (e.g. amide coupling). As a result, the scope of the novel process was expanded on a vast number of systems (representative examples are depicted in **Scheme 2.19**); all of them consist of three main parts:



Scheme 2.19

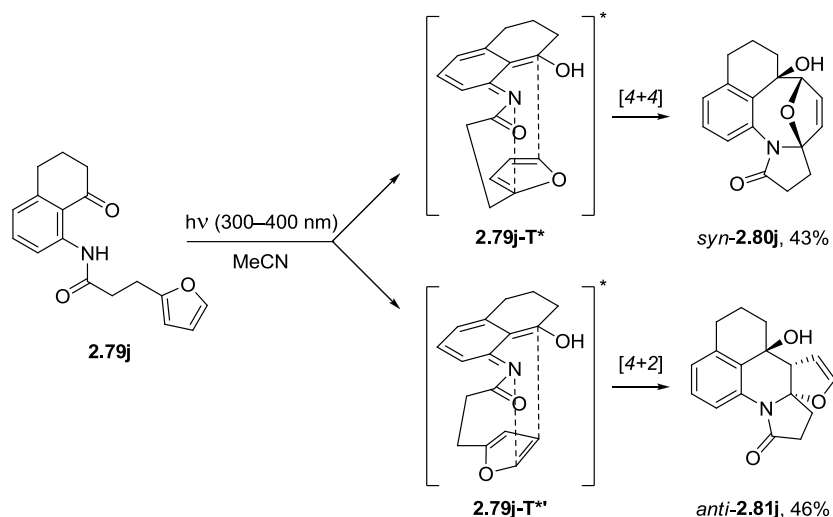
- *Photoactive core* based on *o*-amino-substituted aromatic carbonyl compounds: benzaldehyde (**2.79a–c**), acetophenones (either with plain methyl group, **2.79d**, or α -functionalized, **2.79e,i**), benzophenone (**2.79f**), or cyclic ketones (**2.79g,h**);
- *Linker* attached to ESIPT-reactive moiety either through the amide bond (“south” bridge, **2.79a–d,f–i**) or via the ketone arm (“north” bridge, **2.79e**);
- *Unsaturated pendant* responsible for intercepting the photogenerated *o*-azaxylylene; cycloaddition-competent groups include electron-rich heterocycles, e.g. furan (**2.79a,c,e,g,i**), thiophene (**2.79d**) and pyrrole (**2.79h**), as well as all-carbon cyclopentene (**2.79b**) and norbornene (**2.79f**).

Variations in all these fragments, combined with the availability of two cycloaddition channels, enabled rapid access to a diverse collection of *N,O,S*-polyheterocyclic scaffolds. Irradiation of furan-containing precursors afforded products with *O*-bridged benzazocine (*anti*-**2.80a**, *syn*-**2.80c**, *anti*-**2.80e**, *syn*-**2.80g**) and furo[2,3-*b*]quinoline cores (*syn*-**2.81a**, *anti*-**2.81g**) formed by [4+4] and [4+2] pathways, respectively. At the same time, thiophene and *N*-linked pyrrole rings participate only in [4+2] addition, leading to dihydrothiophene *anti*-**2.81d** and 2-pyrroline *syn*-**2.81h**, respectively (due to its instability, *syn*-**2.81h** was converted to the isolable *N*-sulfonyl amidine **2.82**). Additional heterocyclic rings in the photoproducts are introduced as a result of linker folding: for instance, by selecting appropriate spacers between photoactive units and unsaturated pendants, important pharmacophore moieties were installed, such as β -lactam (**Scheme 2.19**, reaction a) and 2,5-diketopiperazine (**Scheme 2.19**, reaction c).

Furthermore, a special precursor system with the “double” photoactive core was

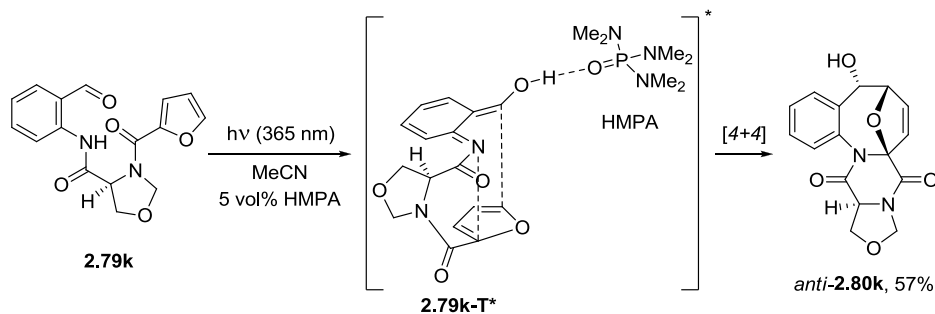
designed, which enabled the cascade sequence of two [4+2] reactions furnishing exceptionally complex structures with a fully saturated furan (**Scheme 2.19**, reaction i).

Overall, the photocycloaddition process is highly diastereoselective; however, due to substantial variety of photoprecursor structure topologies, the unified model that would consistently rationalize all observed stereochemical outcomes was not suggested. For the reactions with furans, thiophenes and pyrroles linked to the rest of the precursor at 2-position, *endo* approach of an unsaturated ring to the azaxylylene was proposed (**Scheme 2.20**). If the hydroxy group in the reactive intermediate is positioned “*in*”, i.e. towards the amide nitrogen – e.g. in case of the tetralone-based photoprecursor **2.79j** having non-rotatable carbonyl group – the resulting [4+4] product has *syn* relationship between OH and the newly formed heteroatom-containing bridge (*syn*-**2.80j**), whereas [4+2] cycloadduct is *anti* (*anti*-**2.81j**) [7].



Scheme 2.20: *endo*-Addition of furan to *in*-OH-*o*-azaxylylene.

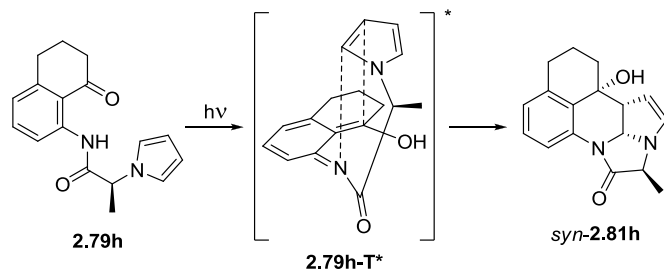
The opposite stereoconfiguration is obtained in the presence of hydrogen-bonding additives, such as HMPA or water, which are used to accelerate the reaction by providing stabilization to hydroxy-*o*-azaxylylene (**Scheme 2.21**) [48]. Binding of the additive to the hydroxy group forces a precursor with a rotatable carbonyl (e.g. **2.79k**) to form azaxylylene with *out*-OH (**2.79k-T***), and consequently leads to *anti*-[4+4] product *anti*-**2.80k** [48].



Scheme 2.21: *endo*-Addition of furan to *out*-OH-*o*-azaxylylene bound to HMPA.

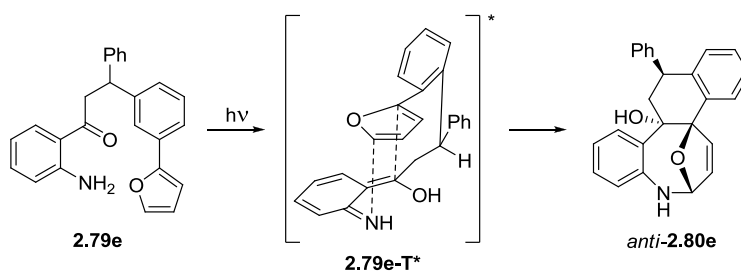
While this *endo*-cycloaddition model generally works well, in some cases it fails to explain diastereoselectivity. For instance, irradiation of **2.79c** in presence of HMPA afforded *syn*-[4+4] photoproduct *syn*-**2.80c** (**Scheme 2.19**, reaction c) [7], even though the reaction is predicted to proceed via “*out*”-OH intermediate.

Also, the model is not applicable to the systems containing the pyrrole pendant attached through the heteroatom: reaction of the photoprecursor **2.79h** yields *syn*-[4+2] cycloadduct *syn*-**2.81h** [49], suggesting the preference of *exo*-approach (**Scheme 2.22**).



Scheme 2.22: *exo*-Addition of pyrrole to *in*-OH-*o*-azaxylylene.

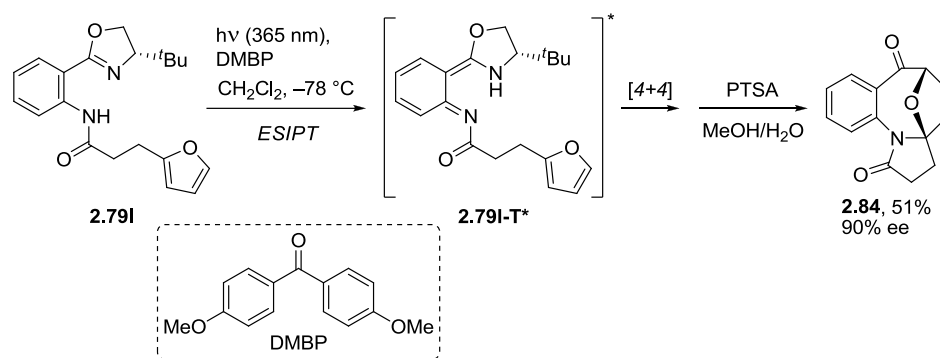
For the systems with “north” linker topology, a reactive conformation rationalizing the observed formation of *anti*-[4+4] products was proposed (**Scheme 2.23**) [8]. Such folding places the phenyl group (or another bulky substituent) in the less sterically hindered pseudo-equatorial position; however, the *exo*-orientation of furan with respect to azaxylylene does not agree with the *endo*-cycloaddition hypothesis suggested for “south-bridged” systems.



Scheme 2.23: *exo*-Addition of furan in systems with “north” linkers.

The *o*-azaxylylene-based diversity-oriented methodology was adapted for the preparation of enantiopure molecules [7, 48, 49]. By using amino acids as starting materials, chiral center can be easily embedded into the linker; photolysis of the resulting precursors, such as proline-derived **2.79c** and phenylalanine-based **2.79h**, leads to diastereoselective cycloaddition, where the chiral information is transferred from the tether to the rest of the molecule (**Scheme 2.19**, reactions c and h).

Furthermore, an asymmetric variant of the photocycloaddition was demonstrated for the systems where the primary source of chirality can be tracelessly removed after the irradiation [50]. For example, employing *L-tert*-leucinol-derived 2-oxazoline as a surrogate for the aldehyde group in the photoactive core enabled a stereocontrolled reaction, which afforded product **2.84** with 90% ee after hydrolytic removal of the chiral auxiliary (Scheme 2.24). Another remarkable feature of this system is that an oxazoline-based photoprecursor undergoes ESIPT to the nitrogen atom, as opposed to previously covered cases, where carbonyl oxygen plays a role of proton acceptor.



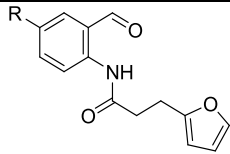
Scheme 2.24

In order to maintain low reaction temperature that is essential for obtaining high ee, this process required a “cool” UV light source (365 nm) instead of heat-generating Hanovia lamps with a wide emission spectrum. Due to weak absorption of oxazoline-functionalized anilides at this wavelength (their λ_{max} is blue-shifted to 320–330 nm), the photocycloaddition proceeded extremely slowly; however, it is significantly accelerated in the presence of 4,4'-dimethoxybenzophenone (DMBP), a known triplet sensitizer that is highly absorbing up to 400 nm. This crucial observation strongly suggests that the ESIPT in azaxylylene precursors can occur in the triplet manifold, because selective production of $T_1(N)$ species is induced under these conditions.

Numerous experimental observations indicate that the cycloaddition step, most likely, proceeds via triplet intermediates as well [52]:

- Bromine-substituted precursor **2.79n** reacts more than 4 times faster than the corresponding non-halogenated compound **2.79m**, as evidenced by their photocycloaddition quantum yields (**Table 2.3**). In addition, bromine significantly suppresses LWE from $S_1(T)$ species (**Figure 2.12**). The reasonable explanation of these phenomena is based on bromine's heavy-atom effect that facilitates conversion of singlets to triplets by ISC.
- The reaction rate exhibits progressive deceleration with the increase in concentration of a triplet quencher (e.g. *trans*-piperylene **2.85**, **Figure 2.13**).
- Results of time-resolved fluorescence studies on a series of photoprecursors reveal that replacing the unreactive acetyl substituent for the cycloaddition-competent furanpropanoyl pendant does not affect the decay of singlet species.

Table 2.3: Absolute Quantum Yields of Photocycloaddition^a
(Adapted with permission from ref. [52]; Copyright © 2014, American Chemical Society)

	QY
2.79m , R = H	0.18 ± 0.01
2.79n , R = Br	0.75 ± 0.06

^aDetermined by comparing conversion rates of 0.01 M photoprecursor solutions and the benzophenone–benzhydrol actinometer system ($\Phi = 0.57$).

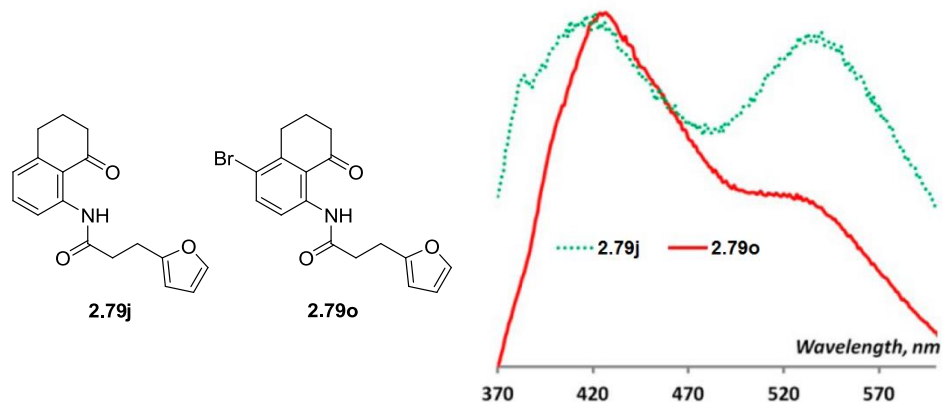


Figure 2.12: Normalized fluorescence spectra of tetralone derivatives **2.79j** and **2.79o**. Adapted with permission from ref. [52]. Copyright © 2014, American Chemical Society.

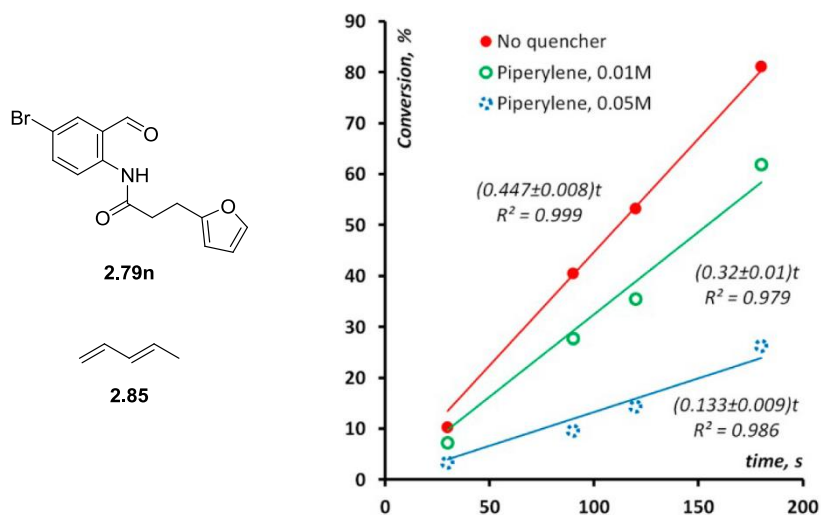
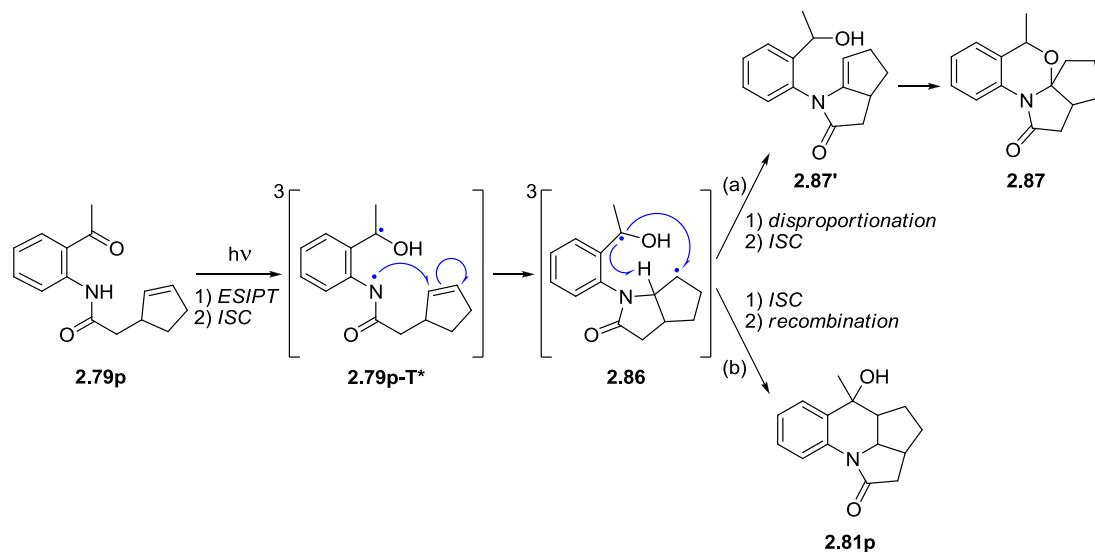


Figure 2.13: *trans*-Piperylene (**2.85**) quenching of **2.79n** in benzene. Adapted with permission from ref. [52]. Copyright © 2014, American Chemical Society.

It is conceivable that triplet-state cycloaddition occurs in a stepwise manner, with the *o*-azaxylylene intermediate represented as a biradicaloid (**2.79p-T***, **Scheme 2.25**). This hypothesis is supported by the formation of hemiaminal side-products (e.g. **2.87**) from certain slow-reacting cycloalkenyl derivatives, such as **2.79p**, which is rationalized by intramolecular radical disproportionation of a common “semi-cyclized” intermediate **2.86** followed by addition of alcohol to the enamine double bond [7].

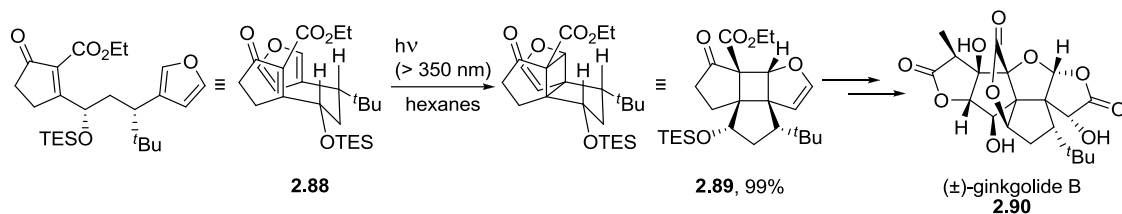


Scheme 2.25

Synthetic Utility of Dearomative Photocycloadditions to Selected Arenes

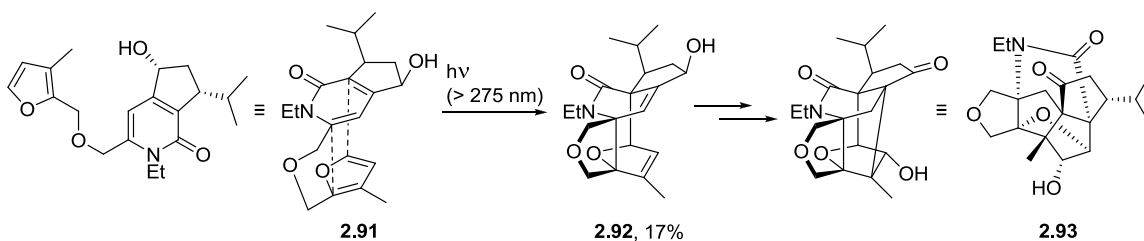
The reactions of ESIPT-generated *o*-azaxylylenes with heteroarene pendants perfectly illustrate how a photoinduced cycloaddition can serve as an effective tool for the removal of aromaticity. The fact that this method allows for the transformation of flat arenes into a diverse set of C(sp³)-enriched three-dimensional structures clearly underscores the synthetic power of the dearomatization approach.

This strategy of using ubiquitous heteroaromatics to access complex molecular architectures through photochemical dearomatizations can also be applied in a target-oriented setting, as demonstrated by Crimmins' total synthesis of ginkgolide B (**Scheme 2.26**) [53]. Intramolecular [2+2] photocycloaddition of cyclopentenone to furan enabled quick assembly of a polycyclic system with established stereochemistries at two vicinal quaternary chiral centers.



Scheme 2.26

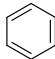
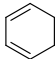
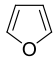
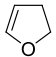
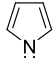
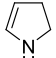
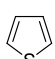
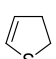
In another illustrative example, Sieburth and co-workers showed that heteroarene photocycloadditions with [4+4] topology can be utilized for the construction of natural-like scaffolds (**Scheme 2.27**) [54]. The photoinduced reaction between the 2-pyridone and the furan moieties furnished product **2.92** with four new stereogenic centers, which was then transformed into the complex triquinane model system **2.93**.



Scheme 2.27

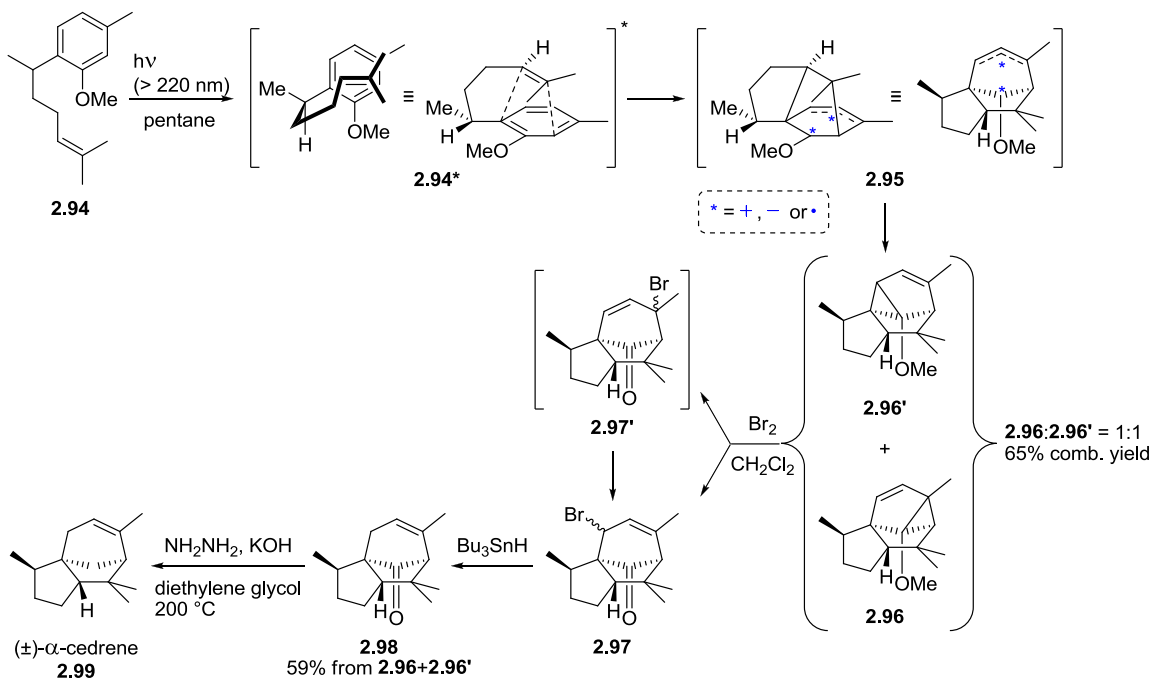
Compared to most heterocyclic arenes, benzene has a higher degree of aromaticity: its hydrogenation to 1,3-cyclohexadiene is endothermic, whereas furan, pyrrole and thiophene possess negative enthalpies of monohydrogenation (**Table 2.4**) [55]. However, the ability of light to deposit substantial amount of energy into reactants leads to the production of highly reactive electronically excited states; and therefore, unlocks the opportunities to involve benzenoid systems in the dearomative photocycloadditions.

Table 2.4: Enthalpies of Hydrogenations for Benzene, Furan, Pyrrole and Thiophene
(Adapted with permission from ref. [55]; Copyright © 2007, American Chemical Society)

A	B	$\Delta H(\mathbf{A} \rightarrow \mathbf{B}), \text{kJ} \cdot \text{mol}^{-1}$
		21.65 ± 1.13
		-37.55 ± 0.41
		-4.90 ± 1.30
		-24.30 ± 2.30

The most widely utilized mode of benzene photodearomatization is [3+2] or *meta* cycloaddition. Since its discovery in 1966 [56, 57], this reaction found multiple applications in concise construction of fused cyclopentane units in natural products [58, 59]. A classic example illustrating the power of this method is Wender's synthetic campaign towards a series of sesquiterpenes: (\pm)- α -cedrene [60], (\pm)-isocomene [61] and (\pm)-silphinene [62]. For instance, irradiation of easily accessible compound **2.94** quickly delivered the structural core of α -cedrene (**Scheme 2.28**) [60]. The observed photochemical reactivity of **2.94** was rationalized by the formation of singlet-state intramolecular *exo* exciplex **2.94*** resembling the stable conformation of *cis*-bicyclo[3.3.0] octane, where C-2 methyl assumes less sterically hindered β -orientation, and methoxy group stabilizes radical/cationic center [11] developing a radical at the adjacent carbon during the cycloaddition. Remarkably, the lack of selectivity in the cyclopropane ring formation was compensated by the subsequent convergence of both isomers **2.96'** and **2.96** into a single bromination product, the more

stable secondary allyl bromide **2.97**. Racemic α -cedrene **2.99** was obtained in just two additional steps, reductive debromination and Wolff–Kishner reduction of the carbonyl group.

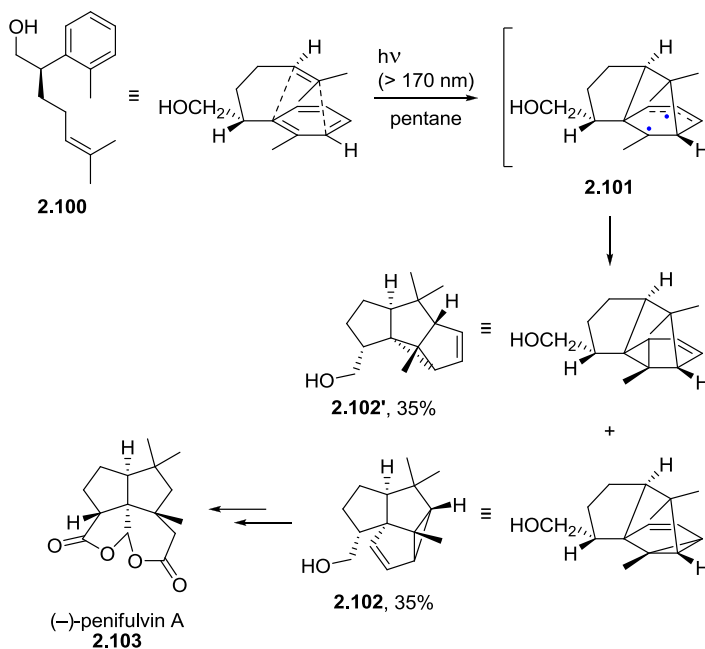


Scheme 2.28

The more recent elegant example of employing [3+2] photocycloaddition to benzene as a shortcut toward a complex natural target is Mulzer's enantioselective synthesis of (–)-penifulvin A (**Scheme 2.29**) [63]. Photoinduced cyclization of the chiral precursor **2.100** yielded equimolar mixture of enantiopure cyclopropane-fused triquinanes **2.102** and **2.102'**. The authors proposed that the substrate **2.100** adapts essentially the same geometry² that was previously suggested by Wender for the analogous substrate **2.94** upon excitation (**Scheme 2.28**), avoiding 1,3-allylic strain between methyl and

² It was implicitly specified that this conformation is achieved in ground state (as opposed to exciplex formation suggested by Wender).

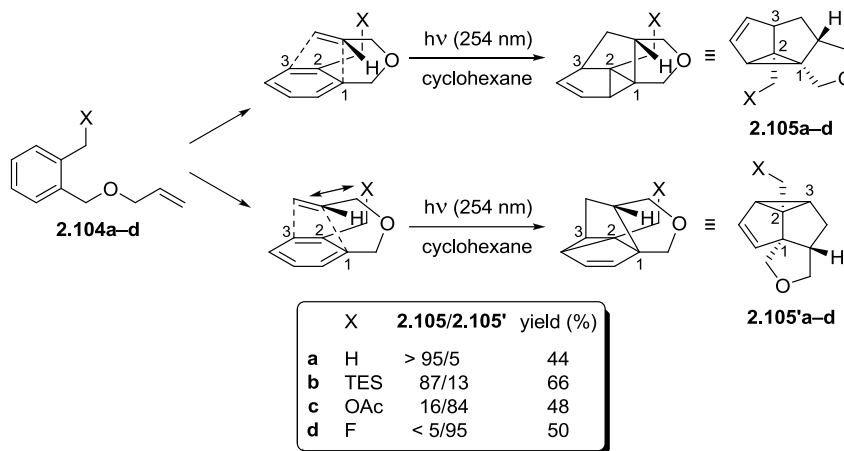
hydroxymethyl groups. The angular product **2.102** was chromatographically separated from the linear isomer **2.102'** and then converted into the desired (–)-penifulvin A **2.103** in four straightforward steps.



Scheme 2.29

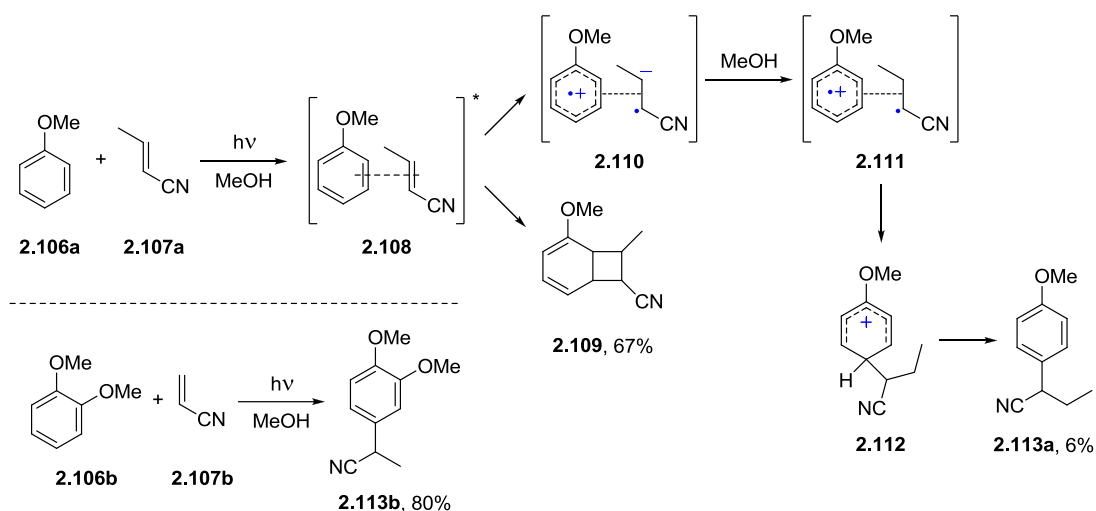
The problem of low regioselectivity at the cyclopropane construction step was addressed in the study by Bach and co-workers [64]. Their crucial finding is that the preference for linear or angular product is strongly influenced by the nature of the X group in the CH_2X substituent located at the *ortho* position relative to the tethered alkene (**Scheme 2.30**). It was postulated that substrates with a three-atom methyloxymethyl tether between arene and olefin (**2.104a–d**) typically adopt a conformation where the internal alkenic carbon is in a close proximity to the aromatic C1. Therefore, the bond-forming event starts occurring earlier at C1 rather than at C3; consequently, C1 acquires significant amount of sp^3 -hybridization before C3 and thus has a stronger preference for being a part of cyclopropane ring, which eventually leads to the linear isomer (**2.105a–d**).

In accordance with this hypothesis, the opposite situation, when arene begins to form a C–C bond with C3 first, favors the formation of angular product (**2.105'a–d**). This reversal in the regioselectivity is achieved in the presence of heteroatomic functions introducing electrostatic repulsions between lone pairs on X and alkene π density; and therefore, forcing the terminal olefinic carbon to occupy the position near C3.



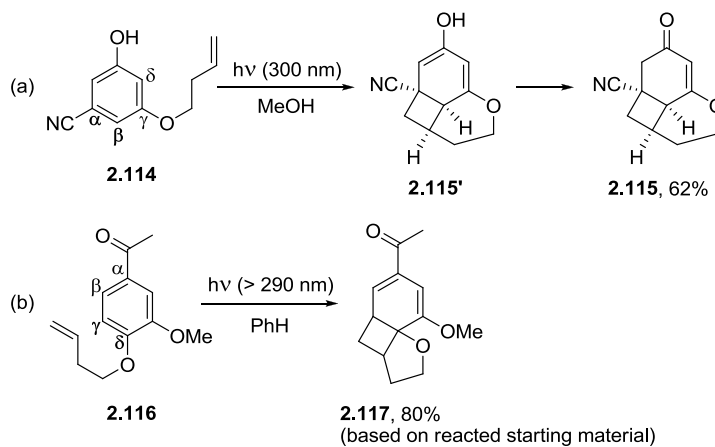
Scheme 2.30

[2+2] or *ortho* cycloaddition to benzene aromatics, which was first reported in 1950s [65], found much smaller number of synthetic applications compared to [3+2] reactions. The rare example of an intermolecular [2+2] process is the addition of an electron-poor crotonitrile **2.107a** to an electron-rich anisole **2.106a** resulting in the cyclohexadiene-fused cyclobutane **2.109** (Scheme 2.31) [66]. The reaction is proposed to proceed via singlet-state exciplex **2.108** that can also undergo electron transfer from an aromatic system to an olefin followed by abstraction of a proton from the solvent, leading to a substitution product **2.113a**. This competing process becomes predominant for more easily oxidizable dimethoxy-functionalized benzenes (e.g. **2.106b**) and alkenes with higher electron affinity (such as acrylonitrile **2.107b**).



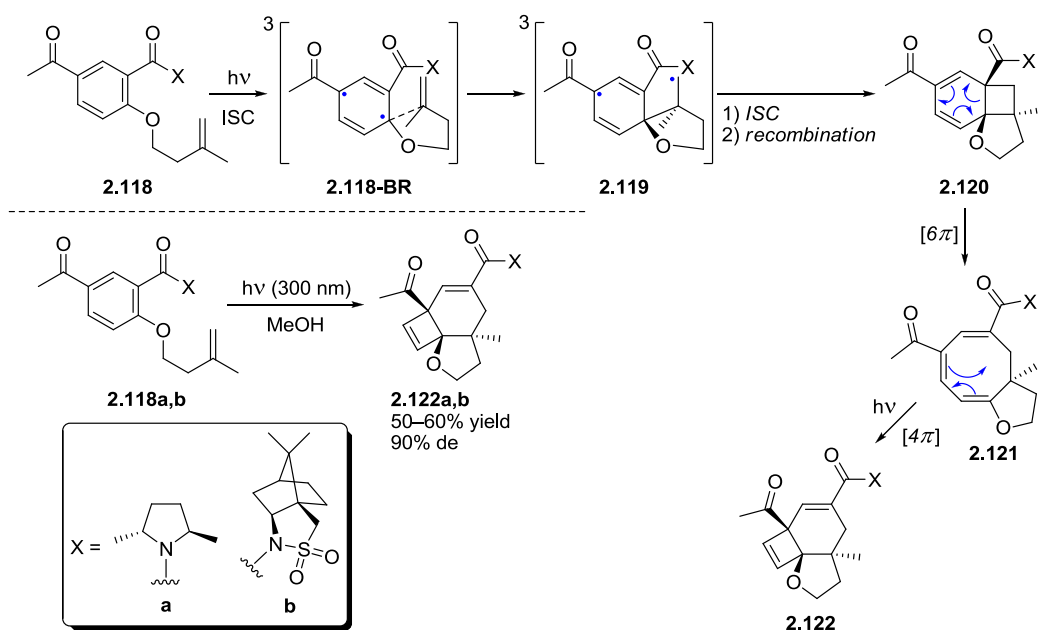
Scheme 2.31

Intramolecular *ortho* photocycloaddition to benzene is also known, yet the preparative examples of this transformation are scarce [67-69]. These reactions are reminiscent of [2+2] additions of alkenes to electronically excited enones [11], since they occur from $^3(\pi,\pi^*)$ state of arene [67] and require the presence of electron-withdrawing groups, such as acetyl and cyano, that direct the addition to either α,β - or γ,δ -positions. For instance, photolysis of benzonitrile **2.114** yields the α,β -adduct **2.115** (Scheme 2.32, reaction a) [68], whereas acetophenone **2.116** regioselectively cyclizes at γ and δ centers (Scheme 2.32, reaction b) [70].



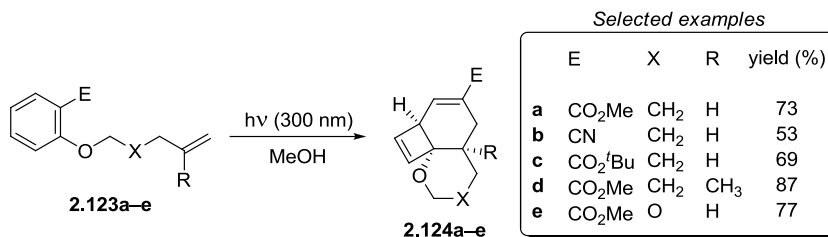
Scheme 2.32

Asymmetric dearomatization cascade, initiated by *ortho* cycloaddition, was reported by Wagner's group [71]. 5-Acetylsalicylic acid derivative **2.118** outfitted with chiral auxiliary at the amide function undergoes photoinduced stepwise [2+2] reaction, followed by a series of electrocyclic disrotatory transformations: thermal [6 π] ring opening of intermediate **2.120** to cyclooctatriene **2.121** and [4 π] photocyclization to cyclobutene **2.122** (Scheme 2.33). The authors noted that the stereocontrol is achieved at the formation of the biradical **2.119** but did not suggest a well-defined model explaining the outstanding diastereoselectivity.



Scheme 2.33

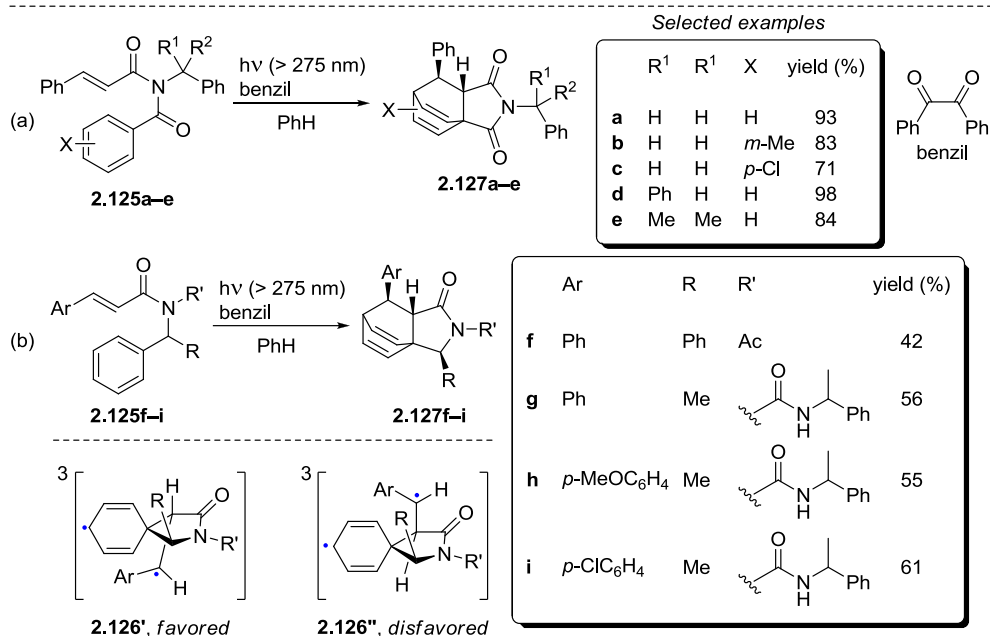
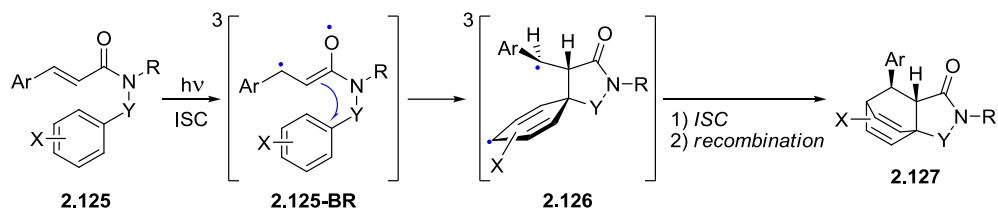
Bach has recently developed a practical synthetic method based on the same sequence of events occurring in “one pot” (Scheme 2.34) [69]. A number of functionalized salicylates with extended four-atom linkers between arene and alkene moieties were smoothly converted into complex tricycles possessing cyclobutachromene scaffold with high yields.



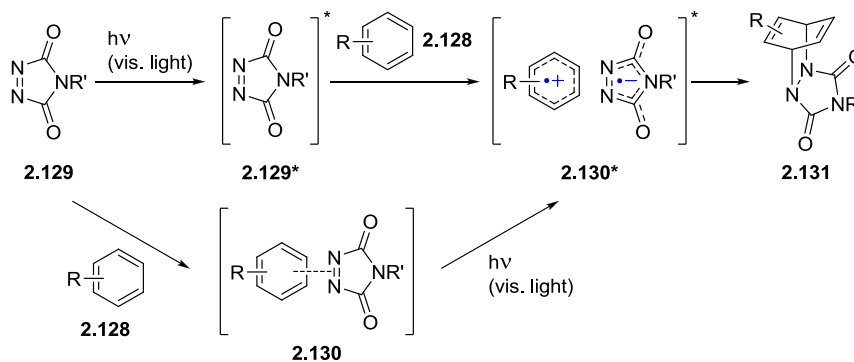
Scheme 2.34

Besides light-driven [3+2] and [2+2] processes, [4+2] or *para* cycloadditions involving benzenoid systems are also feasible [72-75]. For instance, such reactivity was observed for *N*-benzoyl- and *N*-benzyl-substituted cinnamamides (**2.125**, **Scheme 2.35**) [72]. Upon irradiation, these precursors efficiently transform into various bicyclo[2.2.2]-octadienes fused with succinimide (**2.127a–e**) and butyrolactam rings (**2.127f–i**). Given that this reaction occurs only in the presence of triplet sensitizer benzil, the stepwise radical addition mechanism was proposed. The complete diastereoselectivity was rationalized by the conformation of spiro-biradical **2.126** with an *anti* relationship between phenyl and amide carbonyl groups. Furthermore, for the substrates with α -substituted benzyl group the authors suggested that the reaction proceeds via the more favorable intermediate **2.126'**, where repulsions between R' and benzyl substituents in the pyrrolidinone ring are avoided.

Sarlah's group has recently developed a powerful synthetic methodology based on [4+2] photocycloadditions of benzene aromatics **2.128** to *N*-substituted 1,2,4-triazoline-3,5-diones **2.129** (**Scheme 2.36**) [75]. This reaction is enabled by visible light irradiation producing electronically excited arenophile **2.129***, which interacts with the ground-state arene **2.128** and leads to the formation of charge-transfer exciplex (**2.130***) collapsing



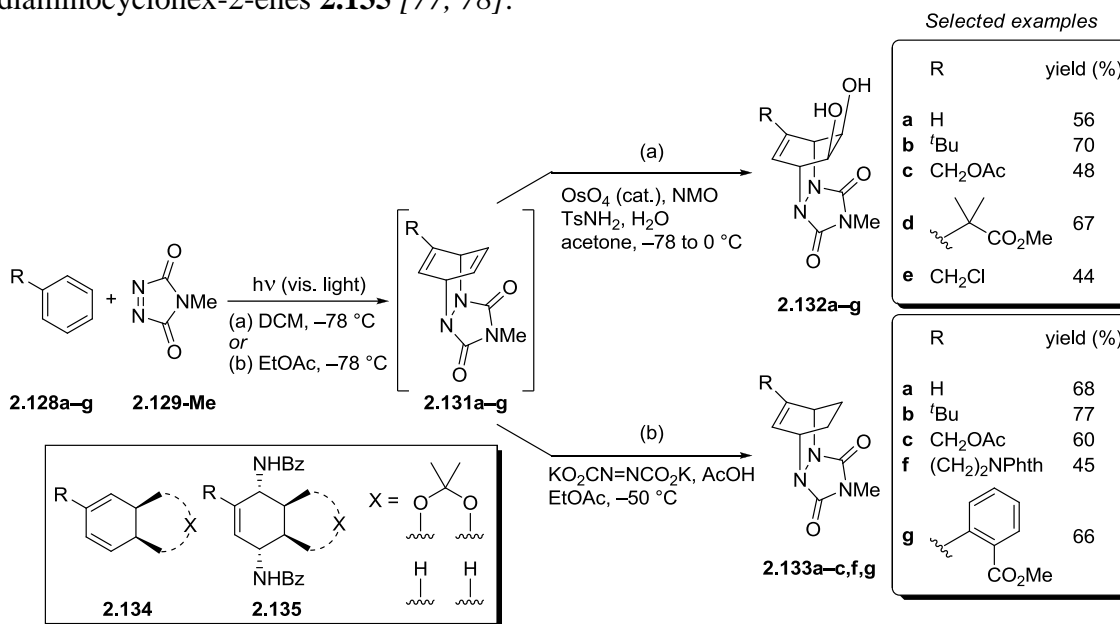
Scheme 2.35



Scheme 2.36

into the product **2.131**; alternatively, the exciplex **2.130*** can be generated by direct excitation of the ground-state complex **2.130** [76].

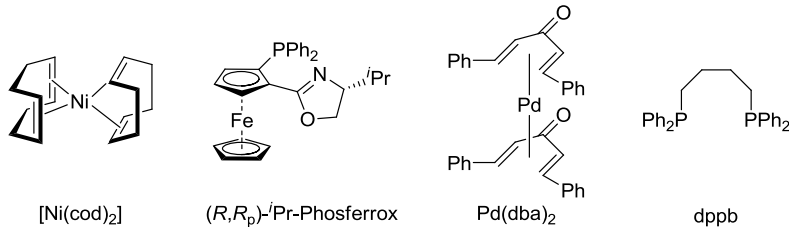
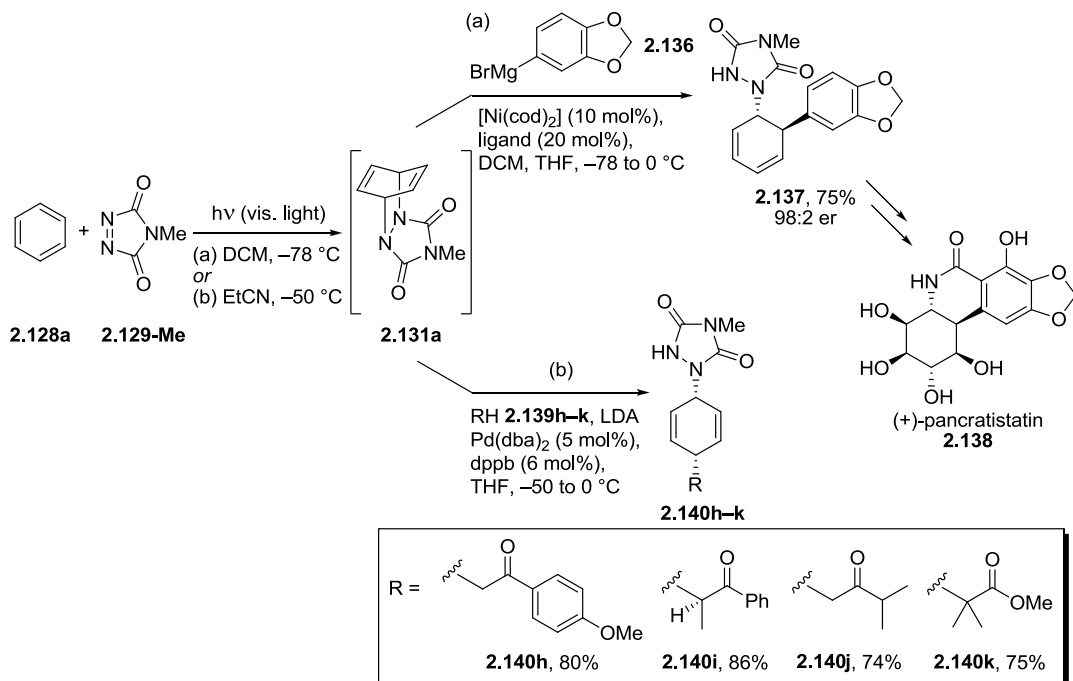
Since the resulting diazabicyclo[2.2.2]octadienes undergo facile retrocycloaddition to the starting materials above $-20\text{ }^{\circ}\text{C}$, these [4+2] processes are carried out at low temperatures and are immediately followed by post-photochemical reactions that (i) convert labile cycloadducts into stable compounds and (ii) highlight the synthetic utility of dearomatized products. Examples of such transformations include Upjohn dihydroxylation (**Scheme 2.37**, reaction a) [77] and reduction of alkene with *in situ* generated diimide (**Scheme 2.37**, reaction b) [78]. The products **2.132** and **2.133** can be further transformed into functionalized cyclohexadienes **2.134** and *syn*-1,4-diaminocyclohex-2-enes **2.135** [77, 78].



Scheme 2.37

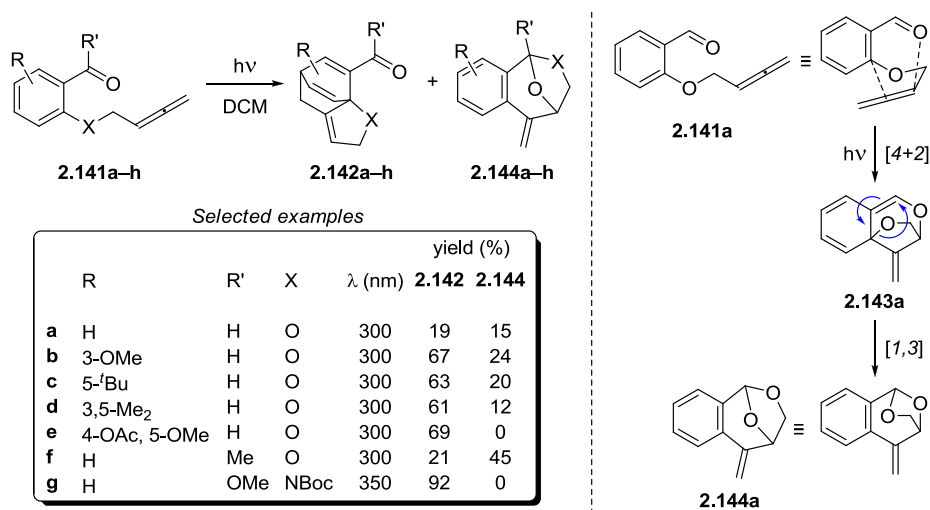
Importantly, it was also demonstrated that urazole-outfitted [4+2] adducts are useful synthons for C–C bond-forming processes, which can be utilized for the assembly of natural products. For instance, dearomatized compound **2.131a** was engaged in diastereo- and enantioselective coupling reaction with aryl Grignard **2.136**, promoted by nickel(0)-based catalyst $\text{Ni}(\text{cod})_2$ in conjunction with chiral ligand (*R,R*)-*i*-Pr-Phosferrox (**Scheme**

2.38, reaction a) [79]. This transformation delivered enantiopure *anti*-1,2-carboaminated product **2.137**, a precursor for the alkaloid (+)-pancratistatin **2.138** obtained after seven additional steps. In another example, a different carboamination topology was achieved: palladium-catalyzed nucleophilic allylic substitutions with lithium enolates afforded *syn*-1,4-substituted derivatives **2.140** (**Scheme 2.38**, reaction b) [80]. These remarkable dearomative transformations allowed for the conversion of benzene, a readily available feedstock chemical, into functionalized cyclohexadienes with two stereocenters.



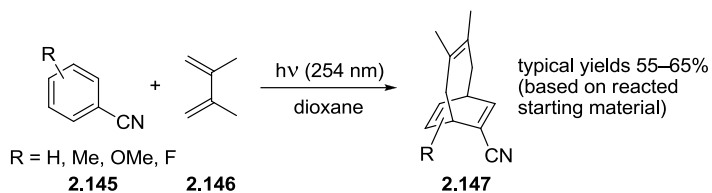
Scheme 2.38

[4+2] Photocycloaddition can also be initiated by the excitation of an aromatic system, as demonstrated by Bochet and co-workers [73, 74]. They discovered that benzene rings equipped with electron-withdrawing chromophore groups are capable of reacting with tethered allenes in a [4+2] fashion, generating complex bicyclo[2.2.2]-octadienes (**2.142**, **Scheme 2.39**) [74]. For benzaldehydes and ketones, significant amounts of benzoxepine side-products (**2.144**) were often obtained; it is conceivable that such compounds result from an alternative [4+2] pathway involving an enone-like fragment followed by [1,3]-sigmatropic migration of an oxymethylene bridge [73].



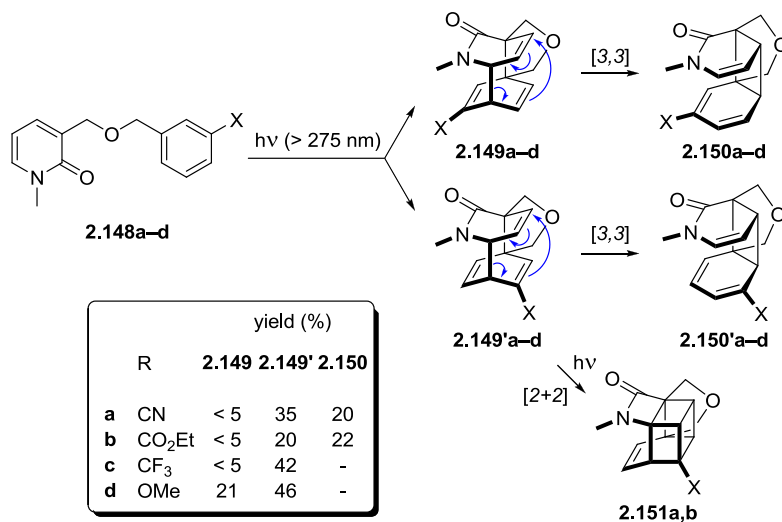
Scheme 2.39

Aside from alkenes, certain dienes can play a role of a second component in *para* photocycloadditions to benzene and lead to [4+4] products; however, the systems reacting through this topology are extremely rare [81-83]. This process was first documented by Okumura for benzonitrile and 2,3-dimethyl-1,3-butadiene (**2.146**) [81]; Gilbert later extended the scope of the reaction on various methyl-, methoxy- and fluoro-substituted benzonitriles **2.145** that afforded functionalized bicyclo[4.2.2]deca-3,7,9-trienes **2.147** (**Scheme 2.40**) [82].



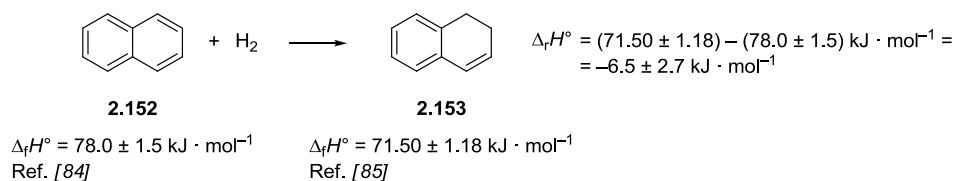
Scheme 2.40

A unique case of intramolecular [4+4] was observed between benzenoid aromatics and 2-pyridone pendants (**Scheme 2.41**) [83]. The resulting cycloadducts **2.149** and **2.149'** were not isolated, because they contain an unstable 1,5-hexadiene moiety that is prone to thermal [3,3] Cope rearrangement (**2.150** and **2.150'**) and a secondary photochemical [2+2] reaction (**2.151**).



Scheme 2.41

When benzene ring is a part of a polycyclic aromatic structure, its dearomatization is more facile. For instance, monohydrogenation of naphthalene is predicted to be exothermic according to the calculation from the standard molar enthalpies of formation [84, 85] (**Scheme 2.42**).



Scheme 2.42

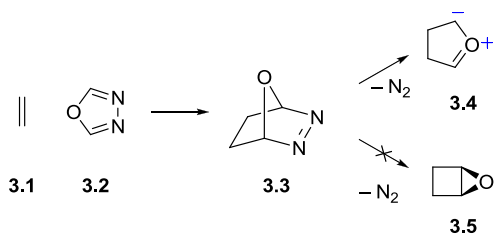
Consequently, dearomative photocycloadditions that involve polyaromatics, such as naphthalene [86-92], anthracene [89, 92-94] and phenanthrene [95] have been described. However, since these systems are not studied in the present work, their reactions are not covered in this review.

Besides photoinduced dearomatizations, a number of ground-state transformations that convert arenes into C(sp³)-containing cycles are known: typical examples include Birch reduction [96], hydrogenation [97, 98], oxidation of phenols [99-102] and transition metal-assisted reactions [103-106]. While all these processes are interesting, they are not immediately relevant to this work, and therefore are also not discussed here; curious reader is advised to consult Porco's review of the synthetic applications of these reactions [107].

Chapter Three: Results and Discussion

Project 1: Photogenerated Diketopiperazine-Spiro-Oxiranes as Versatile Synthons for Accessing Diverse Polyheterocyclic Scaffolds [108]

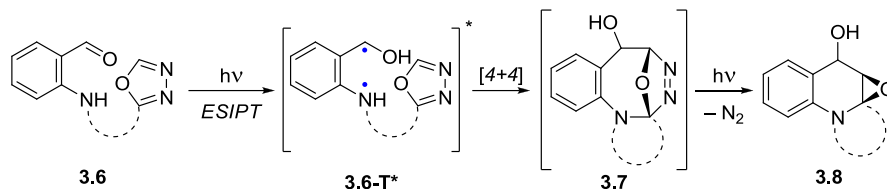
Thermolytic or photochemical extrusion of molecular nitrogen from substituted 1,3,4-oxadiazolines gives access to functionalized epoxides [109-112], which are stable, but at the same time reactive synthons used in a multitude of useful transformations. This mode of reactivity, however, has not been known for oxadiazolines that are part of bicycles, presumably because the main route towards these systems is based on hetero-Diels–Alder chemistry involving alkenes **3.1** and 1,3,4-oxadiazoles **3.2** (Scheme 3.1). These reactions afford oxadiazabicyclo[2.2.1]heptane scaffolds **3.3** that upon the loss of dinitrogen produce carbonyl ylides **3.4** – highly reactive zwitterionic intermediates utilized by Boger in the powerful tandem [4+2]/[3+2]-based methodology [113-115]. Intramolecular formation of a C–C bond that would lead to oxiranes (**3.5**) is not feasible in this case, because it would impose substantial strain on the bridgehead carbon atoms.



Scheme 3.1

We envisioned that the likelihood of producing bicyclic epoxides would increase if the bridge between two oxadiazoline carbons is extended, making the overall framework more flexible. Such systems could be obtained by dearomative intramolecular [4+4]

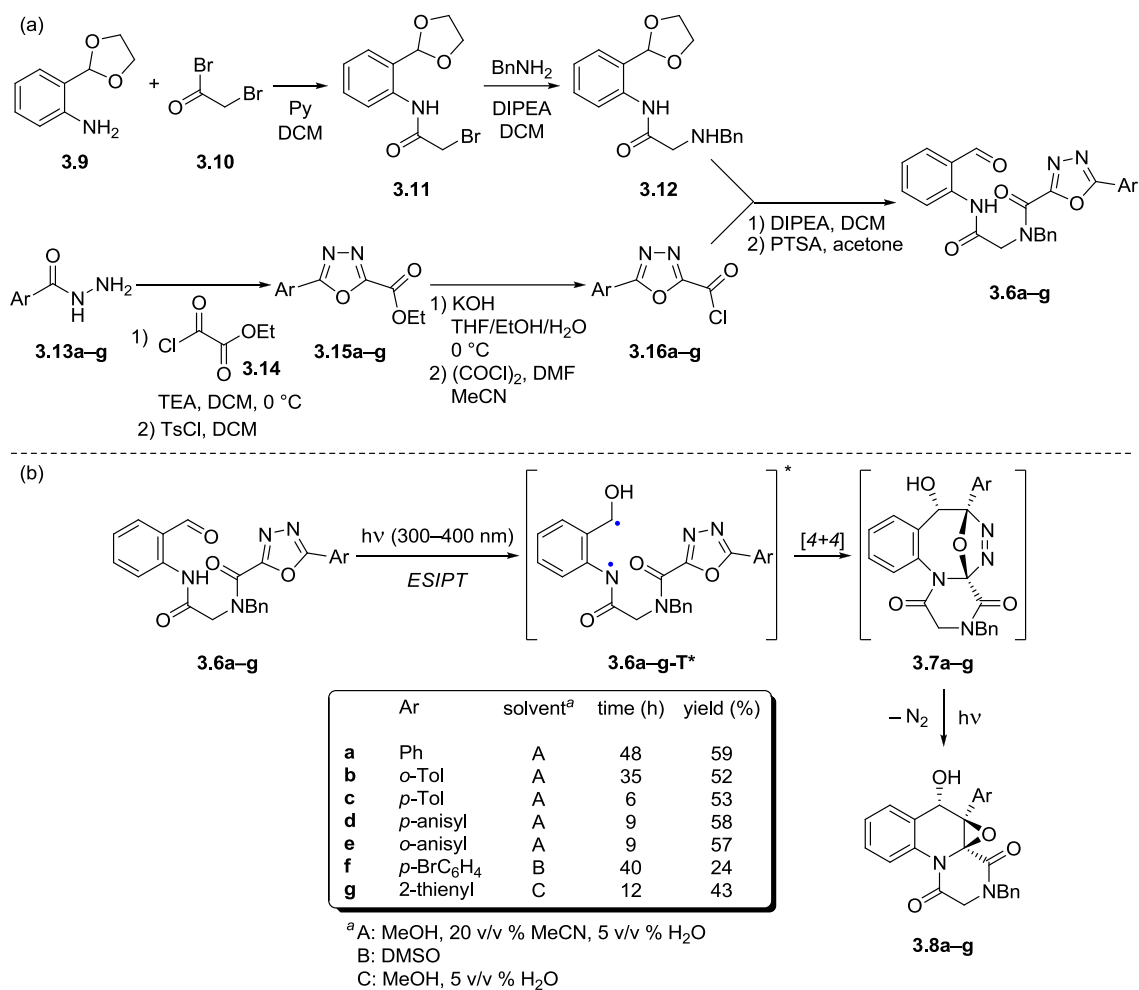
cycloaddition of ESIPT-generated *o*-azaxylylenes to oxadiazoles (**Scheme 3.2**), in a way similar to the previously described formation of *O*-bridged benzazocines from furan-containing precursors [7]. Photoirradiation required to initiate this process could also input enough energy into the primary oxadiazoline **3.7** to trigger the extrusion of dinitrogen, making the entire conversion of oxadiazole **3.6** into epoxide **3.8** “one pot”.



Scheme 3.2

To test the hypothesis, an *o*-amino-benzaldehyde-based precursor **3.6a** was assembled from simple building blocks by peptoid synthesis-inspired methods (**Scheme 3.3**, a). Initially, the required oxadiazole-containing fragment **3.16a** was prepared by tosyl chloride-mediated bis-hydrazide cyclodehydration [116] followed by ester hydrolysis. The substrate **3.6a** was then obtained by a series of high-yielding reactions: (i) acylation of the protected *o*-aminobenzaldehyde **3.9** with bromoacetyl bromide **3.10**, (ii) subsequent coupling of the resulting primary alkyl bromide **3.11** with benzylamine, (iii) acylation of the secondary amine **3.12** with 5-phenyl-1,3,4-oxadiazole-2-carbonyl chloride **3.16a** and (iv) acid-promoted aldehyde deprotection. The obtained photoprecursor **3.6a** was subjected to photolysis with Rayonet RPR-3500 lamps (broadband emission centered at 350 nm) that induced the desired [4+4] cycloaddition/oxirane formation cascade (**Scheme 3.3**, b). The scope of this methodology was extended on a range of substrates with various aryl substituents in an oxadiazole

ring, which after irradiation afforded complex epoxide-fused 2,5-diketo-piperazinoquinolinols (**3.8a–g**) as single diastereomers in good yields.³

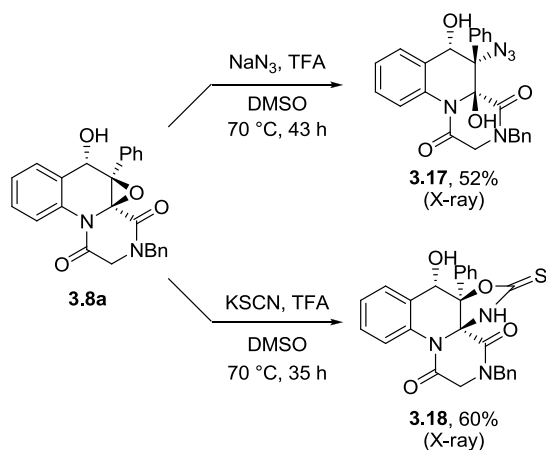


Scheme 3.3

Given the high reactivity of epoxides towards a wide array of nucleophiles, the oxirane moiety in the photoproduct represents an attractive handle for further so-called *post-photochemical modifications* that provide opportunity to increase the overall structure complexity and to diversify a collection of final compounds. Therefore, we

³ The original discovery of the photochemical process belongs to the collaborator Dr. N. N. Bhuvan Kumar, who also optimized conditions for the preparation and irradiation of the photoprecursors and investigated the reaction scope (except *o*-tolyl example **b**).

explored epoxide ring opening in **3.8a** with azide and thiocyanate under acidic conditions (**Scheme 3.4**). Interestingly, these reactions led to different regio- and diastereochemical outcomes, as revealed by X-ray crystallography of the isolated products: azide in adduct **3.17** is located at the position 3 of quinolinol and is *anti* to the former epoxide oxygen, whereas the structure of **3.18** shows the attachment of thiocyanate at C-2 and is indicative of *syn* addition of the nucleophile.

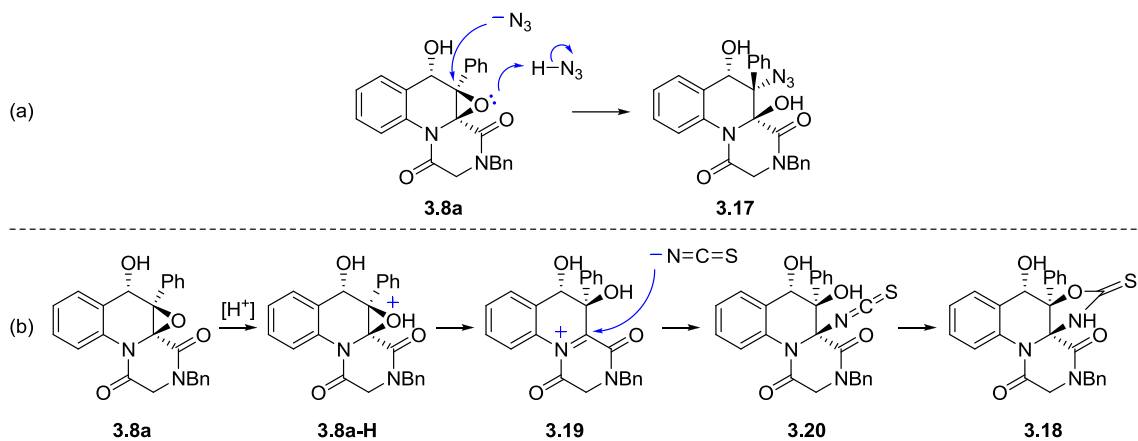


Scheme 3.4

To rationalize this discrepancy, we suggested the following mechanistic proposals:

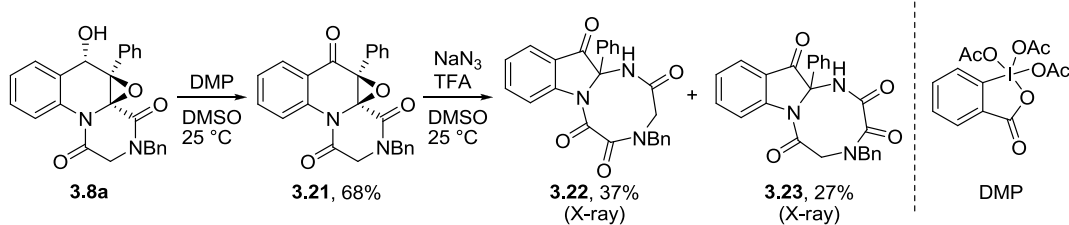
- The relatively weak acid HN_3 ($\text{p}K_a = 4.7$ [117]) is involved in *general acid catalysis* of the azide addition that proceeds via S_N2 mechanism, with the nucleophile attacking from the face opposite to the epoxide ring and consequently leading to the *anti* product (**Scheme 3.5**, reaction a).
- In the case of thiocyanate reaction, only strong acids are present in the mixture ($\text{p}K_a$ values for HSCN and TFA are -1.85 and 0.0 , respectively [118]); therefore, *specific acid catalysis* of S_N1 reaction takes place: oxirane gets fully protonated and then cleaves with the formation of a more stable iminium (not

benzylic) cation, which is trapped by thiocyanate at the “hard” *N*-terminus in a *syn* fashion (**Scheme 3.5**, reaction b).



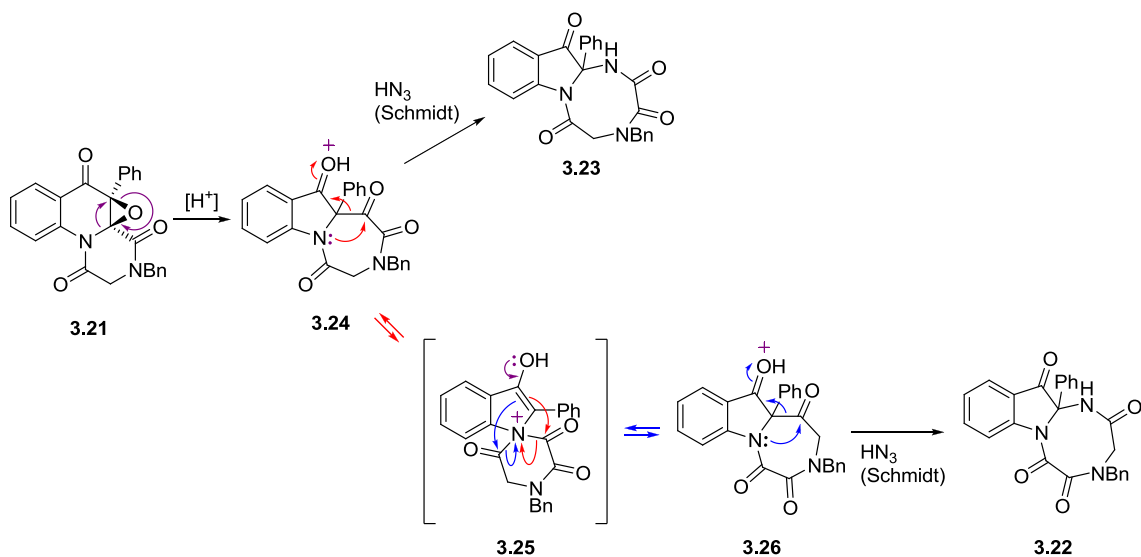
Scheme 3.5

Even though eventually we managed to obtain single crystals of **3.17** and **3.18** for X-ray analysis, which was essential for the determination of regio- and stereochemistry, our initial attempts to crystallize these compounds did not seem promising. For that reason, we decided to convert benzylic OH in **3.8a** into ketone and then run the reactions with the same nucleophiles, hoping that the final products would exhibit greater tendency for crystallization. We proceeded with oxidation of the epoxy-alcohol **3.8a** with Dess–Martin periodinane (DMP) followed by the treatment of the resulting quinolinone with NaN_3/TFA . To our surprise, instead of the anticipated ring opening, the epoxy-ketone **3.21** rearranged into triazocano-indolinones **3.22** and **3.23** (**Scheme 3.6**; the structures were established by X-ray crystallography).



Scheme 3.6

Our plausible explanation for this unusual reactivity is outlined in the **Scheme 3.7**. We proposed that the acid-catalyzed epoxide cleavage is accompanied by the shift of the quinolinol nitrogen, leading to the rearrangement of the 6/6 bicycle into the 5/7-fused system **3.24**; given that no changes were observed in the absence of NaN_3 , it is likely that this step requires nucleophilic catalysis by the azide. Subsequent Schmidt reaction converts aliphatic ketone in **3.24** into the amide, yielding **3.23**. Because the second product, triazocane **3.22**, differs from **3.23** only by the position of one carbonyl group, we believe that this isomer is formed by a similar Schmidt reaction from the intermediate **3.26**. Two benzodiazepines **3.24** and **3.26**⁴ are presumably equilibrated via reversible migrations of acyl groups occurring through the spiroammonium intermediate **3.25**.

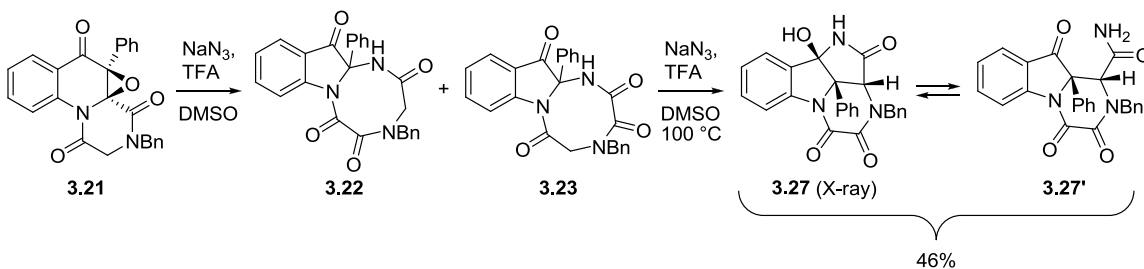


Scheme 3.7

As we were curious to see whether elevated temperature would affect the distribution of the products, we tried subjecting the keto-epoxide **3.21** to the same conditions

⁴ Intermediates **3.24** and **3.26** were not detected in the mixture, most likely due to their rapid reaction with HN_3 .

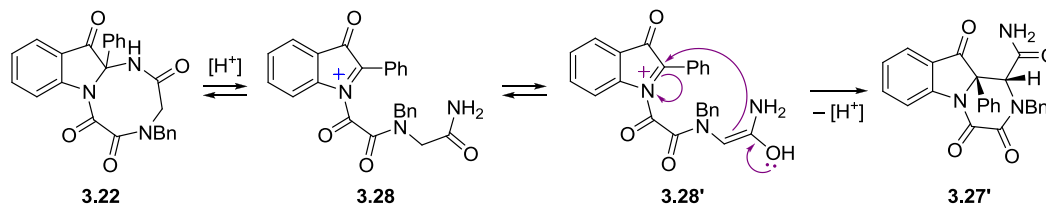
(NaN₃/TFA in DMSO) at 100 °C, and we observed the formation of two completely new compounds. Careful monitoring of the reaction by ¹H NMR showed that these products start forming after the starting material **3.21** is completely converted into the triazocanes **3.22** and **3.23**. Furthermore, the same mixture of two compounds was produced from both pure **3.22** and **3.23** after they were separately heated with sodium azide in acidic DMSO. X-ray analysis of the crystalline material obtained after a large-scale experiment revealed that there was only one secondary product, which is the 2,3-diketopiperazino-fused indolinol **3.27** (Scheme 3.8). The presence of two different sets of peaks in the NMR spectra was rationalized by the equilibrium between closed hemiaminal (**3.27**) and open keto-amide (**3.27'**) forms that takes place in solution; evidence for the formation of **3.27'** was provided by ¹³C NMR spectroscopy that revealed the keto-carbonyl peak at 195 ppm.



Scheme 3.8

The conversion of triazocanes **3.22** and **3.23** into **3.27** does not involve the addition of azide; however, no reaction occurred in the absence of NaN₃. Therefore, the azide anion conceivably plays a role of a base creating buffer solution in conjunction with TFA, which is needed to maintain pH in a certain range that is required for the transformation. This hypothesis was supported by the fact that sodium acetate, which has similar basicity, promotes the same reaction.

While the mechanism of the formation of **3.27** from the triazocane **3.23** remains unclear, the rearrangement of **3.22** presumably starts with acid-assisted opening of the triazocane ring (**Scheme 3.9**). After tautomerization of the resulting glycine amide intermediate **3.28**, the enol moiety recaptures the iminium cation in **3.28'**, furnishing the product **3.27'** as a single diastereomer.



Scheme 3.9

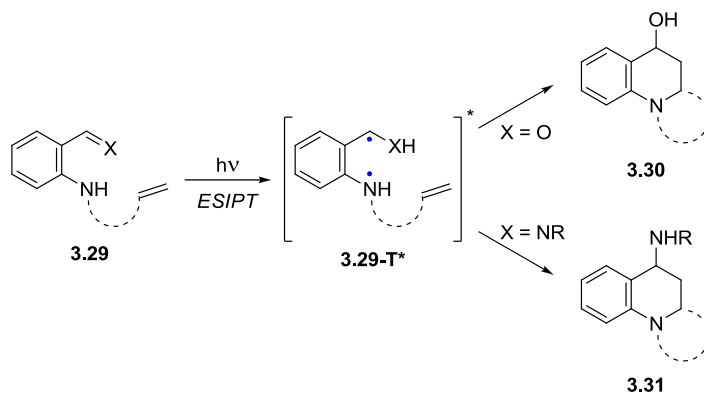
To summarize, we have shown that 1,3,4-oxadiazole is dearomatized by the intramolecular [4+4] cycloaddition to ESIPT-generated *o*-azaxylylene under mild UV irradiation conditions; this process is immediately followed by the extrusion of dinitrogen leading to the oxirane-equipped 2,5-diketopiperazino-quinolinols. Importantly, we have demonstrated that the presence of a reactive epoxide moiety in the photoproducts makes them incredibly useful synthons for further post-photochemical modifications, that enable the increase in molecular complexity and provide the access to diverse scaffolds.

Project 2: Synthesis of Complex Enantiopure Polyheterocycles by Cycloadditions of Amino-*o*-Azaxylylenes to Pyrroles [119]

Previous studies in Kutateladze's group showed that the hydroxy-*o*-azaxylylene intermediates produced by ESIPT in aromatic *o*-amidoaldehydes and *o*-amidoketones can be efficiently engaged into the intramolecular cycloadditions. These reactions generate

complex polyheterocyclic scaffolds containing quinolinol cores with OH group at the benzylic position (**Scheme 3.10**, X = O) [7].

It was envisioned that the introduction of an amino functionality into these products would be synthetically appealing, since it would create an additional diversity input and therefore would allow for the expansion of the collection of molecular architectures synthesized by the azaxylylene photocycloaddition methodology. This task requires utilizing anilides that are outfitted with *ortho* functionalities containing proximal C–N double bond, such as imines or nitrogenated heterocycles (examples of ESIPT-reactive systems with C=N proton acceptors can be found in the “Literature Review” chapter). Upon photoexcitation, these starting materials are expected to tautomerize into the amino-*o*-azaxylylenes that could react with unsaturated pendants (**Scheme 3.10**, X = NR).



Scheme 3.10

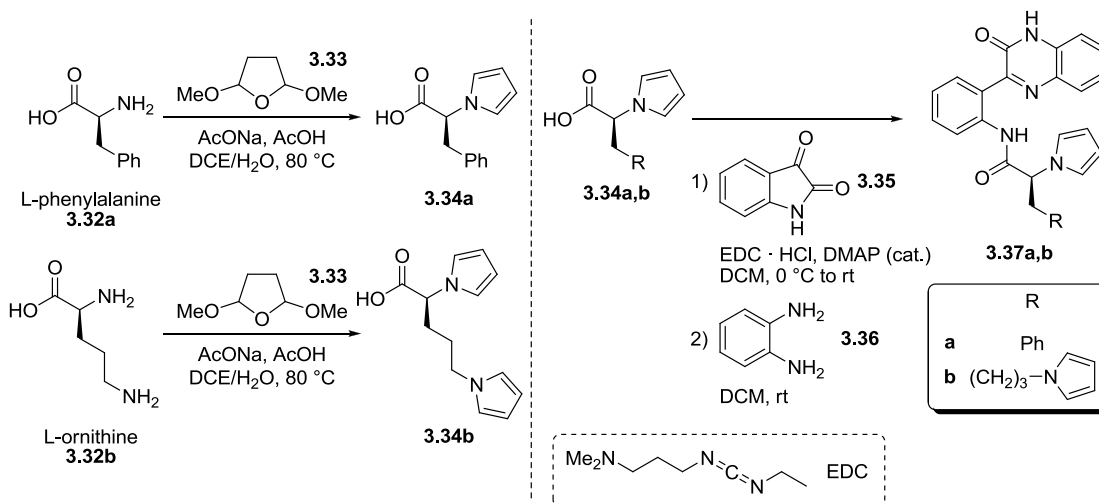
We chose to install quinoxalinone as a proton-accepting moiety into our photoprecursors for several reasons:

- The resulting *o*-azaxylylenes would be equipped with an additional carbonyl group, which could accelerate the cycloaddition by making these

intermediates more electron-deficient; and therefore, more reactive towards electron-rich heterocycles;

- Furthermore, there is an opportunity to amplify this electron-depleting effect by using oxophilic Lewis acids that could enhance the polarization of the azaxylenes by binding to the carbonyl oxygen;
- Quinoxalinone-containing photoprecursors can be easily synthesized in a modular fashion by the ring opening of isatins with *o*-phenylenediamine [120].

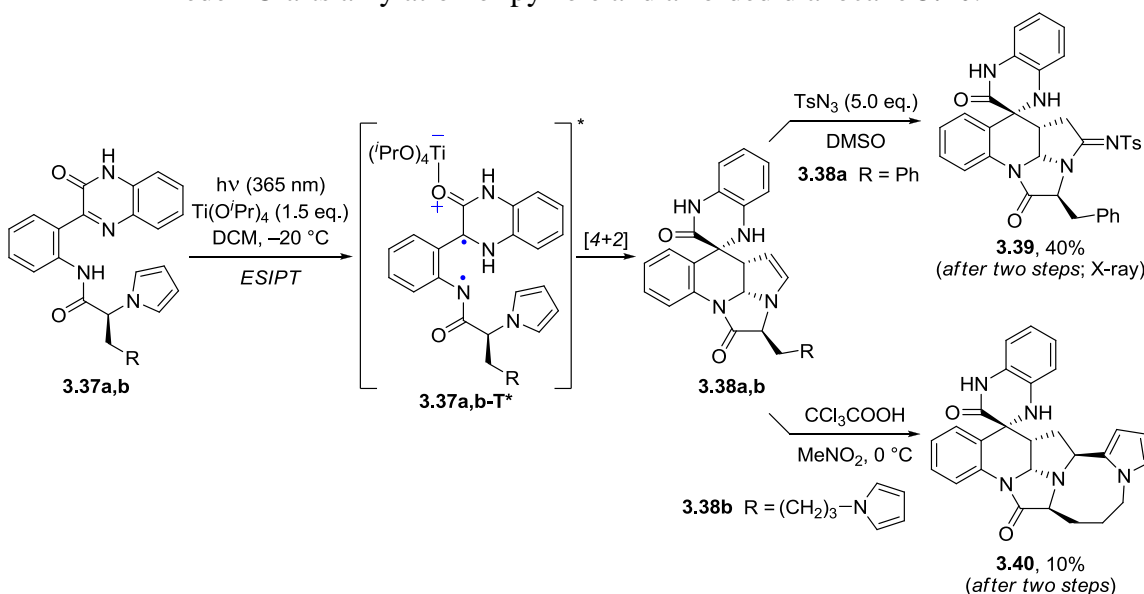
To prepare the required substrates, we first installed pyrrole rings in the chiral aminoacids, L-phenylalanine (**3.32a**) and L-ornithine (**3.32b**) by Paal–Knorr reaction (**Scheme 3.11**). Isatin **3.35** was then coupled with acids **3.34a** and **3.34b** using carbodiimide reagent EDC hydrochloride, followed by the ring opening with *o*-phenylenediamine **3.36**, which afforded enantiopure photoprecursors **3.37a** and **3.37b**.



Scheme 3.11

Irradiation of **3.37a** and **3.37b** with 365 nm UV LEDs⁵ in the presence of titanium(IV) isopropoxide⁶ induced the desired dearomative [4+2] cycloaddition of the Ti-bound *o*-azaxylylenes (**3.37a-T*** and **3.37b-T***) to pyrrole pendants, leading to the pyrrolines **3.38a** and **3.38b**; formation of single diastereomers was observed by ¹H NMR in both cases (**Scheme 3.12**). In order to “fix” the labile enamine fragment and to increase the structure complexity, the primary photoproducts were further modified by the post-photochemical transformations:

- **3.38a** was subjected to 1,3-dipolar cycloaddition with *p*-toluenesulfonyl azide, delivering sulfonylamidine **3.39** after the extrusion of nitrogen;
- **3.38b** was treated with trichloroacetic acid that promoted intramolecular Friedel–Crafts alkylation of pyrrole and afforded diazocane **3.40**.



Scheme 3.12

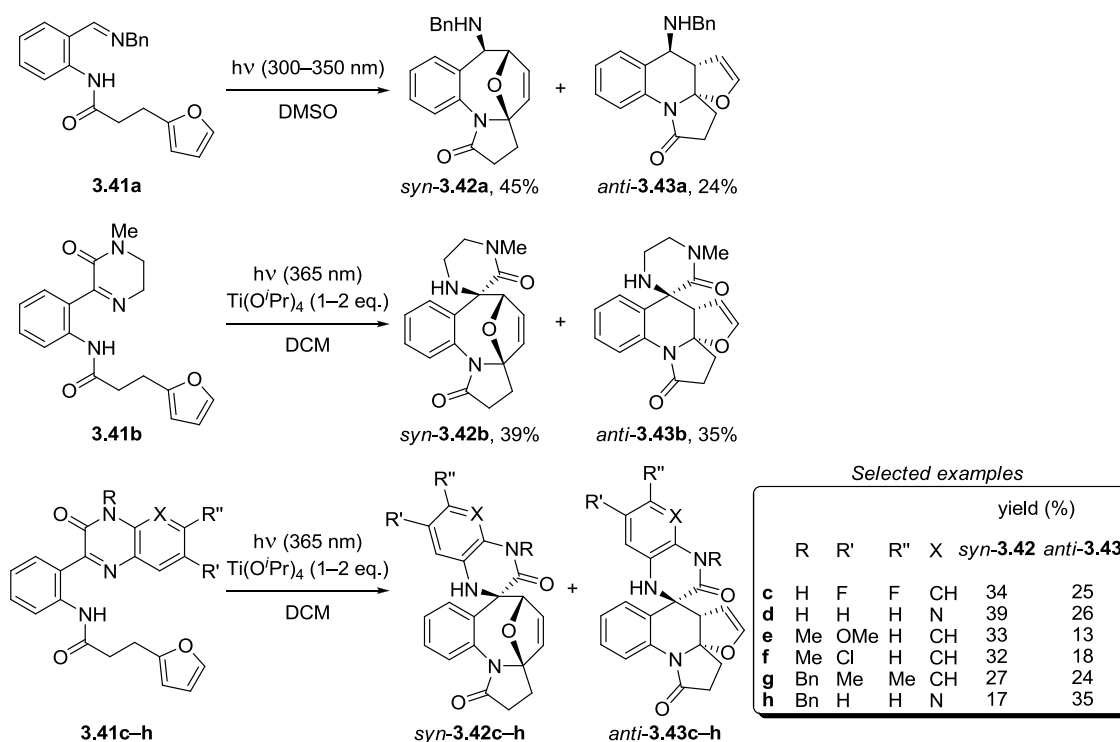
⁵ According to the data obtained by the collaborator Dr. Olga Mukhina, *o*-quinoxalinone-functionalized anilides have a broad UV absorption with a maximum at around 360 nm.

⁶ Accelerating effect of Ti-based Lewis acids on the photoreaction of similar furan-containing precursors was also discovered by Dr. O. Mukhina.

The diastereochemistry of the cycloaddition was established on the basis of X-ray crystallography of product **3.39**, which revealed *syn* relationship between the newly formed benzylic amino group and the nitrogen atom of the pyrrolidine moiety. This finding is consistent with the previously reported *syn*-selective reaction between hydroxy-*o*-azaxylylenes and pyrroles [49].

The obtained results complement those of Drs. Olga Mukhina and Teresa Cowger, who studied furan-outfitted systems bearing both acyclic and cyclic imines, as well as quinoxalinones in the photoactive cores; the representative examples are shown in

Scheme 3.13.



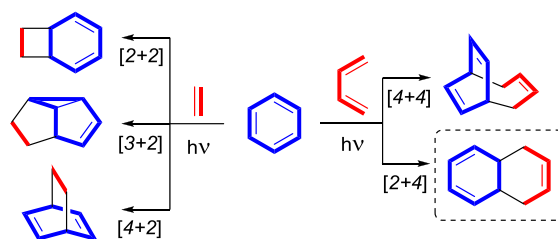
Scheme 3.13

In conclusion, it has been demonstrated that ES IPT-produced amino-*o*-azaxylylenes are capable of the intramolecular dearomative cycloadditions to electron-rich heterocyclic units, such as pyrroles. We have also shown that the reactive pyrroline moiety in the

photoproducts can be utilized for further modifications, affording even more complex structures. Even though the yields of the final compounds are modest, these sophisticated and enantiopure molecular architectures are accessed in a two-step one-pot reaction from readily available precursors.

Project 3: Dearomatization of Benzenoid Arenes with *o*-Azaxylylenes via an Unprecedented [2+4] Reaction Topology [121]

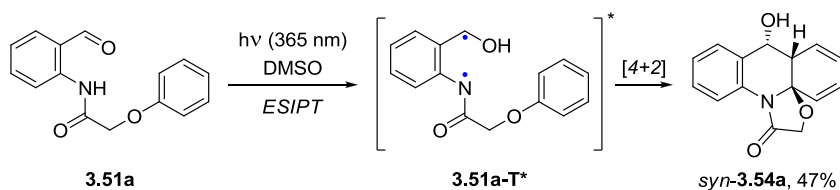
Photoinduced cycloadditions to benzene rings constitute a powerful strategy for the rapid access to a diverse set of C(sp³)-rich molecular scaffolds from ubiquitous arenes [11, 122]. Known variants of these transformations include synthetically valuable [3+2] and [4+2] reactions, as well as less frequently used [2+2] and [4+4] cycloadditions (Scheme 3.14; an overview of these processes with representative examples can be found in the “Literature Review” chapter). To the best of our knowledge, photochemical [2+4] cycloadditions, where a benzenoid arene would play a role of 2π component, have not been reported.



Scheme 3.14

We envisaged that the reaction with missing [2+4] topology could be achieved by the intramolecular cycloaddition of a phenyl group to an ESIPT-generated *o*-azaxylylene, similar to the previously described transformations involving heterocycles, such as furan, pyrrole and thiophene [7, 49]. It was proposed that the addition of the triplet azaxylylene

starts with the attack of the electrophilic *N*-centered radical on an unsaturated moiety, which explains the facile reactivity of electron-rich heteroarenes in these processes [52]. Consistent with this mechanistic hypothesis, we decided to test a donor-substituted benzenoid arene for the feasibility of the [2+4] cycloaddition. Gratifyingly, easily accessible substrate **3.51a** outfitted with the electron-rich phenoxyacetic pendant reacted in the desired manner, furnishing cyclohexadieno-quinolinol *syn*-**3.54a** upon irradiation in DMSO with 365 nm UV LEDs (Scheme 3.15).⁷

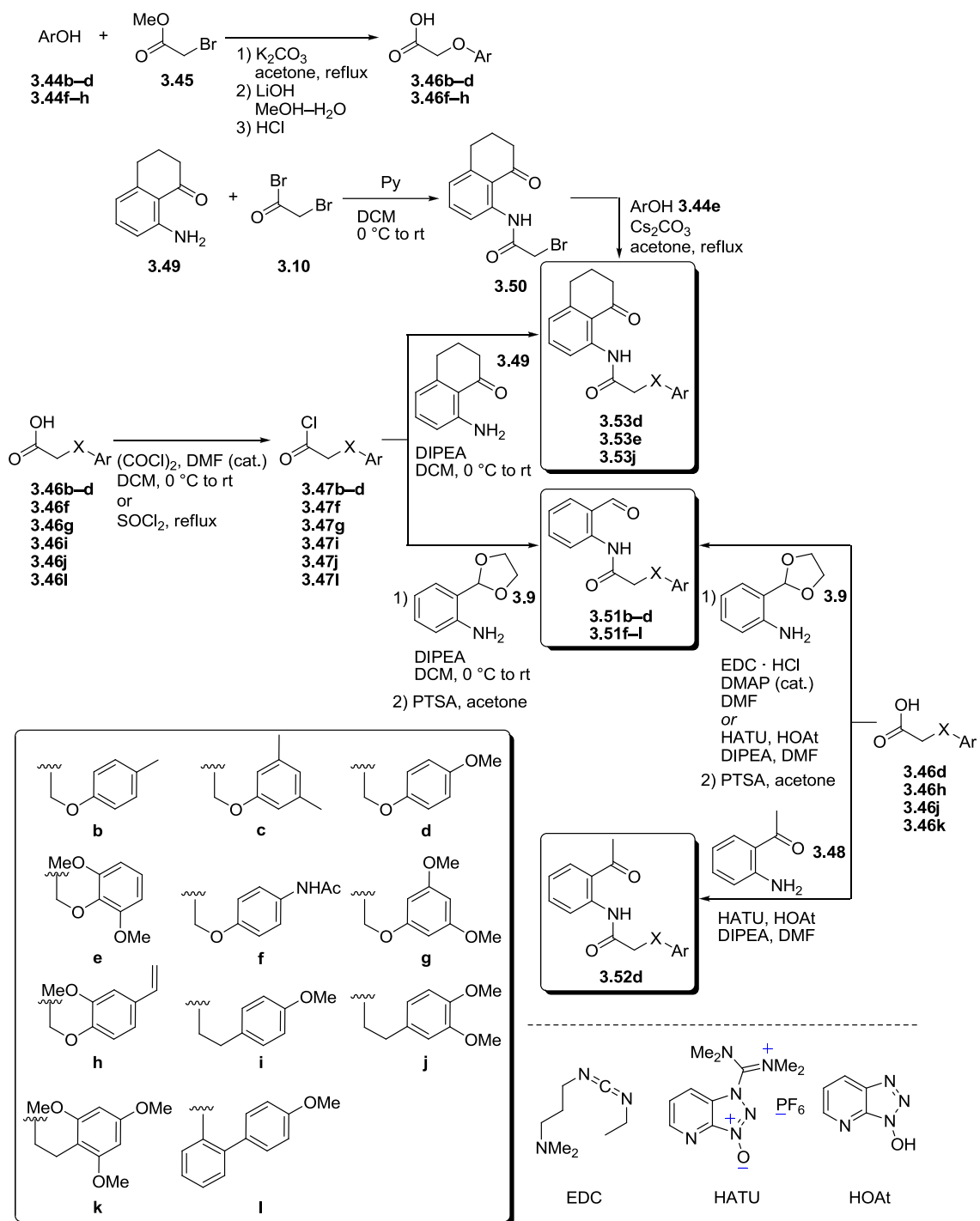


Scheme 3.15

Inspired by this initial success, we proceeded with exploring a scope of the new dearomative transformation. For this purpose, we synthesized an array of substrates based on three different photoactive cores (*o*-aminobenzaldehyde **3.51**, *o*-aminoacetophenone **3.52**, and *o*-aminotetralone **3.53**), equipped with twelve various electron-rich aromatic pendants (derivatives of aryloxyacetic- (**a–h**) and arylpropanoic- (**i–k**) acids, as well as *o*-anisylbenzoic moiety **l**), bearing methoxy- (**d, e, g–l**), methyl- (**b, c**) and acetamido-functionalized (**f**) benzene rings. The preparation of these precursors was accomplished in a modular fashion using the high-yielding methods (Scheme 3.16):

- Alkylation of phenols **3.44** with methyl bromoacetate **3.45** followed by ester hydrolysis, affording aryloxyacetic acids **3.46**;

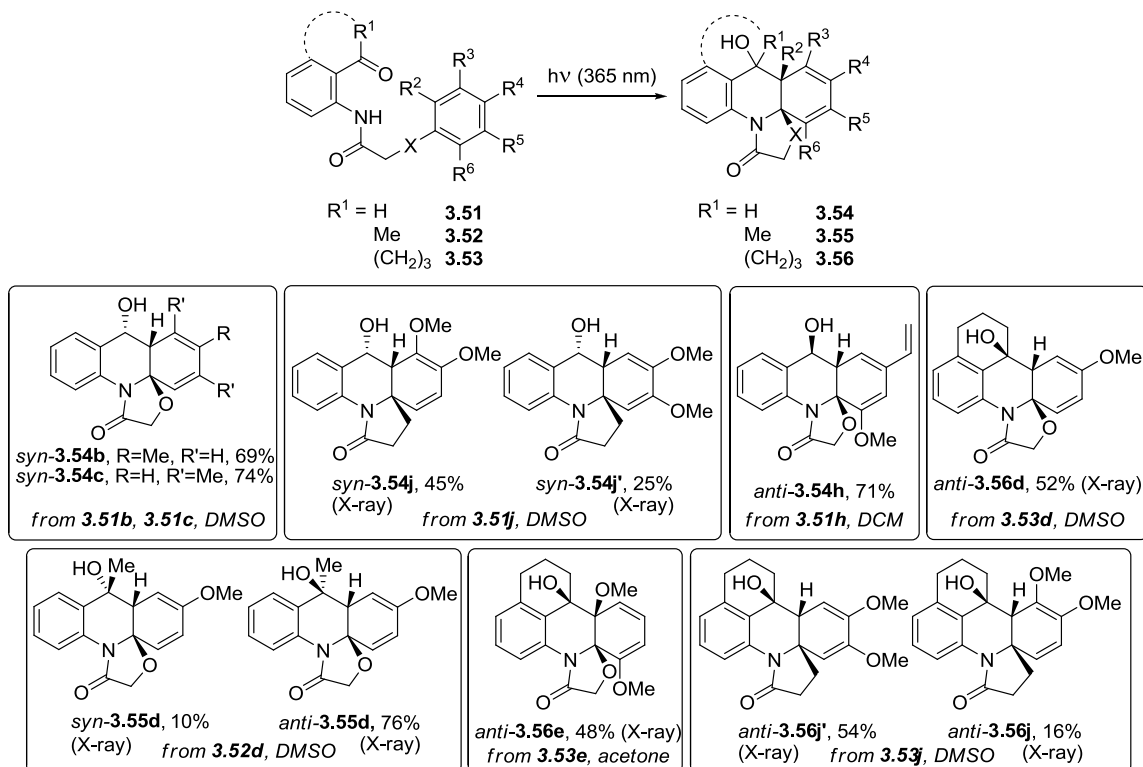
⁷ This reaction was discovered and optimized by the collaborator Dr. O. Mukhina.



Scheme 3.16

- Amide bond formation, which was achieved either by the reaction of acyl chloride (**3.47**) with aniline (**3.9**, **3.48**, **3.49**), or by the peptide coupling promoted by EDC · HCl or azabenzotriazole-uronium salt HATU.

Substrates were then photolyzed on NMR scale in various solvents. 365 nm UV LEDs were used as a light source, because *o*-amidoketones generally have broad absorption with $\lambda_{\max} \approx 350$ nm [7]. These preliminary solvent screening experiments revealed that the majority of the precursors react cleanly in DMSO; in rare cases, other solvents were found to be optimal, such as DCM (**3.51h**) or acetone (**3.53e**). Subsequent preparative scale irradiations afforded the anticipated cyclohexadiene products in good yields (**Scheme 3.17**). In cases where aryl group is unsymmetrically substituted (**3.51j**,



Scheme 3.17

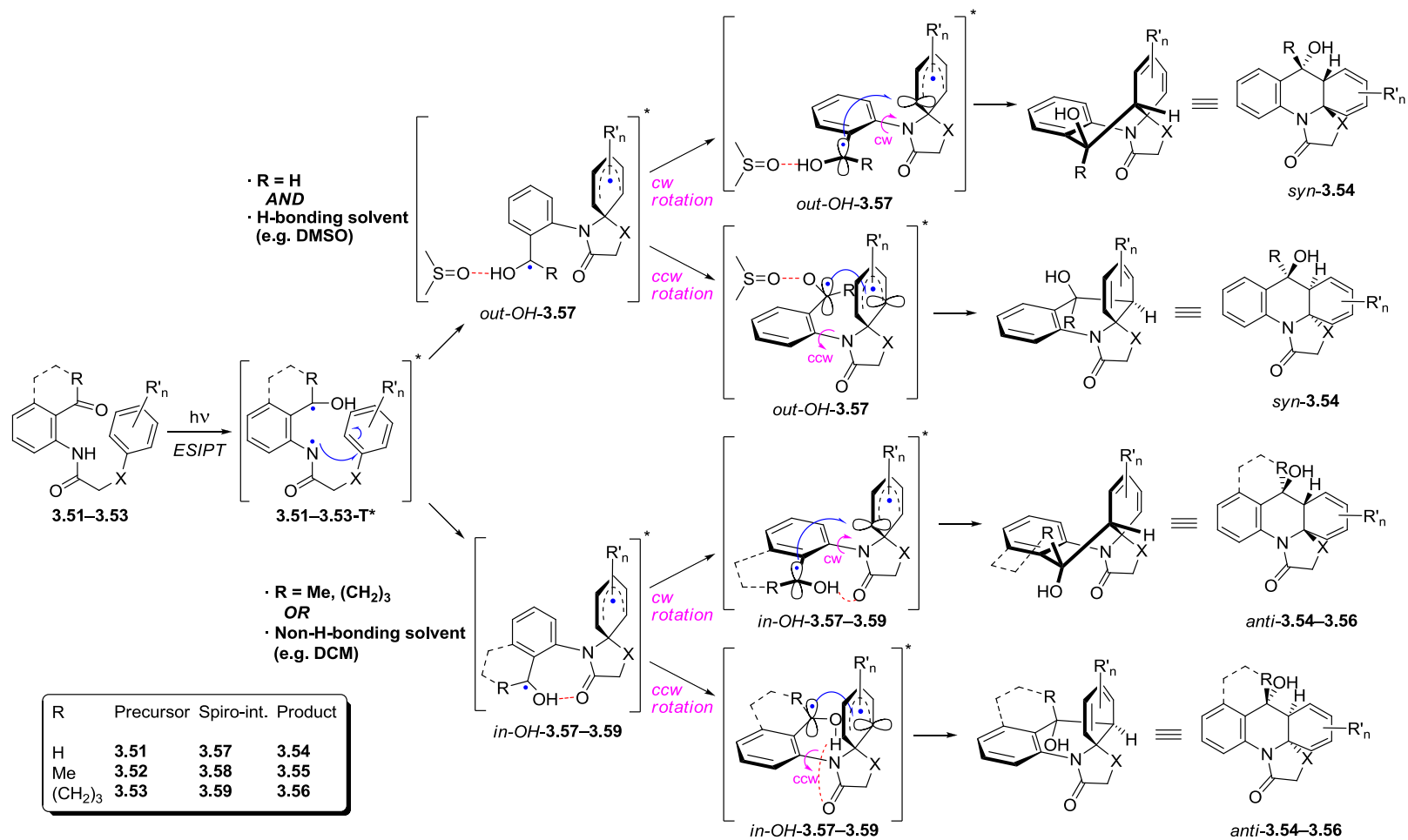
3.53j), two regioisomers were isolated, with a notable exception of the styrene derivative **3.51h** that was converted to the sole adduct *anti*-**3.54h**.

In most cases, diastereochemical outcomes were unambiguously established by X-ray of the photoproducts. For the compounds that were not obtained in a crystalline form, the structures were confirmed by comparing experimental spin-spin coupling constants (SSCCs) obtained by ^1H NMR with those calculated using relativistic force field (RFF) *DU8c* method⁸ [123, 124]. Fortunately, the products, for which X-ray data are not available, are all derived from the aminobenzaldehyde precursors, and therefore diastereochemistry in these cases can be assigned based on vicinal SSCCs between benzylic and bridgehead protons: computed values for *syn*⁹ isomers are in the 5.5–6.5 Hz range, whereas *anti* compounds are predicted to have larger constants of ca. 9 Hz. The accuracy of NMR calculations was corroborated by the fact that the two *syn* photoproducts with X-ray structures, *syn*-**3.54j** and *syn*-**3.54j'**, have the experimental 3J values of 5.9 and 5.3 Hz, respectively. Also, the prediction of greater constants for *anti* isomers is in keeping with the expectation for systems with large dihedral angles (i.e. approaching 180°) based on Karplus equation [125].

With the established structures of products, it is possible to recognize several trends in the diastereoselectivity of the cycloaddition, for which we suggest the rationale outlined in **Scheme 3.18**.

⁸ Calculations were performed by the advisor, Dr. A. Kutateladze. This method was also used to validate the structures of non-crystalline post-photochemical products, which will be discussed later in this chapter.

⁹ Consistent with the previously described products of azaxylylene photocycloadditions, *syn/anti* nomenclature refers to a relative position of the hydroxy group and the cyclohexadiene ring.



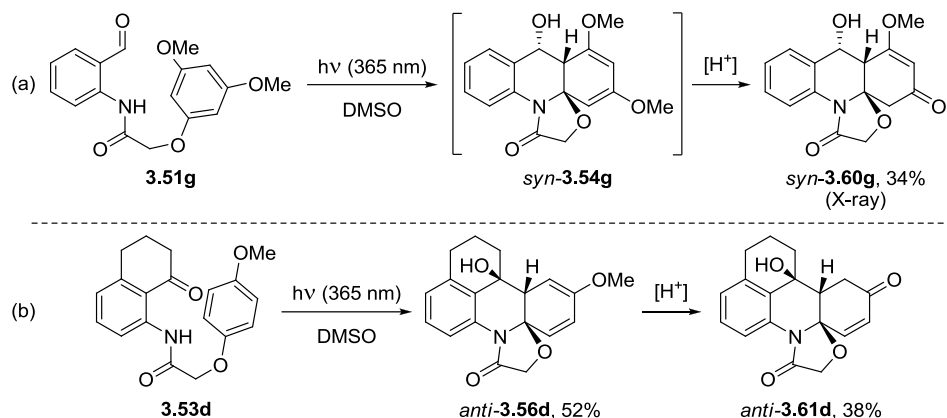
Scheme 3.18

We propose that the addition of *o*-azaxylylene is stepwise, with the initial *ipso*-attack of the nitrogen-centered radical on the aromatic system [52]. In this mechanism, the position of hydroxymethylene radical group in the resulting spiro-intermediate (**3.57**–**3.59**) dictates the stereochemical outcome of the reaction. In the case of aminobenzaldehyde derivatives, hydroxymethylene is small and rotatable; therefore, in these systems, DMSO produces the effect that is similar to the one previously suggested for HMPA [48]: due to external hydrogen bonding, the OH is forced to occupy “*out*” position (*out-OH-3.57*), leading to the predominant production of *syn* isomers (*syn-3.54*). In DCM, however, a conformation with *in*-OH becomes preferable, presumably because of an intramolecular hydrogen bonding of the hydroxy to amide carbonyl; consequently, *anti* product is obtained in this solvent (*anti-3.54*). Formation of *anti* cycloadducts (*anti-3.55*, *anti-3.56*) also predominates for the acetophenone-based compounds, where hydroxymethylene is mostly rotated “*in*” to avoid possible steric interactions between the methyl substituent and the spirocyclic fragment (*in-OH-3.58*), and is the only option available for the tetralone derivatives, which have the OH group permanently locked in “*in*” position (*in-OH-3.59*).

Dearomatization of electron-rich aromatics produces potentially reactive donor-substituted cyclohexadienes. Therefore, in certain cases, instead of the primary cycloadducts (or in addition to them), we obtained the products of secondary post-photochemical transformations, which are primarily acid-catalyzed.

Vinyl ether fragment present in the compound *syn-3.54g* underwent spontaneous hydrolysis, leading to the cyclohexenone *syn-3.60g* (Scheme 3.19, reaction a). The same

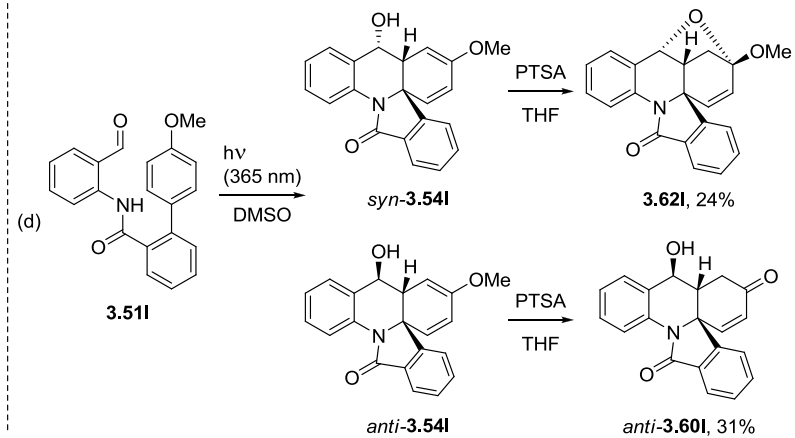
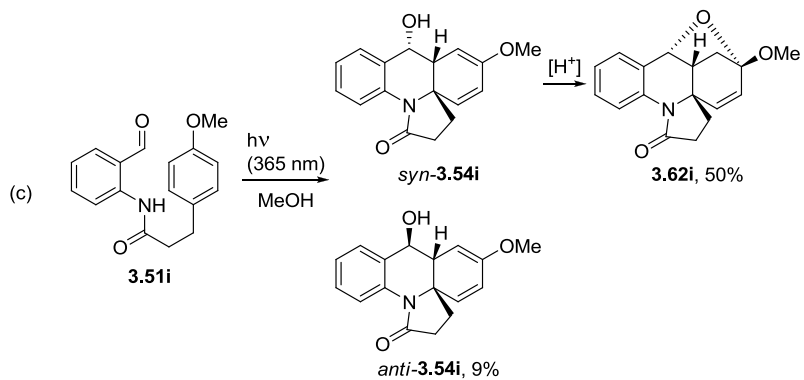
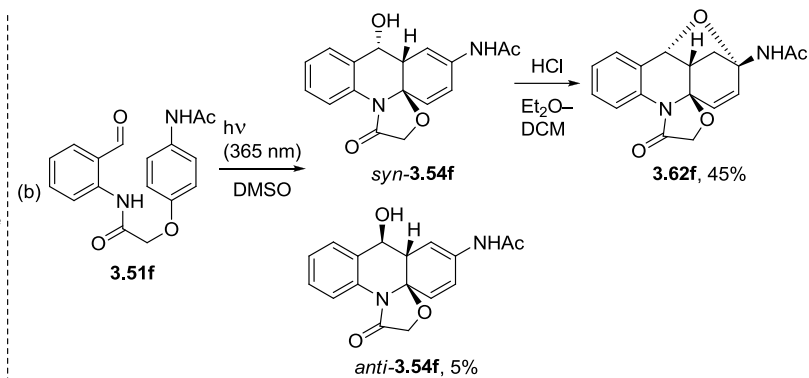
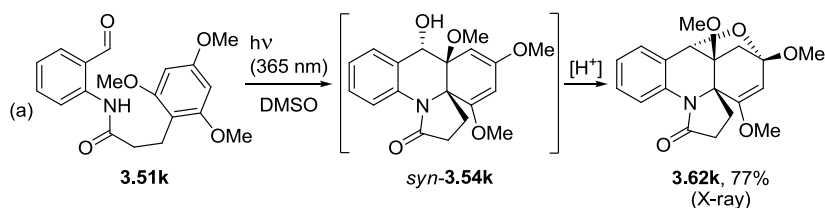
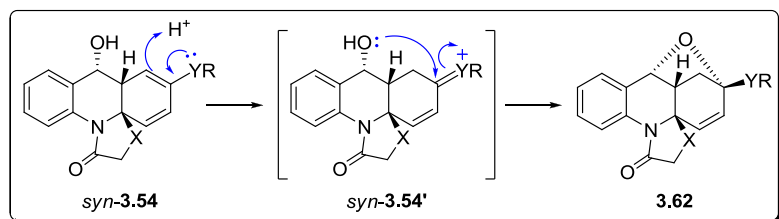
process partially took place in the product *anti*-**3.56d** during chromatographic purification on silica gel (Scheme 3.19, reaction b).



Scheme 3.19

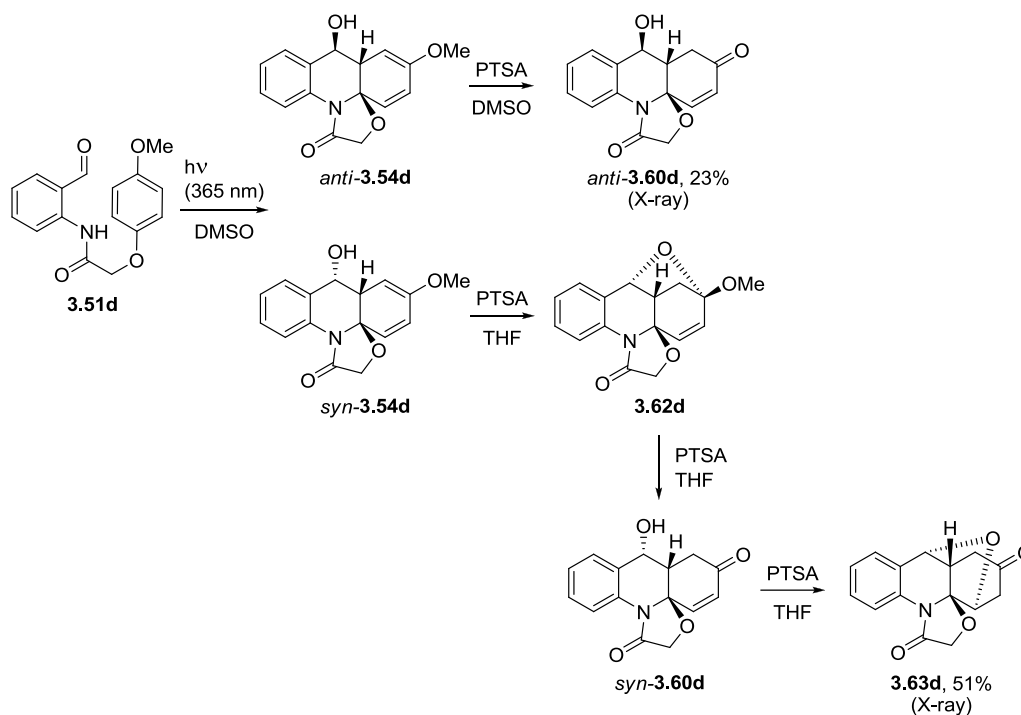
Spatial proximity of the benzylic hydroxy group to the electron-rich double bond in *syn* compounds enables formation of cyclic ketals by the nucleophilic attack on the protonated vinyl ether or enamide (Scheme 3.20). Such reactivity was observed for the *syn* isomers formed from precursors **3.51f**, **3.51i**, **3.51k** and **3.51l**; instructively, the *anti* photoproducts either remained unreacted (*anti*-**3.54f**, *anti*-**3.54i**), or hydrolyzed (*anti*-**3.60l**) under the same conditions.

A unique example of acid-catalyzed transformation was observed in the case of aldehyde-based precursor **3.51d** (Scheme 3.21). Irradiation of this compound resulted in two primary photoproducts, *anti*-**3.54d** and *syn*-**3.54d**, that were subsequently treated with tosic acid. Under these conditions, *anti*-**3.54d** completely hydrolyzed to α,β -unsaturated ketone *anti*-**3.60d**, whereas the isomeric *syn*-**3.54d** transformed into two compounds: ketal **3.62d** and enone *syn*-**3.60d**. Presumably, *syn*-**3.60d** forms as a result of the hydrolysis of **3.62d**; therefore, with the intention to reduce the number of products by converting all **3.62d** into *syn*-**3.60d**, we subjected the mixture to an extended reaction



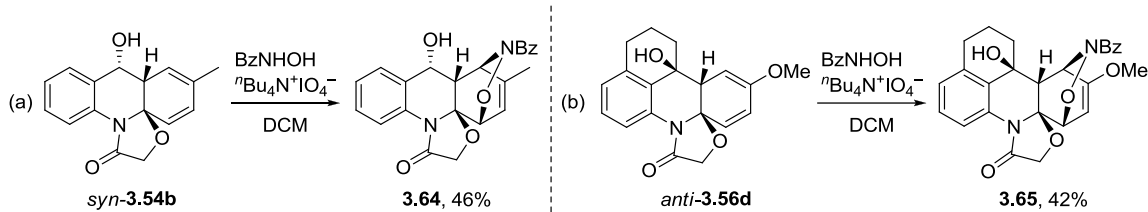
Scheme 3.20

with acid. After 3 days, it was found that **3.62d** was entirely consumed; however, proton NMR spectrum of the final product was lacking characteristic doublets in the alkenic region (4.5–6.5 ppm) with the SSCC \approx 10 Hz, which would be indicative of the cyclohexenone moiety. X-ray analysis of the isolated pure material revealed that this new compound is the cyclic ether **3.63d** formed from *syn*-**3.60d** by intramolecular Michael addition of the benzylic OH to the carbonyl-activated double bond.



Scheme 3.21

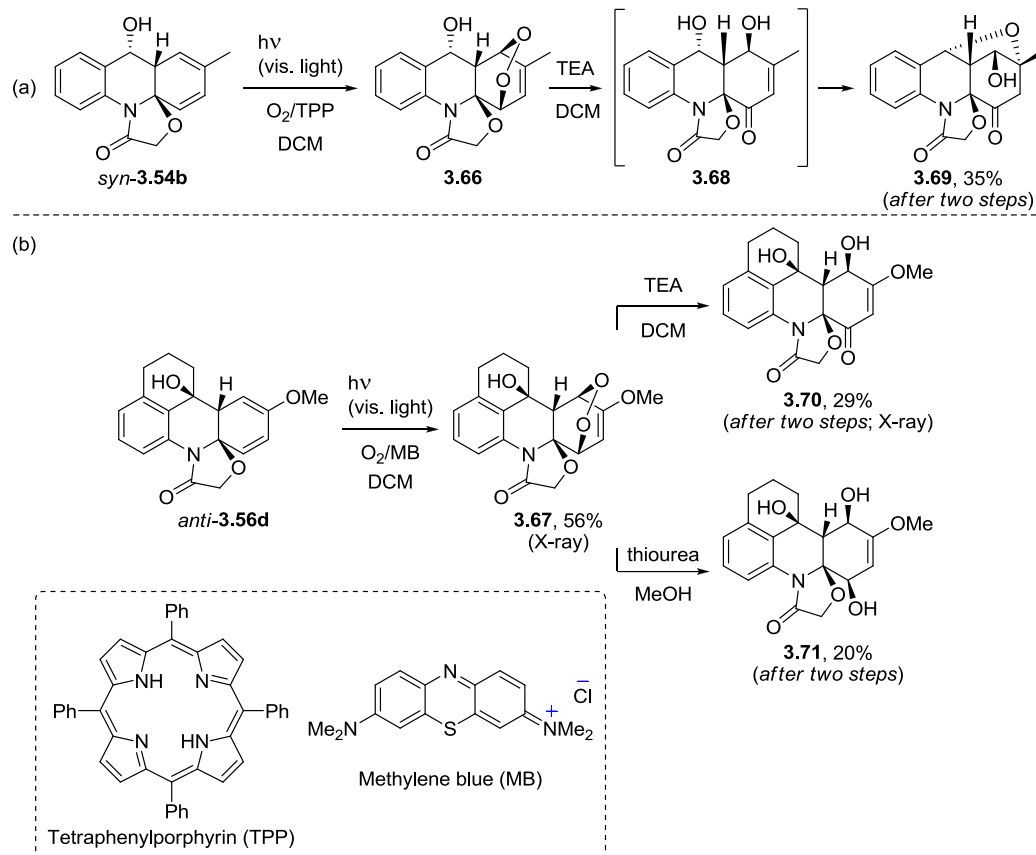
Cyclohexadiene fragment present in the photoproducts provides an appealing opportunity to diversify and grow the complexity of the core scaffolds by post-photochemical [4+2] cycloadditions. To prove the viability of this strategy, we reacted *syn*-**3.54b** and *anti*-**3.56d** with benzoyl-nitroso dienophile that was generated *in situ* by the oxidation of benzhydroxamic acid [126] (**Scheme 3.22**).



Scheme 3.22

Furthermore, we engaged the cyclohexadiene units in hetero-Diels–Alder reactions with singlet oxygen to access endo-peroxides (**3.66** and **3.67**, **Scheme 3.23**) – the method that found applications in the syntheses of numerous peroxy-containing natural products [127]. In addition to being an important structural element responsible for antitumor, antibacterial and antimalarial activities [128, 129], peroxy bridge possesses significant synthetic utility, which we demonstrated by subjecting **3.66** and **3.67** to further modifications (**Scheme 3.23**):

- Base-promoted Kornblum–DeLaMare rearrangement leading to keto-alcohols **3.68** and **3.70**; interestingly, compound **3.68** underwent spontaneous intramolecular Michael reaction between *syn*-OH and enone moiety, affording cyclic ether **3.69** as a final product;
- Reductive ring opening of endo-peroxide with thiourea that converted **3.67** into the corresponding diol **3.71**.



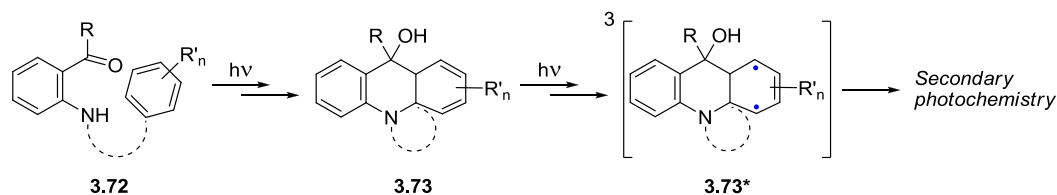
Scheme 3.23

In summary, we have developed a novel method for the dearomatization of benzenoid arenes. Our approach is based on the intramolecular photocycloaddition proceeding via an unprecedented [2+4] topology, with the arene reacting as a 2π component and the ESIPT-produced *o*-azaxylylene playing a role of a 4π counterpart. The primary photoproducts accessed by this strategy contain reactive electron-rich cyclohexadiene fragments, which can be utilized as handles for the experimentally simple post-photochemical transformations to further expand scaffold diversity and complexity.

Project 4: Access to Complex Polyheterocyclic Architectures by Photoinduced Dearomatization Cascade Reactions of Oxalyl Anilides [130]

Both diversity-oriented and target-oriented approaches in drug discovery share the goal of obtaining complex molecular structures [131]. Therefore, development of new synthetic methodologies that enable quick growth in scaffold complexity is highly desirable; “step-economical” strategies, i.e. those that require minimum number of steps, are especially appealing [132].

In the previous section of this chapter, we have described an effective method for the assembly of various polyheterocyclic molecules, which is based on photoinduced [2+4] cycloadditions of ESIPT-generated *o*-azaxylylenes to benzenoid arenes [121]. Given that the resulting compounds contain diene moieties, known “sinks” for triplet energy [133-138], we hypothesized that through the secondary excitation and subsequent ISC it would be possible to produce triplet dienes, which could participate in further reactions leading to an additional increase in molecular complexity (**Scheme 3.24**). Ideally, the entire transformation would occur in “one pot”, using a single light source for inducing both primary and secondary steps.



Scheme 3.24

365 nm irradiation of the substrates containing oxyacetic and propionic linkers leads only to [2+4] cycloadducts and does not promote any secondary photochemistry involving diene functionalities. This observation suggests that the quinolinolo-cyclohexadiene products have reduced UV absorptivity at this wavelength in comparison

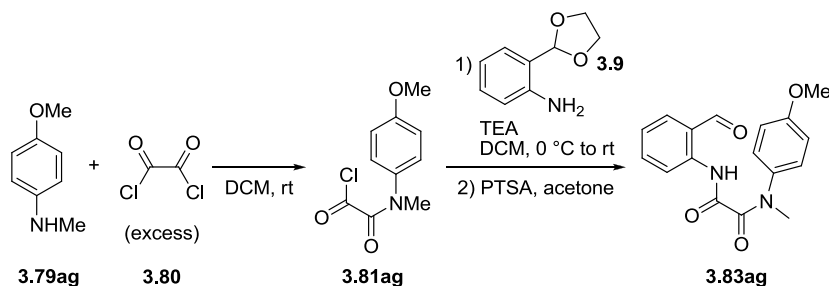
to the corresponding photoprecursors, presumably due to decreased π -conjugation caused by the lack of aromatic carbonyl. In order to solve this problem, we decided to incorporate a *multifunctional linker* between photoactive cores and benzenoid groups in the starting materials. The ideal tether would not only enhance light-harvesting properties of the molecule, but also act as a triplet sensitizer for the diene and thus enable further photoinduced transformations. In addition, the new linker would preferably bring other benefits, such as (i) straightforward and high-yielding assembly of photoprecursor and (ii) formation of an additional pharmacophore in the final product.

We envisioned that oxalyl unit is the most suitable candidate for the role of multifunctional linker in our photoprecursors, for the following reasons:

- The presence of two carbonyl groups adjacent to each other would presumably improve UV absorption of the resulting primary photoproduct by extending π -conjugation;
- α -Dicarbonyl compounds, such as benzil [139] and biacetyl [140], are known triplet sensitizers due to efficient ISC;
- Photoprecursors can be readily assembled by using oxalyl chloride to “zip” two aniline fragments, one of which is the photoactive core and the second is the unsaturated moiety that is dearomatized during [2+4] photoreaction;
- Upon cycloaddition, oxalyl amide would fold into imidazolidine-4,5-dione, a potential pharmacophore group [141-145].

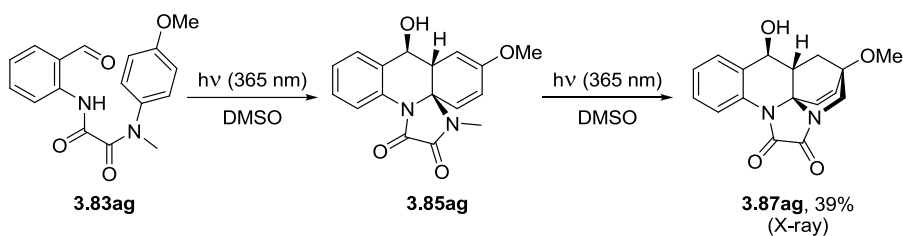
In order to test the feasibility of secondary photoreactions in oxalyl-equipped systems, we prepared the substrate **3.83ag** through the straightforward synthetic route: first, we reacted *N*-methylanisidine **3.79ag** with the excess of oxalyl chloride **3.80** and

then coupled the resulting acyl chloride **3.81ag** with 1,3-dioxolane-protected *o*-amino-benzaldehyde **3.9**; finally, acid-catalyzed deprotection of the aldehyde yielded the precursor **3.83ag** (Scheme 3.25).



Scheme 3.25

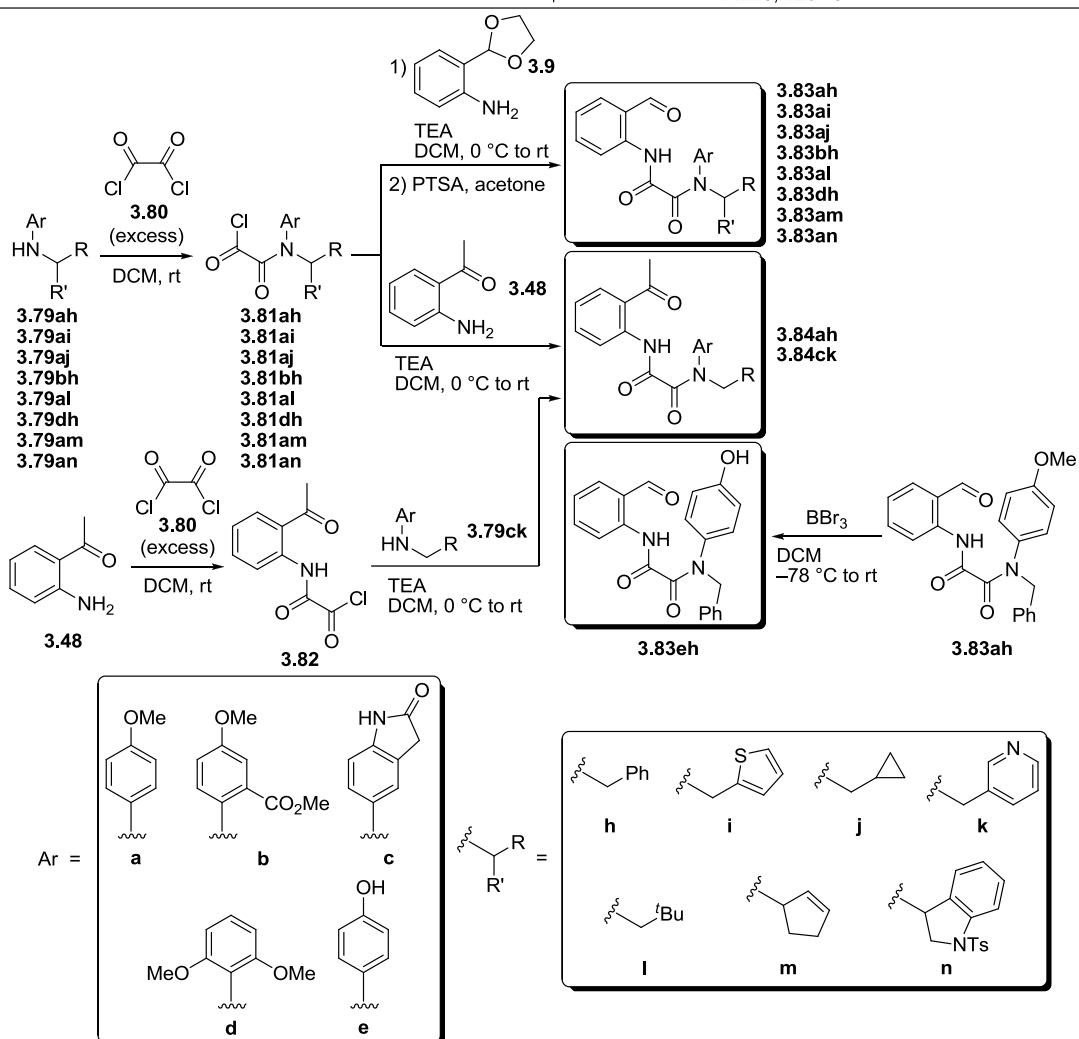
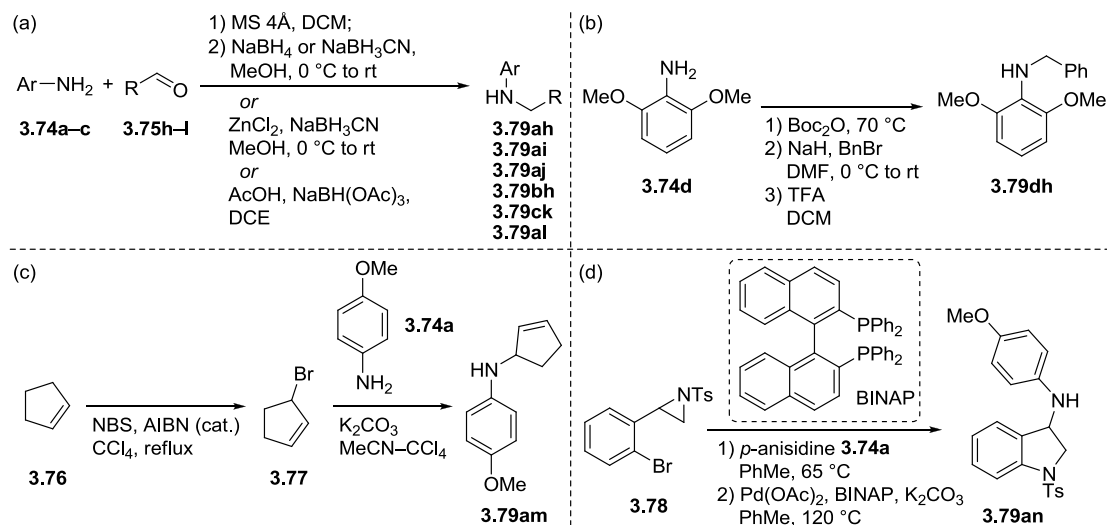
The oxalyl amide substrate **3.83ag** was then irradiated under the conditions previously optimized for the aryloxyacetic and arylpropionic precursors, i.e. with 365 nm LEDs and in DMSO as a solvent. To our delight, monitoring the reaction progress by proton NMR revealed that the initially formed cyclohexadiene **3.85ag** was depleted upon extended photolysis and converted into the 2-azabicyclo[2.2.2]octene product **3.87ag**, whose structure was established by X-ray crystallography (Scheme 3.26).



Scheme 3.26

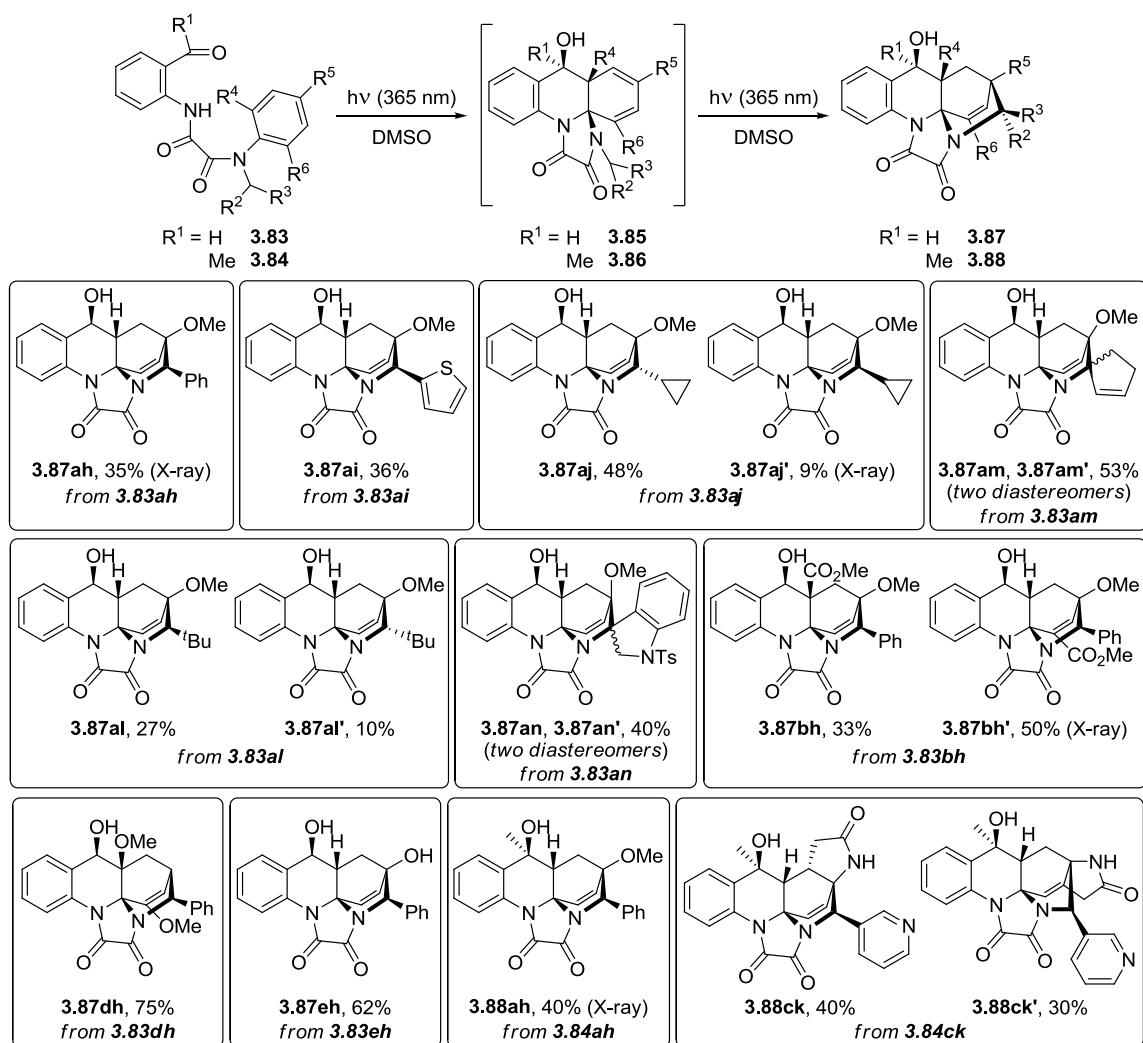
This result clearly demonstrates that the introduction of the oxalyl tether allows the achievement of a cascade transformation, where both photochemical steps (**3.83ag** → **3.85ag** and **3.85ag** → **3.87ag**) occur consecutively in a single pot, producing polycyclic scaffolds that are more complex than the primary cyclohexadiene-outfitted structures.

To probe the scope of the new photocascade, we synthesized a diverse set of benzaldehyde- (**3.83**) and acetophenone-derived substrates (**3.84**) based on *N*-alkylanilines having various substituents in benzene ring, such as methoxy (**a**, **b**, **d**), methoxycarbonyl (**b**), γ -lactam (**c**) and hydroxy (**e**) groups, as well as different functionalities in the α -position to the tertiary nitrogen atom: phenyl (**h**), 2-thienyl (**i**), cyclopropyl (**j**), 3-pyridyl (**k**), *tert*-butyl (**l**), 3-cyclopentenyl (**m**) and 3-indolyl (**n**; **Scheme 3.27**). Initially, we prepared an array of *N*-alkylanilines (**3.79**) either by reductive amination (reaction a), or by monoalkylation of aromatic amine with RBr (reactions b, c); in one case, *p*-anisidine derivative **3.79an** was accessed through ring-opening of aziridine **3.78** followed by intramolecular Buchwald–Hartwig reaction [146] (reaction d). The majority of photoprecursors were then assembled by coupling *N*-alkylanilines **3.79** with the excess of oxalyl chloride **3.80** to get 2-anilino-2-oxoacetyl chlorides **3.81**, which were then used to acylate protected *o*-aminobenzaldehyde **3.9** or *o*-aminoacetophenone **3.48**. For the substrate **3.84ck**, however, we inverted the order of amide couplings, because aniline **3.79ck** underwent decomposition upon treatment with 10 equivalents of oxalyl chloride. Additionally, phenol derivative **3.83eh** was accessed by demethylation of the anisole precursor **3.83ah** with boron tribromide [147].



Scheme 3.27

The photochemical cascade observed for compound **3.83ag** was consistently reproduced on all other substrates, providing the corresponding 2-azabicyclo[2.2.2]-octenes (**3.87**, **3.88**) in 35–75% yields (**Scheme 3.28**). Structures of the four products (**3.87ah**, **3.88ah**, **3.87aj'**, **3.87bh'**) were unambiguously determined by X-ray; other compounds were characterized by ^1H and ^{13}C NMR, and their structures were verified with the help of *DU8+* NMR computations [123, 124, 148, 149].¹⁰



¹⁰ NMR calculations were performed by the advisor, Dr. A. Kutateladze. This method was also used to validate the structures of non-crystalline post-photochemical products, which will be discussed later in this chapter.

Diastereomers **3.87aj** and **3.87aj'** were distinguished by analyzing the multiplicity of the low-field alkenic signal in proton NMR. In compound **3.87aj**, the cyclopropyl substituent is oriented in such a way that the proton H_A has two small SSCCs (≈ 1 Hz) with methine proton H_B and methylene proton H_C (**Figure 3.1**, a); these long-range constants are present due to the *W*-arrangement of the bonds between the nuclei [150]. The isomer **3.87aj'**, on the other hand, lacks the *W*-type coupling interaction between H_A and H_B; therefore, its low-field olefin signal has only one small SSCC (**Figure 3.1**, b). This rationale is consistent with *DU8+* NMR calculations that confirmed the existence of two small *W*-constants in **3.87aj** and one in **3.87aj'**; furthermore, the structure of **3.87aj'** was additionally validated by X-ray crystallography. The same criterion (absence or presence of the *W*-type SSCC between the alkene and methine protons) was also used to differentiate the epimers **3.87al** and **3.87al'** (**Figure 3.2**).

Structures of the obtained photoproducts indicate that the cycloaddition step occurs with the exclusive *anti*-diastereoselectivity, as opposed to our previous dearomatization of benzenoid arenes [121]. Consistent with the mechanistic rationale for [2+4] photocycloaddition depicted in **Scheme 3.18**, we suggest that the observed stereochemical outcome originates from the predominant formation of *in*-OH rotamer (*in*-OH-**3.89**, *in*-OH-**3.90**), which could be explained by the propensity of oxalyl amide to create exceptionally tight intramolecular hydrogen bonds with the hydroxy group (**Scheme 3.29**).

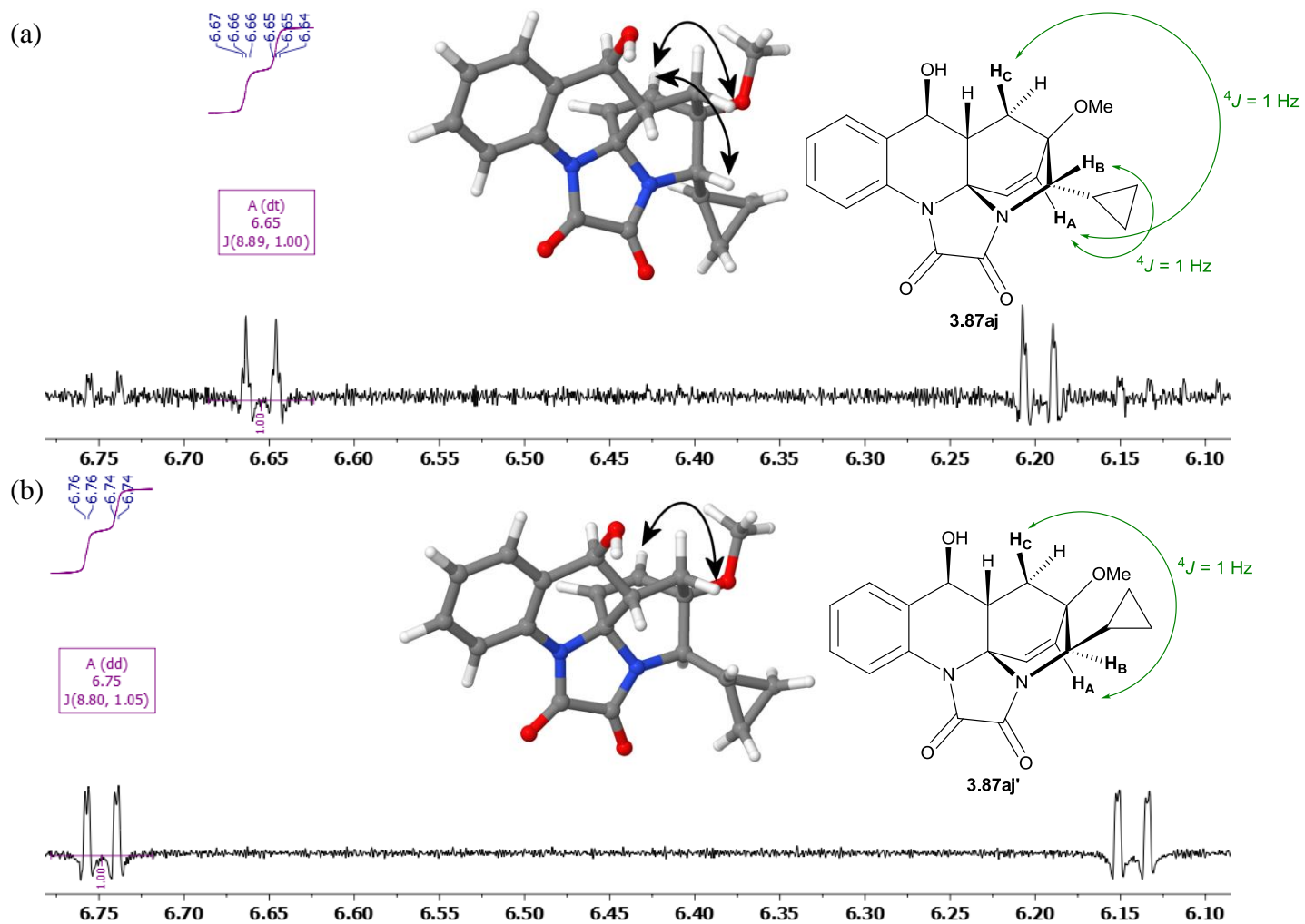


Figure 3.1: Alkenic region of ^1H NMR spectra of **3.87aj** and **3.87aj'**.

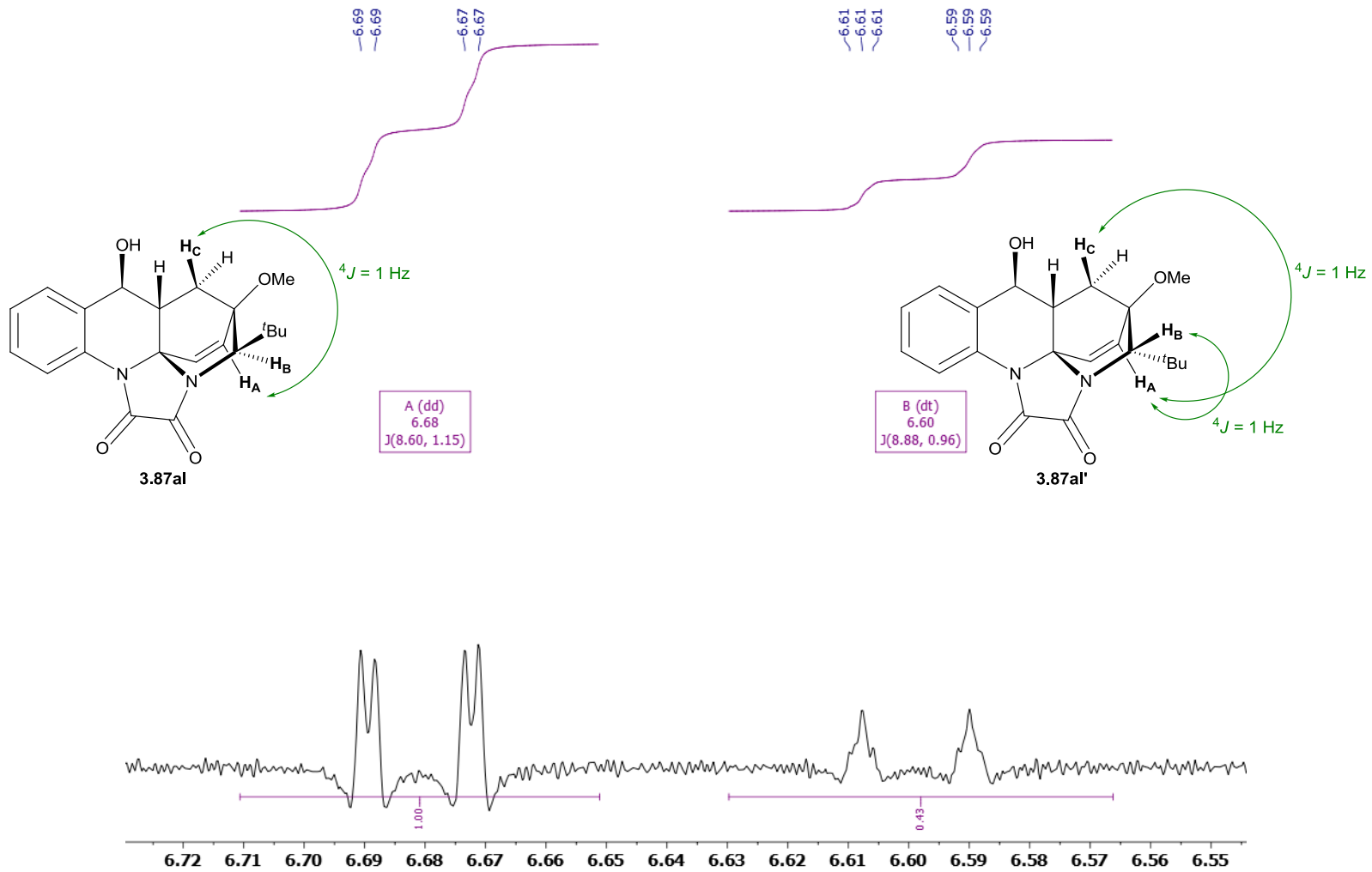
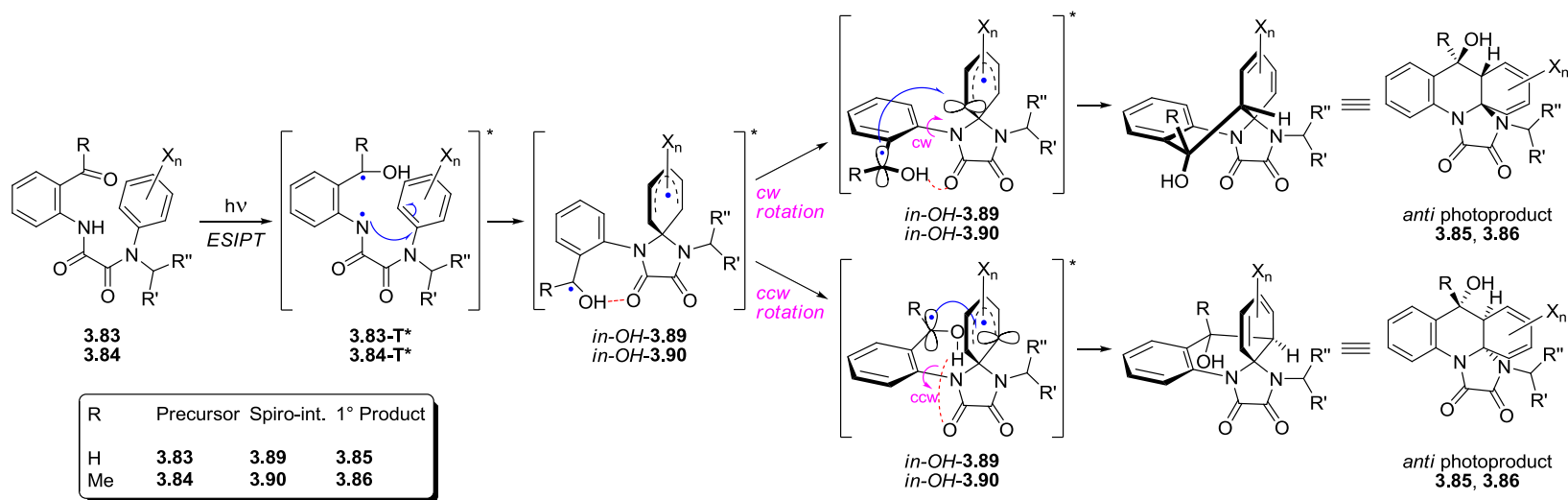


Figure 3.2: Alkenic region of ^1H NMR spectrum of **3.87al** and **3.87al'**.



Scheme 3.29

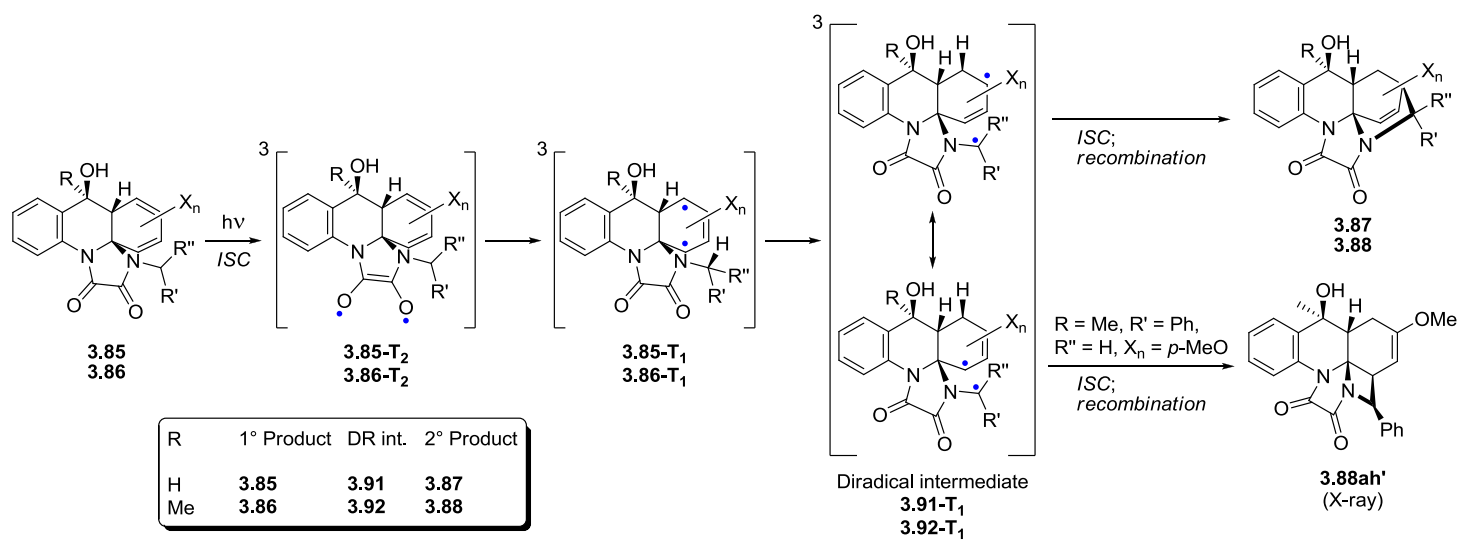
For the secondary photochemical reaction, i.e. the formation of azabicyclo[2.2.2]-octenes from the primary photoproducts, we propose the mechanism, which is based on our hypothesis about the role of oxalyl tether and involves the following steps

(Scheme 3.30):

- Excitation of the oxalyl anilide chromophore followed by ISC into the triplet manifold (**3.85**, **3.86** → **3.85-T₂**, **3.86-T₂**);
- Triplet energy transfer from the dicarbonyl fragment to the cyclohexadiene moiety (**3.85-T₂**, **3.86-T₂** → **3.85-T₁**, **3.86-T₁**);
- 1,5-hydrogen atom transfer (HAT) from the N-CH_n-R,R' carbon to the terminal dienic carbon, resulting in the intermediate with two conjugated radicals (**3.85-T₁**, **3.86-T₁** → **3.91-T₁**, **3.92-T₁**);
- ISC with subsequent recombination of two radical centers (**3.91-T₁**, **3.92-T₁** → **3.87**, **3.88**).

For the simplest *N*-methyl derivative **3.87ag** (R = R' = R'' = H, X_n = *p*-OMe), all intermediates and HAT transition state were calculated by DFT method at the B3LYP/6-311+G(d,p) level of theory¹¹, which supported the proposed reaction pathway. Computational results revealed that the triplets in T₂ and T₁ states of the primary product are indeed localized on α-dicarbonyl and diene, respectively (as indicated by changes in bond lengths in these moieties). Importantly, the energy of **3.85ag-T₁** is ca. 20 kcal/mol lower than that of **3.85ag-T₂**, which corroborates earlier suggested hypothesis that the dienic unit serves as a “triplet sink”. The next step, 1,5-HAT, is predicted to be fast

¹¹ Calculations were performed by the advisor, Dr. A. Kutateladze.

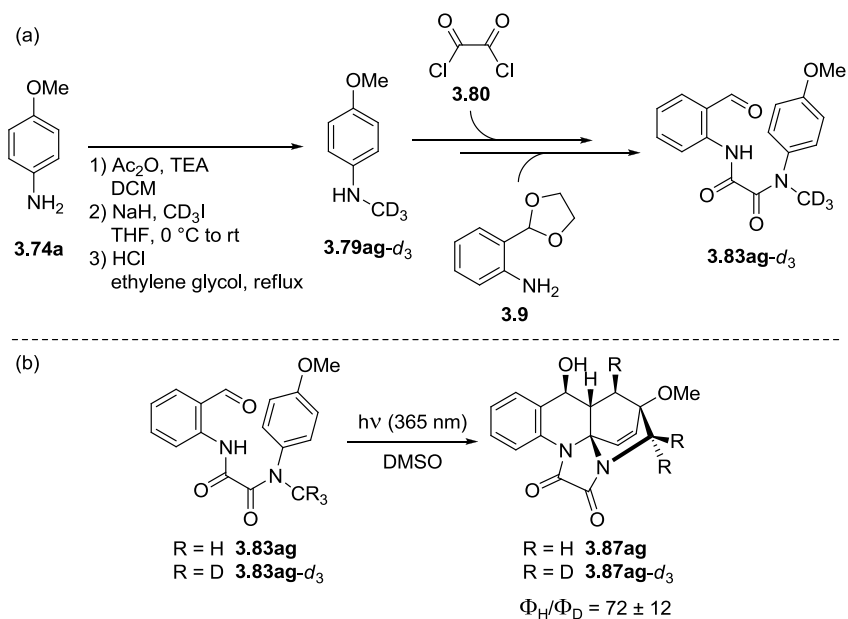


Scheme 3.30

(calculated activation barrier is 15.9 kcal/mol) and exergonic on the triplet hypersurface (diradical **3.91ag-T₁** is ca. 8 kcal/mol “downhill” compared to **3.85ag-T₁**).

Additional evidence for the biradical mechanism was provided by the discovery of diaza-benzofenestrane **3.88ah'** (Scheme 3.30), which was isolated in trace quantities after the irradiation of acetophenone-based precursor **3.84ah** and was characterized by X-ray. Formation of this minor product is rationalized by recombination of **3.92ah-T₁** at the alternative terminus of the allylic radical.

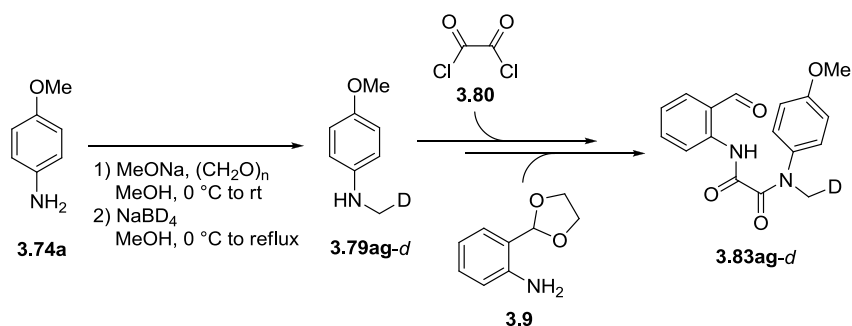
In order to gain more mechanistic information about the 1,5-HAT step, we compared relative quantum yields of the azabicyclo[2.2.2]octene production for the protic substrate **3.83ag** and its trideuteromethyl analogue **3.83ag-d₃**, which was prepared by alkylation of the protected *p*-anisidine with iodomethane-*d*₃, followed by deprotection and the same steps previously used to access **3.83ag** (Scheme 3.31).



Scheme 3.31

By comparing the reactivity of **3.83ag** and **3.83ag-d₃**, we expected to get evidence for a primary kinetic isotope effect (KIE), because the proposed HAT step involves breaking C–H/C–D bond. The experiment was carried out by running NMR scale irradiations of these compounds on a “carousel” photoreactor to average out the influence of LED-to-sample distance on the reaction rate. From the obtained NMR data, we derived an extremely large $\Phi_{\text{H}}/\Phi_{\text{D}}$ value of 72 ± 12 ¹² that implies quantum tunneling [151].

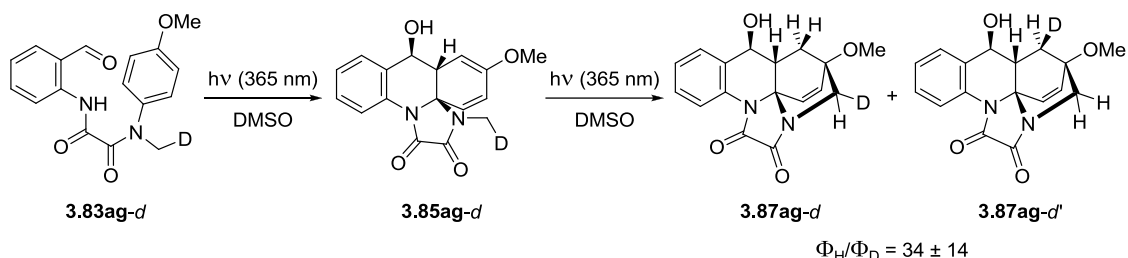
Since the secondary photoreaction is a multi-step process, we recognized that this number might reflect not only the difference in HAT rates between protic and deuterated compounds, but also the isotope effects on lifetimes of the excited state species along the reaction coordinate. Therefore, with the intention to get a more accurate KIE value for HAT by minimizing the possible influence of isotopic composition on lifetimes of the intermediates, we synthesized the monodeuterated photoprecursor **3.83ag-d**; the required isotopically labeled aniline **3.79ag-d** was prepared by sodium borodeuteride reduction of the imine intermediate formed from *p*-anisidine **3.74a** and formaldehyde (**Scheme 3.32**).



Scheme 3.32

¹² Calculation details can be found in the “Experimental Section” chapter.

3.83ag-d was then irradiated under standard conditions, and the resulting product mixture was analyzed by proton NMR. Based on acquired data, we determined the percentages of azabicyclo[2.2.2]octenes deuterated at different positions (**3.83ag-d** and **3.83ag-d'**, **Scheme 3.33**); using these numbers and applying statistical correction for two hydrogens vs. one deuterium atom, we obtained the ratio $\Phi_{\text{H}}/\Phi_{\text{D}} = 34 \pm 14$.¹³ Given that this number is lower than the one calculated in the previous experiment, we rationalize that D substitution has an effect on lifetimes of excited species. At the same time, this value exceeds the maximum possible room temperature primary KIE by a factor of 4, and thereby indicates that 1,5-HAT occurs through quantum tunneling [151]. This phenomenon is not unprecedented: for instance, KIEs of 5–55 were reported for the proton-transfer step in the enzyme methylamine dehydrogenase [152]; also, significant contributions of hydrogen atom tunneling were found for 1,5-HAT from the methyl group to the excited-state carbonyl oxygen [153–157].



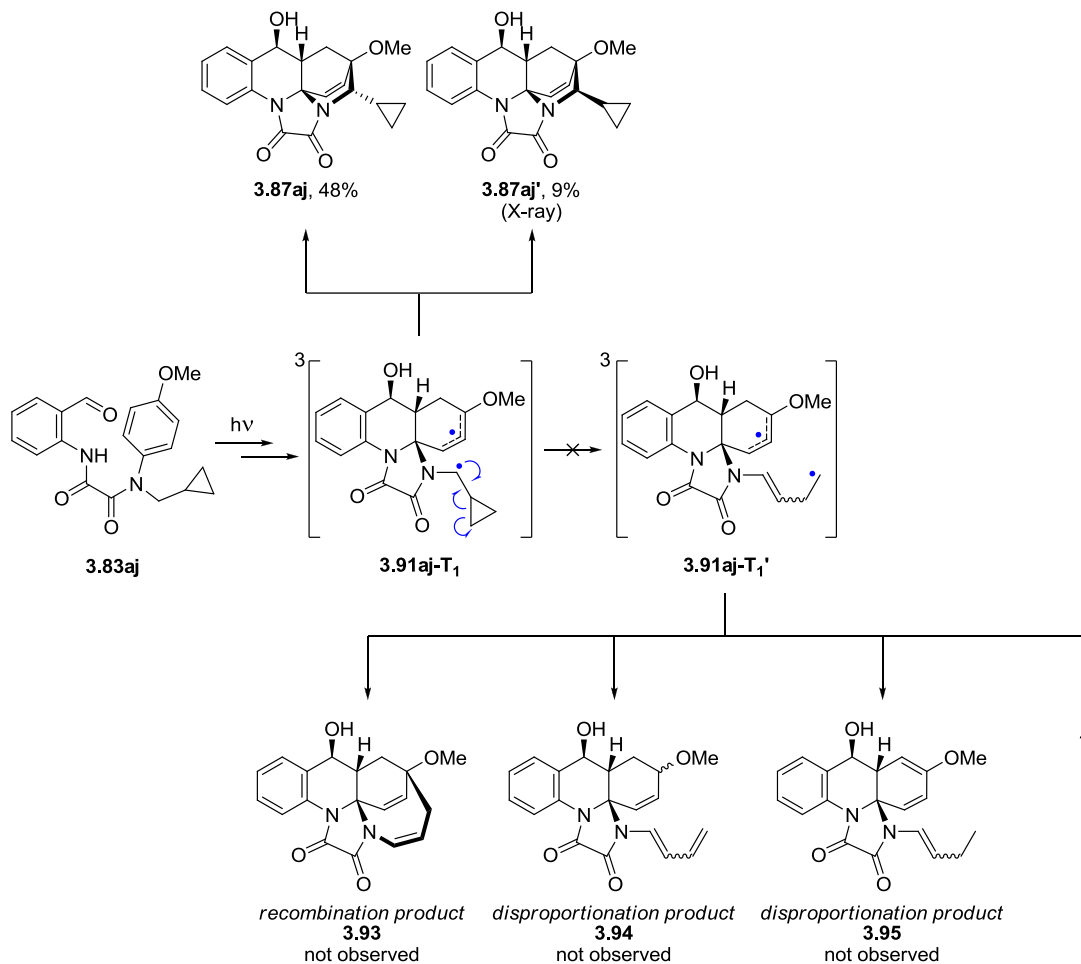
Scheme 3.33

The processes that follow HAT in the mechanism of the azabicyclo[2.2.2]octene formation, i.e. ISC and radical recombination (**3.91-T₁**, **3.92-T₁** → **3.87**, **3.88**;

Scheme 3.30), also proceeded with remarkably fast rates, as demonstrated by the

¹³ Calculation details can be found in the “Experimental Section” chapter.

photolysis of precursor with cyclopropylmethyl radical clock (**3.83aj**, **Scheme 3.34**) that did not generate any ring-opened side products, such as **3.93**, **3.94** or **3.95**. This result suggests that the collapse of the diradical **3.91aj-T₁** is so rapid that it outcompetes strain-relieving rearrangement of the cyclopropane.¹⁴



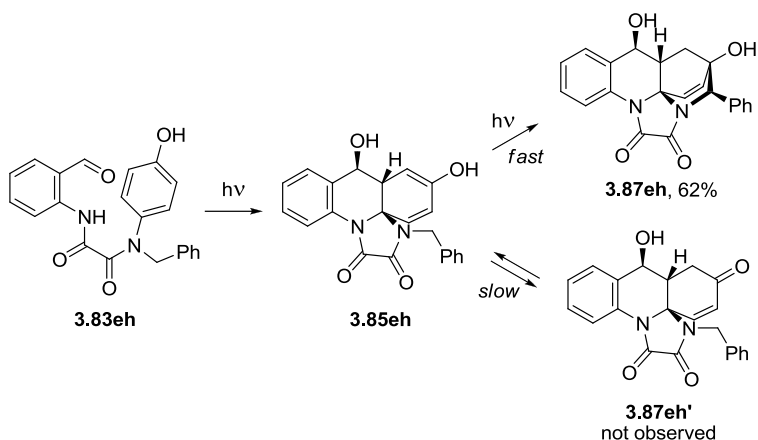
Scheme 3.34

The overall efficiency of the secondary photoreaction is illustrated by the fact that all cyclohexadiene intermediates (except methyl-substituted **3.85ag**) are barely detectable in the irradiation mixtures by NMR. It is conceivable that alkyl or aryl R' groups (which are

¹⁴ It is important to note that faster radical clocks [158], such as 2,2-diphenylcyclobutylmethyl [159] and bicyclo[2.1.0]pent-2-yl [160], might undergo rearrangements at rates comparable to that of HAT.

absent in the *N*-methylated system) provide additional stabilization to the radical center in **3.91-T₁**/**3.92-T₁** and thus facilitate the transformation of primary compounds **3.85**/**3.86** into cyclized photoproducts **3.87**/**3.88**.

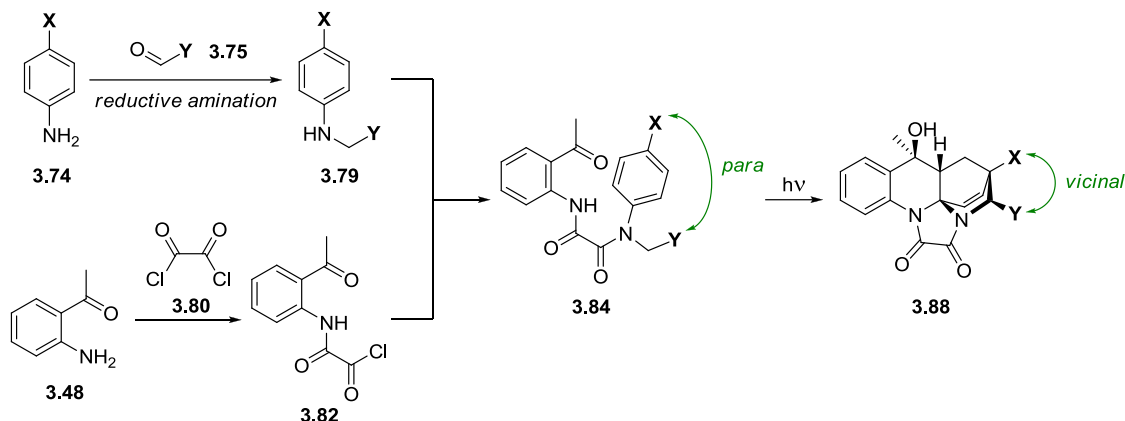
The fast rate of the second photocascade step is further supported by the exclusive formation of tertiary alcohol **3.87eh** from the phenolic substrate **3.83eh** (Scheme 3.35). The initially produced dienol **3.85eh** undergoes rapid and complete conversion into the corresponding secondary photoproduct **3.87eh** and does not tautomerize into the enone **3.87eh'**, which was not observed by NMR at any point during the reaction.



Scheme 3.35

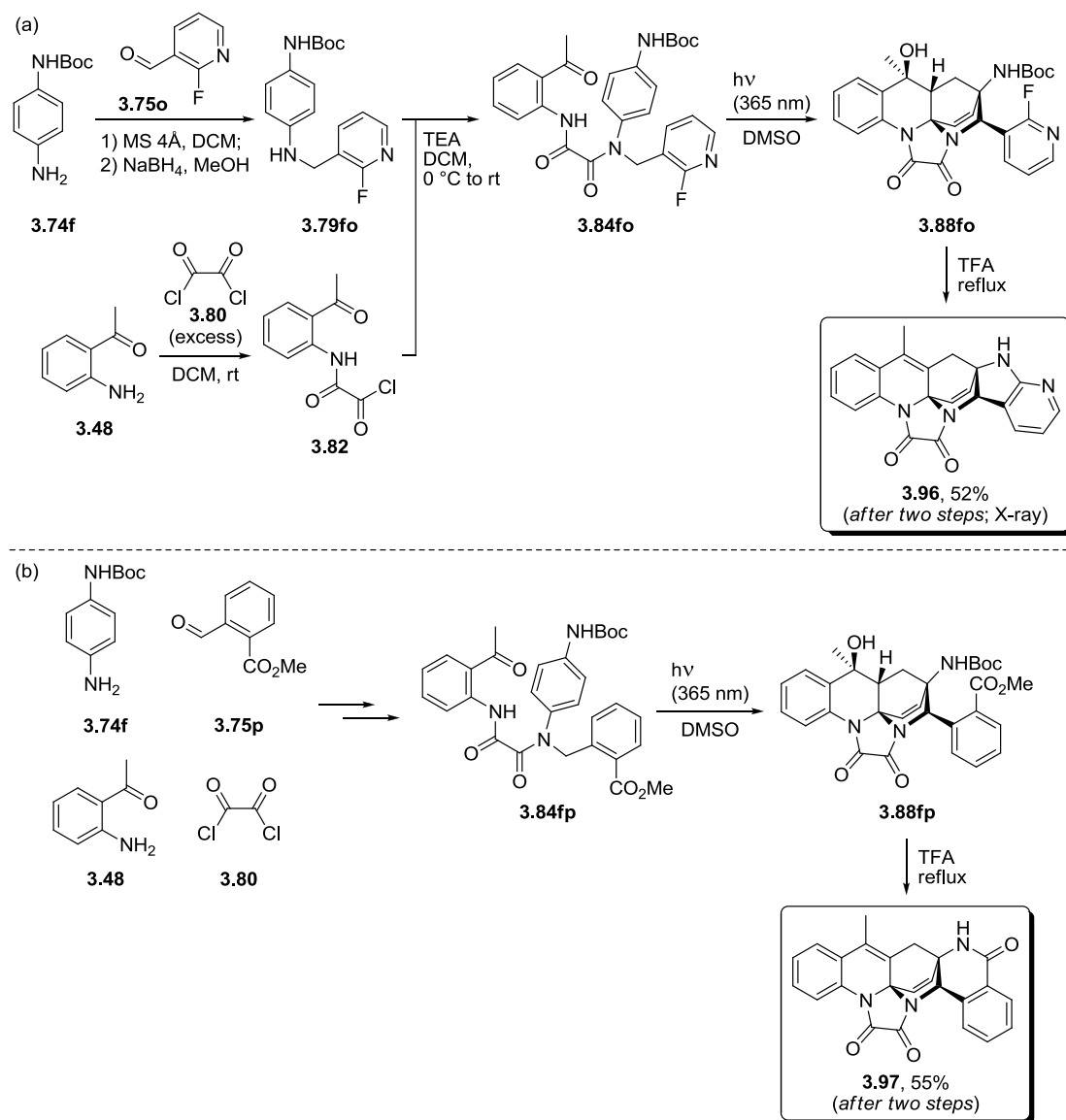
After identifying several important mechanistic aspects of the new photoinduced cascade, we turned our attention to the additional synthetic potential offered by this reaction. We recognized that X and Y groups originally located at the opposite ends in *p*-substituted *N*-alkylaniline (**3.79**, Scheme 3.36) are brought into a vicinal relationship as a result of the photochemical dearomatization (**3.88**). These moieties can be easily varied, due to the wide selection of *p*-functionalized anilines **3.74** and aldehydes **3.75** that are used as starting materials for the modular assembly of the photoprecursors **3.84**. We decided to take advantage of this feature and synthesize azabicyclo[2.2.2]octenes bearing

specific X and Y substituents (**3.88**), with the intention to demonstrate the utility of these groups as “handles” for post-photochemical ring formations enabling further increase in the molecular complexity.



Scheme 3.36

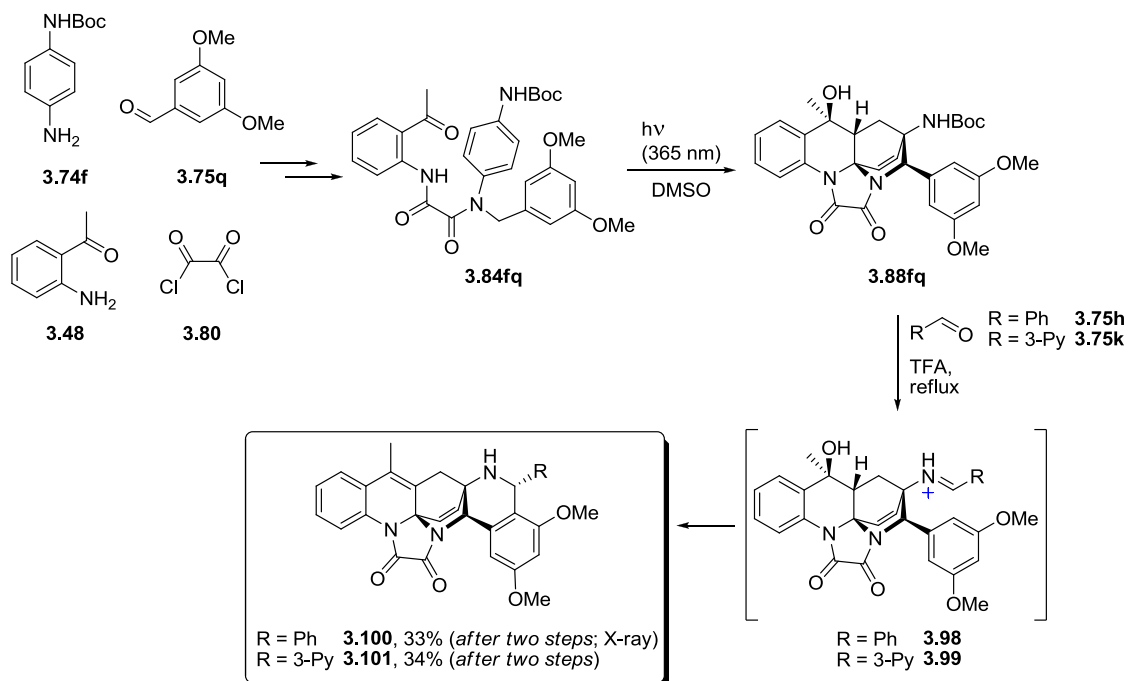
We prepared photoprecursor **3.84fo** in two straightforward steps, by (i) reductive amination of 2-fluoro-nicotinaldehyde **3.75o** with mono-Boc-protected *p*-phenylenediamine **3.74f**, followed by (ii) coupling the resulting aniline **3.79fo** with acyl chloride **3.82** readily obtained from *o*-aminoacetophenone **3.48** and oxalyl chloride **3.80** (Scheme 3.37, a). Irradiation of **3.84fo** provided the secondary photoproduct **3.88fo** outfitted with nucleophilic (NHBoc) and electrophilic (fluoropyridyl) functionalities that are strategically prearranged for further cyclization. We were pleased to discover that simple heating of **3.88fo** in trifluoroacetic acid (TFA) deprotects the amino group and simultaneously activates the electrophilic moiety, enabling the desired formation of the azaindoline **3.96**. This approach was also extended on 2-(methoxycarbonyl)phenyl derivative **3.88fp** that underwent acid-induced lactamization, leading to the dihydroisoquinolone **3.97** (Scheme 3.37, b).



Scheme 3.37

Furthermore, we found that the same conditions are capable of promoting Pictet–Spengler reaction, where the iminium intermediate **3.98/3.99**, generated *in situ* from the amine and the external aldehyde (**3.75h/3.75k**), diastereoselectively alkylates the electron-rich 3,5-dimethoxyphenyl moiety (**Scheme 3.38**). This transformation assembles

the tetrahydroisoquinoline unit decorated with additional functionality, such as phenyl (**3.100**) or 3-pyridyl (**3.101**).



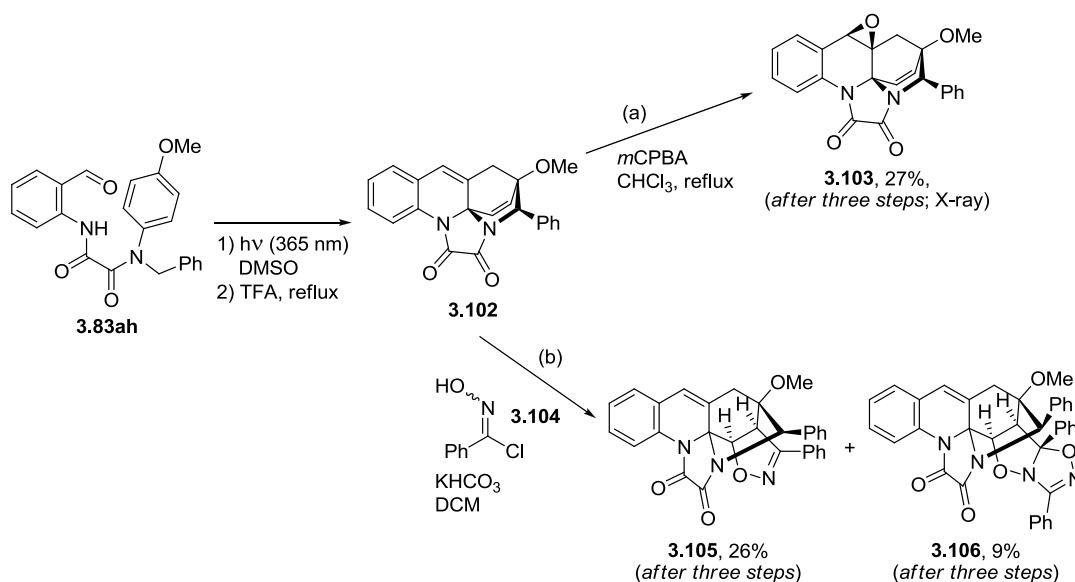
Scheme 3.38

In addition to various cyclizations, treatment with TFA induces dehydration of benzylic alcohol that forms a styrenic double bond. As a result, modified photoproducts contain two alkene fragments that can also be subjected to further transformations enhancing the complexity of the final products.

We discovered that the styrenic olefin can be selectively oxidized with *m*-chloro-peroxybenzoic acid (*m*CPBA): oxirane **3.103** was obtained in 27% after three steps (photocascade, dehydration and epoxidation; **Scheme 3.39**, reaction a). Importantly, the double bond in the azabicyclo[2.2.2]octene core remained intact, presumably due to the effect of the neighboring aminal fragment responsible for $\pi(\text{C}=\text{C}) \rightarrow \sigma^*(\text{C}-\text{N})$ interactions that deplete the alkene of the π density. Furthermore, superior reactivity of

the styrene double bond in the electrophilic epoxidation could be attributable to its enhanced nucleophilic character imparted by the electron donation from *o*-nitrogen. Even though amide nitrogens usually exhibit relatively weak electron-donating properties, this system might be an exception, because structural constraints could lead to misalignment of the lone pair on N atom with the carbonyl group, reducing the $n(\text{N}) \rightarrow \pi^*(\text{C}=\text{O})$ interaction [161].

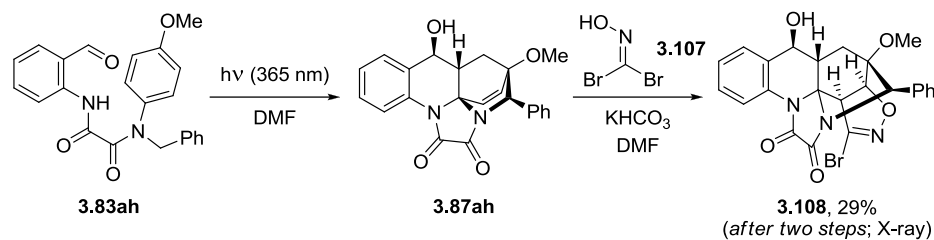
In contrast to the reaction with *m*CPBA, 1,3-dipolar cycloaddition with the *in situ* generated benzonitrile oxide exclusively affected the azabicyclo[2.2.2]octene moiety, furnishing isoxazoline **3.105**, as well as the product of double addition **3.106** (Scheme 3.39, reaction b).



Scheme 3.39

An even more direct route towards isoxazoline-outfitted structures was implemented by running the photochemical cascade in DMF with the subsequent addition of dibromoformaldoxime **3.107** and base (Scheme 3.40). This “one-pot” procedure, carried out with

a single purification, afforded diastereochemically pure bromoisoxazoline **3.108** containing seven contiguous stereocenters and a fully saturated benzene ring.



Scheme 3.40

To summarize, we have developed a new methodology based on the photoinduced two-step cascade reaction that yields complex polyheterocyclic architectures with azabicyclo-[2.2.2]octene core. In the primary photoprocess, ESIPT-generated *o*-azaxylylene undergoes intramolecular dearomative [4+2] cycloaddition to an aniline pendant. The second step of the photocascade involves triplet sensitization of 1,3-cyclohexadiene by the oxalyl amide moiety, 1,5-HAT from the N-CH_n-R,R' carbon to the triplet diene, and the collapse of the diradical intermediate to form [2.2.2]-bicyclic structure; remarkably, KIE studies provide evidence for quantum tunneling in the 1,5-HAT process. The central role in this chemistry belongs to the oxalyl linker, which (i) enables quick modular assembly of the substrates from feedstock chemicals and (ii) initiates a secondary photochemical step. The novel cascade reaction can be used to access photoproducts containing specific functional groups, in order to exploit them in further complexity-building modifications.

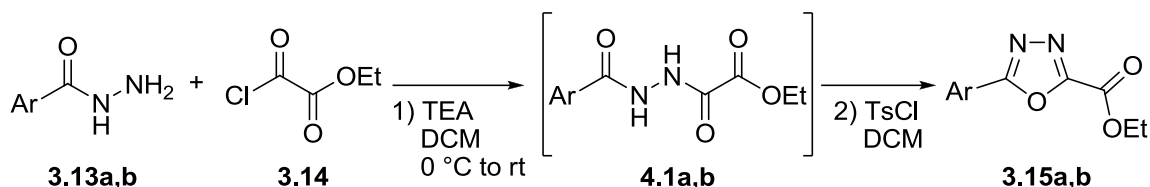
Chapter Four: Experimental Section

General Methods

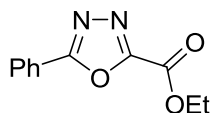
Common solvents were purchased from Fisher Scientific and used as is, except for THF, which was refluxed over and distilled from sodium benzophenone ketyl prior to use. Common reagents were purchased from Sigma-Aldrich, TCI America, AK Scientific, Oakwood Chemical or AstaTech and used without additional purification. NMR spectra were recorded at 25 °C on a Bruker Avance III 500 MHz instrument; spectra are referenced to TMS ($\delta = 0$ ppm, ^1H ; 0 ppm, ^{13}C) or the residual protic solvents: chloroform ($\delta = 7.26$ ppm, ^1H ; 77.16 ppm, ^{13}C), DMSO ($\delta = 2.50$ ppm, ^1H ; 39.52 ppm, ^{13}C), methanol ($\delta = 3.31$ ppm, ^1H ; 49.00 ppm, ^{13}C), DMF ($\delta = 2.75$ ppm, ^1H ; 34.89 ppm, ^{13}C), DCM ($\delta = 54.00$ ppm, ^{13}C), acetone ($\delta = 2.05$ ppm, ^1H). High resolution mass spectra were obtained on a Waters Synapt G2 HDMS Quadrupole/ToF mass spectrometer with electrospray ionization (Central Analytical Laboratory, University of Colorado Boulder). Flash column chromatography was performed using Teledyne Isco RediSep[®] Rf Normal Phase Silica Gel (230–400 mesh or 400–632 mesh) on a Teledyne Isco CombiFlash[®] Rf 200 instrument. X-ray structures were obtained with a Bruker SMART APEX II diffractometer (see Appendix A).

Experimental Section for Project 1

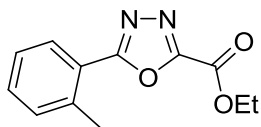
Synthesis of Photoprecursors



General Procedure A for the Synthesis of Ethyl 5-Aryl-1,3,4-oxadiazole-2-carboxylates. Used a modified literature protocol [116]. Under nitrogen, aryl-2-carbohydrazide (**3.13**; 7.00 mmol) and TEA (21.0 mmol) were dissolved in DCM (50 mL), the solution was cooled to 0 °C, and then ethyl oxalyl chloride (**3.14**; 7.70 mmol) was added dropwise. The reaction mixture was slowly warmed to room temperature, stirred for 8 h, and treated with TsCl (7.00 mmol). After stirring overnight, the mixture was diluted with DCM (40 mL) and washed 3 times with sat. aq. NaHCO₃ (2 mL) diluted with water (10 mL), and then with water (20 mL). The organic layer was dried over anhydrous Na₂SO₄, filtered, and the solvent was removed *in vacuo* to yield the desired oxadiazole ester (**3.15**; if necessary, the product was additionally purified by flash chromatography on silica gel).

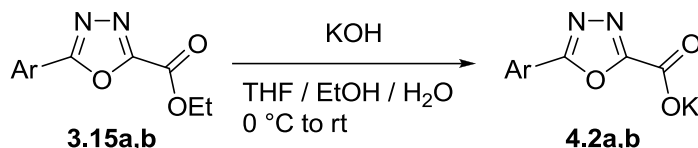


Ethyl 5-Phenyl-1,3,4-oxadiazole-2-carboxylate (3.15a). General procedure **A** was followed on a 36.5 mmol scale of benzhydrazide (**3.13a**), which after flash chromatography on silica gel (gradient elution: hexane → hexane–ethyl acetate 80:20) afforded 6.32 g (79%) of the title compound. ¹H NMR (500 MHz, CDCl₃) δ 8.09 – 8.03 (m, 2H), 7.54 – 7.49 (m, 1H), 7.48 – 7.42 (m, 2H), 4.48 (q, *J* = 7.2 Hz, 2H), 1.40 (t, *J* = 7.2 Hz, 3H). ¹³C NMR (126 MHz, CDCl₃) δ 166.3, 156.4, 154.3, 132.7, 129.2, 127.5, 122.7, 63.4, 14.0.

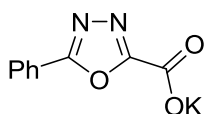


Ethyl 5-(2-Methylphenyl)-1,3,4-oxadiazole-2-carboxylate

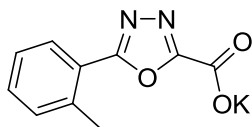
(3.15b). General procedure **A** was followed in a 6.73 mmol scale of *o*-toluic hydrazide (**3.13b**), which afforded 1.53 g (98%) of the title compound. ¹H NMR (500 MHz, CDCl₃) δ 8.05 (dd, *J* = 7.8, 1.4 Hz, 1H), 7.48 (td, *J* = 7.6, 1.5 Hz, 1H), 7.41 – 7.33 (m, 2H), 4.56 (q, *J* = 7.1 Hz, 2H), 2.75 (s, 3H), 1.48 (t, *J* = 7.1 Hz, 3H). ¹³C NMR (126 MHz, CDCl₃) δ 166.9, 156.2, 154.6, 139.3, 132.3, 132.0, 129.7, 126.4, 122.0, 63.5, 22.1, 14.2.



General Procedure B for the Synthesis of Potassium 5-Aryl-1,3,4-oxadiazole-2-carboxylates. 5-Aryl-1,3,4-oxadiazole-2-carboxylic acid ethyl ester (**3.15**; 4.00 mmol) was dissolved in THF (14 mL) and EtOH (3 mL). The solution was cooled to 0 °C and treated with KOH (4.20 mmol) in H₂O (1 mL). The resulting mixture was stirred at ambient temperature for 1 h. The product (**4.2**) precipitated out of the solution and was separated by filtration.



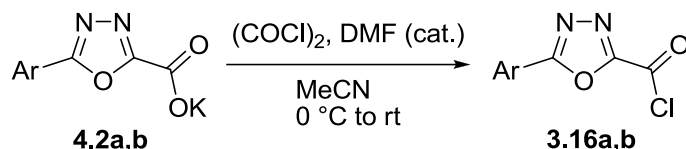
Potassium 5-Phenyl-1,3,4-oxadiazole-2-carboxylate (4.2a). General procedure **B** was followed on a 14.2 mmol scale of **3.15a**, which afforded 2.66 g (82%) of the title compound. ¹H NMR (500 MHz, MeOD) δ 8.15 – 8.11 (m, 2H), 7.65 – 7.55 (m, 3H). ¹³C NMR (126 MHz, MeOD) δ 166.4, 163.1, 159.5, 133.4, 130.4, 128.2, 125.0.



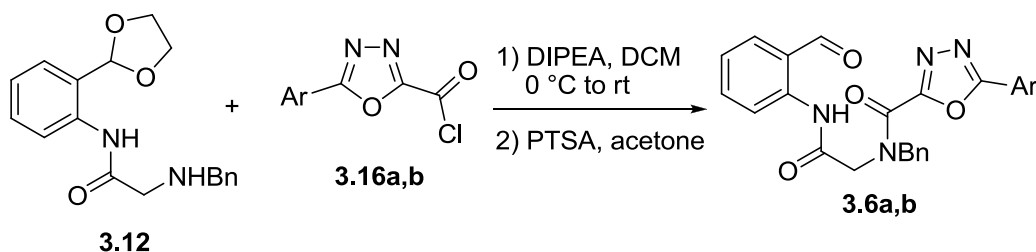
Potassium 5-(4-Methylphenyl)-1,3,4-oxadiazole-2-carboxylate

(4.2b). General procedure **B** was followed on a 6.59 mmol scale of

3.15b with 8.24 mmol of KOH, which afforded 1.46 g (92%) of the title compound. ^1H NMR (500 MHz, MeOD) δ 8.01 (dd, $J = 7.8, 1.4$ Hz, 1H), 7.48 (td, $J = 7.5, 1.5$ Hz, 1H), 7.43 – 7.40 (m, 1H), 7.40 – 7.36 (m, 1H), 2.69 (s, 3H). ^{13}C NMR (126 MHz, MeOD) δ 166.7, 162.7, 159.6, 139.8, 132.8, 132.8, 130.4, 127.4, 124.1, 21.9.



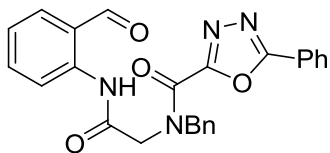
General Procedure C for the Synthesis of Acyl Chlorides. Under nitrogen, to a stirred suspension of potassium 5-aryl-1,3,4-oxadiazole-2-carboxylate (**4.2**; 2.50 mmol) in acetonitrile (10 mL) cooled to 0 °C, oxalyl chloride (2.62 mmol) was added dropwise over 10 min. DMF (3 drops, ca. 0.03 mL) was added to the reaction mixture, and vigorous gas evolution was observed. The resulting reaction mixture was stirred for 2 h and used for the next step without purification.



General Procedure D for Amide Coupling Followed by Dioxolane Deprotection.

Under nitrogen, *N*-(2-(1,3-dioxolan-2-yl)phenyl)-2-(benzylamino)acetamide [7] (**3.12**; 2.00 mmol) was dissolved in DCM (10 mL), the solution was treated with DIPEA (6.00 mmol) and cooled to 0 °C, and then suspension of acyl chloride (**3.16**; 1.4 mmol) in

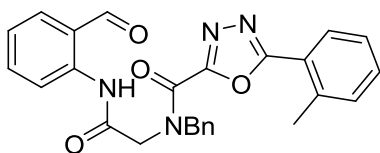
acetonitrile (prepared according to general procedure **C**) was added dropwise. The reaction mixture was stirred at 0 °C for 30 min, and then at ambient temperature overnight. The reaction was quenched with water (5 mL), and aqueous layer was extracted with DCM (2×25 mL). The combined organic layers were dried over anhydrous Na₂SO₄, filtered, and the solvent was removed *in vacuo* to yield crude dioxolane-protected photoprecursor, which was then purified by flash chromatography on silica gel (gradient elution: hexane → hexane–ethyl acetate 70:30) and subsequently deprotected by stirring with TsOH·H₂O (0.400 mmol) in acetone (15 mL) at ambient temperature for 1 day. Solvent was removed *in vacuo*, and the residue was dissolved in DCM (25 mL). The solution was washed with sat. aq. NaHCO₃ (2×5 mL) and then with water (5 mL). The organic layer was dried over anhydrous Na₂SO₄, filtered and concentrated *in vacuo*. Further purification by flash chromatography on silica gel yielded the desired photoprecursor (**3.6**).



***N*-Benzyl-*N*-(2-(2-formylphenylamino)-2-oxoethyl)-5-phenyl-1,3,4-oxadiazole-2-carboxamide (**3.6a**).** General procedure **C** was followed on an 11.7 mmol scale of **4.2a**,

and the resulting acyl chloride **3.16a** was coupled with 9.75 mmol of **3.12** according to general procedure **D**, which after flash chromatography on silica gel (gradient elution: hexane → hexane–ethyl acetate 70:30) afforded 2.37 g (55% after two steps) of the title compound in a form of two equilibrating rotamers (*A* and *B*). ¹H NMR (500 MHz, CDCl₃) δ 11.51 (s, 1H, *A*), 11.49 (s, 1H, *B*), 9.87 (d, *J* = 0.7 Hz, 1H, *B*), 9.86 (d, *J* = 0.7 Hz, 1H, *A*), 8.71 (d, *J* = 8.4 Hz, 1H, *A*), 8.66 (d, *J* = 8.4 Hz, 1H, *B*), 8.19 – 8.16 (m, 2H, *A*), 8.16 – 8.14 (m, 2H, *B*), 7.70 – 7.47 (m, 11H, *A+B*), 7.44 – 7.29 (m, 11H, *A+B*), 7.27

(dd, $J = 7.4, 1.0$ Hz, 1H, *B*), 7.24 (dd, $J = 7.4, 1.0$ Hz, 1H, *A*), 5.46 (s, 2H, *A*), 4.96 (s, 2H, *B*), 4.86 (s, 2H, *B*), 4.33 (s, 2H, *A*). ^{13}C NMR (126 MHz, CDCl_3) δ 195.7, 195.7, 167.1, 166.5, 165.9, 165.8, 158.4, 158.1, 155.8, 155.6, 140.3, 140.3, 136.4, 136.3, 136.1, 136.0, 135.3, 135.1, 132.7, 129.3, 129.3, 129.1, 129.1, 128.9, 128.4, 128.4, 128.3, 127.8, 127.7, 123.6, 123.1, 123.0, 122.0, 122.0, 120.1, 120.1, 53.9, 52.5, 51.5, 50.4. HRMS (ESI) calcd for $\text{C}_{25}\text{H}_{21}\text{N}_4\text{O}_4^+$ (MH^+) 441.1563, found 441.1557.

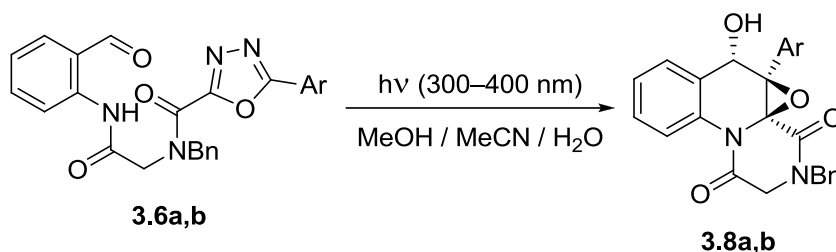


***N*-Benzyl-*N*-(2-(2-formylphenylamino)-2-oxoethyl)-5-(2-methylphenyl)-1,3,4-oxadiazole-2-carboxamide**

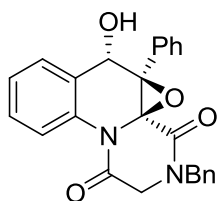
(3.6b). General procedure **C** was followed on an 5.87

mmol scale of **4.2b**, and the resulting acyl chloride **3.16b** was coupled with 4.19 mmol of **3.12** according to general procedure **D**, which after flash chromatography on silica gel (gradient elution: hexane \rightarrow hexane–ethyl acetate 70:30) afforded 0.368 g (19% after two steps) of the title compound in a form of two equilibrating rotamers (*A* and *B*). ^1H NMR (500 MHz, CDCl_3) δ 11.50 (s, 1H, *A*), 11.49 (s, 1H, *B*), 9.84 (s, 1H, *A* + 1H, *B*), 8.70 (d, $J = 8.5$ Hz, 1H, *A*), 8.65 (d, $J = 8.5$ Hz, 1H, *B*), 8.06 (t, $J = 6.4$ Hz, 1H, *A* + 1H, *B*), 7.68 – 7.62 (m, 1H, *A* + 1H, *B*), 7.59 (q, $J = 8.9$ Hz, 1H, *A* + 1H, *B*), 7.49 – 7.19 (m, 9H, *A* + 9H, *B*), 5.45 (s, 2H, *B*), 4.94 (s, 2H, *A*), 4.87 (s, 2H, *A*), 4.32 (s, 2H, *B*), 2.75 (s, 3H, *A*), 2.70 (s, 3H, *B*). ^{13}C NMR (126 MHz, CDCl_3) δ 195.6, 195.6, 167.1, 166.4, 166.2, 166.0, 157.9, 157.6, 155.9, 155.6, 140.2, 140.2, 139.2, 139.2, 136.3, 136.2, 136.0, 136.0, 135.3, 135.1, 132.1, 132.0, 131.9, 129.8, 129.7, 129.0, 129.0, 128.9, 128.4, 128.3, 128.2, 126.4, 126.4, 123.5, 122.1, 122.0, 121.9, 120.0, 120.0, 53.8, 52.4, 51.4, 50.4, 22.3, 22.2. HRMS (ESI) calcd for $\text{C}_{26}\text{H}_{23}\text{N}_4\text{O}_4^+$ (MH^+) 455.1714, found 455.1701.

Photochemical Reactions



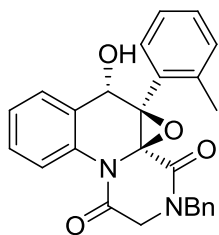
General Procedure E for the Photoassisted Synthesis of Epoxides. Photoprecursor (**3.6**; 1.00 mmol) was dissolved in MeCN (16 mL). MeOH (64 mL) and water (4.5 mL) were added, and the solution was degassed by bubbling nitrogen or argon for 30 min. The mixture was irradiated in a Pyrex reaction vessel using Rayonet photoreactor equipped with RPR-3500 UV lamps (broadband 300-400 nm UV source with peak emission at 350 nm), with the reaction progress monitored by ¹H NMR. After completion, solvents were removed *in vacuo*, and the solid residue was washed with methanol (10 mL), filtered and air-dried to yield the desired epoxide photoproduct (**3.8**).



***anti*-9-Hydroxy-3-benzyl-10-phenyl-7,8-benzo-11-oxa-3,6-**

diazatricyclo[8.1.0.0^{1,6}]undeca-7-ene-2,5-dione (3.8a**).** General

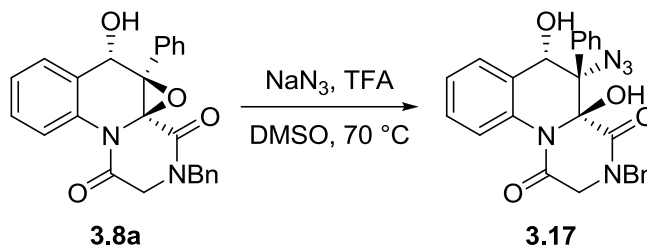
procedure **E** was followed on a 0.953 mmol scale of **3.6a**, which afforded 0.230 g (59%) of the title compound. ¹H NMR (500 MHz, CDCl₃) δ 7.68 – 7.62 (m, 2H), 7.56 (dt, *J* = 8.0, 0.7 Hz, 1H), 7.49 – 7.39 (m, 4H), 7.40 – 7.34 (m, 3H), 7.32 (td, *J* = 7.4, 1.2 Hz, 1H), 7.27 (dd, *J* = 7.5, 1.6 Hz, 1H), 7.21 – 7.10 (m, 2H), 5.24 (d, *J* = 4.2 Hz, 1H), 4.79 (d, *J* = 14.4 Hz, 1H), 4.35 (d, *J* = 14.4 Hz, 1H), 4.06 (s, 2H), 2.72 (d, *J* = 4.2 Hz, 1H). ¹³C NMR (126 MHz, CDCl₃) δ 164.2, 158.3, 134.9, 133.3, 131.9, 130.5, 129.6, 129.1, 129.0, 129.0, 128.7, 128.5, 128.3, 127.8, 127.7, 126.7, 74.2, 70.7, 69.4, 50.2, 49.4. HRMS (ESI) calcd for C₂₅H₂₀N₂NaO₄⁺ (MNa⁺) 435.1321, found 435.1345.



anti-9-Hydroxy-3-benzyl-10-(2-methylphenyl)-7,8-benzo-11-oxa-3,6-diazatricyclo[8.1.0.0^{1,6}]undeca-7-ene-2,5-dione (3.8b). General procedure **E** was followed on a 0.722 mmol scale of **3.6b**, which afforded 0.160 g (52%) of the title compound in a form of two

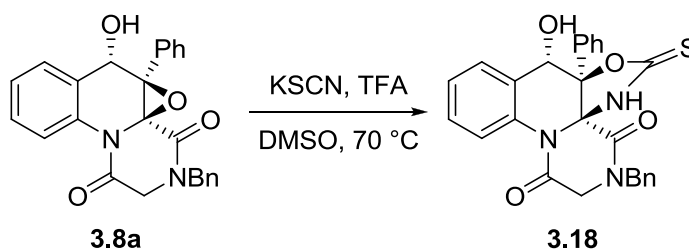
equilibrating rotamers (*A* and *B*). ¹H NMR (500 MHz, DMSO) δ 7.64 – 7.17 (m, 12H, *A* + 11H, *B*), 7.15 – 6.99 (m, 1H, *A* + 2H, *B*), 6.08 (s, 1H, *B*), 5.96 (d, *J* = 7.6 Hz, 1H, *A*), 5.04 (d, *J* = 7.5 Hz, 1H, *A* + 1H, *B*), 4.91 (d, *J* = 14.5 Hz, 1H, *A*), 4.61 (d, *J* = 14.3 Hz, 1H, *B*), 4.51 (d, *J* = 14.4 Hz, 1H, *B*), 4.44 – 4.28 (m, 2H, *A* + 2H, *B*), 4.25 (d, *J* = 14.5 Hz, 1H, *A*), 2.34 (s, 3H, *A*), 2.08 (s, 3H, *B*). ¹³C NMR (126 MHz, DMSO) δ 163.6, 157.9, 136.1, 135.7, 131.8, 131.7, 131.5, 130.3, 130.2, 129.2, 128.8, 128.6, 128.4, 128.0, 127.8, 126.7, 125.9, 124.2, 71.3, 70.7, 68.7, 49.6, 49.1, 18.6. HRMS (ESI) calcd for C₂₆H₂₃N₂O₄⁺ (MH⁺) 427.1653, found 427.1671.

Post-Photochemical Modifications



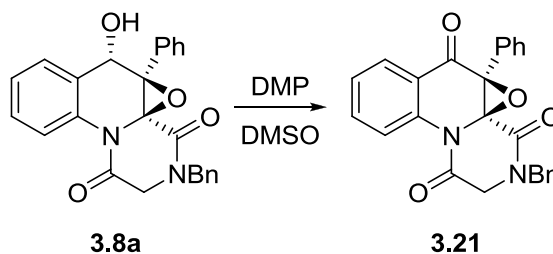
(±)-(4a*S*,5*S*,6*S*)-5-Azido-3-benzyl-4a,6-dihydroxy-5-phenyl-2,3,5,6-tetrahydro-1*H*-pyrazino[1,2-*a*]quinoline-1,4(4a*H*)-dione (3.17). *Safety note:* sodium azide and trifluoroacetic acid can produce highly toxic hydrazoic acid [162]; furthermore, care should be taken when inorganic azides are used in the presence of DCM, due to potential formation of explosive diazidomethane [163, 164]. Epoxide **3.8a** (0.116 g, 0.281 mmol) was dissolved in DMSO (2.81 mL) under nitrogen. Trifluoroacetic acid (108 μL, 1.41

mmol) and sodium azide (0.274 g, 4.22 mmol) were added, and the mixture was stirred at 70 °C for 43 h. The reaction mixture was allowed to cool down to ambient temperature and was concentrated under high vacuum (60 °C/0.15 Torr). The residue was taken in DCM (40 mL) and washed with water (4x10 mL). The product was extracted from aqueous layer with DCM (2x20 mL). The combined organic layers were dried over anhydrous Na₂SO₄, filtered, and the solvent was removed *in vacuo*. Further purification by flash chromatography on silica gel pretreated with pyridine (gradient elution: hexane → hexane–ethyl acetate + 1% TEA 50:50) afforded 0.067 g (52%) of the title compound. ¹H NMR (500 MHz, CDCl₃) δ 7.77 – 7.72 (m, 1H), 7.56 – 7.46 (m, 6H), 7.45 – 7.34 (m, 5H), 7.29 (dd, *J* = 7.6, 1.9 Hz, 2H), 6.14 (d, *J* = 6.3 Hz, 1H), 4.84 (s, 1H), 4.66 (d, *J* = 14.2 Hz, 1H), 4.48 (d, *J* = 17.8 Hz, 1H), 4.47 (d, *J* = 14.2 Hz, 1H), 4.08 (d, *J* = 17.8 Hz, 1H), 2.24 (d, *J* = 6.3 Hz, 1H). ¹³C NMR (126 MHz, CDCl₃) δ 164.1, 163.0, 134.4, 134.3, 132.8, 130.0, 129.3, 129.2, 129.2, 129.1, 128.8, 127.9, 127.8, 127.5, 127.0, 126.7, 86.9, 72.7, 72.7, 51.2, 50.9. HRMS (ESI) calcd for C₂₅H₂₁N₅NaO₄⁺ (MNa⁺) 478.1486, found 478.1514.



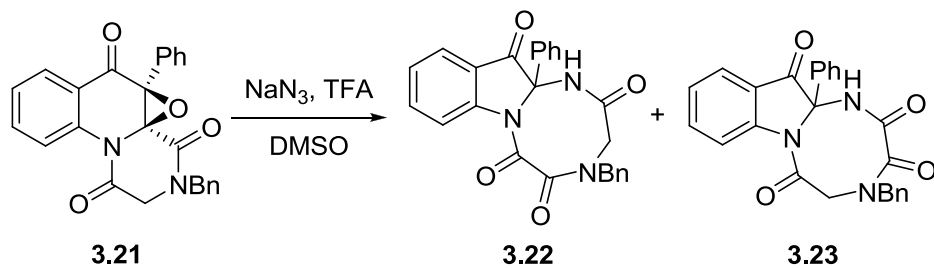
(±)-(4¹R,7aS,8S)-3-Benzyl-8-hydroxy-7a-phenyl-6-thioxo-2,3,5,6,7a,8-hexahydrooxazolo[4,5-*b*]pyrazino[1,2-*a*]quinoline-1,4-dione (3.18). Epoxide **3.8a** (0.197 g, 0.478 mmol) was dissolved in DMSO (16.0 mL) under nitrogen. Trifluoroacetic acid (73.2 μL, 0.955 mmol) and potassium thiocyanate (0.465 g, 4.78 mmol) were added,

and the mixture was stirred at 70 °C for 35 h. The reaction mixture was allowed to cool to ambient temperature and concentrated under high vacuum (60 °C/0.15 Torr). The residue was taken in DCM (70 mL) and washed with water (3×20 mL). The product was extracted from aqueous layer with DCM (50 mL). The combined organic layers were dried over anhydrous Na₂SO₄, filtered, and the solvent was removed *in vacuo*. Further purification by flash chromatography on silica gel pretreated with pyridine (gradient elution: hexane → hexane–ethyl acetate + 1% TEA 50:50) afforded 0.134 g (60%) of the title compound. ¹H NMR (500 MHz, MeOD) δ 7.63 – 7.56 (m, 2H), 7.49 (ddd, *J* = 7.8, 6.9, 2.0 Hz, 1H), 7.45 – 7.30 (m, 9H), 7.27 (dd, *J* = 7.5, 2.0 Hz, 2H), 4.62 (s, 1H), 4.56 (d, *J* = 14.3 Hz, 1H), 4.43 (d, *J* = 18.7 Hz, 1H), 4.35 (d, *J* = 14.3 Hz, 1H), 4.23 (d, *J* = 18.7 Hz, 1H). ¹³C NMR (126 MHz, MeOD) δ 188.3, 164.8, 162.4, 137.2, 136.6, 135.8, 135.6, 130.4, 130.2, 130.2, 130.0, 129.6, 129.4, 129.4, 129.2, 128.9, 127.5, 98.1, 85.1, 74.3, 51.2, 49.8. HRMS (ESI) calcd for C₂₆H₂₂N₃O₄S⁺ (MH⁺) 472.1326, found 472.1320.



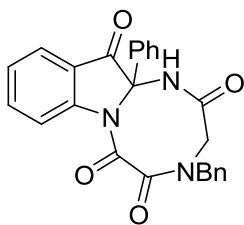
(±)-(4¹*S*,5a⁵*S*)-3-Benzyl-5a-phenyl-2,3-dihydrooxireno[2,3-*b*]pyrazino[1,2-*a*]quinoline-1,4,6(5a*H*)-trione (**3.21**). Hydroxy-epoxide **3.8a** (0.688 g, 1.67 mmol) was dissolved in DMSO (16.7 mL) under nitrogen. Dess–Martin periodinane (0.849 g, 2.00 mmol) was added, and the mixture was stirred at room temperature for 17 h. The reaction mixture was concentrated under high vacuum (60 °C/0.15 Torr), then the residue was taken in chloroform (90 mL) and washed with saturated aq. NaHCO₃ (10 mL) and

water (3×20 mL). The product was extracted from aqueous layer with chloroform (50 mL). The combined organic layers were dried over anhydrous Na₂SO₄, filtered, and the solvent was removed *in vacuo*. Further purification by flash chromatography on silica gel pretreated with pyridine (gradient elution: hexane → hexane–ethyl acetate + 1% TEA 80:20) afforded 0.465 g (68%) of the title compound. ¹H NMR (500 MHz, CDCl₃) δ 7.85 (dd, *J* = 7.7, 1.6 Hz, 1H), 7.71 (dd, *J* = 8.2, 1.1 Hz, 1H), 7.64 (ddd, *J* = 8.4, 7.4, 1.6 Hz, 1H), 7.51 – 7.36 (m, 6H), 7.32 (qd, *J* = 3.9, 1.8 Hz, 3H), 7.14 – 7.07 (m, 2H), 4.70 (d, *J* = 14.4 Hz, 1H), 4.33 (d, *J* = 14.4 Hz, 1H), 4.16 (d, *J* = 18.6 Hz, 1H), 4.07 (d, *J* = 18.6 Hz, 1H). ¹³C NMR (126 MHz, CDCl₃) δ 189.5, 163.1, 156.0, 134.6, 134.4, 133.8, 129.3, 129.1, 128.7, 128.6, 128.3, 128.0, 127.7, 127.6, 127.4, 126.6, 125.8, 72.7, 70.7, 50.4, 49.4. HRMS (ESI) calcd for C₂₅H₁₈N₂NaO₄⁺ (MNa⁺) 433.1159, found 433.1173.

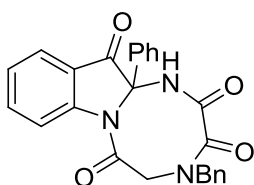


4-Benzyl-12a-phenyl-1,3,4,12a-tetrahydro-[1,3,6]triazocino[1,2-*a*]indole-2,5,6,12-tetraone (3.22) and **4-Benzyl-12a-phenyl-1,4,5,12a-tetrahydro-[1,3,6]triazocino[1,2-*a*]indole-2,3,6,12-tetraone (3.23)**. Keto-epoxide **3.21** (0.137 g, 0.333 mmol) was dissolved in DMSO (11.1 mL) under nitrogen. Trifluoroacetic acid (25.5 μL, 0.333 mmol) and sodium azide (65 mg, 0.999 mmol) were added, and the mixture was stirred at room temperature for 13 h. The reaction mixture was concentrated under high vacuum (60 °C/0.15 Torr), and further purification by flash chromatography on silica gel

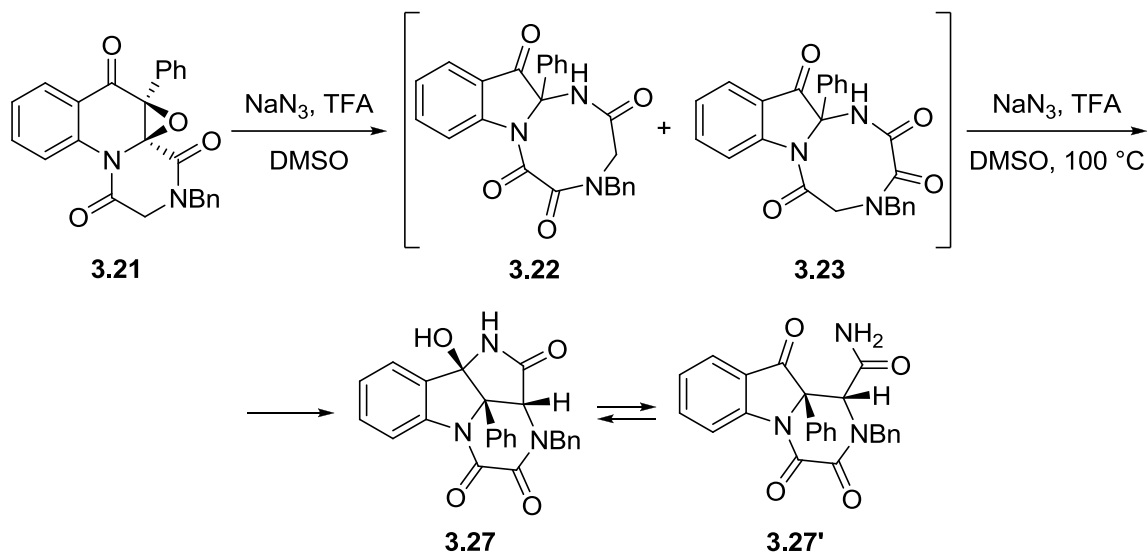
pretreated with pyridine (gradient elution: hexane → hexane–ethyl acetate + 1% TEA 70:30) afforded 0.052 g (37%) of **3.22** and 0.039 g (27%) of **3.23**.



3.22: ^1H NMR (500 MHz, CDCl_3) δ 8.75 (dd, $J = 9.1, 0.9$ Hz, 1H), 7.95 – 7.87 (m, 2H), 7.49 (td, $J = 7.5, 0.9$ Hz, 1H), 7.48 – 7.42 (m, 3H), 7.36 – 7.29 (m, 3H), 7.29 – 7.20 (m, 4H), 6.63 (s, 1H), 4.66 (dd, $J = 14.4, 1.5$ Hz, 1H), 4.30 (dd, $J = 17.1, 1.6$ Hz, 1H), 3.83 (d, $J = 17.2$ Hz, 1H), 3.56 (d, $J = 14.6$ Hz, 1H). ^{13}C NMR (126 MHz, CDCl_3) δ 192.2, 168.0, 162.7, 161.5, 152.4, 139.2, 134.1, 133.9, 130.6, 129.7, 129.1, 129.0, 128.4, 127.2, 126.5, 125.0, 119.7, 119.7, 78.2, 50.1, 48.9. HRMS (ESI) calcd for $\text{C}_{25}\text{H}_{19}\text{N}_3\text{NaO}_4^+$ (MNa^+) 448.1268, found 448.1284.



3.23: ^1H NMR (500 MHz, CDCl_3) δ 8.68 (d, $J = 8.5$ Hz, 1H), 7.81 (ddd, $J = 8.6, 7.3, 1.4$ Hz, 1H), 7.73 (d, $J = 7.4$ Hz, 1H), 7.71 (dd, $J = 7.8, 1.5$ Hz, 1H), 7.49 (t, $J = 7.8$ Hz, 1H), 7.37 (tt, $J = 7.4, 1.2$ Hz, 1H), 7.36 – 7.23 (m, 6H), 7.21 (dd, $J = 7.5, 2.0$ Hz, 2H), 7.11 (d, $J = 8.0$ Hz, 1H), 4.52 (dd, $J = 17.1, 1.6$ Hz, 1H), 4.45 (dd, $J = 14.6, 1.6$ Hz, 1H), 3.97 (d, $J = 17.1$ Hz, 1H), 3.36 (d, $J = 14.6$ Hz, 1H). ^{13}C NMR (126 MHz, CDCl_3) δ 192.0, 165.7, 165.3, 161.7, 151.4, 138.7, 134.0, 133.6, 130.4, 129.1, 129.0, 128.4, 128.4, 128.3, 126.4, 126.1, 123.5, 119.2, 119.2, 80.2, 51.4, 49.0. HRMS (ESI) calcd for $\text{C}_{25}\text{H}_{19}\text{N}_3\text{NaO}_4^+$ (MNa^+) 448.1268, found 448.1286.

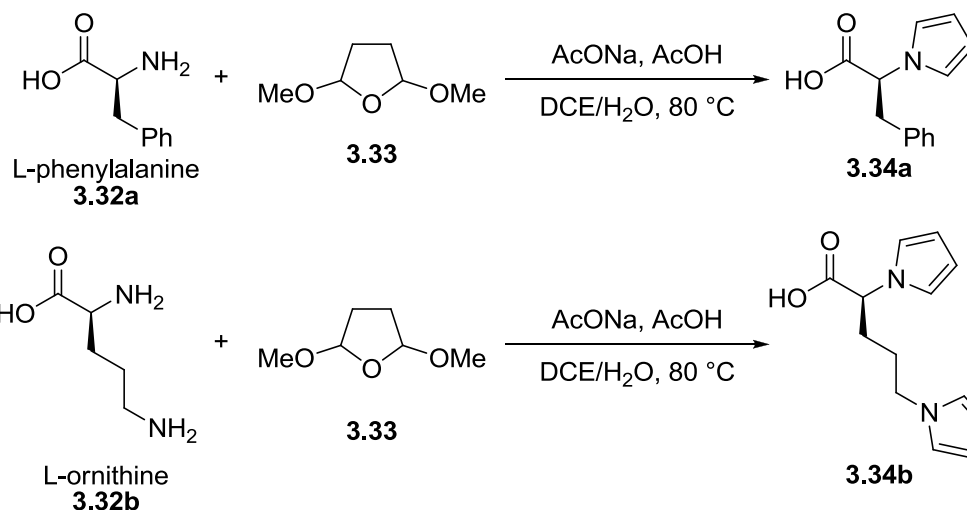


(±)-(2a_S,2a¹_S,9b_R)-3-Benzyl-9b-hydroxy-2a¹-phenyl-1,3,5a-triaza-2a,3-dihydro-1*H*-cyclopenta[*jk*]fluorene-2,4,5(2a¹_H,5a_H,9b_H)-trione (**3.27**) and (±)-(1*R*,10a_S)-2-Benzyl-3,4,10-trioxo-10a-phenyl-1,2,3,4,10,10a-hexahydropyrazino[1,2-*a*]indole-1-carboxamide (**3.27'**). Keto-epoxide **3.21** (0.200 g, 0.487 mmol) was dissolved in DMSO (16.2 mL) under nitrogen. Trifluoroacetic acid (37.3 μL, 0.487 mmol) and sodium azide (0.475 g, 7.31 mmol) were added, and the mixture was stirred at room temperature for 2 h, and then at 100 °C for 2 h. The reaction mixture was concentrated under high vacuum (60 °C/0.15 Torr), and further purification by flash chromatography on silica gel pretreated with pyridine (gradient elution: hexane → hexane–ethyl acetate + 1% TEA 50:50) afforded 0.095 g (46%) of the product in a form of two equilibrating isomers, **3.27** and **3.27'**. ¹H NMR (500 MHz, MeOD) δ 8.53 (d, *J* = 8.4 Hz, 1H, **3.27'**), 8.18 (d, *J* = 8.0 Hz, 1H, **3.27**), 7.87 (ddd, *J* = 8.5, 7.4, 1.4 Hz, 1H, **3.27'**), 7.71 (d, *J* = 7.7 Hz, 1H, **3.27'**), 7.53 (td, *J* = 7.8, 1.4 Hz, 1H, **3.27**), 7.45 (dd, *J* = 7.6, 1.2 Hz, 1H, **3.27**), 7.39 (td, *J* = 7.6, 0.9 Hz, 1H, **3.27'**), 7.37 – 7.27 (m, 1H, **3.27**, 3H, **3.27'**), 7.26 (td, *J* = 7.4, 1.2 Hz, 2H,

3.27), 7.25 – 7.18 (m, 3H, **3.27'**), 7.15 (td, $J = 7.8, 1.4$ Hz, 4H, **3.27**), 7.11 (t, $J = 7.7$ Hz, 2H, **3.27'**), 6.97 (d, $J = 8.1$ Hz, 4H, **3.27**), 6.88 (d, $J = 7.5$ Hz, 2H, **3.27'**), 5.55 (d, $J = 14.7$ Hz, 1H, **3.27**), 5.06 (s, 1H, **3.27'**), 5.03 (s, 1H, **3.27**), 4.91 (d, $J = 14.8$ Hz, 1H, **3.27'**), 4.28 (d, $J = 14.7$ Hz, 1H, **3.27**), 4.02 (d, $J = 14.7$ Hz, 1H, **3.27'**). ^{13}C NMR (126 MHz, MeOD) δ 194.7, 171.8, 169.5, 159.8, 157.5, 155.9, 155.2, 152.0, 141.3, 139.3, 135.9, 135.6, 135.5, 133.8, 133.5, 131.9, 130.4, 130.4, 130.0, 129.9, 129.7, 129.7, 129.6, 129.6, 129.2, 129.0, 128.2, 128.0, 127.6, 126.1, 126.0, 124.8, 124.1, 119.5, 118.8, 93.3, 74.6, 73.2, 63.5, 61.3, 51.7, 51.6, 49.6. HRMS (ESI) calcd for $\text{C}_{25}\text{H}_{20}\text{N}_3\text{O}_4^+$ (MH^+) 426.1449, found 426.1469.

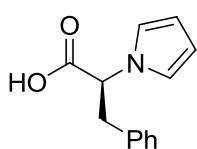
Experimental Section for Project 2

Synthesis of Photoprecursors



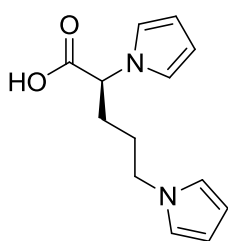
General Procedure A for the Synthesis of 2-(1H-Pyrrol-1-yl)alkanoic acids. Used a modified literature protocol [49]. Amino acid (**3.32**; 60.6 mmol) and anhydrous sodium acetate (5.02 g, 61.2 mmol) were dissolved in water (81 mL), glacial AcOH (27 mL) and DCE (81 mL). The mixture was stirred at 80 °C for 10 min, treated with

2,5-dimethoxytetrahydrofuran (**3.33**; 7.92 mL, 8.08 g, 60.6 mmol), and stirred at 80 °C for 7–14 h. After cooling to ambient temperature, the product was extracted with DCM (3×100 mL), the combined organic layers were subsequently washed with sat. aq. NaCl (50 mL) and water (50 mL), dried over anhydrous Na₂SO₄, filtered and concentrated *in vacuo*. The residue was filtered through silica gel. Two fractions were collected: first fraction was obtained by eluting with 500 mL of hexanes–ethyl acetate 98:2, second fraction was obtained by eluting with 1000 mL of hexanes–ethyl acetate 50:50. The second fraction was concentrated *in vacuo* to afford the desired pyrrole derivative (**3.34**).



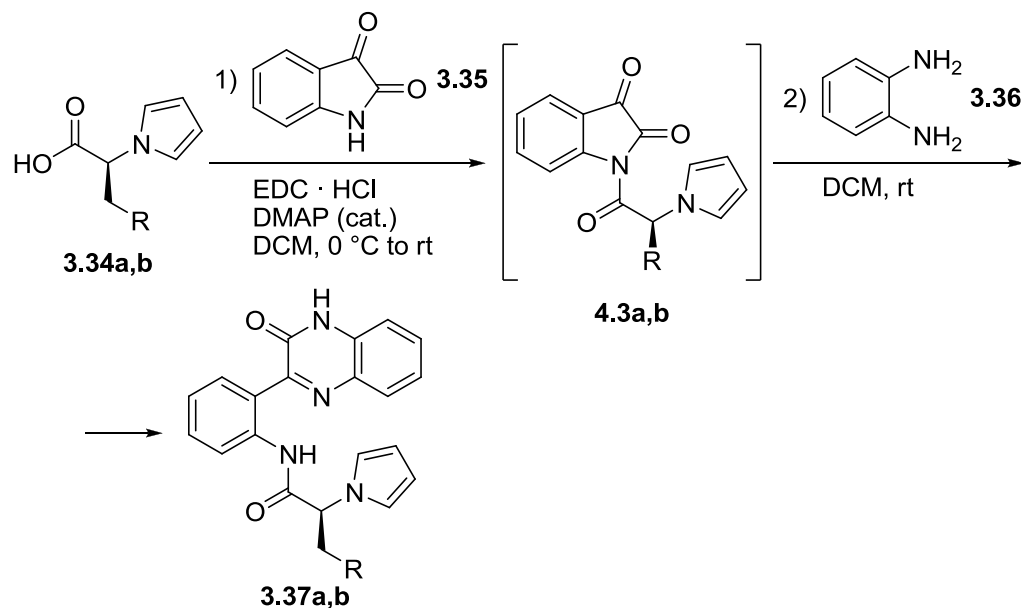
(S)-3-Phenyl-2-(1H-pyrrol-1-yl)propanoic acid (3.34a). General procedure **A** was followed on a 60.6 mmol scale of L-phenylalanine (**3.32a**), which afforded 5.36 g (41%) of the title compound. ¹H NMR

(500 MHz, CDCl₃) δ 7.24 (m, 3H), 7.02 (dd, *J* = 7.6, 1.9, 2H), 6.71 (t, *J* = 2.2, 2H), 6.17 (t, *J* = 2.1, 2H), 4.80 (dd, *J* = 9.2, 5.9, 1H), 3.46 (dd, *J* = 14.0, 5.9, 1H), 3.30 (dd, *J* = 14.0, 9.2, 1H).

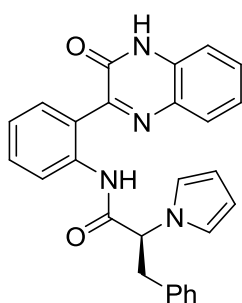


(S)-2,5-Di(1H-pyrrol-1-yl)pentanoic acid (3.34b). General procedure **A** was followed on a 11.9 mmol scale of L-ornithine monohydrochloride (**3.32b**) with 23.7 mmol of sodium acetate and 23.7 mmol of **3.33**, which afforded 1.38 g (50%) of the title

compound. ¹H NMR (500 MHz, CDCl₃) δ 6.68 (t, *J* = 2.2, 2H), 6.60 (t, *J* = 2.1, 2H), 6.20 (t, *J* = 2.2, 2H), 6.15 (t, *J* = 2.1, 2H), 4.44 (dd, *J* = 10.3, 5.4, 1H), 3.86 (t, *J* = 6.8, 2H), 2.12 (m, 1H), 2.02 (m, 1H), 1.75 (m, 1H), 1.65 (m, 1H).



General Procedure B for One-Pot Coupling and Isatin Opening. Under nitrogen, acid (**3.34**; 2.40 mmol) was dissolved in DCM (12 mL), the solution was cooled to 0 °C and treated with isatin (**3.35**; 2.00 mmol), EDC·HCl (2.40 mmol) and DMAP (0.20 mmol). The reaction mixture was stirred at ambient temperature for 3 h, treated with solution of 1,2-phenylenediamine (**3.36**; 2.40 mmol) in DCM (3 mL), and stirred overnight. Solvent was removed *in vacuo*, and further purification by flash chromatography on silica gel yielded the desired photoprecursor (**3.37**).



(*S*)-*N*-(2-(3-Oxo-3,4-dihydroquinoxalin-2-yl)phenyl)-3-phenyl-2-

(1*H*-pyrrol-1-yl)propanamide (**3.37a**). General procedure **B** was

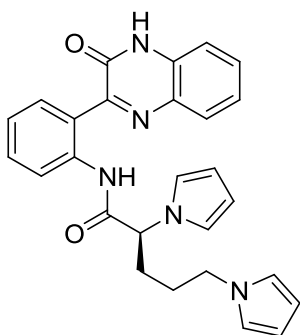
followed on a 4.92 mmol scale of **3.34a**, which after flash

chromatography on silica gel (gradient elution: hexane → hexane–

ethyl acetate 50:50) afforded 1.54 g (72%) of the title compound. ¹H

NMR (500 MHz, CDCl₃) δ 10.87 (s, 1H), 9.68 (s, 1H), 8.17 (d, *J* = 8.3, 1H), 7.91 (dd, *J* = 7.8, 1.6, 1H), 7.76 (dd, *J* = 8.1, 1.3, 1H), 7.59 (ddd, *J* = 8.4, 7.3, 1.4, 1H), 7.52 (td, *J* =

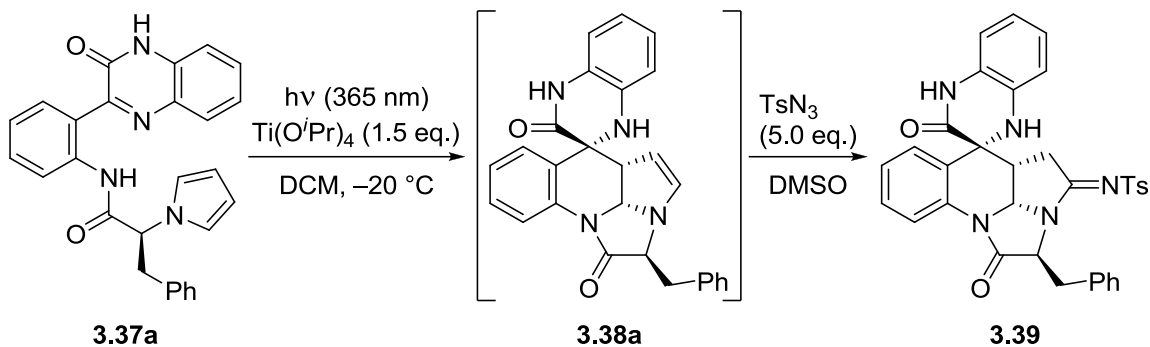
8.4, 7.9, 1.6, 1H), 7.40 (ddd, $J = 8.3, 7.3, 1.3$, 1H), 7.28 (m, 2H), 7.03 (m, 3H), 6.89 (m, 2H), 6.55 (t, $J = 2.1$, 2H), 5.89 (t, $J = 2.1$, 2H), 4.67 (dd, $J = 9.4, 5.6$, 1H), 3.63 (dd, $J = 14.1, 5.6$, 1H), 3.13 (dd, $J = 14.1, 9.4$, 1H). ^{13}C NMR (126 MHz, CDCl_3) δ 168.5, 156.1, 154.7, 137.2, 136.1, 132.6, 131.4, 131.2, 131.0, 130.9, 129.6, 128.8, 128.4, 126.7, 126.7, 124.8, 124.7, 124.1, 120.1, 115.8, 109.5, 66.2, 38.9. HRMS (ESI) calcd for $\text{C}_{27}\text{H}_{22}\text{N}_4\text{NaO}_2^+$ (MNa^+) 457.1635, found 457.1647.



(S)-N-(2-(3-Oxo-3,4-dihydroquinoxalin-2-yl)phenyl)-2,5-di(1H-pyrrol-1-yl)pentanamide (3.37b). General procedure B was followed on a 5.34 mmol scale of **3.34b**, which after flash chromatography on silica gel (gradient elution: hexane \rightarrow hexane–ethyl acetate 30:70) afforded 1.54 g (64%) of the title

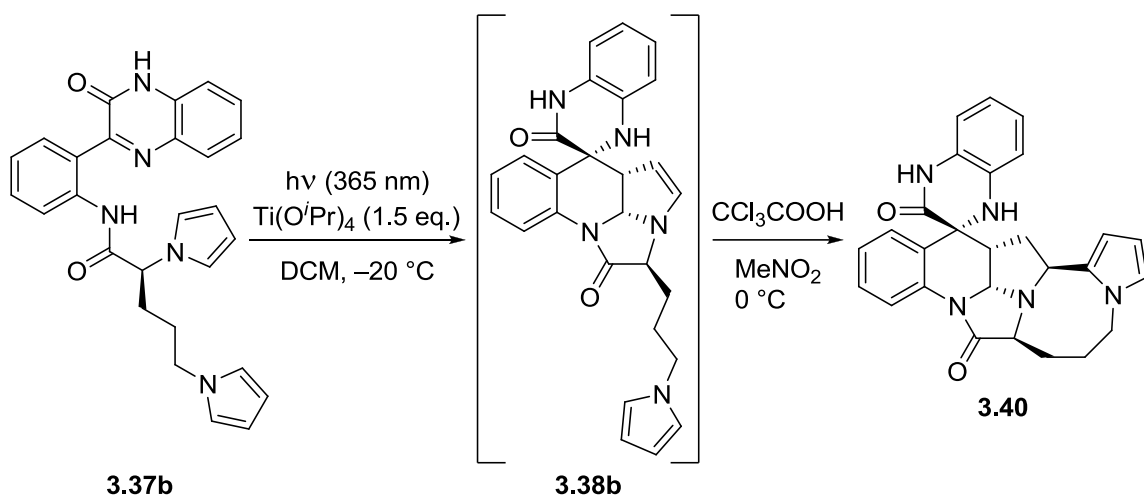
compound. ^1H NMR (500 MHz, CDCl_3) δ 11.34 (br, 1H), 9.29 (s, 1H), 8.12 (d, $J = 8.3$, 1H), 7.86 (d, $J = 7.8$, 1H), 7.78 (d, $J = 8.1$, 1H), 7.59 (t, $J = 7.7$, 1H), 7.51 (t, $J = 7.9$, 1H), 7.42 (t, $J = 7.7$, 1H), 7.28 (m, 2H), 6.54 (s, 2H), 6.51 (s, 2H), 6.06 (s, 2H), 5.88 (s, 2H), 4.36 (dd, $J = 10.4, 4.9$, 1H), 3.78 (m, 2H), 2.30 (m, 1H), 1.90 (m, 1H), 1.59 (m, 2H). ^{13}C NMR (126 MHz, CDCl_3) δ 168.9, 155.5, 155.2, 136.0, 132.6, 131.4, 131.2, 131.2, 130.9, 130.0, 127.0, 124.8, 124.8, 124.1, 120.6, 120.0, 115.5, 109.9, 108.3, 63.9, 49.2, 29.7, 28.1. HRMS (ESI) calcd for $\text{C}_{27}\text{H}_{25}\text{N}_5\text{NaO}_2^+$ (MNa^+) 474.1900, found 474.1913.

Photochemical Reactions Followed by Post-Photochemical Modifications



(2*S*,2*bR*,4*aR*,5*R*)-2-Benzyl-3-(4-methylbenzenesulfonylimino)-2*a*¹,3,4,4*a*-tetrahydro-1'*H*-spiro[2*a*,9*b*-diazapentaleno[1,6-*ab*]naphthalene-5,2'-quinoxaline]-1,3'(2*H*,4'*H*)-dione (3.39). Photoprecursor 3.37a (0.177 g, 0.407 mmol) was dissolved in anhydrous DCM (17 mL) under nitrogen, and the solution was degassed by bubbling nitrogen for 30 min. Titanium (IV) isopropoxide (0.18 mL, 0.632 mmol) was added, and the mixture was irradiated with UV LED-based illuminator (five 250 mW @ 365 nm Nichia chips) at $-20\text{ }^\circ\text{C}$ for 21 h. Then the solution was washed with water (5 mL), and the product was extracted from aqueous layer with DCM (4 mL). The combined organic layers were dried over anhydrous Na_2SO_4 and filtered. DMSO (2.0 mL) and tosyl azide (0.31 mL, 0.40 g, 2.04 mmol) were added, and DCM was removed *in vacuo*. The resulting mixture was stirred at ambient temperature for 2 days, and then concentrated under high vacuum (60 $^\circ\text{C}/0.15$ Torr). Further purification by flash chromatography on silica gel pretreated with pyridine (gradient elution: hexane \rightarrow hexane–ethyl acetate + 1% TEA 50:50) afforded 0.092 g (40% after two steps) of the title compound. ^1H NMR (500 MHz, CDCl_3) δ 8.85 (s, 1H), 7.68 (d, $J = 8.0$, 2H), 7.59 (d, $J = 7.9$, 1H), 7.28 (m, 6H), 7.01 (m, 4H), 6.78 (d, $J = 7.7$, 1H), 6.71 (t, $J = 7.6$, 1H), 6.62 (t, $J = 7.6$, 1H), 6.12 (d, $J = 7.9$, 1H), 4.87 (t, $J = 4.7$, 1H), 4.49 (d, $J = 8.0$, 1H), 4.04 (ddd, $J = 9.9, 8.0, 2.3$ Hz, 1H),

3.92 (dd, $J = 18.8, 2.3$, 1H), 3.88 (s, 1H), 3.47 (dd, $J = 18.7, 9.6$, 1H), 3.38 (dd, $J = 14.1, 4.8$, 1H), 3.29 (dd, $J = 14.1, 4.9$, 1H), 2.25 (s, 3H). ^{13}C NMR (126 MHz, CDCl_3) δ 172.4, 169.0, 165.0, 143.1, 138.8, 135.3, 131.5, 131.1, 130.8, 129.7, 129.6, 129.5, 128.9, 127.8, 126.9, 126.7, 126.0, 124.4, 123.4, 120.8, 116.1, 115.4, 74.8, 63.0, 62.6, 42.6, 36.1, 33.5, 21.6. HRMS (ESI) calcd for $\text{C}_{34}\text{H}_{29}\text{N}_5\text{NaO}_4\text{S}^+$ (MNa^+) 626.1832, found 626.1851.



(13a*S*)-2,3,7,7a,7a¹,13a-Hexahydro-1*H*,1'*H*-spiro[3a,6b¹,12b-triazacyclopenta [4',5']cycloocta[1',2',3':3,4]pentaleno[1,6-*ab*]naphthalene-8,2'-quinoxaline]-3',13(4'*H*,6b*H*)-dione (3.40). Photoprecursor **3.37b** (0.420 g, 0.930 mmol) was dissolved in anhydrous DCM (46.5 mL) under nitrogen, and the solution was degassed by bubbling nitrogen for 30 min. Titanium (IV) isopropoxide (0.41 mL, 1.40 mmol) was added, and the mixture was irradiated with UV LED-based illuminator (five 250 mW @ 365 nm Nichia chips) at -20 °C for 37 h. Then the solution was stirred with sat. aq. NH_4Cl (17 mL) for 30 min. Organic layer was separated, and the product was extracted from aqueous layer with DCM (4×5 mL). The combined organic layers were washed with water (17 mL), dried over anhydrous Na_2SO_4 , filtered and concentrated *in vacuo*. The

residue was redissolved in nitromethane (19 mL), and the resulting solution was filtered through cotton and cooled to 0 °C. Under nitrogen, solution of trichloroacetic acid (0.190 g, 1.16 mmol) in nitromethane (0.5 mL) was added, and the reaction mixture was left at 0 °C for 2 days. Then it was concentrated *in vacuo*, and further purification by flash chromatography on silica gel pretreated with pyridine (gradient elution: hexane → hexane–ethyl acetate + 1% TEA 50:50) afforded 0.040 g (10% after two steps) of the title compound. ¹H NMR (500 MHz, CDCl₃) δ 8.61 (dd, *J* = 8.4, 1.3, 1H), 8.05 (s, 1H), 7.78 (dd, *J* = 7.9, 1.6, 1H), 7.40 (ddd, *J* = 8.5, 7.3, 1.6, 1H), 7.14 (td, *J* = 7.6, 1.3, 1H), 6.97 (td, *J* = 7.7, 1.4, 1H), 6.84 (td, *J* = 7.7, 1.3, 1H), 6.78 (dd, *J* = 7.9, 1.4, 1H), 6.73 (dd, *J* = 7.8, 1.3, 1H), 6.46 (t, *J* = 2.3, 1H), 5.98 (dd, *J* = 3.6, 2.7, 1H), 5.71 (br, 1H), 5.28 (d, *J* = 4.3, 1H), 4.79 (br, 1H), 4.41 (dd, *J* = 10.3, 4.3, 1H), 4.20 (s, 1H), 3.85 (m, 2H), 3.25 (ddd, *J* = 10.5, 9.2, 4.3, 1H), 2.33 (m, 3H), 2.17 (m, 1H), 1.84 (m, 2H). ¹³C NMR (126 MHz, CDCl₃) δ 173.6, 169.2, 135.7, 133.2, 132.0, 130.1, 127.9, 124.9, 124.7, 124.6, 124.2, 123.4, 120.4, 118.4, 115.2, 114.6, 106.5, 105.9, 79.2, 66.0, 61.3, 55.1, 48.8, 41.3, 31.8, 28.4. HRMS (ESI) calcd for C₂₇H₂₆N₅O₂⁺ (MH⁺) 452.2081, found 452.2100.

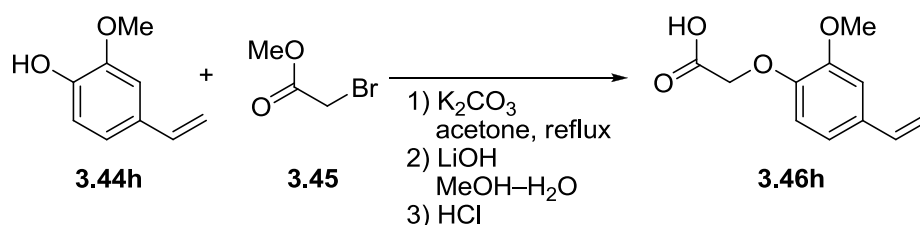
Experimental Section for Project 3

Synthesis of Photoprecursors

The following compounds were synthesized according to previously described procedures (or similarly): 2-(*p*-tolylloxy)acetic acid (**3.46b**) [165], 2-(3,5-dimethylphenoxy)acetic acid (**3.46c**) [166], 2-(4-methoxyphenoxy)acetic acid (**3.46d**) [165], 2-(4-acetamidophenoxy)acetic acid (**3.46f**) [167], 2-(3,5-dimethoxyphenoxy)acetic acid

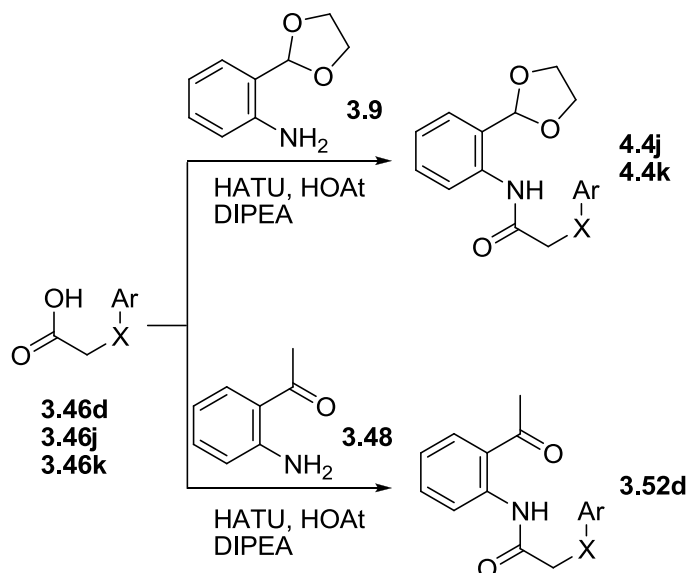
(**3.46g**) [165], 2-(1,3-dioxolan-2-yl)aniline (**3.9**) [7] and 8-amino-3,4-dihydronaphthalen-1(2*H*)-one (**3.49**) [168].

The following compounds are commercially available: 3-(4-methoxyphenyl)propionic acid (**3.46i**), 3-(3,4-dimethoxyphenyl)propionic acid (**3.46j**), 3-(2,4,6-trimethoxyphenyl)propanoic acid (**3.46k**) and bis(4'-methoxy)phenylcarboxylic acid (**3.46l**).



2-(2-Methoxy-4-vinylphenoxy)acetic Acid (3.46h). 2-Methoxy-4-vinylphenol (**3.44h**; 4.00 mL, 4.44 g, 29.6 mmol) was dissolved in anhydrous acetone (30 mL). Methyl bromoacetate (**3.45**; 3.36 mL, 5.43 g, 35.5 mmol) and potassium carbonate (16.3 g, 118 mmol) were added, and the mixture was refluxed for 12 h. Solids were filtered off, and the solvent was removed *in vacuo*. The residue was dissolved in methanol and water (80 mL, 1:1). LiOH (5.68 g, 237 mmol) was added at 0 °C, and the mixture was stirred at ambient temperature overnight. After that, methanol was removed *in vacuo*, 10% aq. HCl was added till pH 1–2, and the product was extracted from the aqueous layer with ethyl acetate (3×150 mL). The combined organic layers were dried over anhydrous Na₂SO₄, filtered, and the solvent was removed *in vacuo* to yield 6.14 g (99%) of the title compound. ¹H NMR (500 MHz, MeOD) δ 7.12 (d, *J* = 1.4 Hz, 1H), 6.98 (dd, *J* = 8.3, 1.5 Hz, 1H), 6.90 (d, *J* = 8.3 Hz, 1H), 6.68 (dd, *J* = 17.6, 10.9 Hz, 1H), 5.68 (d, *J* = 17.6 Hz,

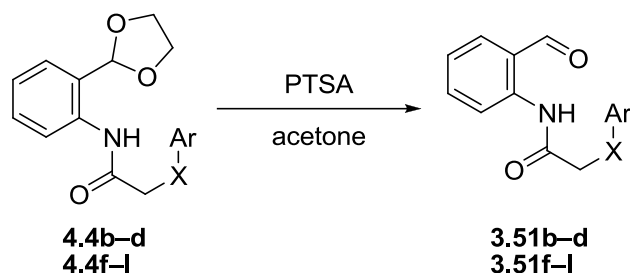
dropwise. The mixture was stirred at ambient temperature overnight, and then diluted with DCM (80 mL). The solution was washed with water (3×15 mL), dried over anhydrous Na₂SO₄, filtered and concentrated *in vacuo* to yield the desired amide. Crude dioxolane-protected photoprecursors (**4.4**) were then deprotected according to general procedure **D**, whereas all other photoprecursors (**3.53**) were purified by flash chromatography on silica gel.



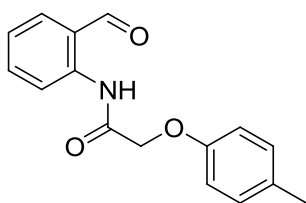
General Procedure C for HATU-Promoted Coupling of Acids with Anilines.

Under nitrogen, acid (**3.46**; 5.49 mmol) was dissolved in anhydrous DMF (9 mL), the solution was treated with HOAt (0.896 g, 6.59 mmol), HATU (2.51 g, 6.59 mmol) and DIPEA (2.39 mL, 1.77 g, 13.7 mmol) and then stirred at ambient temperature for 30 min. Subsequently, aniline (**3.9**, **3.48**; 6.60 mmol) was added, and the mixture was stirred at ambient temperature for 1 day. DMF was removed under high vacuum (50 °C/0.15 Torr), the residue was dissolved in DCM (50 mL) and washed two times with sat. aq. NaHCO₃ (3 mL) diluted with water (30 mL). The organic layer was washed with water (30 mL), dried over anhydrous Na₂SO₄, filtered and concentrated *in vacuo* to yield the desired

amide. Crude dioxolane-protected photoprecursors (**4.4**) were then deprotected according to general procedure **D**, whereas photoprecursor **3.52d** was purified by flash chromatography on silica gel.



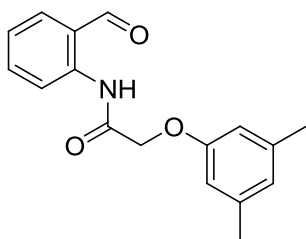
General Procedure D for Dioxolane Deprotection. Dioxolane-protected photoprecursor (**4.4**; 4.94 mmol) was dissolved in acetone (38 mL), TsOH·H₂O (0.988 mmol) was added, and the mixture was stirred at ambient temperature for 1 day. Solvent was removed *in vacuo*, and the residue was dissolved in DCM (90 mL). The solution was washed with sat. aq. NaHCO₃ (2×15 mL) and then with water (25 mL). The organic layer was dried over anhydrous Na₂SO₄, filtered, and the solvent was removed *in vacuo*. Further purification by flash chromatography on silica gel yielded the desired photoprecursor (**3.51**).



***N*-(2-Formylphenyl)-2-(*p*-tolylloxy)acetamide (**3.51b**).**

2-(*p*-Tolyloxy)acetic acid chloride (**3.47b**), which was prepared from 8.47 mmol of 2-(*p*-tolylloxy)acetic acid (**3.46b**) according to general procedure **A**, was coupled to 2-(1,3-dioxolan-2-yl)aniline (**3.9**; 1.04 g, 6.27 mmol) following general procedure **B**. Dioxolane protection was then removed according to general procedure **D**, which after flash chromatography on silica gel (gradient elution: hexane → hexane–DCM 50:50) afforded 1.10 g (65% after two steps) of the title compound. ¹H NMR (500 MHz, CDCl₃) δ 12.16 (s, 1H), 9.97 (s, 1H), 8.83 (d, *J* = 8.4 Hz,

1H), 7.71 (dd, $J = 7.6, 1.7$ Hz, 1H), 7.64 (ddd, $J = 8.9, 7.3, 1.7$ Hz, 1H), 7.28 (td, $J = 7.5, 1.1$ Hz, 1H), 7.14 (m, 2H), 7.02 (m, 2H), 4.63 (s, 2H), 2.31 (s, 3H). ^{13}C NMR (126 MHz, CDCl_3) δ 195.1, 168.5, 155.4, 139.8, 136.1, 136.1, 131.6, 130.3, 123.7, 122.5, 120.2, 114.8, 67.9, 20.7. HRMS (ESI) calcd for $\text{C}_{16}\text{H}_{16}\text{NO}_3^+$ (MH^+) 270.1125, found 270.1131.



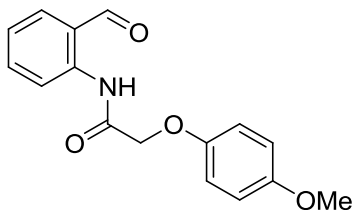
2-(3,5-Dimethylphenoxy)-N-(2-formylphenyl)acetamide

(3.51c). 2-(3,5-Dimethylphenoxy)acetic acid chloride (**3.47c**),

which was prepared from 5.18 mmol of 2-(3,5-dimethyl-

phenoxy)acetic acid (**3.46c**) according to general procedure **A**,

was coupled to 2-(1,3-dioxolan-2-yl)aniline (**3.9**; 0.637 g, 3.86 mmol) following general procedure **B**. Dioxolane protection was then removed according to general procedure **D**, which after flash chromatography on silica gel (gradient elution: hexane \rightarrow hexane-DCM 50:50) afforded 0.931 g (85% after two steps) of the title compound. ^1H NMR (500 MHz, CDCl_3) δ 12.16 (s, 1H), 9.98 (s, 1H), 8.84 (d, $J = 8.4$ Hz, 1H), 7.72 (dd, $J = 7.6, 1.7$ Hz, 1H), 7.64 (ddd, $J = 8.8, 7.3, 1.6$ Hz, 1H), 7.28 (td, $J = 7.5, 1.1$ Hz, 1H), 6.75 (m, 2H), 6.69 (m, 1H), 4.62 (s, 2H), 2.33 (br s, 6H). ^{13}C NMR (126 MHz, CDCl_3) δ 195.0, 168.5, 157.5, 139.9, 139.7, 136.1, 136.1, 124.0, 123.6, 122.5, 120.2, 112.7, 67.6, 21.6. HRMS (ESI) calcd for $\text{C}_{17}\text{H}_{18}\text{NO}_3^+$ (MH^+) 284.1281, found 284.1288.



N-(2-Formylphenyl)-2-(4-methoxyphenoxy)acetamide

(3.51d). 2-(4-Methoxyphenoxy)acetic acid chloride (**3.47d**),

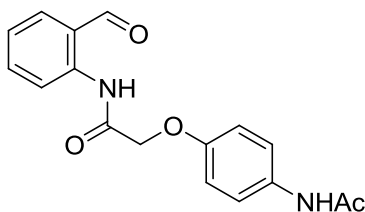
which was prepared from 6.59 mmol of 2-(4-methoxy-

phenoxy)acetic acid (**3.46d**) according to general procedure **A**, was then coupled to 2-

(1,3-dioxolan-2-yl)aniline (**3.9**; 0.815 g, 4.94 mmol) according to general procedure **B**.

Dioxolane protection was then removed according to general procedure **D**, which after

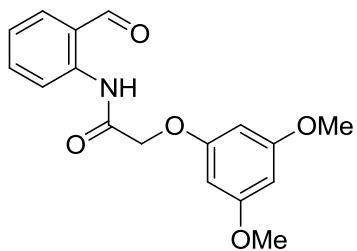
flash chromatography on silica gel (gradient elution: hexane → ethyl acetate) afforded 0.843 g (60% after two steps) of the title compound. ¹H NMR (500 MHz, CDCl₃) δ 12.16 (s, 1H), 9.97 (d, *J* = 0.7 Hz, 1H), 8.83 (d, *J* = 8.4 Hz, 1H), 7.71 (dd, *J* = 7.6, 1.7 Hz, 1H), 7.64 (ddd, *J* = 8.7, 7.3, 1.7 Hz, 1H), 7.28 (td, *J* = 7.5, 1.1 Hz, 1H), 7.06 (m, 2H), 6.89 (m, 2H), 4.61 (s, 2H), 3.78 (s, 3H). ¹³C NMR (126 MHz, CDCl₃) δ 195.1, 168.5, 154.9, 151.7, 139.8, 136.2, 136.1, 123.7, 122.5, 120.2, 115.9, 115.0, 68.5, 55.9. HRMS (ESI) calcd for C₁₆H₁₆NO₄⁺ (MH⁺) 286.1074, found 286.1080.



2-(4-Acetamidophenoxy)-N-(2-formylphenyl)acetamide

(3.51f). General procedure **A** was followed on a 3.46 mmol scale of 2-(4-acetamido-phenoxy)acetic acid (**3.46f**).

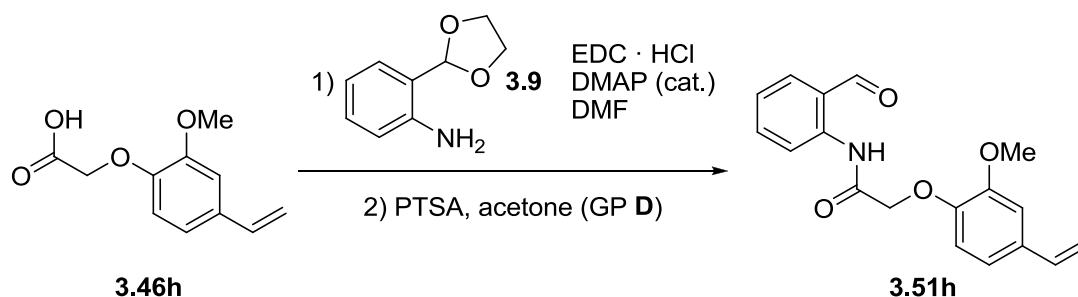
Corresponding acyl chloride (**3.47f**) was redissolved in anhydrous acetonitrile (10 mL) and coupled to 2-(1,3-dioxolan-2-yl)aniline (**3.9**; 0.439 g, 2.66 mmol) according to general procedure **B**. Dioxolane protection was then removed according to general procedure **D**, which after flash chromatography on silica gel (gradient elution: DCM → DCM–methanol 98:2) afforded 0.571 g (69% after two steps) of the title compound. ¹H NMR (500 MHz, CDCl₃) δ 12.16 (s, 1H), 9.96 (d, *J* = 0.8 Hz, 1H), 8.82 (d, *J* = 8.4 Hz, 1H), 7.71 (dd, *J* = 7.7, 1.7 Hz, 1H), 7.64 (ddd, *J* = 8.8, 7.4, 1.7 Hz, 1H), 7.46 (m, 2H), 7.28 (td, *J* = 7.5, 1.1 Hz, 1H), 7.16 (s, 1H), 7.08 (m, 2H), 4.63 (s, 2H), 2.16 (s, 3H). ¹³C NMR (126 MHz, CDCl₃) δ 195.1, 168.3, 168.2, 154.2, 139.8, 136.2, 136.1, 132.4, 123.7, 122.5, 122.0, 120.2, 115.4, 68.0, 24.6. HRMS (ESI) calcd for C₁₇H₁₇N₂O₄⁺ (MH⁺) 313.1183, found 313.1183.



2-(3,5-Dimethoxyphenoxy)-N-(2-formylphenyl)

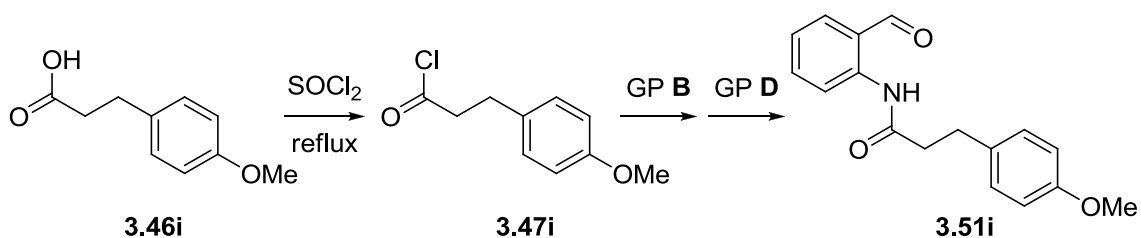
acetamide (3.51g). 2-(3,5-dimethoxyphenoxy)acetic acid chloride (**3.47g**), which was prepared from 1.21 mmol of 2-(3,5-dimethoxyphenoxy)acetic acid (**3.46g**) according to

general procedure **A**, was then coupled to 2-(1,3-dioxolan-2-yl)aniline (**3.9**; 0.154 g, 0.931 mmol) according to general procedure **B**. Dioxolane protection was then removed according to general procedure **D**, which after flash chromatography on silica gel (gradient elution: DCM → DCM–methanol 99:1) afforded 0.143 g (49% after two steps) of the title compound. ¹H NMR (500 MHz, CDCl₃) δ 12.14 (s, 1H), 9.96 (d, *J* = 0.7 Hz, 1H), 8.82 (d, *J* = 8.4 Hz, 1H), 7.71 (dd, *J* = 7.6, 1.7 Hz, 1H), 7.63 (ddd, *J* = 8.9, 7.2, 1.7 Hz, 1H), 7.28 (td, *J* = 7.5, 1.1 Hz, 1H), 6.32 (d, *J* = 2.2 Hz, 2H), 6.16 (t, *J* = 2.2 Hz, 1H), 4.61 (s, 2H), 3.80 (s, 6H). ¹³C NMR (126 MHz, CDCl₃) δ 195.0, 168.1, 161.8, 159.3, 139.8, 136.1, 136.1, 123.7, 122.5, 120.2, 94.4, 94.0, 67.8, 55.6. HRMS (ESI) calcd for C₁₇H₁₈NO₅⁺ (MH⁺) 316.1179, found 316.1187.



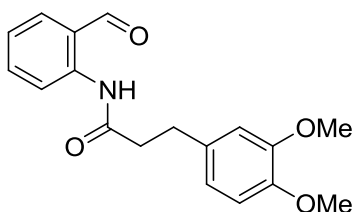
N-(2-Formylphenyl)-2-(2-methoxy-4-vinylphenoxy)acetamide (3.51h). Under nitrogen, 2-(2-methoxy-4-vinylphenoxy)acetic acid (**3.46h**; 0.576 g, 2.77 mmol) was dissolved in anhydrous DMF (5 mL), the solution was treated with EDC·HCl (0.530 g, 2.77 mmol), DMAP (68 mg, 0.55 mmol), and 2-(1,3-dioxolan-2-yl)aniline (**3.9**; 0.549 g, 3.32 mmol) and then was stirred at ambient temperature for 1 day. DMF was removed

under high vacuum (50 °C/0.15 Torr). The residue was dissolved in DCM (50 mL), and the solution was washed with water (3×20mL) and sat. aq. NaHCO₃ (10mL). The organic layer was dried over anhydrous Na₂SO₄, filtered, and the solvent was removed *in vacuo*. Dioxolane protection was then removed according to general procedure **D** with 2.79 mmol of TsOH·H₂O, which after flash chromatography on silica gel (gradient elution: DCM → DCM–methanol 99:1) afforded 0.090 g (10% after two steps) of the title compound. ¹H NMR (500 MHz, CDCl₃) δ 12.03 (s, 1H), 9.95 (s, 1H), 8.83 (d, *J* = 8.4 Hz, 1H), 7.70 (dd, *J* = 7.7, 1.7 Hz, 1H), 7.63 (ddd, *J* = 8.8, 7.3, 1.7 Hz, 1H), 7.28 (td, *J* = 7.5, 1.1 Hz, 1H), 7.03 (d, *J* = 1.9 Hz, 1H), 6.96 (d, *J* = 8.2 Hz, 1H), 6.93 (dd, *J* = 8.2, 1.9 Hz, 1H), 6.66 (dd, *J* = 17.6, 10.8 Hz, 1H), 5.65 (dd, *J* = 17.5, 0.8 Hz, 1H), 5.19 (dd, *J* = 10.9, 0.8 Hz, 1H), 4.70 (s, 2H), 3.98 (s, 3H). ¹³C NMR (126 MHz, CDCl₃) δ 194.8, 168.7, 150.3, 147.1, 139.8, 136.5, 136.0, 136.0, 133.1, 123.7, 122.7, 120.4, 119.4, 115.2, 112.9, 109.9, 69.7, 56.2. HRMS (ESI) calcd for C₁₈H₁₈NO₄⁺ (MH⁺) 312.1230, found 312.1234.



N-(2-Formylphenyl)-3-(4-methoxyphenyl)propanamide (3.51i). 3-(4-Methoxyphenyl)propionic acid (**3.46i**; 0.958 g, 5.32 mmol) was converted into the corresponding acid chloride (**3.47i**) by refluxing in thionyl chloride (5.00 mL, 8.16 g, 68.5 mmol) under nitrogen for 1 day [169]. After removal of volatiles *in vacuo*, the resulting acyl chloride was coupled to 2-(1,3-dioxolan-2-yl)aniline (**3.9**; 0.684 g, 4.15 mmol) according to general procedure **B**. Dioxolane protection was then removed according to general

procedure **D**, which after flash chromatography on silica gel (gradient elution: hexane → hexane–ethyl acetate 90:10) afforded 0.924 g (78% after two steps) of the title compound. ¹H NMR (500 MHz, CDCl₃) δ 11.13 (s, 1H), 9.90 (s, 1H), 8.75 (d, *J* = 8.4 Hz, 1H), 7.66 (dd, *J* = 7.6, 1.6 Hz, 1H), 7.61 (ddd, *J* = 8.6, 7.4, 1.6 Hz, 1H), 7.22 (t, *J* = 7.5 Hz, 1H), 7.18 (d, *J* = 8.3 Hz, 2H), 6.83 (d, *J* = 8.3 Hz, 2H), 3.77 (s, 3H), 3.03 (m, 2H), 2.75 (dd, *J* = 8.7, 6.9 Hz, 2H). ¹³C NMR (126 MHz, CDCl₃) δ 195.6, 171.9, 158.2, 141.1, 136.3, 136.2, 132.6, 129.4, 123.0, 121.7, 120.0, 114.1, 55.4, 40.5, 30.6. HRMS (ESI) calcd for C₁₇H₁₈NO₃⁺ (MH⁺) 284.1281, found 284.1293.

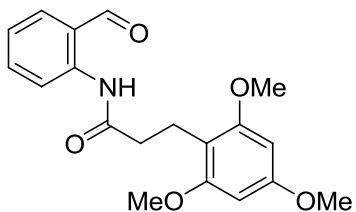


3-(3,4-Dimethoxyphenyl)-N-(2-formylphenyl)

propanamide (3.51j). General procedure **C** was followed

on a 2.38 mmol scale of 3-(3,4-dimethoxyphenoxy)

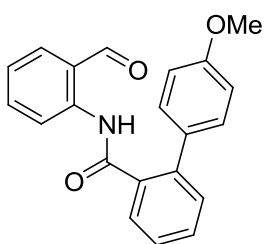
propanoic acid (**3.46j**) with 3.33 mmol of 2-(1,3-dioxolan-2-yl)aniline (**3.9**). Dioxolane protection was then removed according to general procedure **D**, which after flash chromatography on silica gel (gradient elution: hexane → hexane–ethyl acetate 85:15) afforded 0.552 g (74% after two steps) of the title compound. ¹H NMR (500 MHz, CDCl₃) δ 11.11 (s, 1H), 9.88 (s, 1H), 8.75 (d, *J* = 8.5 Hz, 1H), 7.64 (dd, *J* = 7.7, 1.7 Hz, 1H), 7.60 (ddd, *J* = 8.7, 7.3, 1.7 Hz, 1H), 7.21 (td, *J* = 7.5, 1.1 Hz, 1H), 6.78 (m, 3H), 3.84 (s, 3H), 3.83 (s, 3H), 3.02 (dd, *J* = 8.4, 7.1, 2H), 2.75 (dd, *J* = 8.4, 7.1 Hz, 2H). ¹³C NMR (126 MHz, CDCl₃) δ 195.6, 171.8, 149.0, 147.6, 141.0, 136.3, 136.1, 133.1, 123.0, 121.6, 120.3, 119.9, 111.7, 111.4, 56.0, 55.9, 40.4, 31.1. HRMS (ESI) calcd for C₁₈H₂₀NO₄⁺ (MH⁺) 314.1387, found 314.1395.



***N*-(2-Formylphenyl)-3-(2,4,6-trimethoxyphenyl)**

propanamide (3.51k). General procedure **C** was followed on a 1.33 mmol scale of 3-(2,4,6-trimethoxyphenoxy) propanoic acid (**3.46k**) with 1.87 mmol of 2-(1,3-dioxolan-

2-yl)aniline (**3.9**). Dioxolane protection was then removed according to general procedure **D**, which after flash chromatography on silica gel pretreated with pyridine (gradient elution: hexane → hexane–ethyl acetate 85:15) afforded 0.337 g (74% after two steps) of the title compound. ¹H NMR (500 MHz, CDCl₃) δ 11.08 (s, 1H), 9.90 (s, 1H), 8.80 (d, *J* = 8.4 Hz, 1H), 7.65 (dd, *J* = 7.7, 1.7 Hz, 1H), 7.60 (ddd, *J* = 8.7, 7.4, 1.7 Hz, 1H), 7.20 (td, *J* = 7.5, 1.0 Hz, 1H), 6.11 (s, 2H), 3.80 (s, 3H), 3.78 (s, 6H), 3.03 (m, 2H), 2.59 (m, 2H). ¹³C NMR (126 MHz, CDCl₃) δ 195.3, 173.2, 159.8, 158.9, 141.4, 136.2, 136.0, 122.6, 121.6, 119.9, 109.3, 90.5, 55.7, 55.5, 38.5, 19.3. HRMS (ESI) calcd for C₁₉H₂₂NO₅⁺ (MH⁺) 344.1492, found 344.1500.

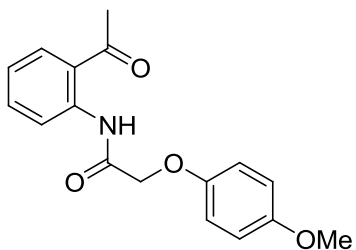


***N*-(2-Formylphenyl)-4'-methoxybiphenyl-2-carboxamide**

(3.51l). 4'-Methoxybiphenyl-2-carbonyl chloride (**3.47l**), which was prepared from 1.39 mmol of 4'-methoxy-biphenyl-2-carboxylic acid (**3.46l**) according to general procedure **A**, was

coupled to 2-(1,3-dioxolan-2-yl)aniline (**3.9**; 0.174 g, 1.05 mmol) following general procedure **B**. Dioxolane protection was then removed according to general procedure **D**, which after flash chromatography on silica gel (gradient elution: hexane → hexane–ethyl acetate 90:10) afforded 0.269 g (77% after two steps) of the title compound. ¹H NMR (500 MHz, C₆D₆) δ 11.44 (s, 1H), 9.25 (d, *J* = 8.5 Hz, 1H), 9.09 (d, *J* = 0.7 Hz, 1H), 7.79 (dd, *J* = 7.7, 1.4 Hz, 1H), 7.48 (m, 2H), 7.27 (dd, *J* = 7.7, 1.3 Hz, 1H), 7.13 (td, *J* = 7.6,

1.5 Hz, 1H), 7.07 (ddd, $J = 8.8, 7.3, 1.7$ Hz, 1H), 7.05 (td, $J = 7.5, 1.3$ Hz, 1H), 6.68 (m, 2H), 6.65 (dd, $J = 7.7, 1.7$ Hz, 1H), 6.54 (td, $J = 7.5, 1.1$ Hz, 1H), 3.12 (s, 3H). ^{13}C NMR (126 MHz, C_6D_6) δ 194.4, 169.3, 159.7, 141.4, 140.3, 137.0, 135.8, 135.8, 132.9, 131.0, 130.7, 130.6, 129.3, 127.4, 122.5, 121.8, 119.9, 114.2, 54.6. HRMS (ESI) calcd for $\text{C}_{21}\text{H}_{18}\text{NO}_3^+$ (MH^+) 332.1281, found 332.1276.



***N*-(2-Acetylphenyl)-2-(4-methoxyphenoxy)acetamide**

(3.52d). General procedure **C** was followed on a 5.49 mmol

scale of 2-(4-methoxy-phenoxy)acetic acid (**3.46d**) with

6.60 mmol of 2'-aminoacetophenone (**3.48**) in 5 mL of

anhydrous DMF, which after flash chromatography on silica gel (gradient elution: hexane

→ hexane–ethyl acetate 85:15) afforded 1.04 g (64%) of the title compound. ^1H NMR

(500 MHz, CDCl_3) δ 12.63 (s, 1H), 8.83 (dd, $J = 8.5, 1.3$ Hz, 1H), 7.92 (dd, $J = 8.0, 1.6$

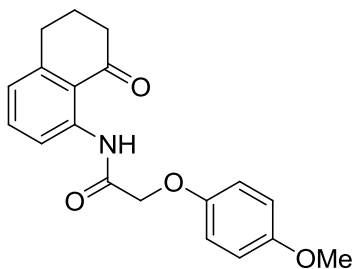
Hz, 1H), 7.57 (ddd, $J = 8.7, 7.2, 1.6$ Hz, 1H), 7.16 (ddd, $J = 8.0, 7.3, 1.2$ Hz, 1H), 7.06

(m, 2H), 6.88 (m, 2H), 4.58 (s, 2H), 3.77 (s, 3H), 2.67 (s, 3H). ^{13}C NMR (126 MHz,

CDCl_3) δ 202.2, 168.3, 154.8, 151.8, 139.9, 135.0, 131.7, 123.1, 122.7, 121.0, 116.0,

114.9, 68.7, 55.8, 28.6. HRMS (ESI) calcd for $\text{C}_{17}\text{H}_{18}\text{NO}_4^+$ (MH^+) 300.1230, found

300.1233.



2-(4-Methoxyphenoxy)-*N*-(8-oxo-5,6,7,8-tetrahydronaphthalen-1-yl)acetamide (3.53d)

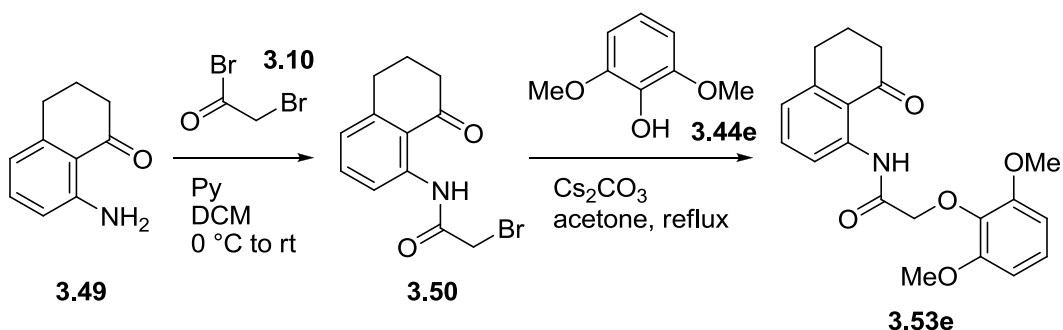
2-(4-Methoxyphenoxy)acetic acid chloride (**3.47d**), which was prepared

from 11.5 mmol of 2-(4-methoxyphenoxy)acetic acid

(3.46d) according to general procedure **A**, was coupled to 8-amino-3,4-dihydro-

naphthalen-1(2*H*)-one (**3.49**; 1.38 g, 8.55 mmol) following general procedure **B**. Further

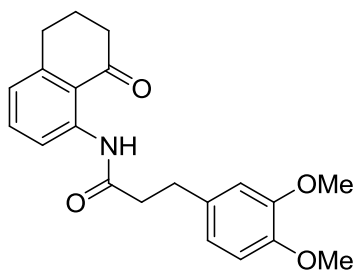
purification by flash chromatography on silica gel (gradient elution: hexane → DCM) afforded 2.03 g (73%) of the title compound. ¹H NMR (500 MHz, CDCl₃) δ 13.04 (s, 1H), 8.70 (dd, *J* = 8.2, 0.9 Hz, 1H), 7.47 (t, *J* = 8.0 Hz, 1H), 7.07 (m, 2H), 6.98 (dd, *J* = 7.6, 1.1 Hz, 1H), 6.88 (m, 2H), 4.59 (s, 2H), 3.78 (s, 3H), 2.98 (t, *J* = 6.1 Hz, 2H), 2.72 (dd, *J* = 7.2, 5.9 Hz, 2H), 2.09 (p, *J* = 6.4 Hz, 2H). ¹³C NMR (126 MHz, CDCl₃) δ 202.8, 168.5, 154.8, 151.9, 146.2, 140.9, 135.0, 123.9, 119.2, 118.6, 116.1, 115.0, 68.8, 55.9, 40.9, 31.1, 22.9. HRMS (ESI) calcd for C₁₉H₂₀NO₄⁺ (MH⁺) 326.1387, found 326.1382.



2-(2,6-Dimethoxyphenoxy)-*N*-(8-oxo-5,6,7,8-tetrahydro-naphthalen-1-yl)

acetamide (3.53e). Under nitrogen, 8-amino-3,4-dihydronaphthalen-1(2*H*)-one (**3.49**; 0.985 g, 6.12 mmol) was dissolved in anhydrous DCM (22 mL), the solution was treated with pyridine (0.74 mL, 0.73 g, 9.2 mmol) and cooled to 0 °C, and then solution of bromoacetyl bromide (**3.10**; 0.60 mL, 1.4 g, 6.7 mmol) in anhydrous DCM (6 mL) was added dropwise. The mixture was stirred at ambient temperature overnight and then quenched with water (10 mL). After 1 h of stirring, the organic layer was separated, and the product was extracted with DCM (3×15 mL). The combined organic layers were washed with water (3×10 mL), dried over anhydrous Na₂SO₄, filtered, and the solvent was removed *in vacuo*. The residue (crude **3.50**) was dissolved in acetone (8 mL), and then 2,6-dimethoxyphenol (**3.44e**; 1.02 g, 6.62 mmol) and cesium carbonate (2.16 g, 6.62

mmol) were added. The mixture was stirred under reflux for 2 h. The solvent was removed *in vacuo*, water (10 mL) and DCM (40 mL) were added, organic layer was separated, and the product was extracted from aqueous layer with DCM (3×20 mL). The combined organic layers were washed with water (10 mL), dried over anhydrous Na₂SO₄, filtered and concentrated *in vacuo*. Further purification by flash chromatography on silica gel (gradient elution: hexane → hexane–ethyl acetate 50:50) afforded 1.47 g (68% after two steps) of the title compound. ¹H NMR (500 MHz, CDCl₃) δ 13.00 (s, 1H), 8.73 (dd, *J* = 8.4, 1.1 Hz, 1H), 7.47 (dd, *J* = 8.5, 7.5 Hz, 1H), 7.02 (t, *J* = 8.4 Hz, 1H), 6.97 (dd, *J* = 7.5, 1.1 Hz, 1H), 6.58 (d, *J* = 8.4 Hz, 2H), 4.57 (s, 2H), 3.82 (s, 6H), 2.98 (t, *J* = 6.1 Hz, 2H), 2.68 (dd, *J* = 7.2, 5.9 Hz, 2H), 2.08 (p, *J* = 6.2 Hz, 2H). ¹³C NMR (126 MHz, CDCl₃) δ 201.9, 169.6, 153.4, 145.9, 141.1, 136.8, 134.7, 124.4, 123.6, 119.5, 118.9, 105.5, 72.8, 56.3, 40.7, 31.2, 22.9. HRMS (ESI) calcd for C₂₀H₂₂NO₅⁺ (MH⁺) 356.1492, found 356.1484.



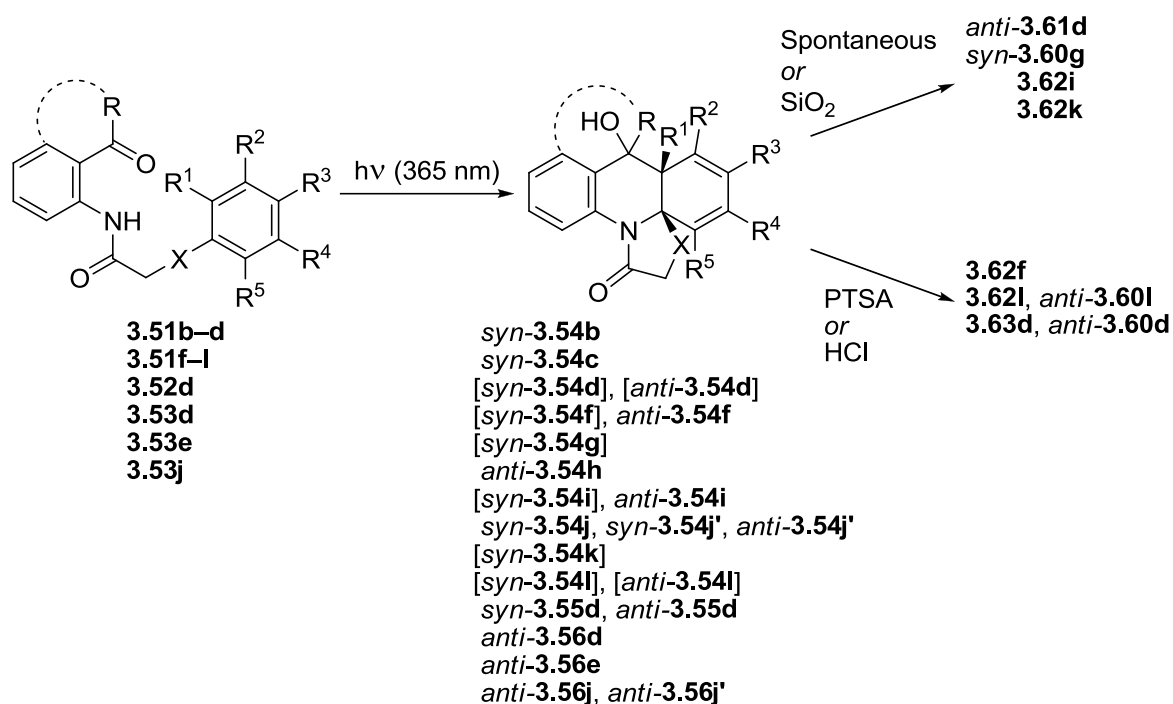
3-(3,4-Dimethoxyphenyl)-N-(8-oxo-5,6,7,8-tetrahydronaphthalen-1-yl)propanamide (3.53j). 3-(3,5-

Dimethoxyphenyl)propionic acid chloride (**3.47j**), which was prepared from 4.76 mmol of 3-(3,5-

dimethoxyphenyl)propionic acid (**3.46j**) with 23.8 mmol of oxalyl chloride in anhydrous benzene (10 mL) according to general procedure **A**, was coupled to 8-amino-3,4-dihydronaphthalen-1(2*H*)-one (**3.49**; 0.639 g, 3.97 mmol) following general procedure **B**. Further purification by flash chromatography on silica gel (gradient elution: hexane → hexane–ethyl acetate 80:20) afforded 0.576 g (41%) of the title compound. ¹H NMR (500 MHz, C₆D₆) δ 12.45 (s, 1H), 9.20 (dd, *J* = 8.5, 1.1 Hz, 1H), 7.10 (dd, *J* = 8.5, 7.5 Hz,

1H), 6.71 (dd, $J = 8.1, 2.1$ Hz, 1H), 6.66 (d, $J = 2.1$ Hz, 1H), 6.55 (d, $J = 8.1$ Hz, 1H), 6.43 (dt, $J = 7.5, 1.0$ Hz, 1H), 3.42 (s, 3H), 3.38 (s, 3H), 3.05 (t, $J = 7.6$ Hz, 2H), 2.61 (t, $J = 7.6$ Hz, 2H), 2.26 (t, $J = 6.1$ Hz, 2H), 2.18 (dd, $J = 7.2, 5.9$ Hz, 2H), 1.36 (p, $J = 6.4$ Hz, 2H). ^{13}C NMR (126 MHz, C_6D_6) δ 202.7, 171.4, 150.2, 148.7, 145.9, 143.0, 135.1, 133.9, 122.6, 120.7, 118.5, 118.4, 113.0, 112.8, 55.7, 55.5, 41.0, 40.6, 31.5, 30.9, 22.7. HRMS (ESI) calcd for $\text{C}_{21}\text{H}_{24}\text{NO}_4^+$ (MH^+) 354.1700, found 354.1706.

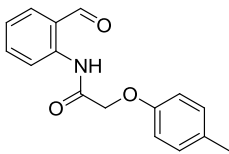
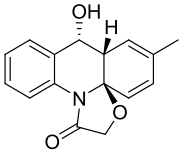
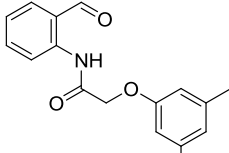
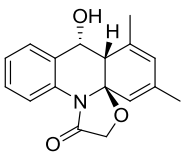
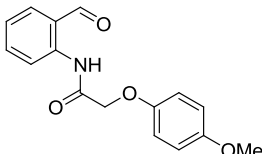
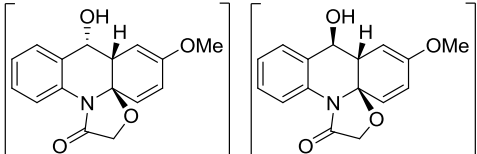
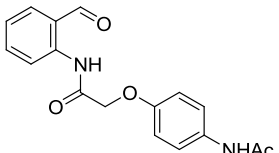
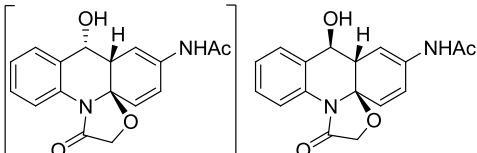
Photochemical Reactions and Acid-Catalyzed Post-Photochemical Modifications

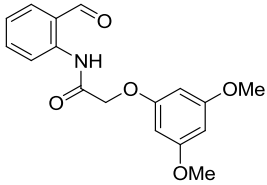
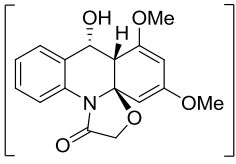
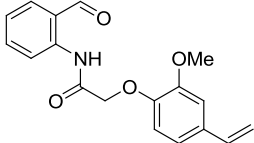
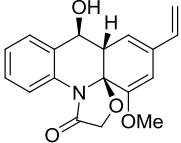
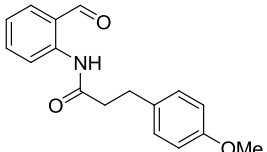
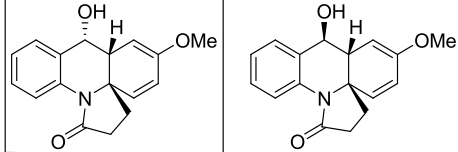
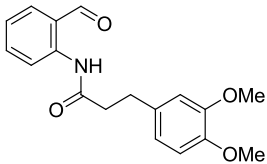
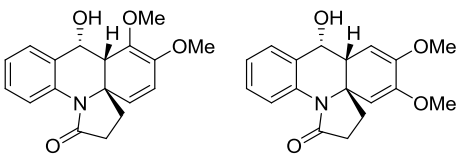
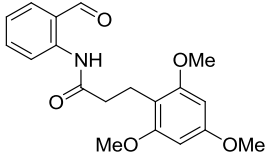
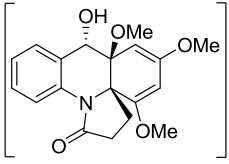
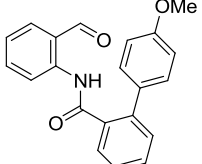
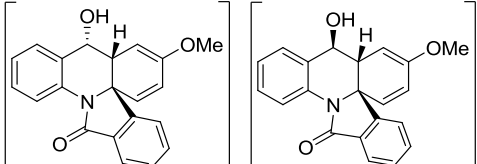


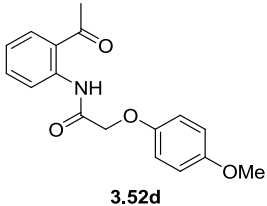
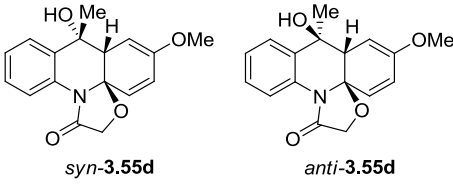
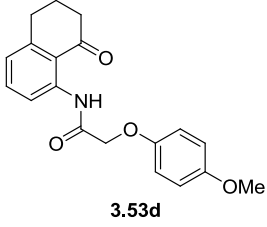
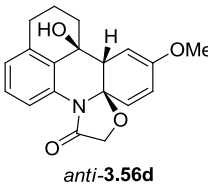
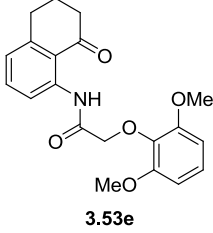
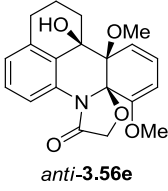
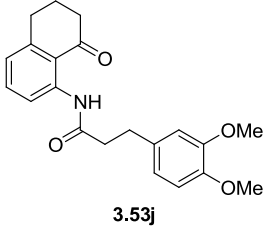
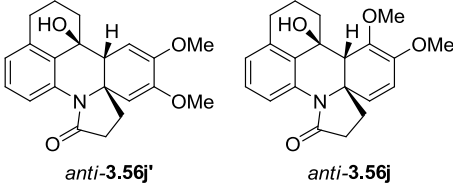
General Procedure E for the Photochemical Reaction. Photoprecursor (**3.51–3.53**; 1.50 mmol) was dissolved in DMSO (500 mL), and the solution was degassed by bubbling nitrogen for 1 h. The mixture was irradiated with UV LED-based illuminator (five 250 mW @ 365 nm Nichia chips) with the reaction progress monitored by ^1H NMR. After completion, the mixture was poured onto ice, and the product was extracted with DCM (4×350 mL). The combined organic layers were washed with water (3×100 mL),

dried over anhydrous Na₂SO₄, filtered, and the solvent was removed *in vacuo*. Crude photoproduct mixtures obtained from the precursors **3.51d**, **3.51f** and **3.51l** were directly subjected to the acid-catalyzed modifications according to general procedure **F**; in all other cases, further purification by flash chromatography on silica gel yielded the desired photoproducts or the hydrolyzed/cyclized derivatives (formed spontaneously during the irradiation or on the column).

Table 4.1: Irradiation Times

Photoprecursor	Photoproduct(s)	Reaction Time (h)
 <p>3.51b</p>	 <p><i>syn</i>-3.54b</p>	4.5
 <p>3.51c</p>	 <p><i>syn</i>-3.54c</p>	10
 <p>3.51d</p>	 <p><i>syn</i>-3.54d <i>anti</i>-3.54d</p>	3
 <p>3.51f</p>	 <p><i>syn</i>-3.54f <i>anti</i>-3.54f</p>	3.5

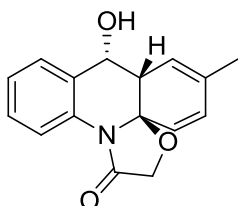
Photoprecursor	Photoproduct(s)	Reaction Time (h)
 <p>3.51g</p>	 <p><i>syn</i>-3.54g</p>	60
 <p>3.51h</p>	 <p><i>anti</i>-3.54h</p>	2.5
 <p>3.51i</p>	 <p><i>syn</i>-3.54i <i>anti</i>-3.54i</p>	4
 <p>3.51j</p>	 <p><i>syn</i>-3.54j <i>syn</i>-3.54j'</p>	4.5
 <p>3.51k</p>	 <p><i>syn</i>-3.54k</p>	4
 <p>3.51l</p>	 <p><i>syn</i>-3.54l <i>anti</i>-3.54l</p>	4

Photoprecursor	Photoproduct(s)	Reaction Time (h)
 <p>3.52d</p>	 <p><i>syn</i>-3.55d <i>anti</i>-3.55d</p>	3.5
 <p>3.53d</p>	 <p><i>anti</i>-3.56d</p>	2.5
 <p>3.53e</p>	 <p><i>anti</i>-3.56e</p>	40
 <p>3.53j</p>	 <p><i>anti</i>-3.56j' <i>anti</i>-3.56j</p>	7.5

General Procedure F for the Acid-Catalyzed Modification. The mixture of photoproducts (0.413 mmol) was dissolved in THF (24 mL), treated with TsOH·H₂O (0.016 g, 0.083 mmol) and stirred at ambient temperature overnight. Solvent was removed *in vacuo*, and the residue was dissolved in DCM (35 mL). The solution was washed with sat. aq. NaHCO₃ (2×5 mL) and then with water (5 mL). The organic layer

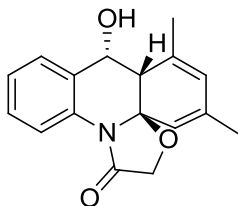
was dried over anhydrous Na₂SO₄ and concentrated *in vacuo*, and the crude products were purified by flash chromatography on silica gel.

***syn*-12-Hydroxy-15-methyl-2-oxa-5-azatetracyclo[11.4.0.0^{1,5}.0^{6,11}]heptadeca-6,8,10,14,16-pentaen-4-one** (*syn*-**3.54b**). General procedure **E** was followed on a 0.346 g (1.28 mmol) scale of **3.51b**, which after flash chromatography on silica gel (gradient elution: DCM → DCM–methanol 98:2) afforded 0.239 g (69%) of *syn*-**3.54b**.



syn-**3.54b**: ¹H NMR (500 MHz, MeOD) δ 7.47 (m, 1H), 7.41 (m, 1H), 7.29 (m, 2H), 5.83 (m, 2H), 5.64 (tq, *J* = 3.4, 1.7 Hz, 1H), 4.96 (dd, *J* = 6.3, 1.0 Hz, 1H), 4.63 (d, *J* = 14.3 Hz, 1H), 4.31 (d, *J* = 14.4 Hz, 1H), 3.53 (ddq, *J* = 6.2, 3.7, 2.6 Hz, 1H), 1.61 (dd, *J* = 2.6, 1.6 Hz, 3H). ¹³C NMR (126 MHz, MeOD) δ 170.1, 137.5, 132.3, 130.7, 130.5, 128.1, 127.6, 125.5, 124.2, 123.9, 120.5, 94.5, 68.0, 66.8, 51.9, 21.3. HRMS (ESI) calcd for C₁₆H₁₆NO₃⁺ (MH⁺) 270.1125, found 270.1133.

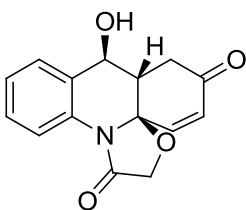
***syn*-12-Hydroxy-14,16-dimethyl-2-oxa-5-azatetracyclo[11.4.0.0^{1,5}.0^{6,11}]heptadeca-6,8,10,14,16-pentaen-4-one** (*syn*-**3.54c**). General procedure **E** was followed on a 0.332 g (1.17 mmol) scale of **3.51c**, which after flash chromatography on silica gel (gradient elution: hexane → hexane–ethyl acetate 70:30) afforded 0.245 g (74%) of *syn*-**3.54c**.



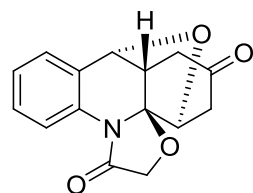
syn-**3.54c**: ¹H NMR (500 MHz, MeOD) δ 8.31 (dd, *J* = 8.3, 1.2 Hz, 1H), 7.53 (dd, *J* = 7.7, 1.5 Hz, 1H), 7.35 (td, *J* = 8.3, 7.9, 1.6 Hz, 1H), 7.20 (td, *J* = 7.5, 1.2 Hz, 1H), 5.87 (s, 1H), 5.46 (s, 1H), 4.85 (d, *J* = 6.1 Hz, 1H), 4.42 (d, *J* = 14.1 Hz, 1H), 4.16 (d, *J* = 14.1 Hz, 1H), 2.78 (d, *J* = 6.1 Hz, 1H), 2.00 (d, *J* = 1.6 Hz, 3H), 1.75 (d, *J* = 1.6 Hz, 3H). ¹³C NMR (126 MHz, MeOD) δ 171.5, 142.5, 136.3, 133.9, 131.5, 131.0, 129.6, 126.2, 125.8, 120.7, 119.5, 94.8, 66.5,

65.0, 51.6, 22.3, 21.5. HRMS (ESI) calcd for C₁₇H₁₈NO₃⁺ (MH⁺) 284.1281, found 284.1284.

***anti*-12-Hydroxy-2-oxa-5-azatetracyclo[11.4.0.0^{1,5}.0^{6,11}]heptadeca-6,8,10,16-tetraene-4,15-dione (*anti*-3.60d) and *N*-[9-Oxo-11,18-dioxa-8-azapentacyclo[13.2.1.0^{2,7}.0^{8,12}.0^{12,17}]octadeca-2,4,6,13-tetraen-15-yl]acetamide (3.63d).** General procedure **E** was followed on a 0.296 g (1.04 mmol) scale of **3.51d**. The crude photoproducts were then subjected to general procedure **F** with 1.05 mmol of TsOH·H₂O, with one modification: the mixture was refluxed for 3 days. Further purification by flash chromatography on silica gel (gradient elution: DCM → DCM–methanol 98:2) afforded 0.066 g (23% after two steps) of *anti*-**3.60d** and 0.145 g (51% after two steps) of **3.63d**.



***anti*-3.60d:** ¹H NMR (500 MHz, CDCl₃) δ 8.22 (dd, *J* = 8.3, 1.2 Hz, 1H), 7.56 (dt, *J* = 7.8, 1.2 Hz, 1H), 7.38 (dddd, *J* = 8.3, 7.3, 1.6, 0.7 Hz, 1H), 7.26 (ddd, *J* = 7.8, 7.3, 1.2 Hz, 1H), 6.73 (dd, *J* = 10.1, 2.3 Hz, 1H), 6.11 (dd, *J* = 10.1, 1.2 Hz, 1H), 4.52 (d, *J* = 14.3 Hz, 1H), 4.49 (dd, *J* = 9.4, 9.2 Hz, 1H), 4.25 (d, *J* = 14.3 Hz, 1H), 3.09 (dd, *J* = 17.5, 4.35 Hz, 1H), 3.01 (ddd, *J* = 17.5, 2.3, 1.2 Hz, 1H), 2.72 (d, *J* = 9.2 Hz, 1H), 2.63 (ddt, *J* = 9.4, 4.35, 2.3 Hz, 1H). ¹³C NMR (126 MHz, CDCl₃) δ 196.2, 167.8, 146.0, 134.0, 132.0, 129.5, 128.5, 128.3, 126.1, 120.1, 91.1, 70.3, 67.5, 46.7, 36.6. HRMS (ESI) calcd for C₁₅H₁₄NO₄⁺ (MH⁺) 272.0917, found 272.0926.

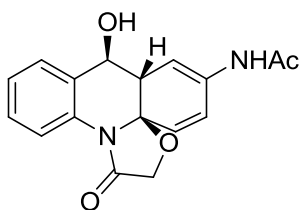


3.63d: ¹H NMR (500 MHz, CDCl₃) δ 8.56 (ddt, *J* = 8.2, 1.1, 0.6 Hz, 1H), 7.37 (ddd, *J* = 8.3, 7.4, 1.6 Hz, 1H), 7.16 (dd, *J* = 7.5, 1.6 Hz, 1H), 7.10 (ddd, *J* = 7.5, 7.4, 1.1 Hz, 1H), 4.84 (s, 1H), 4.60 (d, *J* = 14.2 Hz, 1H), 4.55 (d, *J* = 14.2 Hz, 1H), 4.51 (ddd, *J* = 4.3, 1.3, 1.2 Hz, 1H), 3.00 (ddt, *J*

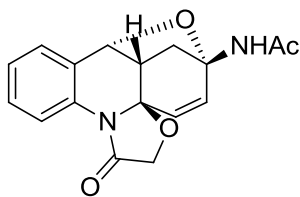
= 18.3, 5.0, 0.9 Hz, 1H), 2.89 (ddt, $J = 17.4, 1.3, 0.8$ Hz, 1H), 2.74 (ddd, $J = 18.3, 2.6, 1.9$ Hz, 1H), 2.69 (m, 2H). ^{13}C NMR (126 MHz, CDCl_3) δ 205.7, 166.6, 134.5, 130.3, 128.7, 126.7, 124.9, 117.9, 99.3, 81.4, 79.6, 68.7, 46.2, 40.8, 40.7. HRMS (ESI) calcd for $\text{C}_{15}\text{H}_{14}\text{NO}_4^+$ (MH^+) 272.0917, found 272.0909.

anti-N-12-Hydroxy-4-oxo-2-oxa-5-azatetracyclo[11.4.0.0^{1,5}.0^{6,11}]heptadeca-6,8,10,14,16-pentaen-15-yl]acetamide (*anti*-3.54f) and N-[9-Oxo-11,18-dioxa-8-azapentacyclo[13.2.1.0^{2,7}.0^{8,12}.0^{12,17}]octadeca-2,4,6,13-tetraen-15-yl]acetamide (3.62f).

General procedure E was followed on a from 0.286 g (0.848 mmol) scale of **3.51f**. Under nitrogen, the crude photoproducts were redissolved in anhydrous DCM (30 mL) and treated with 0.2 M HCl in ether (260 μL , 0.052 mmol). The mixture was refluxed for 5 days, volatiles were removed *in vacuo*, and further purification by flash chromatography on silica gel (gradient elution: DCM \rightarrow DCM–methanol 95:5) afforded 0.014 g (5%) of *anti*-**3.54f** and 0.119 g (45% after two steps) of **3.62f**.

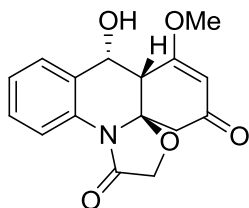


anti-**3.54f**: ^1H NMR (500 MHz, DMSO) δ 9.39 (s, 1H), 8.14 (dd, $J = 8.25, 1.2$ Hz, 1H), 7.46 (d, $J = 7.3$ Hz, 1H), 7.32 (dddd, $J = 8.25, 7.3, 1.6, 0.6$ Hz, 1H), 7.17 (ddd, $J = 8.25, 7.3, 1.2$ Hz, 1H), 6.64 (dd, $J = 6.2, 2.2$ Hz, 1H), 6.25 (dd, $J = 9.85, 2.2$ Hz, 1H), 6.04 (d, $J = 9.85$ Hz, 1H), 5.82 (d, $J = 7.7$ Hz, 1H), 4.44 (d, $J = 14.1$ Hz, 1H), 4.32 (dd, $J = 8.6, 7.8$ Hz, 1H), 4.27 (d, $J = 14.1$ Hz, 1H), 2.78 (ddd, $J = 8.6, 6.2, 1.3$ Hz, 1H), 1.94 (s, 3H). ^{13}C NMR (126 MHz, DMSO) δ 168.5, 132.2, 132.1, 130.9, 128.9, 128.8, 127.9, 127.2, 124.4, 119.1, 110.6, 99.5, 92.1, 71.6, 65.8, 45.0, 23.8. HRMS (ESI) calcd for $\text{C}_{17}\text{H}_{17}\text{N}_2\text{O}_4^+$ (MH^+) 313.1183, found 313.1182.



3.62f: ^1H NMR (500 MHz, DMSO) δ 8.68 (s, 1H), 8.07 (dd, $J = 8.2, 1.3$ Hz, 1H), 7.38 (m, 2H), 7.20 (ddd, $J = 7.7, 7.3, 1.3$ Hz, 1H), 6.50 (dd, $J = 9.6, 1.4$ Hz, 1H), 5.56 (dd, $J = 9.6, 2.2$ Hz, 1H), 5.19 (d, $J = 5.3$ Hz, 1H), 4.57 (d, $J = 14.0$ Hz, 1H), 4.38 (d, $J = 14.0$ Hz, 1H), 3.07 (ddd, $J = 5.3, 5.0, 2.2$ Hz, 1H), 2.50 (m, 1H), 2.27 (d, $J = 11.3$ Hz, 1H), 1.86 (s, 3H). ^{13}C NMR (126 MHz, DMSO) δ 169.8, 167.6, 140.1, 132.0, 130.8, 128.6, 126.5, 125.0, 124.8, 119.2, 92.2, 86.7, 71.7, 66.5, 43.1, 37.7, 23.3. HRMS (ESI) calcd for $\text{C}_{17}\text{H}_{17}\text{N}_2\text{O}_4^+$ (MH^+) 313.1183, found 313.1187.

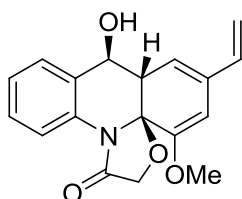
***syn*-12-Hydroxy-14-methoxy-2-oxa-5-azatetracyclo[11.4.0.0^{1,5}.0^{6,11}]heptadeca-6,8,10,14-tetraene-4,16-dione (*syn*-3.60g).** General procedure **E** was followed on a 0.241 g (0.764 mmol) scale of **3.51g**, which after flash chromatography on silica gel (gradient elution: hexane \rightarrow ethyl acetate) afforded 0.079 g (34%) of *syn*-**3.60g**.



***syn*-3.60g:** ^1H NMR (500 MHz, DMSO) δ 8.26 (dd, $J = 8.3, 1.2$ Hz, 1H), 7.50 (dd, $J = 7.7, 1.6$ Hz, 1H), 7.40 (ddd, $J = 8.3, 7.3, 1.6$ Hz, 1H), 7.23 (ddd, $J = 7.7, 7.3, 1.2$ Hz, 1H), 5.94 (d, $J = 5.7$ Hz, 1H), 5.56 (s, 1H), 4.90 (dd, $J = 5.7, 5.3$ Hz, 1H), 4.52 (d, $J = 14.2$ Hz, 1H), 4.25 (d, $J = 14.2$ Hz, 1H), 3.77 (s, 3H), 3.19 (dd, $J = 5.3, 1.9$ Hz, 1H), 2.88 (d, $J = 16.2$ Hz, 1H), 2.64 (dd, $J = 16.2, 1.9$ Hz, 1H). ^{13}C NMR (126 MHz, DMSO) δ 195.0, 173.2, 168.5, 132.0, 131.0, 128.7, 128.1, 124.6, 118.8, 103.9, 92.9, 65.2, 63.5, 56.4, 49.5, 43.2. HRMS (ESI) calcd for $\text{C}_{16}\text{H}_{15}\text{NO}_5\text{Li}^+$ (MLi^+) 308.1105, found 308.1108.

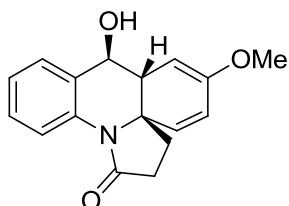
***anti*-15-Ethenyl-12-hydroxy-17-methoxy-2-oxa-5-azatetracyclo[11.4.0.0^{1,5}.0^{6,11}]heptadeca-6,8,10,14,16-pentaen-4-one (*anti*-3.54h).** General procedure **E** was followed on a 0.090 g (0.290 mmol) scale of **3.51h**, with the following modifications: DCM

(96 mL) was used as a solvent, no aqueous workup was performed. Further purification by flash chromatography on silica gel (gradient elution: hexane → hexane–ethyl acetate 60:40) afforded 0.064 g (71%) of *anti*-**3.54h**.



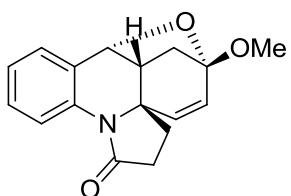
anti-**3.54h**: ^1H NMR (500 MHz, DMSO) δ 8.33 (d, J = 8.3 Hz, 1H), 7.45 (d, J = 7.8 Hz, 1H), 7.31 (t, J = 7.8 Hz, 1H), 7.17 (t, J = 7.5 Hz, 1H), 6.41 (dd, J = 17.6, 10.9 Hz, 1H), 6.04 (d, J = 6.0 Hz, 1H), 5.96 (d, J = 7.9 Hz, 1H), 5.63 (s, 1H), 5.48 (d, J = 17.5 Hz, 1H), 5.11 (d, J = 10.9 Hz, 1H), 4.35 (t, J = 8.6 Hz, 1H), 4.31 (s, 2H), 3.59 (s, 3H), 2.84 (dd, J = 9.3, 6.0 Hz, 1H). ^{13}C NMR (126 MHz, DMSO) δ 169.1, 155.8, 136.5, 132.2, 132.0, 130.2, 128.0, 127.1, 124.4, 122.6, 117.8, 112.7, 93.9, 93.1, 70.5, 66.6, 55.9, 46.8. HRMS (ESI) calcd for $\text{C}_{18}\text{H}_{18}\text{NO}_4^+$ (MH^+) 312.1230, found 312.1239.

***anti*-12-Hydroxy-15-methoxy-5-azatetracyclo[11.4.0.0^{1,5}.0^{6,11}]heptadeca-6,8,10,14,16-pentaen-4-one (*anti*-**3.54i**) and 15-Methoxy-18-oxa-8-azapentacyclo[13.2.1.0^{2,7}.0^{8,12}.0^{12,17}]octadeca-2,4,6,13-tetraen-9-one (**3.62i**)**. General procedure **E** was followed on a 0.308 g (1.09 mmol) scale of **3.51i** with the following modifications: methanol (45 mL) was used as a solvent, no aqueous workup was performed. Further purification by flash chromatography on silica gel (gradient elution: hexane → hexane–ethyl acetate 40:60) afforded 0.027 g (9%) of *anti*-**3.54i** and 0.153 g (50%) of **3.62i**.



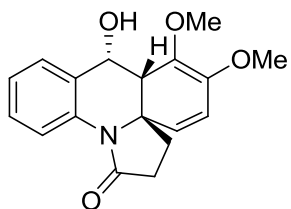
anti-**3.54i**: ^1H NMR (500 MHz, CDCl_3) δ 8.61 (dd, J = 8.4, 1.2 Hz, 1H), 7.55 (d, J = 7.7 Hz, 1H), 7.28 (dddd, J = 8.4, 7.3, 1.6, 0.7 Hz, 1H), 7.12 (ddd, J = 7.7, 7.3, 1.2 Hz, 1H), 5.92 (dd, J = 9.95, 1.7 Hz, 1H), 5.79 (dd, J = 9.95, 2.5 Hz, 1H), 5.21 (dd, J = 6.6, 2.5 Hz, 1H), 4.67 (d, J = 9.15 Hz, 1H), 3.63 (s, 3H), 2.56 (ddd, J = 17.0, 12.1, 8.8, 1H), 2.56 (s, 1H), 2.35

(ddd, $J = 9.15, 6.6, 1.7$ Hz, 1H), 2.23 (m, 2H), 2.02 (td, $J = 12.3, 9.2$ Hz, 1H). ^{13}C NMR (126 MHz, CDCl_3) δ 174.2, 153.8, 136.9, 134.8, 130.8, 128.3, 126.9, 126.3, 124.0, 119.8, 94.5, 71.7, 65.7, 54.7, 45.8, 34.4, 31.4. HRMS (ESI) calcd for $\text{C}_{17}\text{H}_{18}\text{NO}_3^+$ (MH^+) 284.1281, found 284.1288.

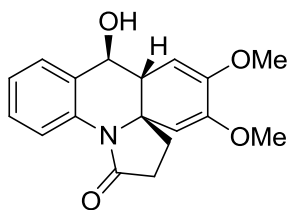


3.62i: ^1H NMR (500 MHz, CDCl_3) δ 8.18 (dd, $J = 8.3, 1.2$ Hz, 1H), 7.47 (dd, $J = 7.7, 1.6$ Hz, 1H), 7.32 (ddd, $J = 8.7, 7.4, 1.6$ Hz, 1H), 7.16 (ddd, $J = 7.7, 7.3, 1.2$ Hz, 1H), 6.07 (dd, $J = 9.6, 1.8$ Hz, 1H), 5.34 (dd, $J = 9.6, 2.2$ Hz, 1H), 5.13 (d, $J = 5.4$ Hz, 1H), 3.49 (s, 3H), 2.78 (ddd, $J = 5.5, 5.4, 2.2$ Hz, 1H), 2.73 (dd, $J = 18.0, 8.5$ Hz, 1H), 2.58 (ddd, $J = 17.5, 8.4, 7.2$ Hz, 1H), 2.47 (ddd, $J = 11.0, 5.5, 1.8$ Hz, 1H), 2.21 (m, 2H), 2.01 (d, $J = 11.0$ Hz, 1H). ^{13}C NMR (126 MHz, CDCl_3) δ 172.9, 136.3, 133.3, 130.6, 129.7, 128.8, 127.6, 125.0, 121.2, 104.2, 72.3, 64.7, 50.6, 45.4, 35.3, 30.5, 30.1. HRMS (ESI) calcd for $\text{C}_{17}\text{H}_{18}\text{NO}_3^+$ (MH^+) 284.1281, found 284.1287.

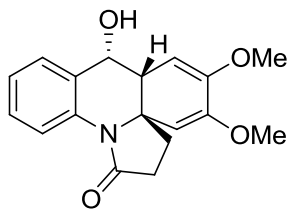
***syn*-12-Hydroxy-14,15-dimethoxy-5-azatetracyclo[11.4.0.0^{1,5}.0^{6,11}]heptadeca-6,8,10,14,16-pentaen-4-one** (*syn*-**3.54j**), ***anti*-12-hydroxy-15,16-dimethoxy-5-azatetracyclo[11.4.0.0^{1,5}.0^{6,11}]heptadeca-6,8,10,14,16-pentaen-4-one** (*anti*-**3.54j'**), ***syn*-12-hydroxy-15,16-dimethoxy-5-azatetracyclo[11.4.0.0^{1,5}.0^{6,11}]heptadeca-6,8,10,14,16-pentaen-4-one** (*syn*-**3.54j'**). General procedure **E** was followed on a 0.338 g (1.08 mmol) scale of **3.51j**, which after flash chromatography on silica gel pretreated with pyridine (gradient elution: hexane \rightarrow hexane–ethyl acetate + 1% TEA 40:60) afforded 0.151 g (45%) of *syn*-**3.54j**, 0.025 g (7%) of *anti*-**3.54j'** and 0.085 g (25%) of *syn*-**3.54j'**.



syn-**3.54j**: $^1\text{H NMR}$ (500 MHz, CDCl_3) δ 8.43 (dd, $J = 8.35, 1.2$ Hz, 1H), 7.55 (dd, $J = 7.8, 1.6$ Hz, 1H), 7.33 (ddd, $J = 8.35, 7.3, 1.7$ Hz, 1H), 7.16 (ddd, $J = 7.8, 7.3, 1.2$ Hz, 1H), 5.94 (d, $J = 9.9$ Hz, 1H), 5.65 (dd, $J = 9.9, 1.2$ Hz, 1H), 4.71 (dd, $J = 9.3, 5.9$ Hz, 1H), 3.91 (s, 3H), 3.61 (s, 3H), 2.82 (dd, $J = 5.85, 1.2$ Hz, 1H), 2.68 (ddd, $J = 17.0, 11.8, 8.8$ Hz, 1H), 2.50 (d, $J = 9.4$ Hz, 1H), 2.46 (ddd, $J = 17.0, 9.05, 1.8$ Hz, 1H), 2.38 (ddd, $J = 12.4, 8.8, 1.8$ Hz, 1H), 2.27 (ddd, $J = 12.4, 11.8, 9.05$ Hz, 1H). $^{13}\text{C NMR}$ (126 MHz, CDCl_3) δ 173.7, 139.1, 137.6, 134.1, 130.3, 129.6, 129.4, 128.9, 126.7, 124.5, 120.7, 65.4, 63.2, 59.3, 59.0, 50.7, 36.6, 30.9. HRMS (ESI) calcd for $\text{C}_{18}\text{H}_{20}\text{NO}_4^+$ (MH^+) 314.1387, found 314.1386.



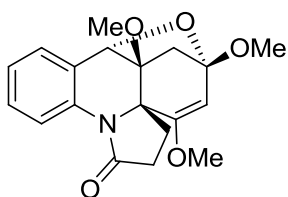
anti-**3.54j**: $^1\text{H NMR}$ (500 MHz, CDCl_3) δ 8.69 (dd, $J = 8.4, 1.7$ Hz, 1H), 7.56 (dt, $J = 7.6, 1.2$ Hz, 1H), 7.30 (ddd, $J = 8.4, 7.3, 1.2$ Hz, 1H), 7.13 (ddd, $J = 7.6, 7.3, 1.7$ Hz, 1H), 5.34 (d, $J = 6.8$ Hz, 1H), 4.82 (d, $J = 1.7$ Hz, 1H), 4.73 (dd, $J = 9.2, 8.5$ Hz, 1H), 3.71 (s, 3H), 3.53 (s, 3H), 2.64 (ddd, $J = 16.9, 12.4, 8.6$ Hz, 1H), 2.35 (ddd, $J = 9.2, 6.8, 1.7$ Hz, 1H), 2.32 (ddd, $J = 16.9, 9.0, 1.4$ Hz, 1H), 2.31 (d, $J = 8.5$ Hz, 1H), 2.26 (ddd, $J = 12.2, 8.6, 1.4$ Hz, 1H), 2.05 (ddd, $J = 12.4, 12.2, 9.0$ Hz, 1H). $^{13}\text{C NMR}$ (126 MHz, CDCl_3) δ 174.2, 150.9, 150.4, 134.8, 130.2, 128.4, 126.7, 123.9, 119.6, 102.4, 97.2, 71.8, 65.7, 55.4, 55.3, 46.2, 35.4, 31.3. HRMS (ESI) calcd for $\text{C}_{18}\text{H}_{20}\text{NO}_4^+$ (MH^+) 314.1387, found 314.1388.



syn-**3.54j'**: $^1\text{H NMR}$ (500 MHz, CDCl_3) δ 8.18 (dd, $J = 8.2, 1.2$ Hz, 1H), 7.43 (dd, $J = 7.7, 1.6$ Hz, 1H), 7.32 (ddd, $J = 8.2, 7.3, 1.6$ Hz, 1H), 7.17 (ddd, $J = 7.7, 7.3, 1.2$ Hz, 1H), 4.88 (d, $J = 5.5$ Hz, 1H), 4.73 (s, 1H), 4.48 (dd, $J = 6.1, 5.3$ Hz, 1H), 3.61 (s, 3H), 3.55 (s, 3H), 3.07 (dd,

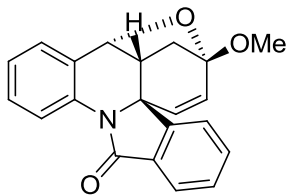
$J = 5.3, 5.5$ Hz, 1H), 2.74 (ddd, $J = 16.95, 12.2, 8.25$ Hz, 1H), 2.52 (d, $J = 6.1$ Hz, 1H), 2.44 (ddd, $J = 16.95, 8.8, 1.2$ Hz, 1H), 2.33 (ddd, $J = 12.4, 8.25, 1.2$ Hz, 1H), 2.17 (ddd, $J = 12.4, 12.2, 8.8$ Hz, 1H). ^{13}C NMR (126 MHz, CDCl_3) δ 173.2, 151.3, 150.8, 134.0, 131.7, 128.4, 127.7, 124.8, 121.6, 99.9, 92.9, 66.8, 63.1, 55.4, 55.3, 47.0, 37.9, 30.6. HRMS (ESI) calcd for $\text{C}_{18}\text{H}_{20}\text{NO}_4^+$ (MH^+) 314.1387, found 314.1385.

13,15,17-Trimethoxy-18-oxa-8-azapentacyclo[13.2.1.0^{2,7}.0^{8,12}.0^{12,17}]octadeca-2,4,6,13-tetraen-9-one (3.62k). General procedure **E** was followed on a 0.232 g (0.675 mmol) scale of **3.51k**, which after flash chromatography on silica gel (gradient elution: hexane \rightarrow hexane–ethyl acetate 80:20) afforded 0.178 g (77%) of **3.62k**.

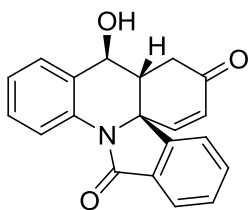


3.62k: ^1H NMR (500 MHz, MeOD) δ 7.90 (dd, $J = 8.2, 1.2$ Hz, 1H), 7.42 (dd, $J = 7.8, 1.5$ Hz, 1H), 7.30 (ddd, $J = 8.6, 7.4, 1.6$ Hz, 1H), 7.18 (td, $J = 7.5, 1.3$ Hz, 1H), 5.05 (m, 2H), 3.52 (s, 3H), 3.42 (s, 3H), 3.34 (s, 3H), 2.96 (dd, $J = 10.5, 1.5$ Hz, 1H), 2.60 (m, 3H), 2.17 (m, 1H), 1.86 (d, $J = 10.5$ Hz, 1H). ^{13}C NMR (126 MHz, MeOD) δ 176.8, 157.2, 133.5, 131.7, 129.2, 129.1, 126.1, 122.4, 106.2, 105.7, 84.0, 72.2, 71.2, 56.0, 51.7, 50.7, 36.1, 32.2, 24.2. HRMS (ESI) calcd for $\text{C}_{19}\text{H}_{22}\text{NO}_5^+$ (MH^+) 344.1492, found 344.1497.

19-Methoxy-22-oxa-8-azahexacyclo[17.2.1.0^{2,7}.0^{8,16}.0^{10,15}.0^{16,21}]docosa-2,4,6,10(15),11,13,17-heptaen-9-one (3.62l) and anti-7-Hydroxy-14-azapentacyclo[12.7.0.0^{1,6}.0^{8,13}.0^{16,21}]henicosa-2,8,10,12,16(21),17,19-heptaene-4,15-dione (anti-3.60l). General procedure **E** was followed on a 0.137 g (0.413 mmol) scale of **3.51l**. The crude photoproducts were then subjected to general procedure **F**, which after flash chromatography on silica gel (gradient elution: hexane \rightarrow hexane–ethyl acetate 80:20) afforded 0.033 g (24%) of **3.62l** and 0.040 g (31%) of *anti*-**3.60l**.



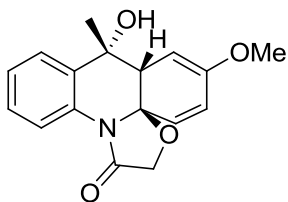
3.62l: ^1H NMR (500 MHz, CDCl_3) δ 8.21 (dd, $J = 8.2, 1.2$ Hz, 1H), 7.98 (dt, $J = 7.4, 1.1$ Hz, 1H), 7.63 (m, 2H), 7.57 (m, 1H), 7.54 (dd, $J = 7.7, 1.4$ Hz, 1H), 7.44 (ddd, $J = 8.2, 7.4, 1.7$ Hz, 1H), 7.22 (ddd, $J = 7.7, 7.4, 1.2$ Hz, 1H), 6.34 (dd, $J = 9.6, 1.1$ Hz, 1H), 5.27 (d, $J = 5.2$ Hz, 1H), 5.16 (dd, $J = 9.6, 2.1$ Hz, 1H), 3.57 (s, 3H), 2.80 (dddd, $J = 5.2, 4.1, 2.1, 2.0$ Hz, 1H), 2.59 (m, 2H). ^{13}C NMR (126 MHz, CDCl_3) δ 165.6, 146.3, 139.1, 132.8, 131.5, 130.4, 129.6, 129.0, 127.6, 127.6, 127.5, 125.1, 124.8, 123.2, 121.8, 104.2, 73.0, 66.2, 50.7, 44.3, 35.8. HRMS (ESI) calcd for $\text{C}_{21}\text{H}_{18}\text{NO}_3^+$ (MH^+) 332.1281, found 332.1288.



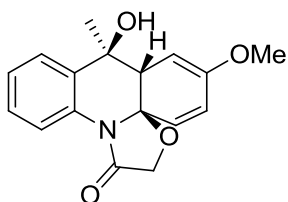
anti-**3.60l:** ^1H NMR (500 MHz, CDCl_3) δ 8.22 (dd, $J = 8.3, 1.2$ Hz, 1H), 8.00 (ddd, $J = 7.4, 1.3, 0.8$ Hz, 1H), 7.66 (td, $J = 7.5, 1.3$ Hz, 1H), 7.62 (dd, $J = 7.4, 1.1$ Hz, 1H), 7.59 (d, $J = 7.6$ Hz, 1H), 7.47 (dddd, $J = 8.3, 7.3, 1.6, 0.7, 0.9$ Hz, 1H), 7.38 (dddd, $J = 8.2, 7.3, 1.7, 0.7$ Hz, 1H), 7.23 (ddd, $J = 7.6, 7.3, 1.2$ Hz, 1H), 6.65 (dd, $J = 10.1, 2.3$ Hz, 1H), 6.20 (dd, $J = 10.1, 0.8$ Hz, 1H), 4.77 (dd, $J = 9.2, 9.0$ Hz, 1H), 3.28 (dd, $J = 18.6, 4.5$ Hz, 1H), 3.22 (ddd, $J = 18.6, 2.1, 0.8$ Hz, 1H), 2.37 (dddd, $J = 9.0, 4.5, 2.3, 2.1$ Hz, 1H), 2.07 (d, $J = 9.4$ Hz, 1H). ^{13}C NMR (126 MHz, CDCl_3) δ 196.2, 165.7, 150.0, 143.5, 133.6, 133.0, 132.3, 131.7, 130.1, 129.1, 128.9, 128.3, 125.6, 125.4, 123.8, 122.2, 69.9, 66.4, 46.9, 38.5. HRMS (ESI) calcd for $\text{C}_{20}\text{H}_{15}\text{NO}_3\text{Li}^+$ (MLi^+) 324.1206, found 324.1209.

***syn*-12-Hydroxy-15-methoxy-12-methyl-2-oxa-5-azatetracyclo[11.4.0.0^{1,5}.0^{6,11}]heptadeca-6,8,10,14,16-pentaen-4-one** (*syn*-**3.55d**) and ***anti*-12-hydroxy-15-methoxy-12-methyl-2-oxa-5-azatetracyclo[11.4.0.0^{1,5}.0^{6,11}]heptadeca-6,8,10,14,16-pentaen-4-one** (*anti*-**3.55d**). General procedure **E** was followed on a 0.449 g (1.50 mmol) scale of

3.52d, which after flash chromatography on silica gel (gradient elution: hexane → ethyl acetate) afforded 0.043 g (10%) of *syn*-**3.55d** and 0.340 g (76%) of *anti*-**3.55d**.



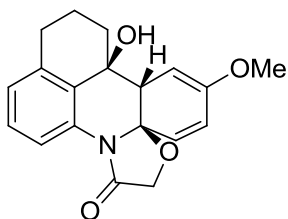
syn-**3.55d**: $^1\text{H NMR}$ (500 MHz, MeOD) δ 7.59 (dd, $J = 7.3, 1.9$ Hz, 1H), 7.56 (dd, $J = 7.8, 1.4$ Hz, 1H), 7.31 (td, $J = 7.6, 1.8$ Hz, 1H), 7.27 (td, $J = 7.5, 1.6$ Hz, 1H), 5.86 (dd, $J = 9.9, 0.7$ Hz, 1H), 5.81 (dd, $J = 9.9, 2.4$ Hz, 1H), 5.00 (dd, $J = 4.3, 2.5$ Hz, 1H), 4.63 (d, $J = 14.5$ Hz, 1H), 4.31 (d, $J = 14.5$ Hz, 1H), 3.47 (s, 3H), 3.39 (d, $J = 4.3$ Hz, 1H), 1.51 (s, 3H).
 $^{13}\text{C NMR}$ (126 MHz, MeOD) δ 170.3, 152.6, 139.9, 131.8, 128.5, 127.7, 127.5, 127.1, 126.2, 124.0, 94.3, 92.5, 72.8, 66.6, 55.3, 54.7, 30.8. HRMS (ESI) calcd for $\text{C}_{17}\text{H}_{18}\text{NO}_4^+$ (MH^+) 300.1230, found 300.1235.



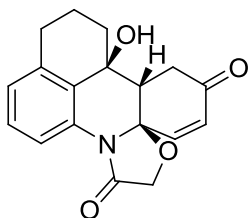
anti-**3.55d**: $^1\text{H NMR}$ (500 MHz, MeOD) δ 7.73 (dd, $J = 7.9, 1.3$ Hz, 1H), 7.52 (dd, $J = 7.7, 1.5$ Hz, 1H), 7.34 (td, $J = 7.7, 1.5$ Hz, 1H), 7.25 (td, $J = 7.6, 1.3$ Hz, 1H), 5.89 (dd, $J = 10.0, 0.8$ Hz, 1H), 5.86 (dd, $J = 9.9, 2.2$ Hz, 1H), 4.78 (dd, $J = 4.9, 2.2$ Hz, 1H), 4.55 (d, $J = 14.1$ Hz, 1H), 4.29 (d, $J = 14.1$ Hz, 1H), 3.51 (s, 3H), 3.38 (d, $J = 4.8$ Hz, 1H), 1.68 (s, 3H).
 $^{13}\text{C NMR}$ (126 MHz, MeOD) δ 171.6, 153.4, 137.9, 133.9, 129.8, 129.3, 128.2, 127.1, 126.9, 124.2, 94.6, 92.4, 73.6, 67.0, 54.9, 54.4, 26.3. HRMS (ESI) calcd for $\text{C}_{17}\text{H}_{18}\text{NO}_4^+$ (MH^+) 300.1230, found 300.1228.

***anti*-12-Hydroxy-9-methoxy-5-oxa-2-azapentacyclo[10.7.1.0^{2,6}.0^{6,11}.0^{16,20}]icosa-1(19),7,9,16(20),17-pentaen-3-one (*anti*-**3.56d**) and *anti*-12-Hydroxy-5-oxa-2-azapentacyclo[10.7.1.0^{2,6}.0^{6,11}.0^{16,20}]icosa-1(19),7,16(20),17-tetraene-3,9-dione (*anti*-**3.61d**)**. General procedure **E** was followed on a 0.187 g (0.575 mmol) scale of **3.53d**,

which after flash chromatography on silica gel (gradient elution: hexane → ethyl acetate) afforded 0.098 g (52%) of *anti*-**3.56d** and 0.072 g (38%) of *anti*-**3.61d**.



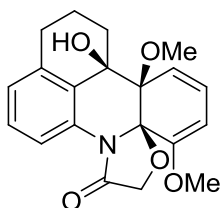
anti-**3.56d**: $^1\text{H NMR}$ (500 MHz, CDCl_3) δ 7.35 (d, $J = 7.8$ Hz, 1H), 7.25 (dd, $J = 7.8, 7.7$ Hz, 1H), 6.99 (dd, $J = 7.7, 1.1$ Hz, 1H), 5.82 (dd, $J = 9.9, 2.4$ Hz, 1H), 5.61 (d, $J = 9.9$ Hz, 1H), 4.65 (dd, $J = 4.8, 2.4$ Hz, 1H), 4.55 (d, $J = 14.1$ Hz, 1H), 4.45 (d, $J = 14.1$ Hz, 1H), 3.63 (d, $J = 4.8$ Hz, 1H), 3.50 (s, 3H), 2.75 (dt, $J = 16.5, 4.5$ Hz, 1H), 2.68 (ddd, $J = 16.4, 10.5, 5.4$ Hz, 1H), 2.24 (ddd, $J = 13.6, 11.6, 3.8$ Hz, 1H), 2.18 (s, 1H), 2.04 (dddd, $J = 13.6, 5.1, 3.0, 1.2$ Hz, 1H), 1.90 (m, 2H). $^{13}\text{C NMR}$ (126 MHz, CDCl_3) δ 169.3, 150.6, 138.5, 133.4, 132.1, 128.6, 127.9, 127.3, 126.5, 122.7, 93.4, 91.0, 71.8, 66.2, 55.0, 54.5, 35.7, 29.7, 19.8. HRMS (ESI) calcd for $\text{C}_{19}\text{H}_{19}\text{LiNO}_4^+$ (MLi^+) 332.1469, found 332.1481.



anti-**3.61d**: $^1\text{H NMR}$ (500 MHz, CDCl_3) δ 7.35 (dd, $J = 7.8, 1.5$ Hz, 1H), 7.32 (dd, $J = 7.8, 7.3$ Hz, 1H), 7.09 (d, $J = 7.3$ Hz, 1H), 6.62 (d, $J = 10.1$ Hz, 1H), 6.03 (dd, $J = 10.1, 0.8$ Hz, 1H), 4.57 (d, $J = 14.4$ Hz, 1H), 4.42 (d, $J = 14.4$ Hz, 1H), 3.20 (dd, $J = 11.8, 6.6$ Hz, 1H), 2.81 (d, $J = 16.5$ Hz, 1H), 2.68 (dd, $J = 16.5, 6.6$ Hz), 2.67 (m, 1H), 2.26 (s, 1H), 1.91 (m, 5H). $^{13}\text{C NMR}$ (126 MHz, CDCl_3) δ 196.3, 171.2, 144.9, 139.1, 132.7, 130.0, 129.0, 128.9, 128.0, 123.7, 90.7, 71.1, 65.6, 50.6, 38.3, 34.2, 29.4, 18.8. HRMS (ESI) calcd for $\text{C}_{18}\text{H}_{17}\text{NO}_4\text{Li}^+$ (MLi^+) 318.1312, found 318.1320.

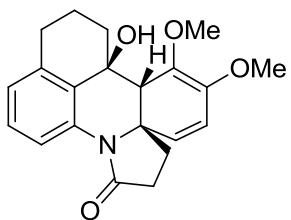
***anti*-12-Hydroxy-7,11-dimethoxy-5-oxa-2-azapentacyclo[10.7.1.0^{2,6}.0^{6,11}.0^{16,20}] icsa-1(19),7,9,16(20),17-pentaen-3-one (*anti*-**3.56e**)**. General procedure **E** was followed on a 0.480 g (1.35 mmol) scale of **3.53e** with the following modifications:

acetone (120 mL) was used as a solvent, no aqueous workup was performed. Further purification by flash chromatography on silica gel (gradient elution: hexane → hexane–ethyl acetate 80:20) afforded 0.232 g (48%) of *anti*-**3.56e**.



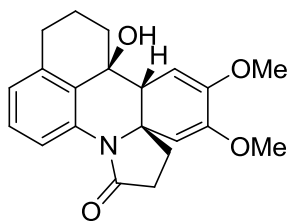
anti-**3.56e**: $^1\text{H NMR}$ (500 MHz, CDCl_3) δ 7.27 (m, 2H), 7.04 (m, 1H), 5.98 (dd, $J = 10.3, 6.6$ Hz, 1H), 5.13 (dd, $J = 10.3, 0.8$ Hz, 1H), 4.91 (dd, $J = 6.7, 0.8$ Hz, 1H), 4.78 (d, $J = 13.3$ Hz, 1H), 4.41 (d, $J = 13.3$ Hz, 1H), 3.68 (s, 3H), 3.50 (s, 3H), 3.07 (s, 1H), 2.77 (dt, $J = 16.2, 3.8$ Hz, 1H), 2.63 (ddd, $J = 16.5, 11.4, 5.2$ Hz, 1H), 2.11 (m, 2H), 1.91 (m, 2H). $^{13}\text{C NMR}$ (126 MHz, CDCl_3) δ 171.4, 158.4, 138.9, 133.5, 130.2, 128.3, 128.2, 127.3, 123.2, 117.3, 93.2, 92.3, 84.1, 74.0, 68.9, 55.8, 53.2, 32.6, 29.6, 19.5. HRMS (ESI) calcd for $\text{C}_{20}\text{H}_{22}\text{NO}_5^+$ (MH^+) 356.1492, found 356.1498.

anti-12-Hydroxy-9,10-dimethoxy-2-azapentacyclo[10.7.1.0^{2,6}.0^{6,11}.0^{16,20}]jicosa-1(19),7,9,16(20),17-pentaen-3-one (*anti*-**3.56j**) and *anti*-12-Hydroxy-8,9-dimethoxy-2-azapentacyclo[10.7.1.0^{2,6}.0^{6,11}.0^{16,20}]jicosa-1(19),7,9,16(20),17-pentaen-3-one (*anti*-**3.56j'**). General procedure **E** was followed on a 0.500 g (1.41 mmol) scale of **3.53j**, which after flash chromatography on silica gel (gradient elution: hexane → hexane–ethyl acetate 50:50) afforded 0.080 g (16%) of *anti*-**3.56j** and 0.268 g (54%) of *anti*-**3.56j'**.



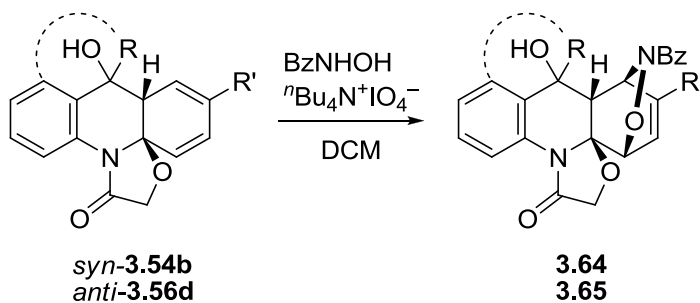
anti-**3.56j**: $^1\text{H NMR}$ (500 MHz, MeOD) δ 7.44 (d, $J = 7.9$ Hz, 1H), 7.19 (t, $J = 7.8$ Hz, 1H), 6.93 (dd, $J = 7.7, 1.1$ Hz, 1H), 5.71 (d, $J = 9.9$ Hz, 1H), 5.14 (dd, $J = 9.9, 1.2$ Hz, 1H), 3.83 (s, 3H), 3.57 (s, 3H), 3.21 (d, $J = 1.3$ Hz, 1H), 2.82 (m, 1H), 2.72 (m, 2H), 2.64 (ddd, $J = 17.3, 9.8, 5.2$ Hz, 1H), 2.56 (ddd, $J = 13.1, 9.8, 5.2$ Hz, 1H), 2.15 (m, 2H), 2.03 (m, 1H), 1.88 (td, $J = 13.2, 3.9$ Hz, 1H), 1.80 (ddq, $J = 13.0, 6.5, 3.6$ Hz, 1H).

^{13}C NMR (126 MHz, MeOD) δ 175.6, 139.8, 139.1, 137.3, 136.8, 136.0, 131.7, 128.5, 127.3, 125.2, 122.2, 70.4, 68.9, 61.6, 58.8, 58.6, 35.0, 32.7, 30.9, 29.9, 19.4. HRMS (ESI) calcd for $\text{C}_{21}\text{H}_{24}\text{NO}_4^+$ (MH^+) 354.1700, found 354.1704.



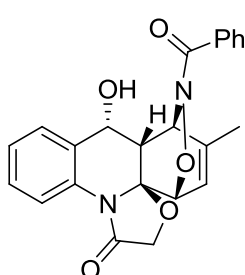
anti-**3.56j**¹: ^1H NMR (500 MHz, MeOD) δ 7.29 (d, $J = 7.8$ Hz, 1H), 7.20 (t, $J = 7.8$ Hz, 1H), 6.97 (dd, $J = 7.7, 1.2$ Hz, 1H), 4.78 (d, $J = 5.0$ Hz, 1H), 4.60 (s, 1H), 3.51 (s, 3H), 3.43 (s, 3H), 3.36 (d, $J = 5.0$ Hz, 1H), 2.79 (m, 2H), 2.69 (ddd, $J = 16.2, 10.4, 5.1$), 2.54 (ddd, $J = 8.1, 5.4, 2.8$), 2.52 (dd, $J = 9.3, 5.8$), 2.30 (m, 1H), 2.20 (ddd, $J = 13.4, 12.0, 3.4$ Hz, 1H), 1.96 (m, 2H), 1.84 (m, 1H). ^{13}C NMR (126 MHz, MeOD) δ 175.3, 150.1, 148.9, 139.6, 137.0, 134.0, 128.4, 127.3, 123.4, 101.7, 95.4, 72.0, 66.4, 56.1, 55.3, 55.1, 39.6, 36.9, 30.8, 30.6, 20.6. HRMS (ESI) calcd for $\text{C}_{21}\text{H}_{24}\text{NO}_4^+$ (MH^+) 354.1700, found 354.1693.

Post-Photochemical Hetero-Diels–Alder Reactions and Further Transformations



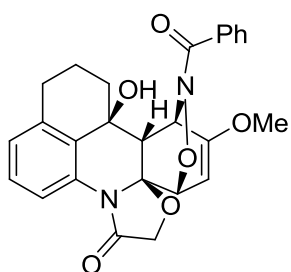
General Procedure G for the Reaction with (Nitrosocarbonyl)benzene. Under nitrogen, the crude photoproduct (1.08 mmol) was dissolved in anhydrous DCM (2 mL), and the solution was treated with tetrabutylammonium periodate (1.23 g, 2.84 mmol). Benzhydroxamic acid (0.411 g, 3.00 mmol) was added portionwise over 1 h, and the mixture was stirred at ambient temperature overnight. After that, the mixture was poured into water (10 mL), and the product was extracted with DCM (2 \times 20 mL). The combined

organic layers were washed with water (3×5 mL), dried over anhydrous Na₂SO₄ and concentrated *in vacuo*. Further purification by flash chromatography on silica gel yielded the desired cycloadduct.



16-Benzoyl-13-hydroxy-19-methyl-3,17-dioxo-6,16-diazapentacyclo[13.2.2.0^{2,6}.0^{2,14}.0^{7,12}]nonadeca-7,9,11,18-tetraen-5-one (3.64). General procedure **E** was followed on a 0.203 g (0.751 mmol) scale of **3.51b**, which afforded crude *syn*-**3.54b**. The

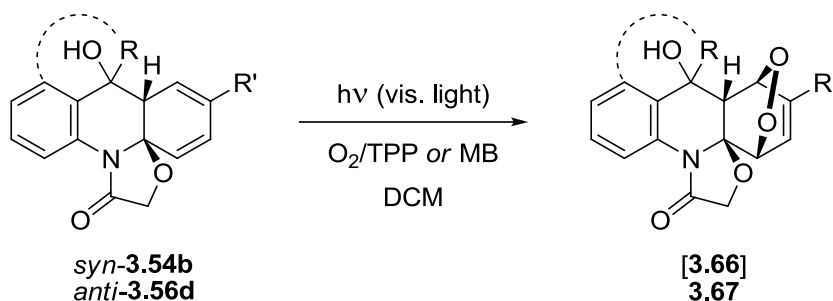
obtained photoproduct was then subjected to general procedure **G**, which after flash chromatography on silica gel (gradient elution: hexane → hexane–ethyl acetate 30:70) afforded 0.140 g (46% after two steps) of the title compound. ¹H NMR (500 MHz, DMSO) δ 7.57 (d, *J* = 7.6 Hz, 2H), 7.48 (m, 4H), 7.30 (m, 2H), 7.18 (br s, 1H), 6.31 (br d, *J* = 3.4 Hz, 1H), 5.47 (br s, 1H), 5.05 (br s, 1H), 4.89 (t, *J* = 5.2 Hz, 1H), 4.62 (d, *J* = 14.2 Hz, 1H), 4.35 (d, *J* = 14.2 Hz, 1H), 3.21 (br s, 1H), 1.27 (br s, 3H). ¹³C NMR (126 MHz, DMSO) δ 168.1, 132.4, 132.4, 131.4, 128.5, 128.2, 128.1, 127.3, 125.1, 124.4, 121.2, 120.3, 93.4, 74.7, 65.1, 63.2, 50.4, 19.3. HRMS (ESI) calcd for C₂₃H₂₁N₂O₅⁺ (MH⁺) 405.1445, found 405.1452.



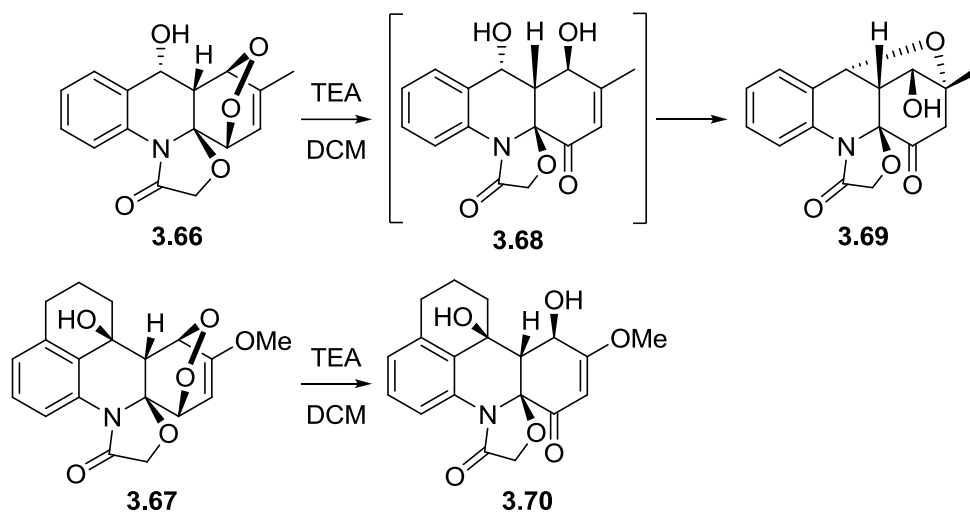
18-Benzoyl-15-hydroxy-21-methoxy-3,19-dioxo-6,18-diazahexacyclo[15.2.2.1^{7,11}.0^{2,6}.0^{2,16}.0^{15,22}]docosa-7,9,11(22),20-tetraen-5-one (3.65). General procedure **E** was followed on a 0.351 mg (1.08 mmol) scale of **3.53d**, which

afforded crude *anti*-**3.56d**. The obtained photoproduct was then subjected to general procedure **G**, which after flash chromatography on silica gel (gradient elution: hexane → hexane–ethyl acetate 60:40) afforded 0.208 g (42% after two steps) of the title

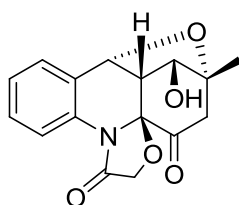
compound. ^1H NMR (500 MHz, CDCl_3) δ 7.77 (d, $J = 7.3$ Hz, 2H), 7.47 (t, $J = 7.4$ Hz, 1H), 7.40 (m, 2H), 7.29 (dd, $J = 7.8, 1.2$ Hz, 1H), 7.25 (dd, $J = 7.8, 7.6$ Hz, 1H), 6.99 (dd, $J = 7.6, 1.2$ Hz, 1H), 5.25 (br s, 1H), 4.63 (d, $J = 6.7$ Hz, 1H), 4.52 (d, $J = 14.5$ Hz, 1H), 4.46 (dd, $J = 6.7, 3.0$ Hz, 1H), 4.44 (d, $J = 14.5$ Hz, 1H), 3.23 (d, $J = 2.8$ Hz, 1H), 2.81 (s, 3H), 2.75 (dt, $J = 17.2, 3.1$ Hz, 1H), 2.65 (ddd, $J = 16.6, 12.2, 4.9$, 1H), 2.22 (s, 1H), 2.06 (m, 2H), 1.95 (m, 1H), 1.83 (qdd, $J = 12.9, 4.3, 2.9$ Hz, 1H). ^{13}C NMR (126 MHz, CDCl_3) δ 171.9, 169.7, 160.2, 138.7, 135.0, 133.3, 131.7, 129.4, 128.9, 128.6, 128.1, 126.7, 121.9, 95.3, 90.6, 77.7, 69.0, 66.1, 55.2, 54.7, 53.6, 34.7, 29.7, 18.9. HRMS (ESI) calcd for $\text{C}_{26}\text{H}_{25}\text{N}_2\text{O}_6^+$ (MH^+) 461.1707, found 461.1710.



General Procedure H for the Reaction with Singlet Oxygen. The crude photoproduct (1.39 mmol) was dissolved in anhydrous DCM (139 mL), and sensitizer (tetraphenylporphyrin or methylene blue; 6.9 μmol) was added. The mixture was placed into water bath and irradiated with fluorescent lamp (visible light) at ambient temperature with constant oxygen bubbling. The reaction progress was monitored by ^1H NMR. After completion, the resulting crude *endo*-peroxide solution was either used directly for the next step, or concentrated *in vacuo* with subsequent purification by flash chromatography on silica gel, which yielded the pure cycloadduct.



General Procedure I for Kornblum–DeLaMare Rearrangement. Solution of crude *endo*-peroxide (0.59 mmol) in anhydrous DCM (36 mL) was treated with TEA (103 μ L, 75 mg, 0.74 mmol). The mixture was stirred at ambient temperature overnight, and then washed with water (2 \times 20 mL). The organic layer was dried over anhydrous Na₂SO₄ and concentrated *in vacuo*. Further purification by flash chromatography on silica gel yielded the desired rearrangement product.

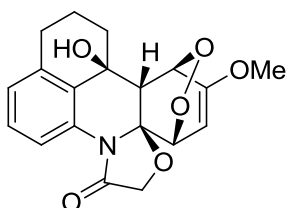


12,14-Dihydroxy-15-methoxy-2-oxa-5-azatetracyclo

[11.4.0.0^{1,5}.0^{6,11}]heptadeca-6,8,10,15-tetraene-4,17-dione (3.69).

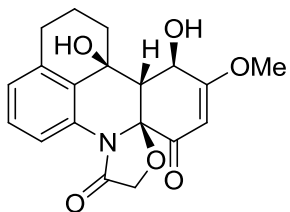
General procedure **E** was followed on a 0.203 g (0.751 mmol) scale of **3.51b**, which afforded crude *syn*-**3.54b**. The obtained photoproduct was then subjected to general procedure **H** (irradiation time = 3 h), yielding the solution of crude *endo*-peroxide **3.66**. After that, general procedure **I** was followed, with several modifications: 30 mL of DCM was used as a solvent, aqueous work-up was not performed. Further purification by flash chromatography on silica gel (gradient elution: DCM \rightarrow DCM–methanol 95:5) afforded 0.080 g (35% after three steps) of the title compound. ¹H NMR (500 MHz, DMSO) δ 8.42 (d, *J* = 8.2 Hz, 1H), 7.39 (m, 2H), 7.16 (td, *J* = 7.5, 1.2 Hz,

1H), 6.11 (d, $J = 3.9$ Hz, 1H), 5.06 (d, $J = 4.3$ Hz, 1H), 4.46 (d, $J = 14.0$ Hz, 1H), 4.44 (dd, $J = 4.5, 3.7$ Hz, 1H), 4.32 (d, $J = 14.0$ Hz, 1H), 3.04 (dd, $J = 4.5, 4.3$ Hz, 1H), 2.99 (d, $J = 17.8$ Hz, 1H), 2.27 (d, $J = 17.8$ Hz, 1H), 1.29 (s, 3H). ^{13}C NMR (126 MHz, DMSO) δ 204.9, 168.6, 132.8, 130.7, 129.6, 124.6, 124.4, 117.1, 90.7, 80.3, 74.9, 70.7, 67.2, 47.6, 45.2, 22.9. HRMS (ESI) calcd for $\text{C}_{16}\text{H}_{16}\text{NO}_5^+$ (MH^+) 302.1023, found 302.1026.



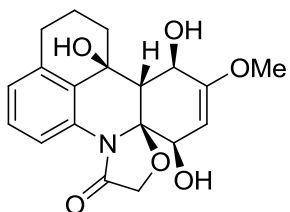
**15-Hydroxy-21-methoxy-3,18,19-trioxa-6-azaheptacyclo
[15.2.2.1^{7,11}.0^{2,6}.0^{2,16}.0^{15,22}]docosa-7,9,11(22),20-tetraen-5-one
(3.67).** General procedure **E** was followed on a 0.151 g

(0.463 mmol) scale of **3.53d**, which afforded crude *anti*-**3.56d**. The obtained photoproduct was then subjected to general procedure **H** (irradiation time = 4 h), which after flash chromatography on silica gel (gradient elution: hexane \rightarrow hexane–ethyl acetate 65:35) afforded 0.093 g (56% after two steps) of the title compound. ^1H NMR (500 MHz, CDCl_3) δ 7.32 (dt, $J = 7.7, 1.1$ Hz, 1H), 7.27 (dd, $J = 7.7, 7.6$ Hz, 1H), 6.99 (d, $J = 7.6$ Hz, 1H), 4.69 (dd, $J = 7.2, 2.7$ Hz, 1H), 4.66 (dd, $J = 7.2, 1.0$ Hz, 1H), 4.63 (ddd, $J = 3.5, 2.7, 1.0$ Hz, 1H), 4.53 (d, $J = 14.6$ Hz, 1H), 4.48 (d, $J = 14.6$ Hz, 1H), 3.29 (d, $J = 3.5$ Hz, 1H), 2.87 (s, 3H), 2.75 (ddt, $J = 16.2, 3.7, 2.0$ Hz, 1H), 2.61 (ddd, $J = 16.4, 11.7, 4.9$ Hz, 1H), 2.07 (s, 1H), 2.02 (m, 1H), 1.87 (m, 3H). ^{13}C NMR (126 MHz, CDCl_3) δ 169.6, 158.6, 138.5, 134.9, 129.0, 128.5, 126.7, 122.0, 93.7, 91.7, 77.1, 75.0, 68.6, 66.0, 55.2, 55.0, 34.5, 29.6, 18.8. HRMS (ESI) calcd for $\text{C}_{19}\text{H}_{20}\text{NO}_6^+$ (MH^+) 358.1285, found 358.1288.



10,12-Dihydroxy-9-methoxy-5-oxa-2-azapentacyclo
[10.7.1.0^{2,6}.0^{6,11}.0^{16,20}]icosa-1(19),8,16(20),17-tetraene-3,7-
dione (3.70). General procedure **E** was followed on a 0.192 g

(0.588 mmol) scale of **3.53d**, which afforded crude *anti*-**3.56d**. The obtained photoproduct was then subjected to general procedure **H** (irradiation time = 4 h), yielding the solution of crude *endo*-peroxide **3.67**. After that, general procedure **I** was followed, which after flash chromatography on silica gel (gradient elution: DCM → DCM–methanol 97:3) afforded 0.061 g (29% after three steps) of the title compound. ¹H NMR (500 MHz, MeOD) δ 7.58 (dd, *J* = 8.0, 1.1 Hz, 1H), 7.26 (t, *J* = 7.8 Hz, 1H), 7.03 (dd, *J* = 7.7, 1.1 Hz, 1H), 5.44 (s, 1H), 4.62 (d, *J* = 13.6 Hz, 1H), 4.39 (d, *J* = 13.5 Hz, 1H), 4.17 (d, *J* = 4.1 Hz, 1H), 3.74 (s, 3H), 3.13 (d, *J* = 4.1 Hz, 1H), 2.89 (dt, *J* = 16.4, 5.0 Hz, 1H), 2.66 (ddd, *J* = 15.9, 9.1, 6.1 Hz, 1H), 2.00 (m, 3H), 1.79 (m, 1H). ¹³C NMR (126 MHz, MeOD) δ 193.3, 178.8, 172.3, 140.7, 134.2, 131.1, 129.5, 127.8, 121.3, 101.6, 93.7, 71.2, 69.1, 67.3, 60.0, 57.5, 35.4, 29.8, 19.4. HRMS (ESI) calcd for C₁₉H₁₉NO₆Li⁺ (MLi⁺) 364.1367, found 364.1371.



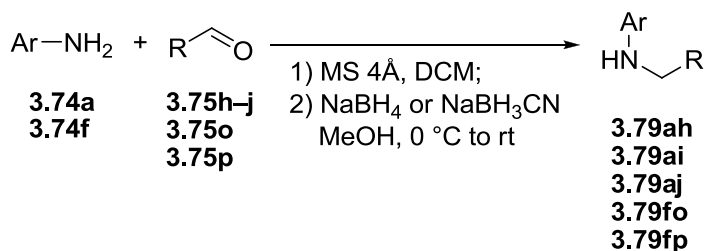
7,10,12-Trihydroxy-9-methoxy-5-oxa-2-azapentacyclo
[10.7.1.0^{2,6}.0^{6,11}.0^{16,20}]icosa-1(19),8,16(20),17-tetraen-3-one
(3.71). General procedure **E** was followed on a 0.151 g

(0.463 mmol) scale of **3.53d**, which afforded crude *anti*-**3.56d**. The obtained photoproduct was then subjected to general procedure **H** (irradiation time = 4 h), yielding the solution of crude *endo*-peroxide **3.67**. Solvent was removed *in vacuo*, and the residue was redissolved in methanol (4.6 mL). Thiourea (0.041 g, 0.543 mmol) was added, and the mixture was stirred at ambient temperature overnight. The solvent was removed *in*

vacuo, and further purification by flash chromatography on silica gel (gradient elution: hexane → ethyl acetate) afforded 0.033 g (20% after three steps) of the title compound (combined fractions were washed with water to remove thiourea). ¹H NMR (500 MHz, MeOD) δ 7.84 (d, *J* = 8.1 Hz, 1H), 7.27 (dd, *J* = 8.1, 7.5 Hz, 1H), 7.03 (dd, *J* = 7.5, 1.0 Hz, 1H), 4.70 (d, *J* = 3.2 Hz, 1H), 4.64 (d, *J* = 13.8 Hz, 1H), 4.40 (d, *J* = 13.8 Hz, 1H), 4.21 (d, *J* = 1.4 Hz, 1H), 4.15 (d, *J* = 3.2 Hz, 1H), 3.53 (s, 3H), 3.08 (dq, *J* = 13.4, 6.9, 5.8 Hz, 1H), 2.99 (d, *J* = 1.4 Hz, 1H), 2.63 (ddd, *J* = 15.2, 6.5, 4.5 Hz, 1H), 2.02 (m, 1H), 1.93 (ddd, *J* = 13.8, 7.9, 4.1 Hz, 1H), 1.71 (ddd, *J* = 13.7, 8.7, 7.3 Hz, 1H), 1.60 (dtdd, *J* = 12.9, 8.7, 6.6, 4.1 Hz, 1H). ¹³C NMR (126 MHz, MeOD) δ 170.9, 159.8, 142.3, 133.5, 130.4, 129.5, 126.8, 120.1, 98.1, 98.0, 71.0, 69.3, 69.0, 67.8, 60.3, 55.5, 32.1, 28.6, 19.2. HRMS (ESI) calcd for C₁₉H₂₁NO₆Li⁺ (MLi⁺) 366.1523, found 366.1514.

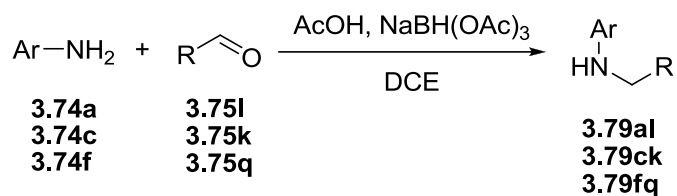
Experimental Section for Project 4

Synthesis of Photoprecursors

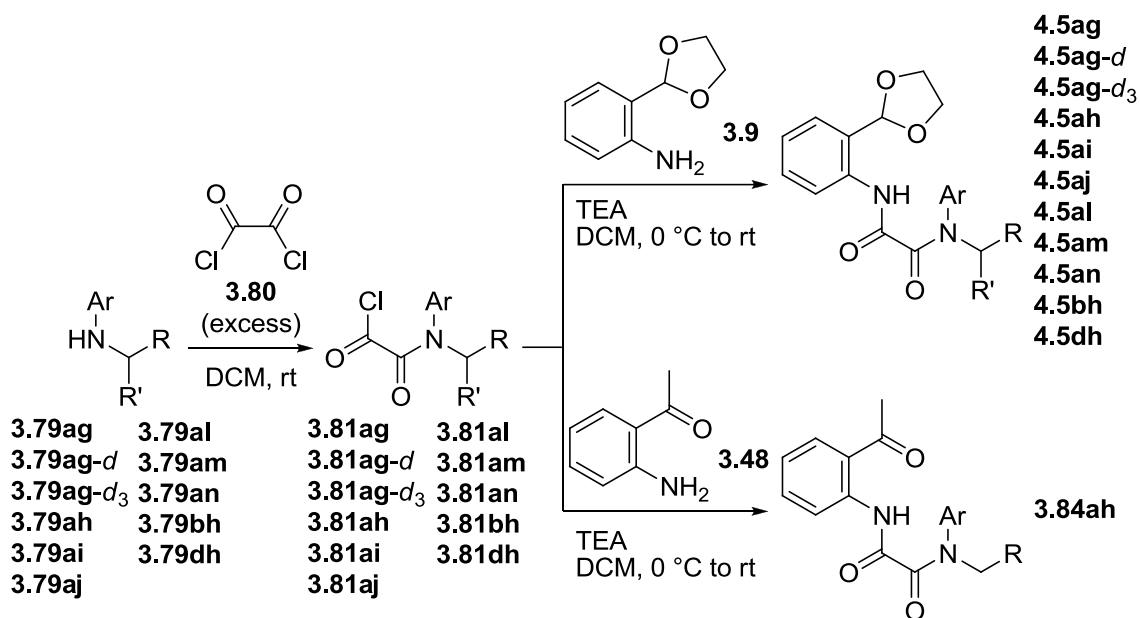


General Procedure A for Reductive Amination. Aniline (**3.74**; 8.29 mmol) was dissolved in anhydrous DCM (25 mL). Aldehyde (**3.75**; 8.7 mmol) and molecular sieves 4Å were added, and the mixture was stirred at ambient temperature till completion (monitored by ¹H NMR). Solids were filtered off and washed with DCM. The filtrate was concentrated *in vacuo*. The residue was dissolved in absolute methanol (30 mL), the

resulting solution was cooled to 0 °C, treated (slowly) with sodium borohydride or sodium cyanoborohydride (9.12 mmol), and stirred overnight. Methanol was removed *in vacuo*, the residue was partitioned between ethyl acetate (100 mL) and water (15 mL). Organic layer was separated, washed with water (2×10 mL) and sat. aq. NaCl (10 mL), dried over anhydrous Na₂SO₄, and the solvent was removed *in vacuo* to afford the desired *N*-alkylaniline (**3.79**; if necessary, the product was additionally purified by flash chromatography on silica gel).

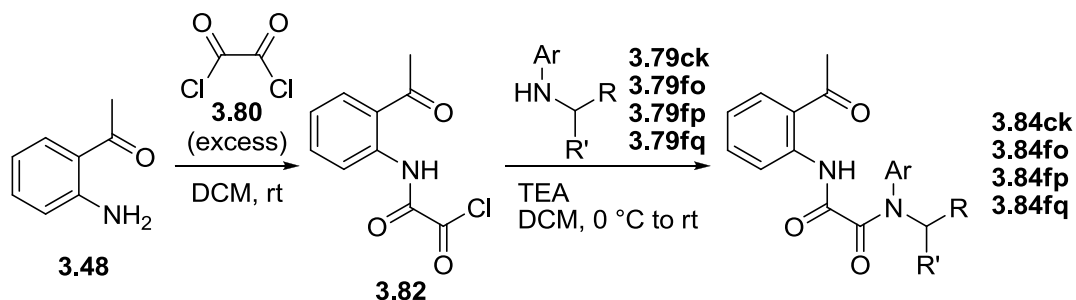


General Procedure B for Reductive Amination. Used a modified literature protocol [170]. Under argon, aldehyde (**3.75**; 1.90 mmol) was dissolved in 1,2-dichloroethane (15 mL), the solution was treated with aniline (**3.74**; 2.09 mmol), glacial acetic acid (1.90 mmol) and sodium triacetoxyborohydride (5.70 mmol) and stirred overnight. Then, the reaction was quenched with sat. aq. NaHCO₃ (10 mL) and stirred for 1 h. Insoluble solids were filtered off and washed with DCM (20 mL). Organic layer was separated. Aqueous layer was mixed with sat. aq. NaHCO₃ (10 mL) and extracted with DCM (3×20 mL; solids formed during extraction were filtered off and washed with the same DCM used for extraction). The combined organic layers were washed with sat. aq. NaHCO₃ (2×10 mL), water (2×10 mL) and sat. aq. NaCl (10 mL), dried over anhydrous Na₂SO₄, and the solvent was removed *in vacuo* to afford the desired *N*-alkylaniline (**3.79**; the products were used for the next steps without chromatographical purification).

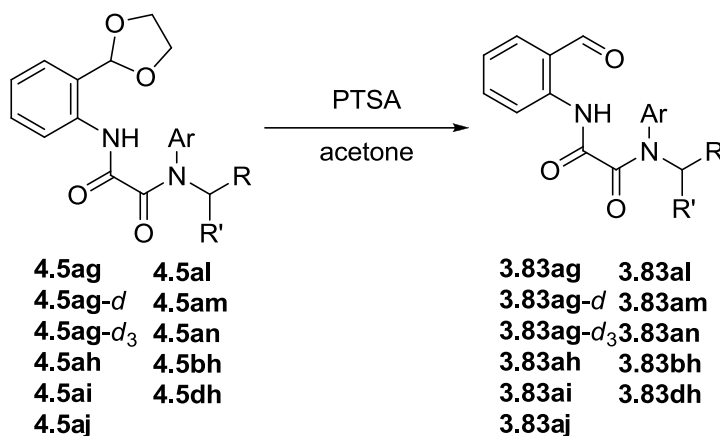


General Procedure C for the Coupling of *N*-Alkylanilines with Photoactive

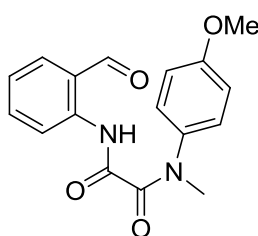
Cores via Oxalyl Linker. Solution of *N*-alkylaniline (**3.79**; 2.00 mmol) in anhydrous DCM (10 mL) was quickly poured into solution of oxalyl chloride (**3.80**; 20 mmol) in anhydrous DCM (10 mL) with vigorous stirring (*note*: slow addition may lead to formation of bis-oxalyl amide), and the mixture was stirred at ambient temperature for 1 h. Volatiles were removed *in vacuo*, and the residue (acyl chloride **3.81**) was redissolved in anhydrous DCM (10 mL) under nitrogen. Solution of primary aniline (**3.9**, **3.48**; 1.89 mmol) and triethylamine (3.0 mmol) in anhydrous DCM (10 mL) was added dropwise at 0 °C under nitrogen. The mixture was stirred at ambient temperature overnight, and then it was diluted with DCM (40 mL) and washed with water (3×10 mL). The organic layer was dried over anhydrous Na₂SO₄, and the solvent was removed *in vacuo*. Crude dioxolane-protected photoprecursors (**4.5**) were then deprotected according to general procedure **E**, whereas photoprecursor **3.84ah** was purified by flash chromatography on silica gel.



General Procedure D for the Coupling of Acid-Sensitive *N*-Alkylanilines with 2'-Aminoacetophenone via Oxalyl Linker. Solution of 2'-aminoacetophenone (**3.48**; 3.05 mmol) in anhydrous DCM (15 mL) was quickly poured into solution of oxalyl chloride (**3.80**; 30 mmol) in anhydrous DCM (15 mL) with vigorous stirring (*note*: slow addition may lead to formation of bis-oxalyl amide), and the mixture was stirred at ambient temperature for 1 h. Volatiles were removed *in vacuo*, and the residue (acyl chloride **3.82**) was redissolved in anhydrous DCM (15 mL) under nitrogen. Solution of *N*-alkylaniline (**3.79**; 1.53 mmol) and triethylamine (0.32 mL, 0.23 g, 2.3 mmol) in anhydrous DCM (15 mL) was added dropwise at 0 °C under nitrogen. The mixture was stirred at ambient temperature overnight, after that it was diluted with DCM (40 mL) and washed 3 times with sat. aq. NaHCO₃ (10 mL) diluted with water (10 mL), and then with water (20 mL). The organic layer was dried over anhydrous Na₂SO₄, and the solvent was removed *in vacuo*. Further purification by flash chromatography on silica gel yielded the desired photoprecursors (**3.84**).



General Procedure E for Dioxolane Deprotection. Dioxolane-protected photoprecursor (**4.5**; 1.89 mmol) was dissolved in acetone (15 mL), TsOH·H₂O (0.567 mmol) was added, and the mixture was stirred at ambient temperature for 1 day. Solvent was removed *in vacuo*, and the residue was dissolved in DCM (50 mL). The solution was washed with sat. aq. NaHCO₃ (2×10 mL) and then with water (10 mL). The organic layer was dried over anhydrous Na₂SO₄, filtered, and the solvent was removed *in vacuo*. Further purification by flash chromatography on silica gel yielded the desired photoprecursor (**3.83**).



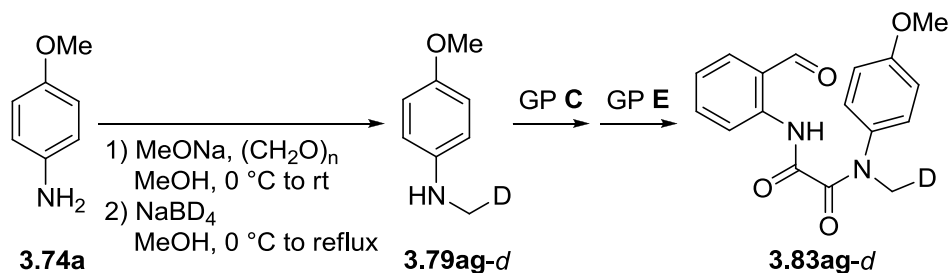
N'-(2-Formylphenyl)-N-(4-methoxyphenyl)-N-

methylethanedi- amide (3.83ag). 4-Methoxy-*N*-methylaniline (**3.74ag**; 1.43 mmol) was coupled with oxalyl chloride (**3.80**;

11 mmol), and the resulting acyl chloride **3.79ag** was coupled with

2-(1,3-dioxolan-2-yl)aniline (**3.9**; 0.873 mmol) according to general procedure **C**, with the following modifications: solid 4-methoxy-*N*-methylaniline was added to a solution of oxalyl chloride in anhydrous DCM (15 mL) at 0 °C; second coupling step was carried out in 6 mL of anhydrous DCM with DIPEA (1.9 mmol) as a base. Dioxolane protection was then removed according to general procedure **E** with 0.18 mmol of TsOH·H₂O, which

after flash chromatography on silica gel (gradient elution: hexane → hexane–ethyl acetate 80:20) afforded 0.178 g (65%) of the title compound. ¹H NMR (500 MHz, CDCl₃) δ 12.30 (s, 1H), 9.97 (d, *J* = 0.7 Hz, 1H), 8.49 (d, *J* = 8.4 Hz, 1H), 7.69 (dd, *J* = 7.7, 1.7 Hz, 1H), 7.51 (ddd, *J* = 8.7, 7.4, 1.7 Hz, 1H), 7.24 (dd, *J* = 7.5, 1.1 Hz, 1H), 7.15 (m, 2H), 6.89 (m, 2H), 3.80 (s, 3H), 3.40 (s, 3H). ¹³C NMR (126 MHz, CDCl₃) δ 194.9, 162.1, 159.7, 159.0, 139.4, 136.4, 136.1, 135.9, 127.2, 124.0, 122.7, 120.2, 114.7, 55.5, 39.5. HRMS (ESI) calcd for C₁₇H₁₆N₂O₄Na⁺ (MNa⁺) 335.1002, found 335.1010.

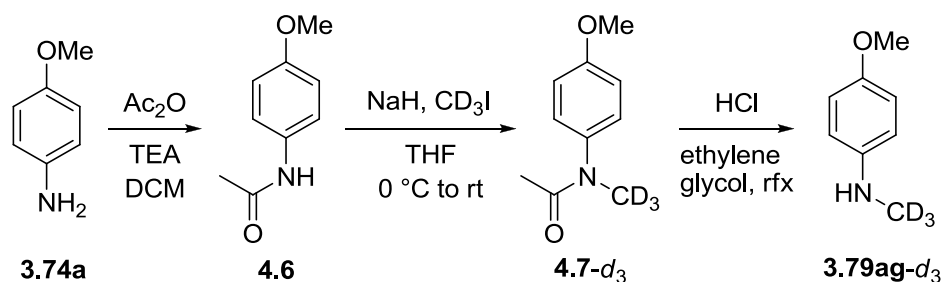


***N'*-(2-Formylphenyl)-*N*-(4-methoxyphenyl)-*N*-(²H₁)methylethanediamide (3.83ag-d).**

Step 1. *4-Methoxy-N-(²H₁)methylaniline (3.79ag-d)*. Prepared according to a modified literature protocol [171]. Under nitrogen, sodium methoxide (1.10 g, 20.4 mmol) was dissolved in absolute methanol (5 mL), and the solution was cooled to 0 °C. Solution of *p*-anisidine (**3.74a**; 0.502 g, 4.08 mmol) in absolute methanol (5 mL) was added. The mixture was stirred for 10 minutes, and then it was added to a solution of paraformaldehyde (0.178 g, 5.93 mmol) in absolute methanol (10 mL) under nitrogen. After 24 h stirring at ambient temperature, sodium borodeuteride (0.171 g, 4.08 mmol) was added portionwise at 0 °C. The reaction mixture was allowed to warm up to room temperature, and then refluxed for 3 h. The product was purified according to general procedure **A**, which afforded 0.534 g of the title compound. The crude product was used

for the next step without chromatographical purification. ^1H NMR (500 MHz, CDCl_3) δ 6.80 (m, 2H), 6.59 (m, 2H), 3.75 (s, 3H), 2.79 (t, $J = 1.8$ Hz, 2H). HRMS (ESI) calcd for $\text{C}_8\text{H}_{11}\text{DNO}^+$ (MH^+) 139.0976, found 139.0983.

Step 2. *N'*-(2-Formylphenyl)-*N*-(4-methoxyphenyl)-*N*-($^2\text{H}_1$)methylethanediamide (**3.83ag-d**). 0.276 g of *N*-alkylaniline **3.79ag-d** was coupled with oxalyl chloride (**3.80**; 20 mmol), and the resulting acyl chloride **3.81ag-d** was coupled with 2-(1,3-dioxolan-2-yl)aniline (**3.9**; 1.88 mmol) according to general procedure **C**. Dioxolane protection was then removed according to general procedure **E** with 0.38 mmol of $\text{TsOH} \cdot \text{H}_2\text{O}$, which after flash chromatography on silica gel (gradient elution: hexane \rightarrow hexane–ethyl acetate 80:20) afforded 0.339 g (58% after two steps) of the title compound. ^1H NMR (500 MHz, CDCl_3) δ 12.30 (s, 1H), 9.97 (s, 1H), 8.49 (d, $J = 8.4$ Hz, 1H), 7.70 (dd, $J = 7.6, 1.5$ Hz, 1H), 7.51 (ddd, $J = 8.7, 7.4, 1.7$ Hz, 1H), 7.25 (t, $J = 7.4$ Hz, 1H), 7.15 (m, 2H), 6.89 (m, 2H), 3.80 (s, 3H), 3.38 (t, $J = 1.8$ Hz, 2H). ^{13}C NMR (126 MHz, CDCl_3) δ 194.9, 162.1, 159.7, 158.9, 139.3, 136.3, 136.0, 135.8, 127.1, 123.9, 122.7, 120.1, 114.7, 55.5, 39.1 (t, $J = 21.5$ Hz). HRMS (ESI) calcd for $\text{C}_{17}\text{H}_{16}\text{DN}_2\text{O}_4^+$ (MH^+) 314.1246, found 314.1255.



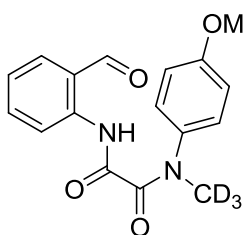
4-Methoxy-*N*-($^2\text{H}_3$)methylaniline (3.79ag-d₃**)**. Prepared according to a modified literature protocol [172].

Step 1. *N*-(4-Methoxyphenyl)acetamide (**4.6**). To a solution of *p*-anisidine (**3.74a**; 1.23 g, 10.0 mmol) in anhydrous DCM (120 mL), triethylamine (1.67 mL, 1.21 g, 12.0 mmol) was added, followed by the dropwise addition of a solution of acetic anhydride (1.13 mL, 1.22 g, 12.0 mmol) in anhydrous DCM (30 mL). The mixture was stirred at ambient temperature overnight, and then volatiles were removed *in vacuo*. Solid residue was washed with water (50 mL), collected by filtration and dried to yield 1.40 g (85%) of the title compound. ¹H NMR (500 MHz, CDCl₃) δ 7.38 (m, 2H), 7.13 (br s, 1H), 6.85 (m, 2H), 3.79 (s, 3H), 2.15 (s, 3H).

Step 2. *N*-(4-Methoxyphenyl)-*N*-(²H₃)methylacetamide (**4.7-d₃**). Under nitrogen, **4.6** (0.731 g, 4.43 mmol) was dissolved in anhydrous THF (8 mL), the solution was cooled to 0 °C and treated with sodium hydride (0.132 g, 5.50 mmol), followed by dropwise addition of iodomethane-*d*₃ (0.33 mL, 0.77 g, 5.3 mmol). The mixture was stirred at ambient temperature overnight, after that it was partitioned between ethyl acetate (50 mL) and sat. aq. NH₄Cl (10 mL). Product was extracted from aqueous layer with ethyl acetate (3×30 mL). The combined organic layers were washed with water (3×10 mL) and sat. aq. NaCl (10 mL), dried over anhydrous Na₂SO₄, and the solvent was removed *in vacuo* to yield 0.870 g of the title compound. The crude product was used for the next step without chromatographical purification. ¹H NMR (500 MHz, CDCl₃) δ 7.10 (m, 2H), 6.91 (m, 2H), 3.83 (s, 3H), 1.85 (s, 3H).

Step 3. 4-Methoxy-*N*-(²H₃)methylaniline (**3.79ag-d₃**) [173]. Crude **4.7-d₃** was dissolved in ethylene glycol (3.33 mL) and treated with conc. HCl (1.11 mL). The mixture was refluxed for one day, after that it was partitioned between water (10 mL) and ethyl acetate (30 mL). 2N NaOH (4 mL) was added to the aqueous layer, and the product

was extracted with ethyl acetate (4×20 mL). The combined organic layers were washed with water (10 mL) and sat. aq. NaCl (10 mL), dried over anhydrous Na₂SO₄, and the solvent was removed *in vacuo*. Further purification by flash chromatography on silica gel (gradient elution: hexane → hexane–ethyl acetate 95:5) afforded 0.427 g (69% after two steps) of the title compound. ¹H NMR (500 MHz, CDCl₃) δ 6.81 (m, 2H), 6.60 (m, 2H), 3.76 (s, 3H), 3.39 (br s, 1H). ¹³C NMR (126 MHz, CDCl₃) δ 152.1, 143.8, 114.9, 113.6, 55.9, 30.8 (sep, *J* = 20.6 Hz). HRMS (ESI) calcd for C₈H₈D₃NOLi⁺ (MLi⁺) 147.1183, found 147.1188.



***N'*-(2-Formylphenyl)-*N*-(4-methoxyphenyl)-*N*-**

(²H₃)methylethanediamide (3.83ag-*d*₃). 4-Methoxy-*N*-

(²H₃)methylaniline (**3.79ag-*d*₃**; 1.24 mmol) was coupled with

oxalyl chloride (**3.80**; 19 mmol), and the resulting acyl chloride

3.81ag-*d*₃ was coupled with 2-(1,3-dioxolan-2-yl)aniline (**3.9**; 0.885 mmol) according to

general procedure **C**, with the following modifications: solution of **3.79ag-*d*₃** in

anhydrous DCM (10 mL) was added dropwise to a solution of oxalyl chloride in

anhydrous DCM (50 mL) at 0 °C; second coupling step was performed in 6 mL of

anhydrous DCM with DIPEA (1.9 mmol) as a base. Dioxolane protection was then

removed according to general procedure **E** with 0.18 mmol of TsOH·H₂O, which after

flash chromatography on silica gel (gradient elution: hexane → hexane–ethyl acetate

80:20) afforded 0.205 g (73% after two steps) of the title compound. ¹H NMR (500 MHz,

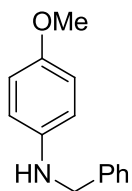
CDCl₃) δ 12.29 (s, 1H), 9.96 (d, *J* = 0.7 Hz, 1H), 8.48 (d, *J* = 8.4 Hz, 1H), 7.69 (dd, *J* =

7.6, 1.7 Hz, 1H), 7.50 (ddd, *J* = 8.7, 7.4, 1.7 Hz, 1H), 7.24 (td, *J* = 7.5, 1.1 Hz, 1H), 7.14

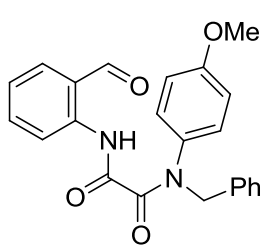
(m, 2H), 6.88 (m, 2H), 3.79 (s, 3H). ¹³C NMR (126 MHz, CDCl₃) δ 194.9, 162.1, 159.6,

158.9, 139.3, 136.3, 136.0, 135.8, 127.1, 123.9, 122.6, 120.1, 114.6, 55.5, 38.7 (sep, $J = 21.3$ Hz). HRMS (ESI) calcd for $C_{17}H_{14}D_3N_2O_4^+$ (MH^+) 316.1371, found 316.1380.

***N'*-Benzyl-*N*-(2-formylphenyl)-*N'*-(4-methoxyphenyl)ethanediamide (**3.83ah**).**



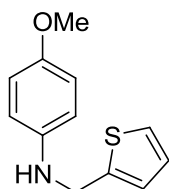
Step 1. *N*-Benzyl-4-methoxyaniline (**3.79ah**). General procedure **A** was followed on a 163 mmol scale of *p*-anisidine (**3.74a**) with 166 mmol of benzaldehyde (**3.75h**) in 250 mL of anhydrous DCM. The resulting imine was then reduced with 163 mmol of sodium borohydride in 250 mL of absolute methanol according to the same general procedure, which afforded 31.93 g of the title compound. The crude product was used for the next step without chromatographical purification. 1H NMR (500 MHz, $CDCl_3$) δ 7.35 (m, 4H), 7.28 (m, 1H), 6.78 (m, 2H), 6.61 (m, 2H), 4.29 (s, 2H), 3.78 (br s, 1H), 3.74 (s, 3H).



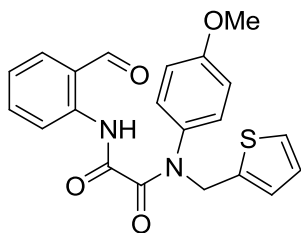
Step 2. *N'*-Benzyl-*N*-(2-formylphenyl)-*N'*-(4-methoxyphenyl)ethanediamide (**3.83ah**). 5.00 g of *N*-alkylaniline **3.79ah** was coupled with oxalyl chloride (**3.80**; 236 mmol), and the resulting acyl chloride **3.81ah** was coupled with 2-(1,3-dioxolan-2-yl)aniline (**3.9**; 21.1 mmol) according to general procedure **C**. Dioxolane protection was then removed according to general procedure **E** with 4.64 mmol of $TsOH \cdot H_2O$, which after flash chromatography on silica gel (gradient elution: hexane \rightarrow ethyl acetate) afforded 5.52 g (67% after two steps) of the title compound. 1H NMR (500 MHz, $CDCl_3$) δ 12.33 (s, 1H), 9.98 (s, 1H), 8.48 (d, $J = 8.4$ Hz, 1H), 7.69 (dd, $J = 7.7, 1.6$ Hz, 1H), 7.50 (ddd, $J = 8.7, 7.4, 1.6$ Hz, 1H), 7.26 (m, 6H), 6.94 (m, 2H), 6.79 (m, 2H), 4.97 (s, 2H), 3.77 (s, 3H). ^{13}C NMR (126 MHz, $CDCl_3$) δ 195.0, 162.1, 159.8, 159.0, 139.4, 136.3, 136.1,

135.9, 134.5, 129.2, 128.7, 128.3, 127.9, 124.0, 122.7, 120.2, 114.4, 55.4, 55.2. HRMS (ESI) calcd for $C_{23}H_{21}N_2O_4^+$ (MH^+) 389.1496, found 389.1500.

***N'*-(2-Formylphenyl)-*N*-(4-methoxyphenyl)-*N*-[(thiophen-2-yl)methyl]ethanediamide (3.83ai).**

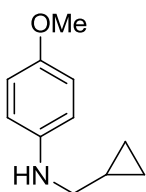


Step 1. *4-Methoxy-N-[(thiophen-2-yl)methyl]aniline* (**3.79ai**). General procedure **A** was followed on a 12.1 mmol scale of *p*-anisidine (**3.74a**) with 12.7 mmol of 2-thiophenecarboxaldehyde (**3.75i**) in 20 mL of anhydrous DCM. The resulting imine was then reduced with 27.0 mmol of sodium cyanoborohydride in 20 mL of absolute methanol according to the same general procedure, which afforded 2.48 g of the title compound. The crude product was used for the next step without chromatographical purification. 1H NMR (500 MHz, $CDCl_3$) δ 7.21 (dd, $J = 5.1, 1.2$ Hz, 1H), 7.00 (dd, $J = 3.4, 1.0$ Hz, 1H), 6.96 (dd, $J = 5.0, 3.5$ Hz, 1H), 6.79 (m, 2H), 6.65 (m, 2H), 4.47 (d, $J = 0.8$ Hz, 2H), 3.75 (s, 3H).



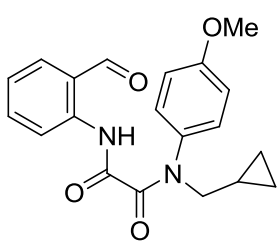
Step 2. *N'*-(2-Formylphenyl)-*N*-(4-methoxyphenyl)-*N*-[(thiophen-2-yl)methyl]ethanediamide (**3.83ai**). 0.228 g of *N*-alkylaniline **3.79ai** was coupled with oxalyl chloride (**3.80**; 16 mmol), and the resulting acyl chloride **3.81ai** was coupled with 2-(1,3-dioxolan-2-yl)aniline (**3.9**; 0.572 mmol) according to general procedure **C**, with the following modifications: solution of **3.79ai** and TEA (1.0 mmol) in anhydrous DCM (6 mL) was added dropwise to a solution of oxalyl chloride in anhydrous DCM (20 mL); second coupling step was performed in 5 mL of anhydrous DCM with 0.72 mmol of TEA. Dioxolane protection was then removed according to general procedure **E** with 0.11 mmol of $TsOH \cdot H_2O$, which after flash chromatography on silica

gel (gradient elution: hexane → hexane–ethyl acetate 85:15) afforded 0.157 g (69% after two steps) of the title compound. ¹H NMR (500 MHz, CDCl₃) δ 12.35 (s, 1H), 9.98 (d, *J* = 0.8 Hz, 1H), 8.47 (d, *J* = 8.4 Hz, 1H), 7.69 (dd, *J* = 7.6, 1.6 Hz, 1H), 7.51 (ddd, *J* = 8.8, 7.7, 1.7 Hz, 1H), 7.24 (m, 2H), 6.99 (m, 2H), 6.91 (m, 2H), 6.83 (m, 2H), 5.09 (s, 2H), 3.79 (s, 3H). ¹³C NMR (126 MHz, CDCl₃) δ 194.9, 161.7, 159.4, 159.2, 139.3, 138.0, 136.1, 135.9, 134.2, 128.3, 126.7, 126.3, 124.0, 122.7, 120.2, 114.5, 100.1, 55.5, 49.9. HRMS (ESI) calcd for C₂₁H₁₉N₂O₄S⁺ (MH⁺) 395.1060, found 395.1064.



***N*-(Cyclopropylmethyl)-4-methoxyaniline (3.79aj)** [174]. General

procedure **A** was followed on a 11.2 mmol scale of *p*-anisidine (**3.74a**) with 11.2 mmol of cyclopropanecarboxaldehyde (**3.75j**) in 10 mL of anhydrous DCM. The resulting imine was then reduced with 16.8 mmol of sodium cyanoborohydride in 10 mL of absolute methanol according to the same general procedure, which after flash chromatography on silica gel (gradient elution: hexane → hexane–ethyl acetate 97:3) afforded 1.03 g (52%) of the title compound. ¹H NMR (500 MHz, CDCl₃) δ 6.78 (m, 2H), 6.60 (m, 2H), 3.75 (s, 3H), 2.91 (d, *J* = 6.9 Hz, 2H), 1.09 (m, 1H), 0.54 (m, 2H), 0.23 (m, 2H).

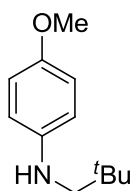


***N*-(Cyclopropylmethyl)-*N'*-(2-formylphenyl)-*N*-(4-methoxyphenyl)ethanediamide (3.83aj).**

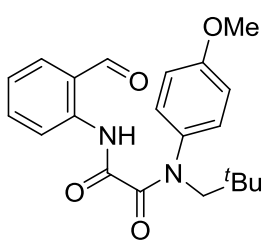
N-(Cyclopropylmethyl)-4-methoxyaniline (**3.79aj**; 1.03 mmol) was coupled with oxalyl chloride (**3.80**; 10 mmol), and the resulting acyl chloride **3.81aj** was coupled with 2-(1,3-dioxolan-2-yl)aniline (**3.9**; 0.964 mmol) according to general procedure **C**. Dioxolane protection was then removed according to general procedure **E** with 0.19 mmol of TsOH·H₂O, which after flash

chromatography on silica gel (gradient elution: hexane → hexane–ethyl acetate 90:10) afforded 0.266 g (78% after two steps) of the title compound. ¹H NMR (500 MHz, CDCl₃) δ 12.27 (s, 1H), 9.97 (s, 1H), 8.49 (d, *J* = 8.4 Hz, 1H), 7.68 (dd, *J* = 7.6, 1.4 Hz, 1H), 7.50 (ddd, *J* = 8.9, 7.5, 1.7 Hz, 1H), 7.24 (m, 1H), 7.18 (m, 2H), 6.88 (m, 2H), 3.80 (s, 3H), 3.67 (d, *J* = 7.2 Hz, 2H), 1.07 (m, 1H), 0.48 (m, 2H), 0.21 (m, 2H). ¹³C NMR (126 MHz, CDCl₃) δ 194.9, 161.9, 160.0, 159.0, 139.4, 136.0, 135.9, 134.9, 128.5, 123.9, 122.7, 120.2, 114.4, 55.8, 55.5, 9.5, 3.9. HRMS (ESI) calcd for C₂₀H₂₀N₂O₄Na⁺ (MNa⁺) 375.1315, found 375.1324.

***N*-(2,2-Dimethylpropyl)-*N'*-(2-formylphenyl)-*N*-(4-methoxyphenyl)ethanediamide (3.83al).**

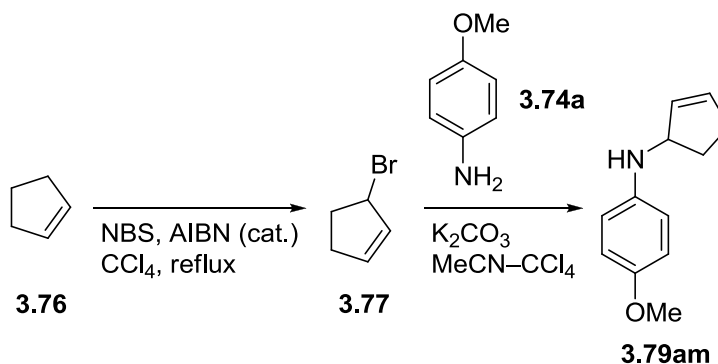


Step 1. *N*-(2,2-Dimethylpropyl)-4-methoxyaniline (**3.79al**). General procedure **B** was followed on a 2.25 mmol scale of pivalaldehyde (**3.75l**) with 2.47 mmol of *p*-anisidine (**3.74a**; *note*: formation of insoluble solids was not observed), which afforded 0.443 g of the title compound. The crude product was used for the next step without chromatographical purification. ¹H NMR (500 MHz, CDCl₃) δ 6.77 (m, 2H), 6.59 (m, 2H), 3.74 (s, 3H), 2.84 (s, 2H), 0.98 (s, 9H).

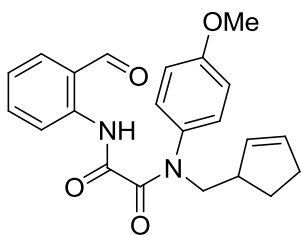


Step 2. *N*-(2,2-Dimethylpropyl)-*N'*-(2-formylphenyl)-*N*-(4-methoxyphenyl)ethanediamide (**3.83al**). 0.243 g of *N*-alkylaniline **3.79al** was coupled with oxalyl chloride (**3.80**; 12 mmol), and the resulting acyl chloride **3.81al** was coupled with 2-(1,3-dioxolan-2-yl)aniline (**3.9**; 1.17 mmol) according to general procedure **C**. Dioxolane protection was then removed according to general procedure **E**, which after flash chromatography on silica gel (gradient elution: hexane → hexane–ethyl acetate 85:15) afforded 0.339 g

(79% after two steps) of the title compound. ^1H NMR (500 MHz, CDCl_3) δ 11.97 (s, 1H), 9.94 (s, 1H), 8.45 (d, $J = 8.4$ Hz, 1H), 7.67 (dd, $J = 7.6, 1.6$ Hz, 1H), 7.51 (ddd, $J = 8.8, 7.5, 1.8$ Hz, 1H), 7.23 (td, $J = 7.6, 1.0$ Hz, 1H), 7.20 (m, 2H), 6.83 (m, 2H), 3.77 (s, 3H), 3.76 (s, 2H), 0.92 (s, 9H). ^{13}C NMR (126 MHz, CDCl_3) δ 195.0, 163.7, 161.0, 158.7, 139.5, 136.0, 135.9, 135.8, 128.1, 123.8, 122.5, 120.2, 114.4, 61.3, 55.5, 34.2, 28.6. HRMS (ESI) calcd for $\text{C}_{21}\text{H}_{25}\text{N}_2\text{O}_4^+$ (MH^+) 369.1809, found 369.1813.



***N*-(Cyclopent-2-en-1-yl)-4-methoxyaniline (3.79am)**. Solution of 3-bromocyclopent-1-ene (**3.77**) in CCl_4 was prepared from 40.0 mmol of cyclopentene (**3.76**) and 10.0 mmol of NBS according to the reported procedure [175], and then reacted with 27.5 mmol of *p*-anisidine (**3.74a**) according to the literature protocol [176], which after flash chromatography on silica gel (gradient elution: hexane \rightarrow hexane–ethyl acetate 97:3) afforded 1.08 g (57% after two steps) of the title compound. ^1H NMR (500 MHz, CDCl_3) δ 6.78 (m, 2H), 6.61 (m, 2H), 5.95 (m, 1H), 5.85 (m, 1H), 4.49 (dd, $J = 4.7, 2.2$ Hz, 1H), 3.75 (s, 3H), 3.35 (br s, 1H), 2.47 (tdq, $J = 10.7, 6.0, 2.7$ Hz, 1H), 2.33 (m, 2H), 1.64 (ddq, $J = 13.7, 9.7, 4.6$ Hz, 1H).



***N*-(Cyclopent-2-en-1-yl)-*N'*-(2-formylphenyl)-*N*-(4-**

methoxyphenyl)ethanediamide (3.83am). *N*-(Cyclopent-2-en-

1-yl)-4-methoxyaniline (**3.79am**; 2.00 mmol) was coupled with

oxalyl chloride (**3.80**; 20 mmol), and the resulting acyl chloride

3.81am was coupled with 2-(1,3-dioxolan-2-yl)aniline (**3.9**; 1.89 mmol) according to

general procedure **C**. Dioxolane protection was then removed according to general

procedure **E**, which after flash chromatography on silica gel (gradient elution: hexane →

hexane–ethyl acetate 85:15) afforded 0.515 g (75% after two steps) of the title

compound. ¹H NMR (500 MHz, CDCl₃) δ 12.18 (s, 1H), 9.96 (m, 1H), 8.45 (d, *J* = 8.5

Hz, 1H), 7.68 (dd, *J* = 7.6, 1.6 Hz, 1H), 7.49 (ddd, *J* = 8.8, 7.4, 1.7 Hz, 1H), 7.23 (td, *J* =

7.5, 1.0 Hz, 1H), 7.05 (m, 2H), 6.81 (m, 2H), 5.86 (ddt, *J* = 14.4, 6.2, 1.8 Hz, 2H), 5.69

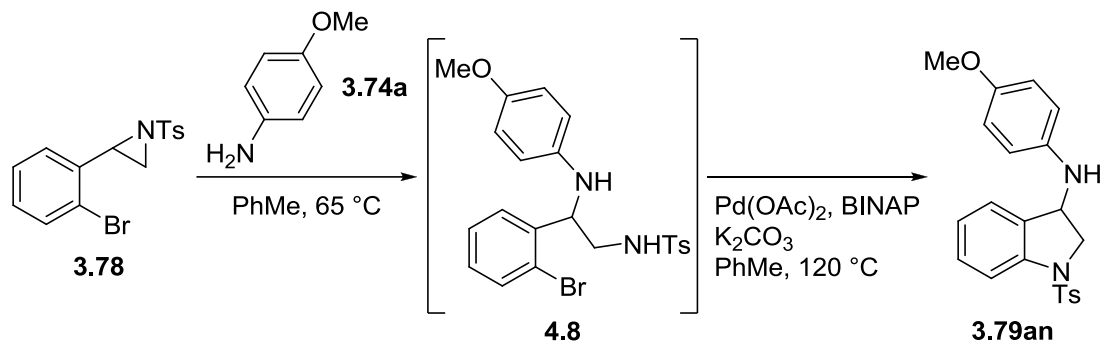
(dq, *J* = 5.6, 2.2 Hz, 1H), 3.78 (s, 3H), 2.32 (dtd, *J* = 14.1, 9.0, 5.4 Hz, 1H), 2.18 (dddq, *J*

= 17.2, 9.0, 4.2, 2.1 Hz, 1H), 1.96 (dddd, *J* = 14.1, 11.5, 5.2, 2.6 Hz, 1H), 1.83 (ddt, *J* =

13.2, 8.7, 4.3 Hz, 1H). ¹³C NMR (126 MHz, CDCl₃) δ 195.0, 162.2, 160.2, 159.2, 139.5,

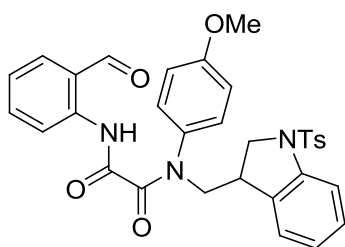
136.3, 136.0, 135.9, 131.0, 130.4, 129.5, 123.8, 122.6, 120.2, 113.8, 63.5, 55.4, 31.6,

27.9. HRMS (ESI) calcd for C₂₁H₂₀N₂O₄Na⁺ (MNa⁺) 387.1315, found 387.1318.



***N*-(4-Methoxyphenyl)-1-tosylindolin-3-amine (3.79an).** Prepared according to a modified literature protocol [146]. In a high-pressure tube, 2-(2-bromophenyl)-1-

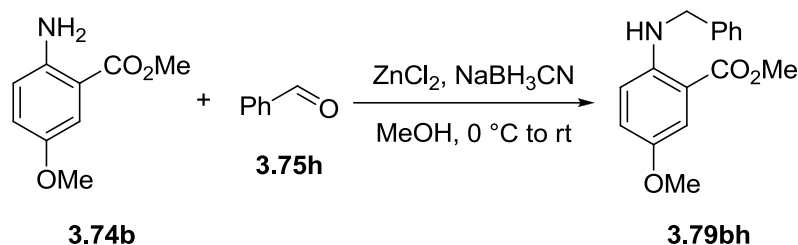
tosylaziridine [177] (**3.78**; 0.230 g, 0.653 mmol) and *p*-anisidine (**3.74a**; 0.084 g, 0.69 mmol) were dissolved in anhydrous toluene (0.40 mL) under argon, and the solution was stirred at 65 °C overnight. After that, palladium acetate (0.031 g, 0.14 mmol), (±)-BINAP (0.165 g, 0.265 mmol), K₂CO₃ (0.227 g, 1.64 mmol) and anhydrous toluene (6.5 mL) were added under argon. The tube was sealed, and the mixture was stirred at 120 °C overnight. Insoluble solids were filtered off, and toluene was removed *in vacuo*. Further purification by flash chromatography on 40–60 μm silica gel pre-treated with pyridine (gradient elution: hexane → hexane–ethyl acetate + 1% TEA 80:20) afforded 0.153 g (59%) of the title compound. ¹H NMR (500 MHz, CDCl₃) δ 7.74 (d, *J* = 8.2 Hz, 1H), 7.61 (m, 2H), 7.34 (tdd, *J* = 7.5, 1.3, 0.7 Hz, 1H), 7.25 (d, *J* = 7.5 Hz, 1H), 7.21 (m, 2H), 7.05 (td, *J* = 7.5, 0.9 Hz, 1H), 6.77 (m, 2H), 6.40 (m, 2H), 4.79 (br m, 1H), 4.09 (dd, *J* = 11.7, 7.4 Hz, 1H), 3.83 (dd, *J* = 11.6, 3.5 Hz, 1H), 3.76 (s, 3H), 2.39 (s, 3H). ¹³C NMR (126 MHz, CDCl₃) δ 152.9, 144.3, 142.1, 139.9, 134.0, 132.7, 130.0, 129.9, 127.4, 125.7, 124.4, 116.0, 115.1, 114.9, 56.7, 55.9, 54.3, 21.7. HRMS (ESI) calcd for C₂₂H₂₃N₂O₃S⁺ (MH⁺) 395.1424, found 395.1433.



***N'*-(2-Formylphenyl)-*N*-(4-methoxyphenyl)-*N*-[1-(4-methylbenzenesulfonyl)-2,3-dihydro-1*H*-indol-3-yl]ethanediamide (**3.83an**). *N*-(4-Methoxyphenyl)-1-tosylindolin-3-amine (**3.79an**; 0.342 mmol) was coupled**

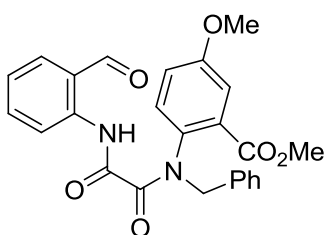
with oxalyl chloride (**3.80**; 3.4 mmol), and the resulting acyl chloride **3.81an** was coupled with 2-(1,3-dioxolan-2-yl)aniline (**3.9**; 0.325 mmol) according to general procedure **C**. Dioxolane protection was then removed according to general procedure **E** with 0.13 mmol of TsOH·H₂O, which after flash chromatography on silica gel (gradient

elution: hexane → hexane–ethyl acetate 70:30) afforded 0.158 g (85% after two steps) of the title compound. ¹H NMR (500 MHz, CDCl₃) δ 12.23 (s, 1H), 9.97 (s, 1H), 8.41 (d, *J* = 8.4 Hz, 1H), 7.69 (dd, *J* = 7.6, 1.5 Hz, 1H), 7.57 (m, 2H), 7.50 (m, 2H), 7.31 (d, *J* = 7.6 Hz, 1H), 7.25 (m, 2H), 7.20 (m, 2H), 7.01 (td, *J* = 7.5, 0.8 Hz, 1H), 6.63 (br m, 4H), 6.37 (dd, *J* = 8.5, 4.6 Hz, 1H), 4.04 (dd, *J* = 11.7, 4.6 Hz, 1H), 4.01 (dd, *J* = 11.7, 8.5 Hz, 1H), 3.72 (s, 3H), 2.38 (s, 3H). ¹³C NMR (126 MHz, CDCl₃) δ 195.1, 162.8, 159.5, 159.4, 144.4, 143.2, 139.2, 136.1, 136.0, 133.7, 130.3, 129.9, 129.7, 129.5, 128.5, 127.4, 126.8, 124.1, 123.7, 122.6, 120.2, 114.1, 114.1, 56.0, 55.3, 53.2, 21.7. HRMS (ESI) calcd for C₃₁H₂₇N₃O₆SLi⁺ (MLi⁺) 576.1775, found 576.1773.



Methyl 2-(Benzylamino)-5-methoxybenzoate (3.79bh). Prepared according to a modified literature protocol [178]. Under nitrogen, methyl 2-methoxy-5-aminobenzoate (**3.74b**; 0.291 g, 1.61 mmol) was dissolved in absolute MeOH (4 mL), the solution was cooled to 0 °C and treated with benzaldehyde (**3.75h**; 0.33 mL, 0.34 g, 3.2 mmol), anhydrous ZnCl₂ (0.374 g, 2.74 mmol) and sodium cyanoborohydride (0.172 g, 2.74 mmol). The mixture was stirred at ambient temperature overnight. After that, the reaction was quenched with sat. aq. NH₄Cl (5 mL), product was extracted with ethyl acetate (3×15 mL). The combined organic layers were washed with sat. aq. NaCl (5 mL), dried over anhydrous Na₂SO₄, and the solvent was removed *in vacuo*. Further purification by flash chromatography on silica gel (gradient elution: hexane → hexane–ethyl acetate

97:3) afforded 0.277 g (63%) of the title compound. ^1H NMR (500 MHz, CDCl_3) δ 7.84 (t, $J = 5.6$ Hz, 1H), 7.45 (d, $J = 3.0$ Hz, 1H), 7.33 (m, 4H), 7.25 (m, 1H), 6.97 (dd, $J = 9.1, 3.1$ Hz, 1H), 6.59 (d, $J = 9.1$ Hz, 1H), 4.42 (d, $J = 5.6$ Hz, 2H), 3.86 (s, 3H), 3.74 (s, 3H). ^{13}C NMR (126 MHz, CDCl_3) δ 168.9, 149.6, 146.4, 139.4, 128.8, 127.2, 127.2, 123.4, 114.6, 113.3, 110.2, 56.1, 51.7, 47.6. HRMS (ESI) calcd for $\text{C}_{16}\text{H}_{18}\text{NO}_3^+$ (MH^+) 272.1281, found 272.1291.



Methyl 2-*N*-Benzyl-1-[(2-formylphenyl)carbamoyl]

formamido]-5-methoxybenzoate (3.83bh). Methyl 2-

(benzylamino)-5-methoxybenzoate (**3.79bh**; 0.840 mmol) was

coupled with oxalyl chloride (**3.80**; 8.4 mmol), and the

resulting acyl chloride **3.81bh** was coupled with 2-(1,3-dioxolan-2-yl)aniline (**3.9**;

0.794 mmol) according to general procedure **C**. Dioxolane protection was then removed

according to general procedure **E**, which after flash chromatography on silica gel

(gradient elution: hexane \rightarrow hexane–ethyl acetate 85:15) afforded 0.239 g (68% after two

steps) of the title compound. ^1H NMR (500 MHz, CDCl_3) δ 12.53 (s, 1H), 10.00 (s, 1H),

8.45 (d, $J = 8.4$ Hz, 1H), 7.69 (d, $J = 7.6$ Hz, 1H), 7.48 (t, $J = 7.9$ Hz, 1H), 7.38 (d, $J =$

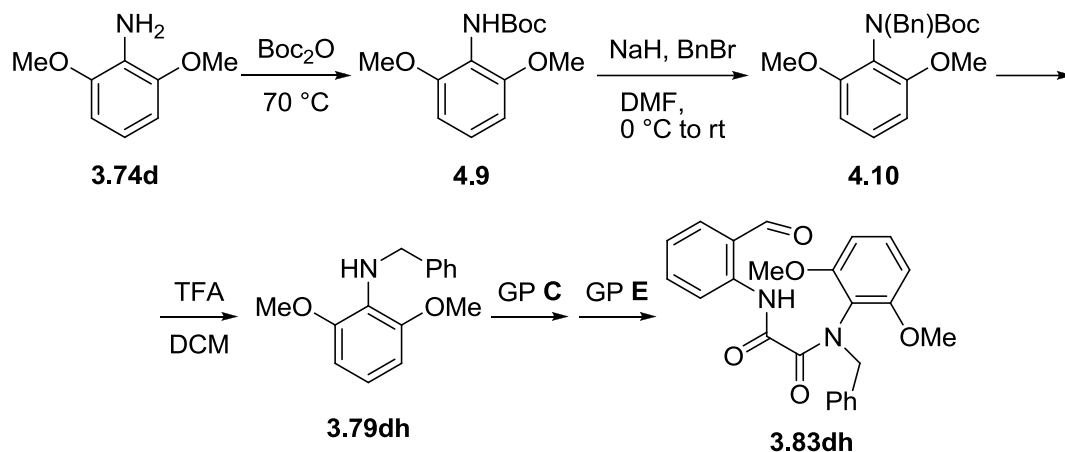
2.4 Hz, 1H), 7.23 (m, 6H), 7.02 (dd, $J = 8.8, 2.3$ Hz, 1H), 6.99 (d, $J = 8.7$ Hz, 1H), 5.03

(d, $J = 13.9$ Hz, 1H), 4.79 (d, $J = 13.9$ Hz, 1H), 3.83 (s, 3H), 3.63 (s, 3H). ^{13}C NMR (126

MHz, CDCl_3) δ 194.6, 165.7, 161.4, 159.3, 158.4, 139.2, 135.9, 135.6, 135.6, 134.5,

130.7, 129.8, 128.5, 128.4, 127.9, 123.7, 122.7, 120.0, 119.0, 115.6, 55.7, 55.5, 52.4.

HRMS (ESI) calcd for $\text{C}_{25}\text{H}_{23}\text{N}_2\text{O}_6^+$ (MH^+) 447.1551, found 447.1561.



***N'*-Benzyl-*N'*-(2,6-dimethoxyphenyl)-*N*-(2-formylphenyl)ethanediamide (3.83dh).**

Step 1. *tert*-Butyl 2,6-dimethoxyphenylcarbamate (**4.9**). Prepared according to a modified literature protocol [179]. Mixture of 2,6-dimethoxyaniline (**3.74d**; 0.620 g, 4.05 mmol) and Boc_2O (2.65 g, 12.2 mmol) was stirred at $70\text{ }^\circ\text{C}$ for 4 h. Further purification by flash chromatography on silica gel (gradient elution: hexane \rightarrow hexane–ethyl acetate 80:20) afforded 0.916 g (89%) of the title compound. ^1H NMR (500 MHz, CDCl_3) δ 7.13 (t, $J = 8.4$ Hz, 1H), 6.57 (d, $J = 8.4$ Hz, 2H), 5.81 (br s, 1H), 3.84 (s, 6H), 1.49 (s, 9H). ^{13}C NMR (126 MHz, CDCl_3) δ 155.5, 154.2, 127.1, 115.2, 104.4, 79.9, 56.1, 28.4. HRMS (ESI) calcd for $\text{C}_{13}\text{H}_{19}\text{LiNO}_4^+$ (MLi^+) 260.1469, found 260.1472.

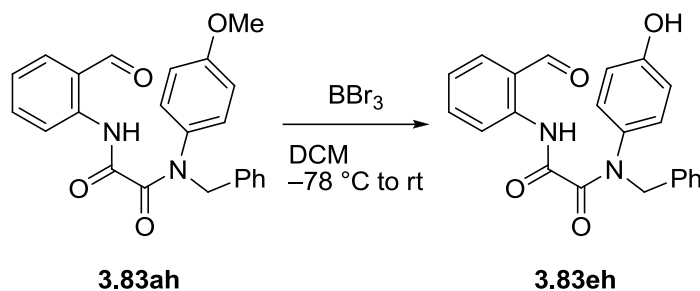
Step 2. *N*-Benzyl-2,6-dimethoxyaniline (**3.79dh**). Prepared according to a modified literature protocol [180]. Under argon, sodium hydride (0.107 g, 4.45 mmol) was suspended in anhydrous DMF (9 mL), the mixture was cooled to $0\text{ }^\circ\text{C}$, and then solution of **4.9** (0.916 g, 3.61 mmol) in anhydrous DMF (9 mL) was added dropwise. After stirring for 30 min, benzyl bromide (0.48 mL, 0.68 g, 4.0 mmol) was added, and the mixture was stirred at ambient temperature overnight. DMF was removed under high vacuum ($50\text{ }^\circ\text{C}/0.15$ Torr), and the residue was partitioned between ethyl acetate (30 mL)

and water (15 mL). Product was extracted from aqueous layer with ethyl acetate (2×30 mL). The combined organic layers were washed with water (15 mL) and sat. aq. NaCl (15 mL), dried over anhydrous Na₂SO₄, and the solvent was removed *in vacuo*. Residue (crude **4.10**) was redissolved in DCM (9 mL) and treated with TFA (9 mL) at 0 °C. The mixture was stirred at ambient temperature overnight. After that, volatiles were removed *in vacuo*, the residue was redissolved in DCM (30 mL) and washed with 2 N NaOH (15 mL). Aqueous layer was extracted with DCM (2×20 mL). The combined organic layers were washed with water (15 mL) and sat. aq. NaCl (15 mL), dried over anhydrous Na₂SO₄, and the solvent was removed *in vacuo* to yield 0.954 g of **3.79dh**. The crude product was used for the next step without chromatographical purification. ¹H NMR (500 MHz, CDCl₃) δ 7.33 (d, *J* = 7.1 Hz, 2H), 7.29 (t, *J* = 7.5 Hz, 2H), 7.22 (t, *J* = 7.2 Hz, 1H), 6.81 (t, *J* = 8.3 Hz, 1H), 6.54 (d, *J* = 8.3 Hz, 2H), 4.41 (s, 2H), 3.81 (s, 6H).

Step 3. *N'*-Benzyl-*N'*-(2,6-dimethoxyphenyl)-*N*-(2-formylphenyl)ethanediamide (**3.83gh**). 0.947 g of *N*-alkylaniline **3.79dh** was coupled with oxalyl chloride (**3.80**; 35 mmol), and the resulting acyl chloride **3.81dh** was coupled with 2-(1,3-dioxolan-2-yl)aniline (**3.9**; 3.39 mmol) according to general procedure **C**. Dioxolane protection was then removed according to general procedure **E**, which after flash chromatography on silica gel (gradient elution: hexane → hexane–ethyl acetate 60:40) afforded 1.22 g (86% after two steps) of the title compound. ¹H NMR (500 MHz, CDCl₃) δ 12.29 (s, 1H), 9.99 (s, 1H), 8.52 (d, *J* = 8.5 Hz, 1H), 7.68 (dd, *J* = 7.6, 1.6 Hz, 1H), 7.48 (ddd, *J* = 8.7, 7.2, 1.7 Hz, 1H), 7.21 (m, 6H), 7.16 (t, *J* = 8.4 Hz, 1H), 6.46 (d, *J* = 8.4 Hz, 2H), 4.92 (s, 2H), 3.57 (s, 6H). ¹³C NMR (126 MHz, CDCl₃) δ 194.7, 163.1, 159.7, 155.6, 139.7, 136.6,

136.0, 135.7, 129.9, 128.8, 127.8, 127.4, 123.5, 122.7, 120.3, 119.5, 104.5, 56.0, 52.3.

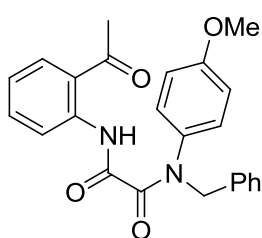
HRMS (ESI) calcd for $C_{24}H_{23}N_2O_5^+$ (MH^+) 419.1601, found 419.1610.



***N'*-Benzyl-*N*-(2-formylphenyl)-*N'*-(4-hydroxyphenyl)ethanediamide (3.83eh).**

Prepared according to a modified literature protocol [147]. Under argon, **3.83ah** (0.380 g, 0.978 mmol) was dissolved in anhydrous DCM (12 mL), and the solution was cooled to $-78\text{ }^\circ\text{C}$. Solution of BBr_3 (0.40 mL, 1.0 g, 4.0 mmol) in anhydrous DCM (24 mL) was added dropwise under argon over 1 h, maintaining the temperature below $-60\text{ }^\circ\text{C}$. The mixture was stirred for 12 h (*note*: longer reaction time leads to formation of by-products), after that it was cooled to $0\text{ }^\circ\text{C}$, carefully quenched with sat. aq. $NaHCO_3$ (20 mL) and stirred until effervescence ceased. The mixture was transferred to separatory funnel, shaken, and layers were separated. Aqueous layer was extracted with ethyl acetate ($3 \times 25\text{ mL}$). The combined organic layers were washed with sat. aq. $NaCl$ (20 mL), dried over anhydrous Na_2SO_4 , and the solvent was removed *in vacuo*. Further purification by flash chromatography on silica gel (gradient elution: hexane \rightarrow hexane–ethyl acetate 75:25) afforded 0.313 g (86%) of the title compound. 1H NMR (500 MHz, $CDCl_3$) δ 12.34 (s, 1H), 9.97 (s, 1H), 8.46 (d, $J = 8.4\text{ Hz}$, 1H), 7.70 (dd, $J = 7.6, 1.5\text{ Hz}$, 1H), 7.51 (ddd, $J = 8.9, 7.4, 1.7\text{ Hz}$, 1H), 7.27 (m, 6H), 6.87 (m, 2H), 6.67 (m, 2H), 5.25 (s, 1H), 4.95 (s, 2H). ^{13}C NMR (126 MHz, $CDCl_3$) δ 195.0, 162.2, 160.1, 155.6, 139.2, 136.2,

136.1, 136.0, 134.1, 129.2, 128.7, 128.4, 127.9, 124.2, 122.8, 120.2, 116.2, 55.1. HRMS (ESI) calcd for $C_{22}H_{19}N_2O_4^+$ (MH^+) 375.1339, found 375.1349.

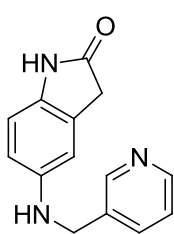


***N'*-(2-Acetylphenyl)-*N*-benzyl-*N*-(4-methoxyphenyl)**

ethanediamide (3.84ah). 0.201 g of *N*-alkylaniline **3.79ah** was coupled with oxalyl chloride (**3.80**; 9.4 mmol), and the resulting acyl chloride **3.81ah** was coupled with 2'-aminoacetophenone

(**3.48**; 0.889 mmol) according to general procedure **C**, which after flash chromatography on silica gel (gradient elution: hexane \rightarrow hexane–ethyl acetate 80:20) afforded 0.321 g (90%) of the title compound. 1H NMR (500 MHz, $CDCl_3$) δ 12.82 (s, 1H), 8.47 (d, J = 8.3 Hz, 1H), 7.89 (dd, J = 8.0, 1.3 Hz, 1H), 7.44 (ddd, J = 8.7, 7.3, 1.7 Hz, 1H), 7.28 (m, 5H), 7.13 (m, 1H), 6.94 (m, 2H), 6.78 (m, 2H), 4.96 (s, 2H), 3.76 (s, 3H), 2.68 (s, 3H). ^{13}C NMR (126 MHz, $CDCl_3$) δ 202.2, 162.5, 159.8, 158.8, 139.4, 136.3, 134.8, 134.5, 131.6, 129.1, 128.5, 128.2, 127.7, 123.3, 122.7, 120.8, 114.3, 55.3, 54.9, 28.5. HRMS (ESI) calcd for $C_{24}H_{23}N_2O_4^+$ (MH^+) 403.1652, found 403.1652.

***N'*-(2-Acetylphenyl)-*N*-(2-oxo-2,3-dihydro-1*H*-indol-5-yl)-*N*-[(pyridin-3-yl)methyl]ethanediamide (3.84ck).**

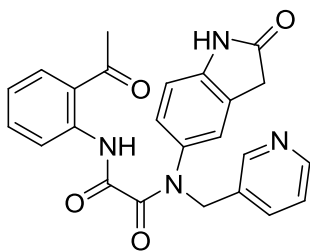


Step 1. 5-(Pyridin-3-ylmethylamino)indolin-2-one (**3.79ck**). General procedure **B** was followed on a 1.91 mmol scale of nicotinaldehyde (**3.75k**) with 2.10 mmol of 5-aminooxindole (**3.74c**), with the one

modification: insoluble solids after aqueous workup were combined with

organic extracts. 0.483 g of the title compound was obtained. The crude product was used for the next step without chromatographical purification. 1H NMR (500 MHz, DMSO) δ 9.95 (s, 1H), 8.56 (dd, J = 2.3, 0.8 Hz, 1H), 8.42 (dd, J = 4.8, 1.6 Hz, 1H), 7.73 (m, 1H),

7.33 (ddd, $J = 7.8, 4.8, 0.8$ Hz, 1H), 6.57 (d, $J = 2.0$ Hz, 1H), 6.54 (d, $J = 8.3$ Hz, 1H), 6.39 (dd, $J = 8.3, 2.1$ Hz, 1H), 5.91 (t, $J = 6.1$ Hz, 1H), 4.24 (m, 2H), 3.32 (m, 2H).

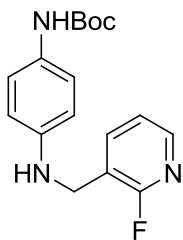


Step 2. *N'*-(2-Acetylphenyl)-*N*-(2-oxo-2,3-dihydro-1H-indol-5-yl)-*N*-[(pyridin-3-yl)methyl]ethanediamide (**3.84ck**).

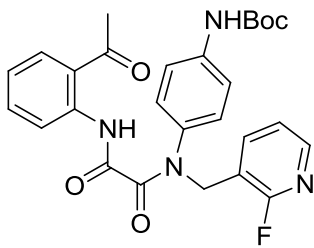
2'-Aminoacetophenone (**3.48**; 1.80 mmol) was coupled with oxalyl chloride (**3.80**; 18 mmol), and the resulting acyl

chloride **3.82** was coupled with 0.231 g of *N*-alkylaniline **3.79ck** according to general procedure **D**, with the following modifications: for the second coupling step, **3.79ck** was used as solution in anhydrous DMF (10 mL); upon completion of the reaction, DMF was evaporated under high vacuum (50 °C/0.15 Torr), the crude product was redissolved in DCM (100 mL) and subjected to aqueous workup, as described in general procedure **D**. Further purification by flash chromatography on silica gel (gradient elution: chloroform → chloroform–methanol 95:5) afforded 0.194 g (50% after two steps) of the title compound. ¹H NMR (500 MHz, CDCl₃) δ 12.95 (s, 1H), 9.20 (s, 1H), 8.53 (dd, $J = 4.8, 1.5$ Hz, 1H), 8.42 (dd, $J = 8.5, 0.9$ Hz, 1H), 8.38 (d, $J = 1.8$ Hz, 1H), 7.90 (dd, $J = 8.0, 1.4$ Hz, 1H), 7.76 (dt, $J = 7.9, 1.9$ Hz, 1H), 7.43 (ddd, $J = 8.7, 7.5, 1.5$ Hz, 1H), 7.26 (m, 1H), 7.13 (ddd, $J = 8.0, 7.4, 1.2$ Hz, 1H), 6.92 (d, $J = 2.1$ Hz, 1H), 6.81 (dd, $J = 8.2, 2.1$ Hz, 1H), 6.74 (d, $J = 8.2$ Hz, 1H), 4.96 (s, 2H), 3.46 (s, 2H), 2.67 (s, 3H). ¹³C NMR (126 MHz, CDCl₃) δ 202.4, 177.4, 162.3, 159.0, 150.2, 149.4, 142.6, 139.2, 137.2, 136.0, 134.9, 131.9, 131.8, 126.9, 126.6, 123.8, 123.7, 123.5, 122.9, 120.8, 110.2, 52.9, 36.4, 28.6. HRMS (ESI) calcd for C₂₄H₂₁N₄O₄⁺ (MH⁺) 429.1557, found 429.1560.

***tert*-Butyl *N*-(4-{1-[(2-acetylphenyl)carbamoyl]-*N*-[(2-fluoropyridin-3-yl)methyl]formamido}phenyl)carbamate (3.84fo).**

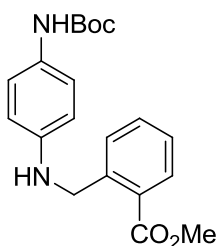


Step 1. *tert*-Butyl 4-((2-fluoropyridin-3-yl)methylamino)phenylcarbamate (3.79fo). General procedure A was followed on a 1.91 mmol scale of *N*-Boc-*p*-phenylenediamine (3.74f) with 2.00 mmol of 2-fluoro-3-pyridinecarboxaldehyde (3.75o) in 7 mL of anhydrous DCM. The resulting imine was then reduced with 2.0 mmol of sodium borohydride in 10 mL of absolute methanol according to the same general procedure, which afforded 0.538 g of the title compound. The crude product was used for the next step without chromatographical purification. ¹H NMR (500 MHz, MeOD) δ 8.05 (ddd, *J* = 4.9, 1.9, 0.9 Hz, 1H), 7.90 (m, 1H), 7.24 (ddd, *J* = 7.0, 4.9, 1.7 Hz, 1H), 7.10 (br m, 2H), 6.56 (m, 2H), 4.35 (s, 2H), 1.48 (s, 9H).



Step 2. *tert*-Butyl *N*-(4-{1-[(2-acetylphenyl)carbamoyl]-*N*-[(2-fluoropyridin-3-yl)methyl]formamido}phenyl)carbamate (3.84fo). 2'-Aminoacetophenone (3.48; 3.05 mmol) was coupled with oxalyl chloride (3.80; 30 mmol), and the resulting acyl chloride 3.82 was coupled with 0.535 g of *N*-alkylaniline 3.79fo according to general procedure D, which after flash chromatography on silica gel (gradient elution: hexane → hexane–ethyl acetate 55:45) afforded 0.687 g (71% after two steps) of the title compound. ¹H NMR (500 MHz, CDCl₃) δ 12.86 (s, 1H), 8.46 (d, *J* = 8.5 Hz, 1H), 8.13 (d, *J* = 3.9 Hz, 1H), 7.96 (ddd, *J* = 9.4, 7.5, 2.0 Hz, 1H), 7.91 (dd, *J* = 8.0, 1.4 Hz, 1H), 7.45 (ddd, *J* = 8.6, 7.4, 1.3 Hz, 1H), 7.32 (m, 2H), 7.19 (ddd, *J* = 6.9, 4.8, 1.5 Hz, 1H), 7.14 (ddd, *J* = 8.3, 7.3, 1.1 Hz, 1H), 7.02 (m, 2H), 6.52 (s, 1H), 5.02 (s, 2H), 2.68 (s, 3H),

1.48 (s, 9H). ^{13}C NMR (126 MHz, CDCl_3) δ 202.4, 163.0, 161.7 (d, $J = 239.7$ Hz), 159.2, 152.5, 147.2 (d, $J = 14.6$ Hz), 141.9 (d, $J = 4.7$ Hz), 139.4, 138.4, 136.2, 135.0, 131.7, 127.3, 123.6, 122.9, 121.9 (d, $J = 4.3$ Hz), 121.0, 118.9, 118.4 (d, $J = 30.0$ Hz), 81.0, 48.2, 28.6, 28.4 (*note*: multiplet assignments for 2-fluoropyridine fragment were made in accordance with ref. [181]). HRMS (ESI) calcd for $\text{C}_{27}\text{H}_{28}\text{FN}_4\text{O}_5^+$ (MH^+) 507.2038, found 507.2047.



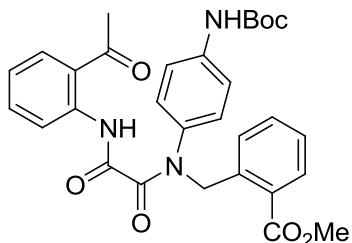
Methyl 2-((4-(*tert*-Butoxycarbonylamino)phenylamino)methyl)

benzoate (3.79fp). General procedure **A** was followed on a

2.39 mmol scale of *N*-Boc-*p*-phenylenediamine (**3.74f**) with

2.52 mmol of methyl *o*-formylbenzoate (**3.75p**) in 10 mL of

anhydrous DCM. The resulting imine was then reduced with 2.4 mmol of sodium borohydride in 10 mL of anhydrous methanol according to the same general procedure, with the following modifications: reaction mixture was stirred for 2 h (*note*: longer reaction time leads to reduced yield), after that methanol was evaporated, the crude product was partitioned between ethyl acetate (60 mL) and water (5 mL) and subjected to aqueous workup, as described in general procedure **A**. Further purification by flash chromatography on silica gel (gradient elution: hexane \rightarrow hexane–ethyl acetate 85:15) afforded 0.494 g (58%) of the title compound. ^1H NMR (500 MHz, MeOD) δ 7.90 (dd, $J = 7.8, 1.4$ Hz, 1H), 7.52 (dd, $J = 7.8, 1.0$ Hz, 1H), 7.44 (td, $J = 7.6, 1.4$ Hz, 1H), 7.30 (td, $J = 7.6, 1.2$ Hz, 1H), 7.07 (br m, 2H), 6.53 (m, 2H), 4.58 (s, 2H), 3.88 (s, 3H), 1.47 (s, 9H). ^{13}C NMR (126 MHz, MeOD) δ 169.5, 156.1, 146.1, 143.1, 133.2, 131.7, 130.4, 130.2, 130.1, 127.9, 122.4, 114.5, 80.3, 52.6, 47.9, 28.8. HRMS (ESI) calcd for $\text{C}_{20}\text{H}_{25}\text{N}_2\text{O}_4^+$ (MH^+) 357.1809, found 357.1819.



Methyl 2-((1-((2-Acetylphenyl)carbamoyl)-N-(4-((tert-butoxy)carbonyl)amino)phenyl)formamido)

methyl)benzoate (3.84fp). 2'-Aminoacetophenone (**3.48**;

2.01 mmol) was coupled with oxalyl chloride (**3.80**;

20 mmol), and the resulting acyl chloride **3.82** was coupled with *N*-alkylaniline **3.79fp**

(0.993 mmol) according to general procedure **D**, which after flash chromatography on

silica gel (gradient elution: hexane → hexane–ethyl acetate 70:30) afforded 0.476 g

(88%) of the title compound. ¹H NMR (500 MHz, CDCl₃) δ 12.80 (s, 1H), 8.48 (d, *J* =

8.4 Hz, 1H), 7.89 (td, *J* = 7.9, 1.3 Hz, 2H), 7.59 (d, *J* = 7.8 Hz, 1H), 7.51 (td, *J* = 7.6, 1.4

Hz, 1H), 7.45 (ddd, *J* = 8.7, 7.3, 1.6 Hz, 1H), 7.32 (td, *J* = 7.8, 1.3 Hz, 1H), 7.26 (m, 2H),

7.13 (ddd, *J* = 8.1, 7.4, 1.2 Hz, 1H), 7.01 (m, 2H), 6.48 (s, 1H), 5.46 (s, 2H), 3.80 (s, 3H),

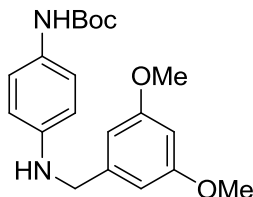
2.67 (s, 3H), 1.47 (s, 9H). ¹³C NMR (126 MHz, CDCl₃) δ 202.2, 167.6, 163.0, 159.9,

152.5, 139.5, 137.9, 137.6, 136.7, 134.9, 132.6, 131.7, 130.9, 129.6, 129.2, 127.4, 127.3,

123.5, 122.9, 121.0, 118.7, 80.9, 52.5, 52.2, 28.6, 28.4. HRMS (ESI) calcd for

C₃₀H₃₂N₃O₇⁺ (MH⁺) 546.2235, found 546.2231.

***tert*-Butyl *N*-(4-{1-[(2-acetylphenyl)carbamoyl]-*N*-[(3,5-dimethoxyphenyl)methyl]formamido}phenyl)carbamate (3.84fq).**



Step 1. *tert*-Butyl 4-(3,5-dimethoxybenzylamino)phenylcarbamate

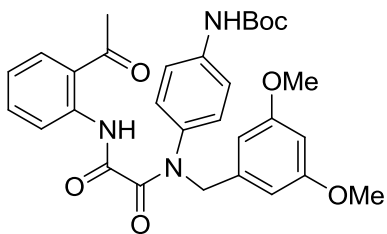
(**3.79fq**). General procedure **B** was followed on a 1.90 mmol scale

of 3,5-dimethoxybenzaldehyde (**3.75q**) with 2.09 mmol of *N*-Boc-

phenylenediamine (**3.74f**), which afforded 0.683 g of the title compound. The crude

product was used for the next step without chromatographical purification. ¹H NMR (500

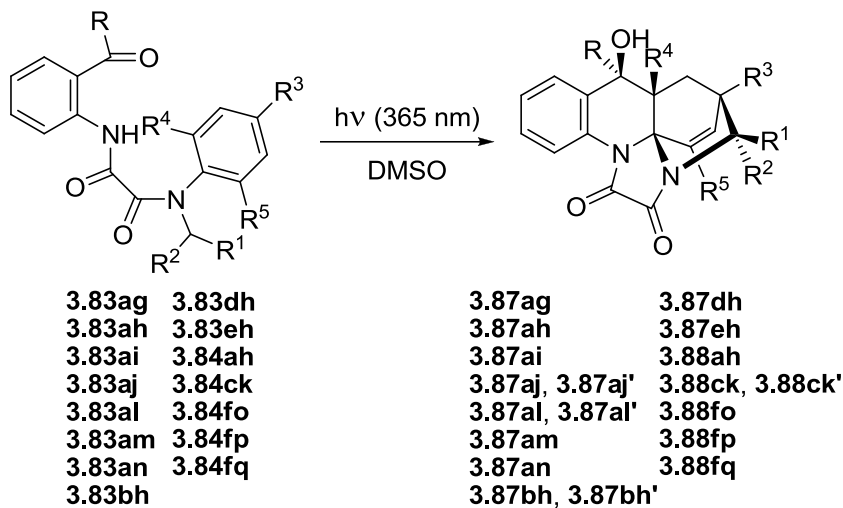
MHz, CDCl₃) δ 7.14 (br m, 2H), 6.58 (m, 2H), 6.52 (d, *J* = 2.3 Hz, 2H), 6.36 (t, *J* = 2.3 Hz, 1H), 6.22 (br s, 1H), 4.24 (s, 2H), 3.77 (s, 6H), 1.49 (s, 9H).



Step 2. *tert*-Butyl *N*-(4-{1-[1-(2-acetylphenyl)carbamoyl]-*N*-[(3,5-dimethoxyphenyl)methyl]formamido}phenyl)carbamate (**3.84fq**). 2'-Aminoacetophenone (**3.48**; 2.33 mmol) was coupled with oxalyl chloride

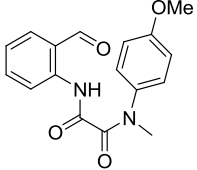
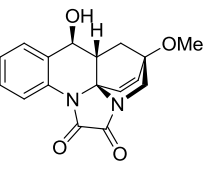
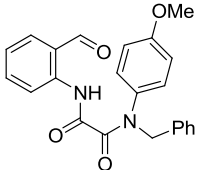
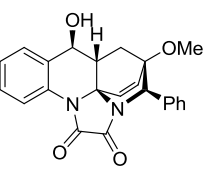
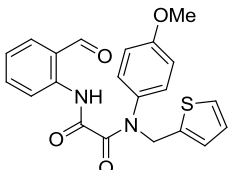
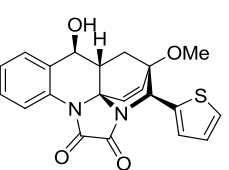
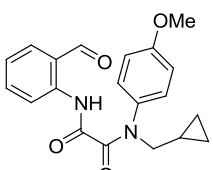
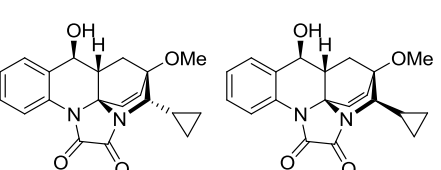
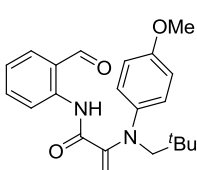
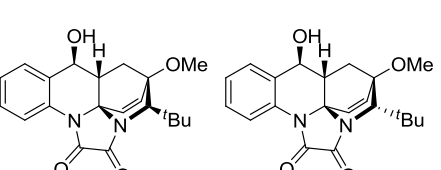
(**3.80**; 24 mmol), and the resulting acyl chloride **3.82** was coupled with 0.418 g of *N*-alkylaniline **3.79fq** according to general procedure **D**, which after flash chromatography on silica gel (gradient elution: hexane → hexane–ethyl acetate 65:35) afforded 0.578 g (91% after two steps) of the title compound. ¹H NMR (500 MHz, CDCl₃) δ 12.81 (s, 1H), 8.44 (d, *J* = 8.4 Hz, 1H), 7.88 (dd, *J* = 8.0, 1.2 Hz, 1H), 7.42 (ddd, *J* = 8.7, 7.4, 1.6 Hz, 1H), 7.28 (m, 2H), 7.11 (m, 1H), 6.97 (m, 2H), 6.65 (s, 1H), 6.42 (d, *J* = 2.2 Hz, 2H), 6.35 (t, *J* = 2.2 Hz, 1H), 4.88 (s, 2H), 3.73 (s, 6H), 2.65 (s, 3H), 1.46 (s, 9H). ¹³C NMR (126 MHz, CDCl₃) δ 202.2, 162.6, 160.9, 159.8, 152.6, 139.4, 138.6, 138.1, 136.4, 134.8, 131.6, 127.6, 123.4, 122.8, 120.9, 118.7, 106.8, 100.0, 80.7, 55.4, 54.8, 28.5, 28.4. HRMS (ESI) calcd for C₃₀H₃₄N₃O₇⁺ (MH⁺) 548.2391, found 548.2393.

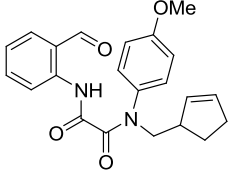
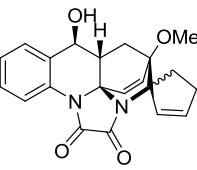
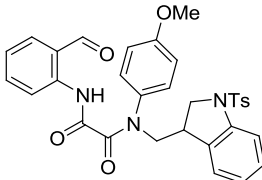
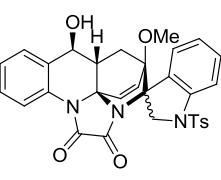
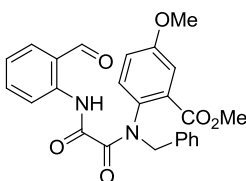
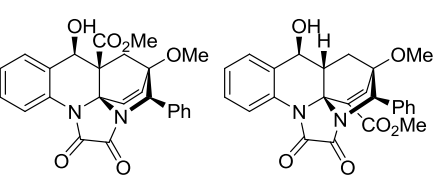
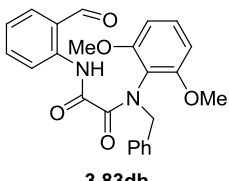
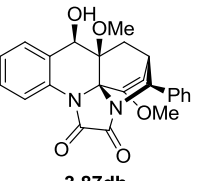
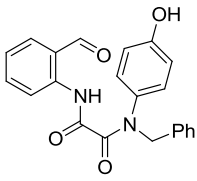
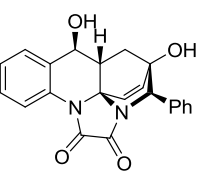
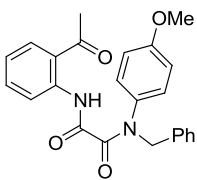
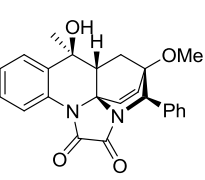
Photochemical Reactions

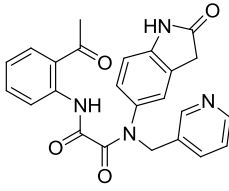
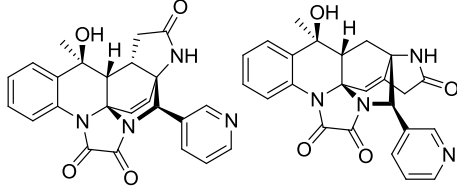
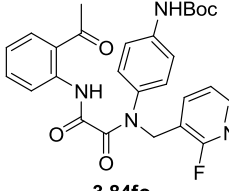
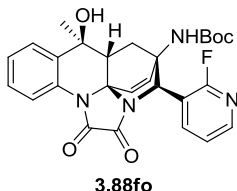
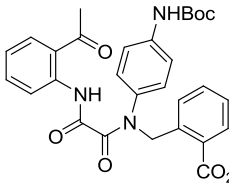
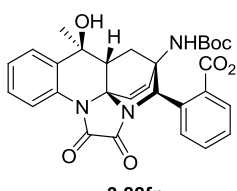
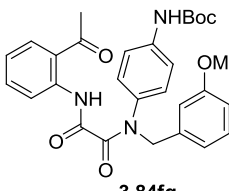
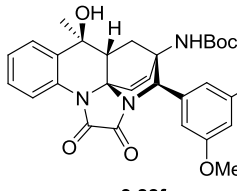


General Procedure F for the Photochemical Reaction. Photoprecursor (**3.83**, **3.84**; 0.394 mmol) was dissolved in DMSO (131 mL), and the solution was degassed by bubbling nitrogen or argon for 1 h. The mixture was irradiated with UV LED-based illuminator, seven 2.9 W @ 365 nm LED Engin chips (or two for **3.83ai**) with the reaction progress monitored by ^1H NMR. After completion, DMSO was evaporated under high vacuum (60 °C/0.15 Torr). Crude photoproducts **3.88fo** and **3.88fp** were directly subjected to the post-photochemical modifications according to general procedure **G**; in all other cases, photoproducts (**3.87**, **3.88**) were purified by flash chromatography on silica gel.

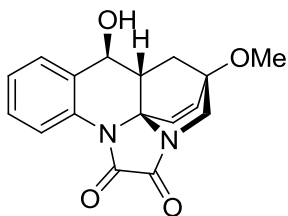
Table 4.2: Irradiation Times

Photoprecursor	Photoproduct(s)	LED power (W)	Reaction Time (h)
 3.83ag	 3.87ag	20	2.5
 3.83ah	 3.87ah	20	4
 3.83ai	 3.87ai	6	7
 3.83aj	 3.87aj 3.87aj'	20	6
 3.83al	 3.87al 3.87al'	20	6.5

Photoprecursor	Photoproduct(s)	LED power (W)	Reaction Time (h)
 <p>3.83am</p>	 <p>3.87am, 3.87am'</p>	20	1.5
 <p>3.83an</p>	 <p>3.87an, 3.87an'</p>	20	2.5
 <p>3.83bh</p>	 <p>3.87bh 3.87bh'</p>	20	7.5
 <p>3.83dh</p>	 <p>3.87dh</p>	20	2.5
 <p>3.83eh</p>	 <p>3.87eh</p>	20	8.5
 <p>3.84ah</p>	 <p>3.88ah</p>	20	32

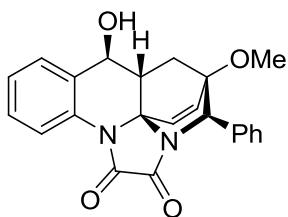
Photoprecursor	Photoproduct(s)	LED power (W)	Reaction Time (h)
 3.84ck	 3.88ck 3.88ck'	20	13
 3.84fo	 3.88fo	20	25
 3.84fp	 3.88fp	20	23
 3.84fq	 3.88fq	20	31.5

(±)-(1*S*,3*R*,4*S*,15*S*)-4-Hydroxy-1-methoxy-11,14-diazapentacyclo [12.3.1.0^{3,15}.0^{5,10}.0^{11,15}]octadeca-5,7,9,16-tetraene-12,13-dione (**3.87ag**). General procedure **F** was followed on a 0.103 g (0.330 mmol) scale of **3.83ag**, which after flash chromatography on silica gel (gradient elution: DCM → DCM–methanol 98:2) afforded 0.040 g (39%) of **3.87ag**.



3.87ag: ^1H NMR (500 MHz, CDCl_3) δ 8.31 (d, $J = 9.0$ Hz, 1H), 7.66 (d, $J = 7.8$ Hz, 1H), 7.44 (t, $J = 7.9$ Hz, 1H), 7.31 (t, $J = 7.6$ Hz, 1H), 6.70 (d, $J = 8.8$ Hz, 1H), 6.16 (d, $J = 8.8$ Hz, 1H), 4.30 (t, $J = 9.9$ Hz, 1H), 3.61 (d, $J = 11.0$ Hz, 1H), 3.51 (s, 3H), 3.47 (dd, $J = 10.9, 2.9$ Hz, 1H), 2.34 (dd, $J = 12.2, 9.4$ Hz, 1H), 2.17 (td, $J = 10.0, 4.0$ Hz, 1H), 2.02 (d, $J = 9.8$ Hz, 1H), 1.98 (dt, $J = 12.8, 3.6$ Hz, 1H). ^{13}C NMR (126 MHz, CDCl_3) δ 156.8, 155.0, 138.3, 132.0, 129.6, 128.9, 128.1, 127.8, 126.5, 120.6, 72.0, 69.1, 52.4, 46.3, 45.6, 32.7, 31.1. HRMS (ESI) calcd for $\text{C}_{17}\text{H}_{17}\text{N}_2\text{O}_4^+$ (MH^+) 313.1183, found 313.1190.

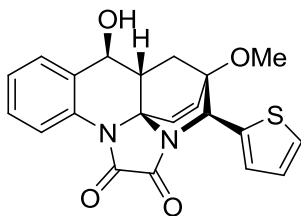
(\pm)-(1*S*,3*R*,4*S*,15*S*,18*R*)-4-Hydroxy-1-methoxy-18-phenyl-11,14-diazapentacyclo[12.3.1.0^{3,15}.0^{5,10}.0^{11,15}]octadeca-5,7,9,16-tetraene-12,13-dione (**3.87ah**). General procedure **F** was followed on a 0.153 g (0.394 mmol) scale of **3.83ah**, which after flash chromatography on silica gel (gradient elution: hexane \rightarrow hexane–ethyl acetate 50:50) afforded 0.054 g (35%) of **3.87ah**.



3.87ah: ^1H NMR (500 MHz, DMSO) δ 8.25 (d, $J = 8.2$ Hz, 1H), 7.65 (d, $J = 8.0$ Hz, 1H), 7.45 (t, $J = 7.7$ Hz, 1H), 7.35 (m, 6H), 7.02 (d, $J = 8.8$ Hz, 1H), 6.42 (d, $J = 8.8$ Hz, 1H), 6.00 (d, $J = 7.2$ Hz, 1H), 4.78 (s, 1H), 4.16 (dd, $J = 10.0, 7.3$ Hz, 1H), 3.43 (s, 3H), 2.63 (td, $J = 9.9, 4.1$ Hz, 1H), 1.76 (dd, $J = 12.6, 9.4$ Hz, 1H), 1.62 (ddd, $J = 13.2, 4.1, 1.4$ Hz, 1H). ^{13}C NMR (126 MHz, DMF) δ 157.9, 155.9, 138.8, 134.5, 133.7, 132.0, 131.0, 129.4, 129.3, 129.3, 129.1, 128.9, 126.5, 120.1, 80.7, 71.7, 70.6, 60.8, 52.9, 44.1, 28.9. HRMS (ESI) calcd for $\text{C}_{23}\text{H}_{20}\text{N}_2\text{O}_4\text{Na}^+$ (MNa^+) 411.1315, found 411.1321.

(±)-(1*S*,3*R*,4*S*,15*S*,18*S*)-4-Hydroxy-1-methoxy-18-(thiophen-2-yl)-11,14-diazapentacyclo[12.3.1.0^{3,15}.0^{5,10}.0^{11,15}]octadeca-5,7,9,16-tetraene-12,13-dione

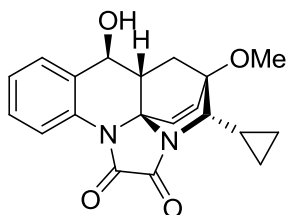
(3.87ai). General procedure **F** was followed on a 0.143 g (0.362 mmol) scale of **3.83ai**, which after flash chromatography on silica gel (gradient elution: hexane → hexane–ethyl acetate 65:35) afforded 0.052 g (36%) of **3.87ai**.



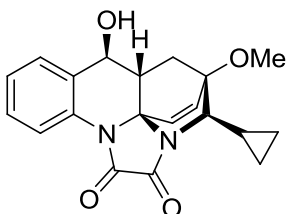
3.87ai: ¹H NMR (500 MHz, CDCl₃) δ 8.48 (dd, *J* = 8.2, 1.3 Hz, 1H), 7.67 (d, *J* = 7.9 Hz, 1H), 7.47 (td, *J* = 7.7, 1.4 Hz, 1H), 7.32 (m, 2H), 7.02 (m, 2H), 6.86 (dd, *J* = 8.6, 0.9 Hz, 1H), 6.28 (dd, *J* = 8.9, 1.3 Hz, 1H), 5.08 (d, *J* = 1.9 Hz, 1H), 4.34 (t, *J* = 10.0 Hz, 1H), 3.55 (s, 3H), 2.39 (dt, *J* = 9.8, 4.4 Hz, 1H), 2.28 (dd, *J* = 12.5, 9.4 Hz, 1H), 1.84 (d, *J* = 9.6 Hz, 1H), 1.79 (ddd, *J* = 13.0, 4.3, 1.7 Hz, 1H). ¹³C NMR (126 MHz, CDCl₃) δ 156.3, 155.2, 138.1, 135.3, 132.0, 129.7, 129.6, 128.8, 127.8, 127.1, 127.1, 126.4, 125.9, 120.0, 79.8, 72.0, 69.6, 56.1, 52.6, 44.1, 29.0. HRMS (ESI) calcd for C₂₁H₁₉N₂O₄S⁺ (MH⁺) 395.1060, found 395.1068.

(±)-(1*S*,3*R*,4*S*,15*S*,18*S*)-18-Cyclopropyl-4-hydroxy-1-methoxy-11,14-diazapentacyclo[12.3.1.0^{3,15}.0^{5,10}.0^{11,15}]octadeca-5,7,9,16-tetraene-12,13-dione (3.87aj)
and (±)-(1*S*,3*R*,4*S*,15*S*,18*R*)-18-Cyclopropyl-4-hydroxy-1-methoxy-11,14-diazapentacyclo[12.3.1.0^{3,15}.0^{5,10}.0^{11,15}]octadeca-5,7,9,16-tetraene-12,13-dione (3.87aj')

(3.87aj). General procedure **F** was followed on a 0.214 g (0.607 mmol) scale of **3.83aj**, which after flash chromatography on silica gel (gradient elution: hexane → ethyl acetate) afforded 0.103 g (48%) of **3.87aj** and 0.020 g (9%) of **3.87aj'**.

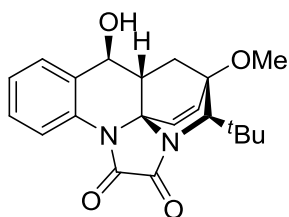


3.87aj: ^1H NMR (500 MHz, DMSO) δ 7.97 (dd, $J = 8.2, 1.2$ Hz, 1H), 7.62 (dt, $J = 8.0, 1.3$ Hz, 1H), 7.43 (dddd, $J = 8.2, 7.4, 1.7, 0.7$ Hz, 1H), 7.32 (td, $J = 7.6, 1.3$ Hz, 1H), 6.65 (d, $J = 8.8$ Hz, 1H), 6.31 (dd, $J = 8.8, 0.9$ Hz, 1H), 5.86 (d, $J = 7.8$ Hz, 1H), 4.08 (dd, $J = 10.5, 7.8$ Hz, 1H), 3.54 (dd, $J = 8.4, 0.9$ Hz, 1H), 3.41 (s, 3H), 2.28 (dd, $J = 11.6, 9.5$ Hz, 1H), 2.11 (td, $J = 10.4, 4.1$ Hz, 1H), 1.77 (dd, $J = 12.2, 3.6$ Hz, 1H), 0.77 (m, 1H), 0.50 (m, 4H). ^{13}C NMR (126 MHz, DMSO) δ 157.1, 153.9, 138.0, 131.7, 131.1, 128.2, 128.1, 126.7, 125.7, 120.3, 79.7, 70.1, 69.2, 63.0, 51.3, 45.7, 30.0, 10.6, 4.5, 3.1. HRMS (ESI) calcd for $\text{C}_{20}\text{H}_{21}\text{N}_2\text{O}_4^+$ (MH^+) 353.1496, found 353.1505.

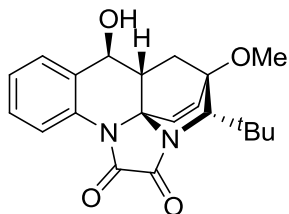


3.87aj': ^1H NMR (500 MHz, DMSO) δ 8.25 (dd, $J = 8.2, 1.0$ Hz, 1H), 7.63 (dt, $J = 7.8, 1.3$ Hz, 1H), 7.42 (dddd, $J = 8.2, 7.3, 1.6, 0.7$ Hz, 1H), 7.30 (td, $J = 7.6, 1.2$ Hz, 1H), 6.86 (d, $J = 8.8$ Hz, 1H), 6.29 (dd, $J = 8.8, 1.1$ Hz, 1H), 5.96 (d, $J = 7.6$ Hz, 1H), 4.08 (dd, $J = 10.3, 7.6$ Hz, 1H), 3.42 (s, 3H), 3.32 (m, 1H, overlaps with HDO), 2.47 (t, $J = 12.6, 9.3$ Hz, 1H), 2.29 (td, $J = 9.6, 4.5$ Hz, 1H), 1.70 (ddd, $J = 12.6, 4.2, 1.4$ Hz, 1H), 1.01 (dddd, $J = 13.4, 10.1, 6.5, 4.1$ Hz, 1H), 0.72 (ddt, $J = 9.4, 4.5, 1.9$ Hz, 1H), 0.60 (m, 1H), 0.52 (m, 2H). ^{13}C NMR (126 MHz, DMSO) δ 156.3, 155.4, 137.5, 131.8, 130.4, 129.3, 128.2, 128.0, 125.4, 118.5, 79.3, 70.1, 69.1, 58.8, 51.8, 41.8, 29.5, 9.3, 3.0, 2.4. HRMS (ESI) calcd for $\text{C}_{20}\text{H}_{21}\text{N}_2\text{O}_4^+$ (MH^+) 353.1496, found 353.1505.

(±)-(1*S*,3*R*,4*S*,15*S*,18*R*)-18-*tert*-Butyl-4-hydroxy-1-methoxy-11,14-diazapentacyclo[12.3.1.0^{3,15}.0^{5,10}.0^{11,15}]octadeca-5,7,9,16-tetraene-12,13-dione (**3.87al**) and (±)-(1*S*,3*R*,4*S*,15*S*,18*S*)-18-*tert*-butyl-4-hydroxy-1-methoxy-11,14-diazapentacyclo[12.3.1.0^{3,15}.0^{5,10}.0^{11,15}]octadeca-5,7,9,16-tetraene-12,13-dione (**3.87al'**). General procedure **F** was followed on a 0.276 g (0.750 mmol) scale of **3.83al**, which after flash chromatography on silica gel (gradient elution: chloroform → chloroform–methanol 98:2) afforded 0.074 g (27%) of **3.87al** and crude **3.87al'** which was additionally purified by flash chromatography on silica gel (gradient elution: hexane → ethyl acetate) to yield 0.027 g (10%) of pure **3.87al'**.



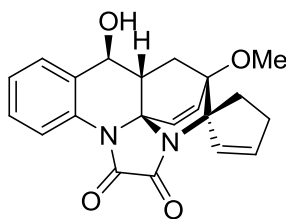
3.87al: ¹H NMR (500 MHz, CDCl₃) δ 8.52 (dd, *J* = 8.3, 1.1 Hz, 1H), 7.66 (dt, *J* = 7.8, 1.3 Hz, 1H), 7.40 (tdd, *J* = 8.2, 1.6, 0.8 Hz, 1H), 7.27 (td, *J* = 7.6, 1.2 Hz, 1H), 6.67 (dd, *J* = 8.6, 1.0 Hz, 1H), 6.12 (dd, *J* = 8.6, 1.1 Hz, 1H), 4.30 (t, *J* = 9.5 Hz, 1H), 3.68 (d, *J* = 1.9 Hz, 1H), 3.45 (s, 3H), 2.66 (ddd, *J* = 12.8, 8.8, 0.9 Hz, 1H), 2.56 (d, *J* = 9.0 Hz, 1H), 2.34 (dddd, *J* = 10.2, 8.9, 4.8, 1.1 Hz, 1H), 1.82 (ddd, *J* = 13.0, 4.8, 2.1 Hz, 1H), 1.25 (s, 9H). ¹³C NMR (126 MHz, CDCl₃) δ 157.6, 156.3, 139.9, 132.0, 130.3, 129.5, 128.5, 127.5, 126.1, 119.3, 80.8, 72.3, 70.3, 63.1, 51.9, 42.1, 36.4, 31.0, 30.8. HRMS (ESI) calcd for C₂₁H₂₅N₂O₄⁺ (MH⁺) 369.1809, found 369.1805.



3.87al': ¹H NMR (500 MHz, DMSO) δ 7.76 (dd, *J* = 8.2, 1.2 Hz, 1H), 7.61 (d, *J* = 7.8 Hz, 1H), 7.44 (td, *J* = 7.8, 1.7 Hz, 1H), 7.34 (td, *J* = 7.6, 1.3 Hz, 1H), 6.71 (d, *J* = 8.9 Hz, 1H), 6.22 (d, *J* = 9.0 Hz, 1H), 5.80 (d, *J* = 8.0 Hz, 1H), 4.10 (s, 1H), 4.03 (dd, *J* = 10.6, 7.9 Hz, 1H), 3.39 (s, 3H), 2.31 (dd, *J* = 12.5, 9.3 Hz, 1H), 1.93 (td, *J* = 10.0, 3.2 Hz, 1H), 1.73 (dd, *J* =

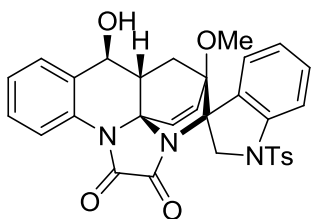
12.5, 3.5 Hz, 1H), 1.05 (s, 9H). ^{13}C NMR (126 MHz, DMSO) δ 157.7, 155.0, 138.1, 131.6, 131.6, 128.2, 128.1, 126.1, 124.1, 121.8, 80.5, 70.5, 70.3, 65.6, 50.8, 48.6, 37.0, 31.2, 30.8. HRMS (ESI) calcd for $\text{C}_{21}\text{H}_{25}\text{N}_2\text{O}_4^+$ (MH^+) 369.1809, found 369.1812.

(\pm)-(1*S*,1'*S*,3'*R*,4'*S*,15'*R*)-4'-Hydroxy-1'-methoxy-11',14'-diazaspiro [cyclopentane-1,18'-pentacyclo[12.3.1.0^{3,15}.0^{5,10}.0^{11,15}]octadecane]-2,5',7',9',16'-pentaene-12',13'-dione (3.87am) and (\pm)-(1*R*,1'*S*,3'*R*,4'*S*,15'*R*)-4'-Hydroxy-1'-methoxy-11',14'-diazaspiro[cyclopentane-1,18'-pentacyclo[12.3.1.0^{3,15}.0^{5,10}.0^{11,15}]octadecane]-2,5',7',9',16'-pentaene-12',13'-dione (3.87am'). General procedure **F** was followed on a 0.160 g (0.439 mmol) scale of **3.83am**, which after flash chromatography on silica gel (gradient elution: DCM \rightarrow DCM–methanol 90:10) afforded 0.084 g (53%) of **3.87am** and **3.87am'** as an inseparable mixture of diastereomers (one pure fraction was obtained; the structure was determined as **3.87am** on the basis of NOE correlation between low-field cyclohexene and high-field cyclopentene alkenic protons [130]).



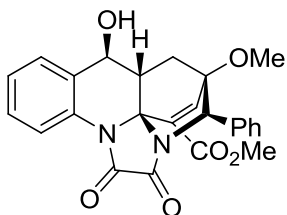
3.87am: ^1H NMR (500 MHz, DMSO) δ 8.04 (dd, $J = 8.2, 1.0$ Hz, 1H), 7.63 (dt, $J = 8.0, 1.2$ Hz, 1H), 7.42 (td, $J = 7.8, 1.6$ Hz, 1H), 7.31 (td, $J = 7.6, 1.2$ Hz, 1H), 6.86 (d, $J = 8.9$ Hz, 1H), 6.34 (dd, $J = 8.9, 1.1$ Hz, 1H), 6.05 (dt, $J = 5.3, 2.1$ Hz, 1H), 5.91 (d, $J = 7.5$ Hz, 1H), 5.12 (dt, $J = 5.6, 2.0$ Hz, 1H), 4.10 (dd, $J = 10.3, 7.6$ Hz, 1H), 3.40 (s, 3H), 2.68 (m, 1H), 2.39 (m, 2H), 2.29 (td, $J = 9.5, 3.3$ Hz, 1H), 2.12 (dd, $J = 12.6, 9.3$ Hz, 1H), 2.05 (m, 1H), 1.95 (dd, $J = 12.8, 4.1$ Hz, 1H). ^{13}C NMR (126 MHz, DMSO) δ 156.9, 152.7, 137.4, 137.1, 131.7, 130.8, 128.2, 128.0, 128.0, 127.4, 125.4, 119.7, 79.8, 75.3, 70.2, 69.5, 51.9, 43.9, 32.0, 28.2, 27.8. HRMS (ESI) calcd for $\text{C}_{21}\text{H}_{21}\text{N}_2\text{O}_4^+$ (MH^+) 365.1496, found 365.1505.

(±)-(1'S,3S,3'R,4'S,15'R)-4'-Hydroxy-1'-methoxy-1-(4-methylbenzenesulfonyl)-1,2-dihydro-11',14'-diazaspiro[indole-3,18'-pentacyclo[12.3.1.0^{3,15}.0^{5,10}.0^{11,15}]octadecane]-5',7',9',16'-tetraene-12',13'-dione (**3.87an**) and (±)-(1'S,3R,3'R,4'S,15'R)-4'-Hydroxy-1'-methoxy-1-(4-methylbenzenesulfonyl)-1,2-dihydro-11',14'-diazaspiro[indole-3,18'-pentacyclo[12.3.1.0^{3,15}.0^{5,10}.0^{11,15}]octadecane]-5',7',9',16'-tetraene-12',13'-dione (**3.87an'**). General procedure **F** was followed on a 0.151 g (0.265 mmol) scale of **3.83an**, which after flash chromatography on silica gel (gradient elution: chloroform → chloroform–methanol 97:3) afforded 0.061 g (40%) of **3.87an** and **3.87an'** as an inseparable mixture of diastereomers.

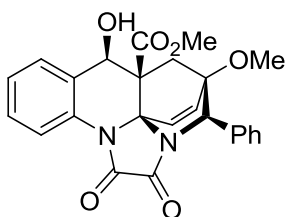


3.87an or **3.87an'**: ¹H NMR (500 MHz, DMSO) δ 8.12 (dd, *J* = 8.2, 1.1 Hz, 1H), 7.79 (m, 2H), 7.65 (dt, *J* = 8.0, 1.3 Hz, 1H), 7.49 (dd, *J* = 8.4, 0.9 Hz, 1H), 7.44 (tdd, *J* = 8.1, 1.6, 0.6 Hz, 1H), 7.40 (m, 2H), 7.32 (m, 2H), 7.25 (dd, *J* = 7.7, 1.2 Hz, 1H), 7.02 (td, *J* = 7.6, 1.0 Hz, 1H), 6.99 (dd, *J* = 8.9, 0.5 Hz, 1H), 6.47 (dd, *J* = 8.8, 0.8 Hz, 1H), 5.99 (d, *J* = 7.2 Hz, 1H), 4.15 (dd, *J* = 10.1, 7.2 Hz, 1H), 4.15 (d, *J* = 11.1 Hz, 1H), 4.04 (d, *J* = 11.1 Hz, 1H), 2.94 (s, 3H), 2.69 (td, *J* = 9.5, 3.9 Hz, 1H), 2.37 (s, 3H), 2.19 (dd, *J* = 12.9, 9.2 Hz, 1H), 1.84 (dd, *J* = 13.3, 4.2 Hz, 1H). ¹³C NMR (126 MHz, DMSO) δ 156.5, 153.0, 144.1, 143.1, 137.2, 134.1, 131.9, 130.9, 130.6, 130.1, 129.7, 128.2, 128.1, 127.4, 126.2, 125.5, 125.2, 122.9, 119.4, 112.8, 81.2, 70.1, 69.5, 67.2, 54.7, 51.6, 43.2, 25.6, 21.0. HRMS (ESI) calcd for C₃₁H₂₈N₃O₆S⁺ (MH⁺) 570.1693, found 570.1692.

(±)-Methyl (1*S*,3*R*,4*S*,15*R*,18*R*)-4-Hydroxy-1-methoxy-12,13-dioxo-18-phenyl-11,14-diazapentacyclo[12.3.1.0^{3,15}.0^{5,10}.0^{11,15}]octadeca-5,7,9,16-tetraene-16-carboxylate (**3.87bh**) and (±)-Methyl (1*S*,3*S*,4*R*,15*S*,18*R*)-4-Hydroxy-1-methoxy-12,13-dioxo-18-phenyl-11,14-diazapentacyclo[12.3.1.0^{3,15}.0^{5,10}.0^{11,15}]octadeca-5,7,9,16-tetraene-3-carboxylate (**3.87bh'**): General procedure F was followed on a 0.233 g (0.522 mmol) scale of **3.83bh**, which after flash chromatography on silica gel (gradient elution: DCM → DCM–methanol 90:10) afforded 0.116 g (50%) of **3.87bh'** and 0.078 g (33%) of **3.87bh**.



3.87bh': ¹H NMR (500 MHz, DMSO) δ 8.28 (dd, *J* = 8.3, 1.3 Hz, 1H), 7.81 (s, 1H), 7.59 (dt, *J* = 7.8, 1.3 Hz, 1H), 7.41 (m, 3H), 7.37 (m, 3H), 7.26 (td, *J* = 7.6, 1.1 Hz, 1H), 5.97 (d, *J* = 7.2 Hz, 1H), 4.89 (d, *J* = 1.2 Hz, 1H), 4.05 (dd, *J* = 10.6, 7.2 Hz, 1H), 3.48 (s, 3H), 3.46 (s, 3H), 2.77 (ddd, *J* = 10.7, 9.1, 4.7 Hz, 1H), 1.78 (dd, *J* = 12.9, 9.1 Hz, 1H), 1.73 (dd, *J* = 13.1, 4.1 Hz, 1H). ¹³C NMR (126 MHz, DMF) δ 161.6, 157.1, 155.1, 146.8, 134.8, 133.0, 132.3, 130.6, 128.7, 128.4, 128.3, 128.3, 127.8, 125.2, 119.0, 79.9, 70.4, 70.2, 59.1, 52.5, 51.9, 43.5, 26.9. HRMS (ESI) calcd for C₂₅H₂₃N₂O₆⁺ (MH⁺) 447.1551, found 447.1557.

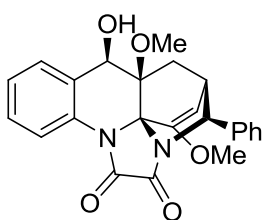


3.87bh: ¹H NMR (500 MHz, DMSO) δ 8.25 (dd, *J* = 8.2, 1.2 Hz, 1H), 7.61 (dt, *J* = 7.8, 1.2 Hz, 1H), 7.48 (t, *J* = 7.4 Hz, 1H), 7.39 (m, 2H), 7.32 (m, 2H), 7.14 (d, *J* = 8.6 Hz, 1H), 7.03 (m, 2H), 6.49 (d, *J* = 6.6 Hz, 1H), 6.33 (d, *J* = 8.6 Hz, 1H), 4.85 (s, 1H), 4.57 (d, *J* = 6.6 Hz, 1H), 3.51 (s, 3H), 3.48 (s, 3H), 2.23 (d, *J* = 13.5 Hz, 1H), 2.15 (dd, *J* = 13.6, 1.5 Hz, 1H). ¹³C NMR (126 MHz, DMSO) δ 169.8, 156.2, 155.9, 138.0, 132.9,

132.0, 130.4, 128.4, 128.3, 128.0, 127.9, 127.8, 127.7, 125.3, 118.6, 79.1, 72.9, 69.5, 59.5, 52.3, 52.2, 49.8, 31.2. HRMS (ESI) calcd for C₂₅H₂₃N₂O₆⁺ (MH⁺) 447.1551, found 447.1558.

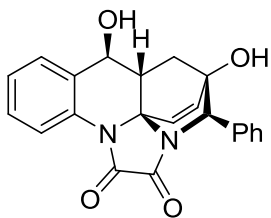
(±)-(1*R*,3*S*,4*R*,15*S*,18*S*)-4-Hydroxy-3,16-dimethoxy-18-phenyl-11,14-diazapentacyclo[12.3.1.0^{3,15}.0^{5,10}.0^{11,15}]octadeca-5,7,9,16-tetraene-12,13-dione

(3.87dh). General procedure **F** was followed on a 0.313 g (0.748 mmol) scale of **3.83dh**, which after flash chromatography on silica gel (gradient elution: DCM → DCM–methanol 97:3) afforded 0.234 g (75%) of **3.87dh**.



3.87dh: ¹H NMR (500 MHz, DMSO) δ 8.21 (dd, *J* = 8.2, 1.1 Hz, 1H), 7.64 (dt, *J* = 7.8, 1.4 Hz, 1H), 7.38 (m, 5H), 7.30 (m, 2H), 6.39 (d, *J* = 6.7 Hz, 1H), 5.49 (d, *J* = 7.4 Hz, 1H), 4.81 (d, *J* = 2.6 Hz, 1H), 4.50 (d, *J* = 6.7 Hz, 1H), 3.46 (s, 3H), 3.24 (s, 3H), 3.20 (dq, *J* = 7.8, 2.8 Hz, 1H), 1.78 (ddd, *J* = 14.0, 3.5, 1.0 Hz, 1H), 1.69 (dd, *J* = 14.1, 2.5 Hz, 1H). ¹³C NMR (126 MHz, DMSO) δ 157.4, 155.3, 155.2, 135.7, 133.4, 129.1, 128.2, 127.6, 127.3, 127.1, 126.9, 125.1, 118.0, 98.1, 74.0, 73.9, 73.3, 59.5, 56.1, 53.7, 37.1, 23.6. HRMS (ESI) calcd for C₂₄H₂₃N₂O₅⁺ (MH⁺) 419.1601, found 419.1606.

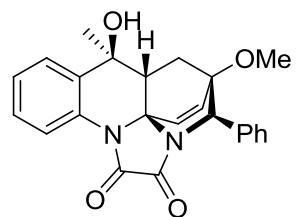
(±)-(1*S*,3*R*,4*S*,15*S*,18*R*)-1,4-Dihydroxy-18-phenyl-11,14-diazapentacyclo[12.3.1.0^{3,15}.0^{5,10}.0^{11,15}]octadeca-5,7,9,16-tetraene-12,13-dione (3.87eh). General procedure **F** was followed on a 0.137 g (0.365 mmol) scale of **3.83eh**, which after flash chromatography on silica gel (gradient elution: chloroform → chloroform–methanol 97:3) afforded 0.085 g (62%) of **3.87eh**.



3.87eh: ^1H NMR (500 MHz, DMF) δ 8.34 (dd, $J = 8.2, 1.1$ Hz, 1H), 7.77 (dt, $J = 7.8, 1.1$ Hz, 1H), 7.53 (m, 2H), 7.49 (dddd, $J = 8.1, 7.4, 1.6, 0.7$ Hz, 1H), 7.38 (m, 4H), 6.77 (dd, $J = 8.5, 0.7$ Hz, 1H), 6.42 (dd, $J = 8.5, 1.0$ Hz, 1H), 6.21 (s, 1H), 6.07 (d, $J = 7.2$ Hz, 1H), 4.59 (d, $J = 1.5$ Hz, 1H), 4.35 (dd, $J = 10.4, 7.2$ Hz, 1H), 2.71 (td, $J = 9.8, 3.9$ Hz, 1H), 2.05 (dd, $J = 12.9, 9.2$ Hz, 1H), 1.60 (ddd, $J = 12.9, 4.1, 1.5$ Hz, 1H). ^{13}C NMR (126 MHz, DMF) δ 157.2, 155.1, 143.4, 133.8, 132.9, 131.4, 128.7, 128.6, 128.4, 128.4, 128.2, 127.9, 125.6, 119.3, 74.1, 71.0, 70.1, 62.6, 43.8, 31.0. HRMS (ESI) calcd for $\text{C}_{22}\text{H}_{19}\text{N}_2\text{O}_4^+$ (MH^+) 375.1339, found 375.1351.

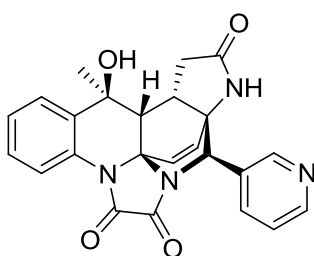
(\pm)-(1S,3R,4S,15S,18R)-4-Hydroxy-1-methoxy-4-methyl-18-phenyl-11,14-diazapentacyclo[12.3.1.0^{3,15}.0^{5,10}.0^{11,15}]octadeca-5,7,9,16-tetraene-12,13-dione

(3.88ah). General procedure **F** was followed on a 0.284 g (0.706 mmol) scale of **3.84ah**, which after flash chromatography on silica gel (gradient elution: hexane \rightarrow hexane–ethyl acetate 50:50) afforded 0.115 g (40%) of **3.88ah**.

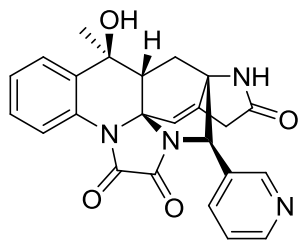


3.88ah: ^1H NMR (500 MHz, CDCl_3) δ 8.33 (dd, $J = 8.2, 1.0$ Hz, 1H), 7.68 (dd, $J = 7.9, 1.3$ Hz, 1H), 7.38 (ddd, $J = 8.3, 7.4, 1.6$ Hz, 1H), 7.34 (m, 3H), 7.29 (m, 1H), 7.26 (m, 2H), 6.82 (d, $J = 8.7$ Hz, 1H), 6.27 (dd, $J = 8.7, 0.8$ Hz, 1H), 4.70 (s, 1H), 3.46 (s, 3H), 2.83 (t, $J = 7.3$ Hz, 1H), 2.31 (s, 1H), 1.94 (d, $J = 7.5$ Hz, 2H), 1.40 (s, 3H). ^{13}C NMR (126 MHz, CDCl_3) δ 157.2, 155.0, 137.2, 134.1, 131.9, 131.0, 129.6, 129.2, 128.6, 128.5, 127.9, 127.6, 126.6, 120.6, 79.7, 71.6, 69.9, 60.0, 52.6, 48.1, 28.5, 24.0. HRMS (ESI) calcd for $\text{C}_{24}\text{H}_{22}\text{N}_2\text{O}_4\text{Na}^+$ (MNa^+) 425.1472, found 425.1475.

(±)-(1*R*,5*S*,6*R*,7*S*,18*S*,21*R*)-7-Hydroxy-7-methyl-21-(pyridin-3-yl)-2,14,17-triazahehexacyclo[15.3.1.0^{1,5}.0^{6,18}.0^{8,13}.0^{14,18}]henicosa-8,10,12,19-tetraene-3,15,16-trione (3.88ck) and (±)-(3*R*,4*S*,15*S*,21*R*)-4-Hydroxy-4-methyl-21-(pyridin-3-yl)-11,14,20-triazahehexacyclo[12.6.1.0^{1,17}.0^{3,15}.0^{5,10}.0^{11,15}]henicosa-5,7,9,16-tetraene-12,13,19-trione (3.88ck'). General procedure **F** was followed on a 0.164 g (0.383 mmol) scale of **3.84ck**, which after flash chromatography on silica gel (gradient elution: chloroform → chloroform–methanol 90:10) afforded 0.065 g (40%) of **3.88ck** and 0.050 g (30%) of **3.88ck'**.



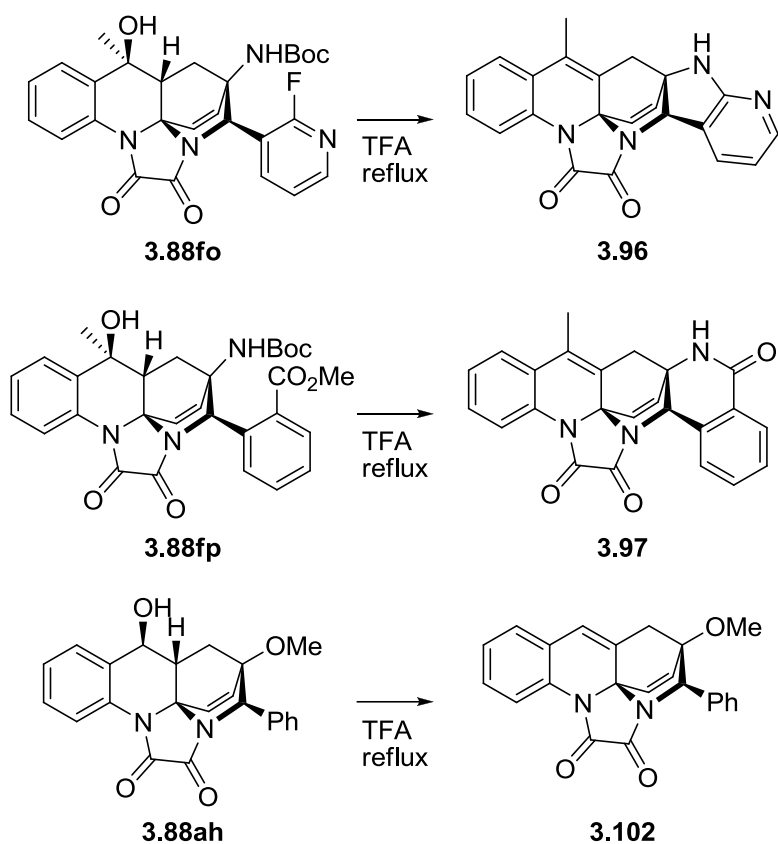
3.88ck: ¹H NMR (500 MHz, DMSO) δ 8.67 (d, *J* = 2.2 Hz, 1H), 8.55 (s, 1H), 8.54 (dd, *J* = 4.9, 1.6 Hz, 1H), 8.30 (dd, *J* = 8.3, 1.2 Hz, 1H), 7.89 (dt, *J* = 8.0, 2.3 Hz, 1H), 7.68 (dd, *J* = 7.9, 1.5 Hz, 1H), 7.41 (m, 2H), 7.32 (td, *J* = 7.6, 1.3 Hz, 1H), 6.75 (d, *J* = 8.3 Hz, 1H), 6.56 (d, *J* = 8.4 Hz, 1H), 5.62 (s, 1H), 4.69 (s, 1H), 3.29 (m, 1H), 2.50 (m, 2H, overlaps with DMSO), 2.21 (m, 1H), 1.41 (s, 3H). ¹³C NMR (126 MHz, DMSO) δ 176.0, 157.1, 155.9, 149.6, 149.1, 137.4, 136.7, 135.7, 132.4, 131.2, 127.7, 126.6, 125.6, 123.1, 123.1, 119.1, 71.8, 71.1, 63.1, 58.5, 47.5, 36.0, 32.9, 32.1. HRMS (ESI) calcd for C₂₄H₂₁N₄O₄⁺ (MH⁺) 429.1557, found 429.1561.



3.88ck': ¹H NMR (500 MHz, DMSO) δ 8.60 (d, *J* = 4.8 Hz, 1H), 8.58 (s, 1H), 8.38 (s, 1H), 8.18 (d, *J* = 8.1 Hz, 1H), 7.78 (d, *J* = 7.9 Hz, 1H), 7.71 (d, *J* = 7.5 Hz, 1H), 7.44 (m, 2H), 7.33 (t, *J* = 7.3 Hz, 1H), 6.29 (t, *J* = 2.0 Hz, 1H), 5.42 (s, 1H), 4.72 (s, 1H), 3.28 (dd, *J* = 22.4, 2.3 Hz, 1H), 3.13 (dd, *J* = 22.2, 2.1 Hz, 1H), 3.06 (dd, *J* = 9.4, 5.1 Hz, 1H), 1.96 (dd, *J* = 13.6, 9.9 Hz, 1H), 1.54 (dd, *J* = 13.7, 4.3 Hz, 1H), 1.25 (s, 3H).

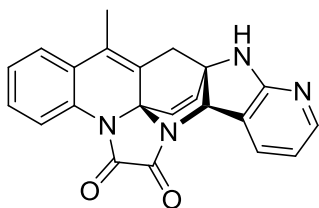
^{13}C NMR (126 MHz, DMSO) δ 174.6, 157.0, 154.4, 149.2, 148.8, 144.4, 136.1, 135.0, 130.9, 128.3, 127.8, 127.8, 125.8, 123.6, 120.8, 119.6, 70.6, 70.2, 63.5, 59.2, 47.1, 33.1, 28.3, 25.6. HRMS (ESI) calcd for $\text{C}_{24}\text{H}_{21}\text{N}_4\text{O}_4^+$ (MH^+) 429.1557, found 429.1560.

Post-Photochemical Modifications



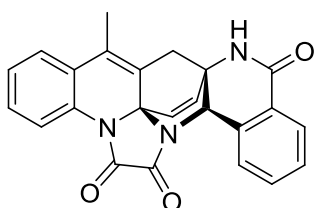
General Procedure G for Acid-Promoted Dehydration/Cyclization. The crude photoproduct (0.395 mmol) was dissolved in TFA (8 mL). Solution was refluxed or stirred in a sealed tube at 80 °C for 1 day. Volatiles were removed *in vacuo*, and the residue was redissolved in DCM (50 mL). Solution was washed 2 times with sat. aq. NaHCO_3 (5 mL) diluted with water (5 mL). Aqueous layer was extracted with DCM (2×10 mL). The combined organic layers were washed with water (10 mL) and sat. aq. NaCl (10 mL), dried over anhydrous Na_2SO_4 , and the solvent was removed *in vacuo*.

Further purification by flash chromatography on silica gel yielded modified photoproduct.



(±)-(1*S*,9*R*,22*S*)-20-Methyl-2,4,10,13-tetraazaheptacyclo[19.3.1.0^{1,9}.0^{3,8}.0^{10,22}.0^{13,22}.0^{14,19}]pentacosa-3(8),4,6,14,16,18,20,23-octaene-11,12-dione

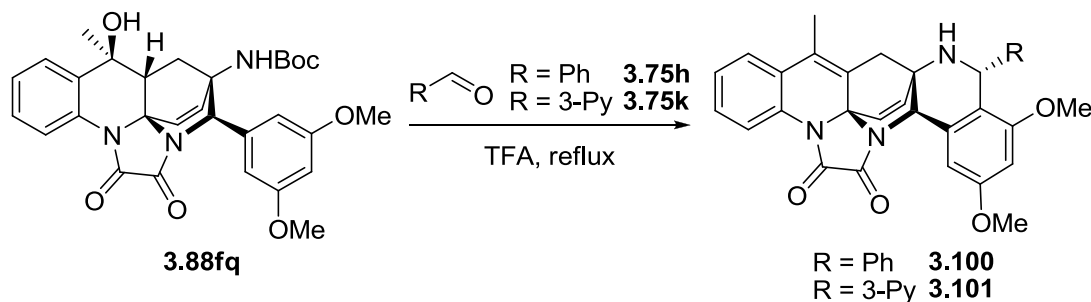
(3.96). General procedure **F** was followed on a 0.200 g (0.395 mmol) scale of **3.84fo**, which afforded crude **3.88fo**. The obtained photoproduct was then subjected to general procedure **G**, which after flash chromatography on silica gel (gradient elution: chloroform → chloroform–methanol 97:3) afforded 0.076 g (52% after two steps) of the title compound. ¹H NMR (500 MHz, CDCl₃) δ 8.06 (dt, *J* = 5.6, 1.1 Hz, 1H), 7.91 (m, 2H), 7.37 (ddd, *J* = 7.9, 6.8, 2.2 Hz, 1H), 7.27 (m, 2H), 6.83 (dd, *J* = 7.2, 5.3 Hz, 1H), 6.78 (d, *J* = 8.6 Hz, 1H), 6.53 (dd, *J* = 8.5, 0.5 Hz, 1H), 5.17 (s, 1H), 4.69 (d, *J* = 1.2 Hz, 1H), 2.75 (d, *J* = 16.2 Hz, 1H), 2.40 (dt, *J* = 16.3, 1.0 Hz, 1H), 1.86 (t, *J* = 1.2 Hz, 3H). ¹³C NMR (126 MHz, CDCl₃) δ 162.6, 158.5, 157.7, 147.8, 135.4, 135.1, 130.6, 129.8, 129.8, 128.6, 127.1, 127.1, 123.9, 123.1, 122.6, 118.5, 116.7, 73.6, 67.0, 63.3, 30.3, 13.4. HRMS (ESI) calcd for C₂₂H₁₇N₄O₂⁺ (MH⁺) 369.1346, found 369.1355.



(±)-(1*S*,10*R*,23*S*)-21-Methyl-2,11,14-triazaheptacyclo[20.3.1.0^{1,10}.0^{4,9}.0^{11,23}.0^{14,23}.0^{15,20}]hexacosa-4(9),5,7,15,17,19,21,24-octaene-3,12,13-trione (**3.97**).

General procedure **F** was followed on a 0.196 g (0.359 mmol) scale of **3.84fp**, which afforded crude **3.88fp**. The obtained photoproduct was then subjected to general procedure **G**, which after flash chromatography on silica gel (gradient elution: chloroform → chloroform–methanol 97:3) afforded 0.078 g (55% after two steps) of the

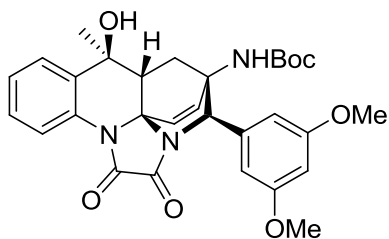
title compound. ^1H NMR (500 MHz, CDCl_3) δ 8.13 (dd, $J = 7.7, 1.2$ Hz, 1H), 8.08 (dd, $J = 8.0, 0.9$ Hz, 1H), 7.67 (s, 1H), 7.61 (td, $J = 7.5, 1.4$ Hz, 1H), 7.55 (dtd, $J = 7.8, 1.3, 0.5$ Hz, 1H), 7.51 (tt, $J = 7.5, 1.1$ Hz, 1H), 7.38 (ddd, $J = 8.0, 7.1, 1.9$ Hz, 1H), 7.26 (m, 2H), 6.76 (dd, $J = 8.3, 0.5$ Hz, 1H), 6.49 (dd, $J = 8.3, 0.7$ Hz, 1H), 5.08 (s, 1H), 2.79 (d, $J = 16.0$ Hz, 1H), 2.48 (dt, $J = 16.7, 1.3$ Hz, 1H), 1.83 (t, $J = 1.3$ Hz, 3H). ^{13}C NMR (126 MHz, CDCl_3) δ 164.9, 158.8, 157.3, 134.8, 134.2, 133.9, 133.5, 130.4, 129.1, 129.0, 128.7, 127.9, 127.1, 126.9, 126.4, 126.2, 124.7, 124.1, 121.6, 72.9, 57.7, 57.7, 32.1, 13.6. HRMS (ESI) calcd for $\text{C}_{24}\text{H}_{18}\text{N}_3\text{O}_3^+$ (MH^+) 396.1343, found 396.1346.



General Procedure H for Pictet–Spengler Reaction. Photoproduct (**3.88fq**;

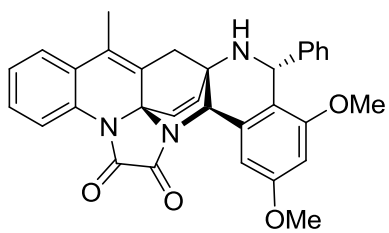
0.369 mmol) was dissolved in TFA (7 mL). Aldehyde (**3.75**; 1.81 mmol) was added, and the mixture was refluxed for 1 day. Volatiles were removed *in vacuo*, and the residue was redissolved in DCM (50 mL). Solution was washed with sat. aq. NaHCO_3 (2×10 mL). Aqueous layer was extracted with DCM (3×20 mL). The combined organic layers were washed with water (3×15 mL) and sat. aq. NaCl (15 mL), dried over anhydrous Na_2SO_4 , and the solvent was removed *in vacuo*. Further purification by flash chromatography on silica gel yielded modified photoproduct.

(±)-(1*S*,3*R*,10*R*,23*S*)-5,7-Dimethoxy-21-methyl-3-phenyl-2,11,14-triazaheptacyclo
[20.3.1.0^{1,10}.0^{4,9}.0^{11,23}.0^{14,23}.0^{15,20}]hexacosa-4(9),5,7,15,17,19,21,24-octaene-12,13-dione
(**3.100**).



Step 1. (±)-*tert*-Butyl *N*-[(1*S*,3*R*,4*S*,15*S*,18*R*)-18-(3,5-
dimethoxyphenyl)-4-hydroxy-4-methyl-12,13-dioxo-
11,14-diazapentacyclo[12.3.1.0^{3,15}.0^{5,10}.0^{11,15}]octadeca-
5,7,9,16-tetraen-1-yl]carbamate (**3.88fq**). General

procedure **F** was followed on a 0.202 g (0.369 mmol) scale of **3.84fq**, which after flash chromatography on silica gel (gradient elution: chloroform → chloroform–methanol 97:3) afforded 0.165 g of **3.88fq**. ¹H NMR (500 MHz, CDCl₃) δ 8.31 (dd, *J* = 8.2, 1.1 Hz, 1H), 7.72 (dd, *J* = 7.9, 1.6 Hz, 1H), 7.38 (ddd, *J* = 8.2, 7.5, 1.6 Hz, 1H), 7.29 (td, *J* = 7.6, 1.3 Hz, 1H), 6.91 (d, *J* = 8.6 Hz, 1H), 6.40 (t, *J* = 2.2 Hz, 1H), 6.35 (d, *J* = 1.8 Hz, 2H), 6.20 (d, *J* = 8.5 Hz, 1H), 5.07 (s, 1H), 4.79 (s, 1H), 3.74 (s, 6H), 2.94 (dd, *J* = 9.4, 4.9 Hz, 1H), 2.01 (dd, *J* = 12.6, 10.4 Hz, 1H), 1.78 (dd, *J* = 13.1, 4.0 Hz, 1H), 1.49 (s, 9H), 1.35 (s, 3H). ¹³C NMR (126 MHz, CDCl₃ + DMSO) δ 161.2, 157.3, 155.0, 154.6, 139.6, 135.2, 134.3, 131.0, 128.7, 127.9, 127.5, 126.4, 120.6, 106.1, 100.1, 80.8, 70.9, 70.0, 58.9, 57.7, 55.5, 48.0, 28.5, 28.4, 26.5. HRMS (ESI) calcd for C₃₀H₃₄N₃O₇⁺ (MH⁺) 548.2391, found 548.2391.

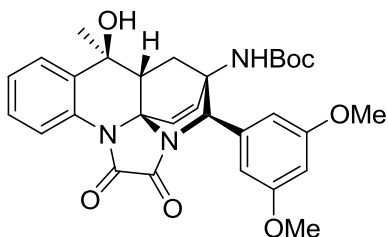


Step 2. (±)-(1*S*,3*R*,10*R*,23*S*)-5,7-Dimethoxy-21-methyl-3-
phenyl-2,11,14-triazaheptacyclo
[20.3.1.0^{1,10}.0^{4,9}.0^{11,23}.0^{14,23}.0^{15,20}]hexacosa-
4(9),5,7,15,17,19,21,24-octaene-12,13-dione (**3.100**).

0.165 g of photoproduct **3.88fq** was subjected to general procedure **H** with 1.81 mmol of

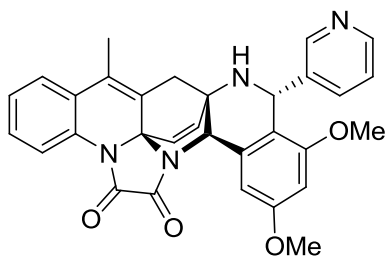
benzaldehyde (**3.75h**), which after flash chromatography on silica gel (gradient elution: hexane → hexane–ethyl acetate 50:50) afforded 0.063 g (33% after two steps) of the title compound. ¹H NMR (500 MHz, CDCl₃) δ 8.07 (dd, *J* = 8.0, 1.1 Hz, 1H), 7.34 (td, *J* = 7.7, 1.6 Hz, 1H), 7.27 (m, 7H), 6.88 (dd, *J* = 2.4, 0.9 Hz, 1H), 6.60 (d, *J* = 8.2 Hz, 1H), 6.39 (dd, *J* = 2.4, 0.4 Hz, 1H), 6.22 (d, *J* = 8.3 Hz, 1H), 5.38 (d, *J* = 0.5 Hz, 1H), 4.66 (s, 1H), 3.77 (s, 3H), 3.52 (s, 3H), 2.76 (dd, *J* = 16.2, 0.9 Hz, 1H), 2.34 (d, *J* = 16.0 Hz, 1H), 1.85 (t, *J* = 1.2 Hz, 3H). ¹³C NMR (126 MHz, CDCl₃) δ 160.4, 159.2, 157.9, 157.0, 144.9, 137.5, 135.1, 132.4, 130.5, 129.1, 128.6, 128.5, 127.5, 127.3, 126.7, 126.6, 123.8, 123.5, 121.3, 117.5, 103.9, 99.4, 73.3, 58.3, 58.0, 55.6, 55.5, 54.9, 30.9, 13.5. HRMS (ESI) calcd for C₃₂H₂₈N₃O₄⁺ (MH⁺) 518.2074, found 518.2072.

(±)-(1*S*,3*R*,10*R*,23*S*)-5,7-Dimethoxy-21-methyl-3-(pyridin-3-yl)-2,11,14-triazaheptacyclo[20.3.1.0^{1,10}.0^{4,9}.0^{11,23}.0^{14,23}.0^{15,20}]hexacosa-4(9),5,7,15,17,19,21,24-octaene-12,13-dione (3.101).



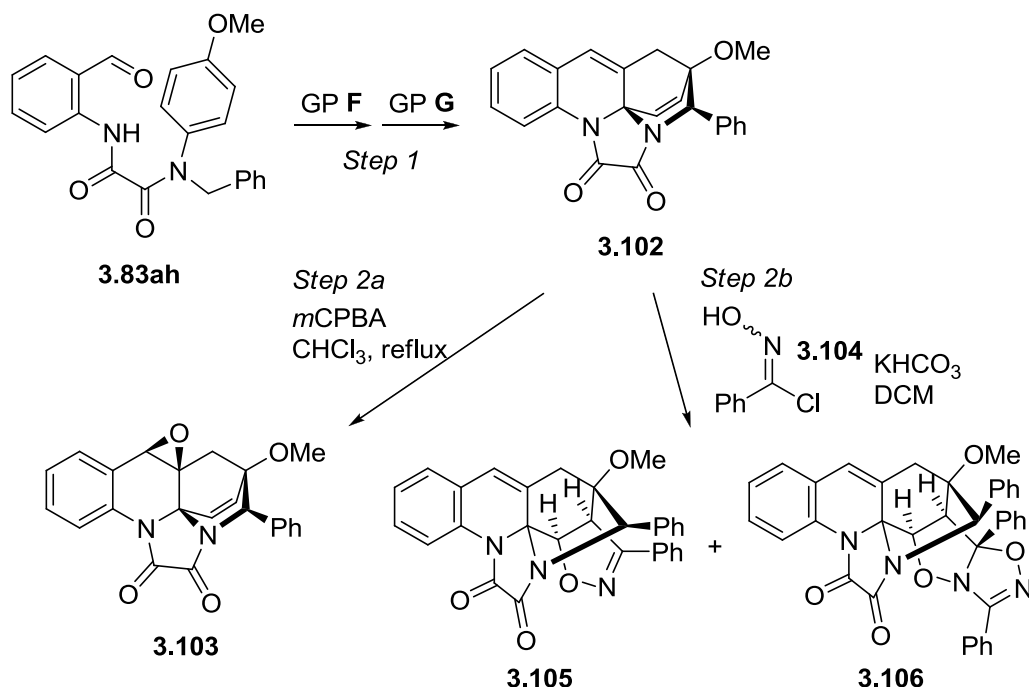
Step 1. (±)-*tert*-Butyl *N*-[(1*S*,3*R*,4*S*,15*S*,18*R*)-18-(3,5-dimethoxyphenyl)-4-hydroxy-4-methyl-12,13-dioxo-11,14-diazapentacyclo[12.3.1.0^{3,15}.0^{5,10}.0^{11,15}]octadeca-5,7,9,16-tetraen-1-yl]carbamate (**3.88fq**). General

procedure **F** was followed on a 0.365 g (0.667 mmol) scale of **3.84fq**, which after flash chromatography on silica gel (gradient elution: hexane → ethyl acetate) afforded 0.190 g of **3.88fq**.



Step 2. (\pm)-(1*S*,3*R*,10*R*,23*S*)-5,7-Dimethoxy-21-methyl-3-(pyridin-3-yl)-2,11,14-triazaheptacyclo
 [20.3.1.0^{1,10}.0^{4,9}.0^{11,23}.0^{14,23}.0^{15,20}]hexacos-
 4(9),5,7,15,17,19,21,24-octaene-12,13-dione (**3.101**).

0.179 g of the photoproduct **3.88fq** was subjected to general procedure **H** with 3.17 mmol of nicotinaldehyde (**3.75k**), which after flash chromatography on silica gel (gradient elution: chloroform \rightarrow chloroform–methanol 97:3) afforded 0.110 g (34% after two steps) of the title compound. ¹H NMR (500 MHz, CDCl₃) δ 8.64 (d, $J = 1.7$ Hz, 1H), 8.48 (dd, $J = 4.8, 1.4$ Hz, 1H), 8.07 (dd, $J = 8.0, 0.9$ Hz, 1H), 7.53 (dt, $J = 7.9, 1.8$ Hz, 1H), 7.34 (ddd, $J = 8.0, 7.3, 1.7$ Hz, 1H), 7.24 (m, 3H), 6.89 (dd, $J = 2.3, 0.8$ Hz, 1H), 6.62 (d, $J = 8.3$ Hz, 1H), 6.38 (d, $J = 2.2$ Hz, 1H), 6.24 (d, $J = 8.3$ Hz, 1H), 5.42 (d, $J = 0.7$ Hz, 1H), 4.69 (s, 1H), 3.76 (s, 3H), 3.54 (s, 3H), 2.78 (d, $J = 16.4$ Hz, 1H), 2.33 (dt, $J = 16.2, 1.4$ Hz, 1H), 1.85 (t, $J = 1.2$ Hz, 3H). ¹³C NMR (126 MHz, CDCl₃) δ 160.7, 159.3, 157.8, 156.6, 149.4, 148.2, 140.7, 137.3, 135.4, 135.2, 132.5, 130.5, 128.8, 128.6, 126.7, 126.6, 123.9, 123.7, 123.7, 121.3, 116.2, 104.1, 99.3, 73.3, 58.1, 58.0, 55.6, 55.3, 52.7, 31.0, 13.5. HRMS (ESI) calcd for C₃₁H₂₇N₄O₄⁺ (MH⁺) 519.2027, found 519.2031.

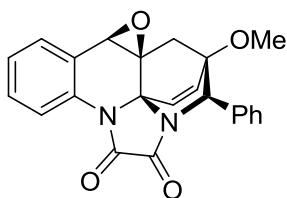


(±)-(1*S*,3*R*,14*R*,15*S*,18*S*)-15-Methoxy-14-phenyl-2-oxa-10,13-diazahexacyclo[13.3.1.0^{1,3}.0^{4,9}.0^{10,18}.0^{13,18}]nonadeca-4,6,8,16-tetraene-11,12-dione (3.103), (±)-(1*S*,16*R*,20*S*,21*R*)-1-Methoxy-19,21-diphenyl-17-oxa-11,14,18-triazahexacyclo[12.6.1.0^{3,15}.0^{5,10}.0^{11,15}.0^{16,20}]heneicosa-3,5(10),6,8,18-pentaene-12,13-dione (3.105) and (±)-(1*S*,16*R*,22*R*,23*S*,24*R*)-1-Methoxy-19,22,24-triphenyl-17,21-dioxa-11,14,18,20-tetraazaheptacyclo[12.9.1.0^{3,15}.0^{5,10}.0^{11,15}.0^{16,23}.0^{18,22}]tetracos-3,5(10),6,8,19-pentaene-12,13-dione (3.106).

Step 1. (±)-(1*S*,15*S*,18*R*)-1-Methoxy-18-phenyl-11,14-diazapentacyclo[12.3.1.0^{3,15}.0^{5,10}.0^{11,15}]octadeca-3,5,7,9,16-pentaene-12,13-dione (3.102). General procedure F was followed on a 0.297 g (0.765 mmol) scale of 3.83ah, which afforded crude 3.87ah. The obtained photoproduct was then subjected to general procedure G, which afforded 0.271 g of crude 3.102. ¹H NMR (500 MHz, CDCl₃) δ 7.98 (dq, *J* = 8.0, 0.5 Hz, 1H), 7.35 (m, 4H), 7.25 (m, 2H), 7.21 (td, *J* = 7.6, 1.2 Hz, 1H), 7.11 (dd, *J* = 7.5,

1.4 Hz, 1H), 6.74 (dd, $J = 8.7, 0.7$ Hz, 1H), 6.65 (dd, $J = 8.7, 0.8$ Hz, 1H), 6.20 (t, $J = 1.9$ Hz, 1H), 4.84 (d, $J = 1.7$ Hz, 1H), 3.45 (s, 3H), 2.61 (dd, $J = 16.7, 2.0$ Hz, 1H), 2.49 (dt, $J = 16.8, 1.9$ Hz, 1H).

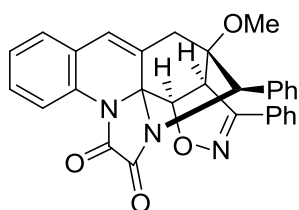
Step 2a. (\pm)-(1*S*,3*R*,14*R*,15*S*,18*S*)-15-Methoxy-14-phenyl-2-oxa-10,13-diazahexacyclo [13.3.1.0^{1,3}.0^{4,9}.0^{10,18}.0^{13,18}]nonadeca-4,6,8,16-tetraene-11,12-dione (**3.103**). 0.135 g of crude **3.102** was dissolved in chloroform (15 mL). The solution was treated with *m*CPBA (0.200 g, 1.16 mmol) and refluxed for 4 h. The mixture was then diluted with DCM (50 mL) and washed 2 times with sat. aq. NaHCO₃ (5 mL) diluted with water (5 mL). Aqueous layer was extracted with DCM (2×10 mL). The combined organic layers were washed with water (10 mL) and sat. aq. NaCl (10 mL), dried over anhydrous Na₂SO₄, and the solvent was removed *in vacuo*. Further purification by flash chromatography on silica gel pre-treated with pyridine (gradient elution: hexane → hexane–ethyl acetate + 1% TEA 60:40) afforded 0.040 g (27% after three steps) of **3.103**.



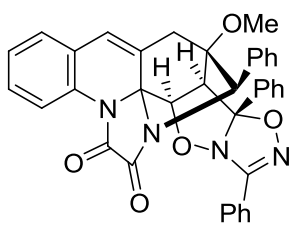
3.103: ¹H NMR (500 MHz, CDCl₃) δ 7.92 (ddd, $J = 7.9, 1.2, 0.6$ Hz, 1H), 7.50 (m, 2H), 7.41 (m, 4H), 7.35 (m, 1H), 7.29 (td, $J = 7.6, 1.2$ Hz, 1H), 6.96 (d, $J = 8.8$ Hz, 1H), 6.38 (d, $J = 8.8$ Hz, 1H), 4.90 (d, $J = 1.5$ Hz, 1H), 4.01 (s, 1H), 3.42 (s, 3H), 2.36 (dd, $J = 13.8, 1.7$ Hz, 1H), 2.09 (d, $J = 13.8$ Hz, 1H). ¹³C NMR (126 MHz, CDCl₃) δ 157.3, 154.7, 140.6, 131.8, 131.6, 130.8, 130.6, 128.8, 128.8, 128.7, 128.5, 126.8, 124.4, 123.3, 80.1, 69.9, 67.0, 60.8, 59.1, 52.7, 29.9. HRMS (ESI) calcd for C₂₃H₁₉N₂O₄⁺ (MH⁺) 387.1339, found 387.1342.

Step 2b. (\pm)-(1*S*,16*R*,20*S*,21*R*)-1-Methoxy-19,21-diphenyl-17-oxa-11,14,18-triazahexacyclo [12.6.1.0^{3,15}.0^{5,10}.0^{11,15}.0^{16,20}]heneicosa-3,5(10),6,8,18-pentaene-12,13-

dione (**3.105**) and (\pm)-(1*S*,16*R*,22*R*,23*S*,24*R*)-1-Methoxy-19,22,24-triphenyl-17,21-dioxo-11,14,18,20-tetraazaheptacyclo[12.9.1.0^{3,15}.0^{5,10}.0^{11,15}.0^{16,23}.0^{18,22}]tetracos-3,5(10),6,8,19-pentaene-12,13-dione (**3.106**). Under nitrogen, 0.135 g of crude **3.102** was dissolved in anhydrous DCM (8 mL), and the solution was treated with *N*-hydroxybenzimidoyl chloride [182] (**3.104**; 0.598 g, 3.85 mmol) and potassium bicarbonate (0.460 g, 4.60 mmol). The mixture was stirred at ambient temperature for 1 day, and then quenched with water (5 mL). Aqueous layer was extracted with DCM (3×20 mL). The combined organic layers were washed with water (2×10 mL) and sat. aq. NaCl (10 mL), dried over anhydrous Na₂SO₄, and the solvent was removed *in vacuo*. Further purification by flash chromatography on silica gel (gradient elution: hexane → hexane–ethyl acetate 60:40) afforded 0.049 g (26% after three steps) of **3.105** and crude **3.106** which was additionally purified by flash chromatography on silica gel (gradient elution: hexane → chloroform) to yield 0.022 g (9% after three steps) of pure **3.106**.

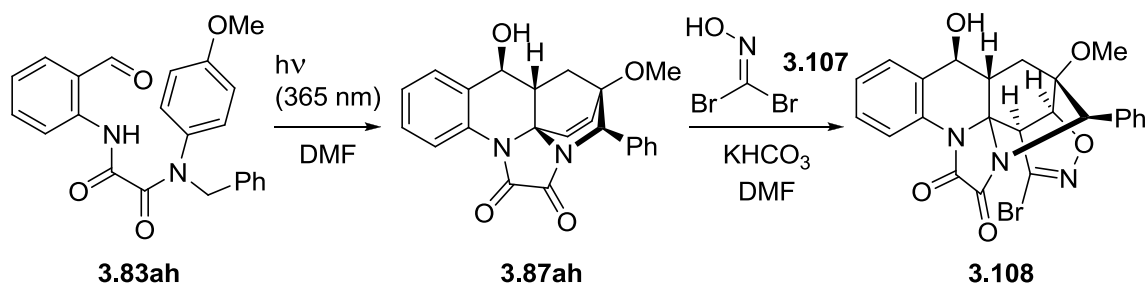


3.105: ¹H NMR (500 MHz, CDCl₃) δ 7.47 (m, 2H), 7.37 (m, 5H), 7.32 (m, 3H), 7.26 (td, *J* = 7.6, 1.3 Hz, 1H), 7.20 (m, 3H), 6.41 (t, *J* = 2.3 Hz, 1H), 5.65 (d, *J* = 1.5 Hz, 1H), 5.38 (d, *J* = 11.5 Hz, 1H), 4.64 (d, *J* = 11.5 Hz, 1H), 3.43 (s, 3H), 2.77 (dd, *J* = 18.2, 2.4 Hz, 1H), 2.70 (dt, *J* = 18.3, 1.7 Hz, 1H). ¹³C NMR (126 MHz, CDCl₃+DMSO) δ 156.2, 154.4, 154.0, 132.9, 131.5, 131.1, 130.0, 129.6, 129.3, 128.6, 128.5, 128.0, 127.8, 127.7, 127.6, 127.0, 124.6, 122.2, 122.2, 81.7, 76.3, 70.2, 57.4, 56.1, 52.5, 28.2. HRMS (ESI) calcd for C₃₀H₂₄N₃O₄⁺ (MH⁺) 490.1761, found 490.1769.



3.106: ^1H NMR (500 MHz, CDCl_3) δ 7.99 (m, 2H), 7.49 (m, 8H), 7.40 (m, 2H), 7.32 (m, 3H), 7.26 (td, $J = 7.6, 1.2$ Hz, 1H), 7.15 (m, 3H), 6.30 (t, $J = 2.2$ Hz, 1H), 5.86 (d, $J = 1.4$ Hz, 1H), 4.99 (d, $J = 9.1$ Hz, 1H), 3.89 (d, $J = 9.1$ Hz, 1H), 3.20 (s, 3H),

2.65 (dd, $J = 18.2, 2.3$ Hz, 1H), 2.57 (dt, $J = 18.2, 1.8$ Hz, 1H). ^{13}C NMR (126 MHz, CD_2Cl_2) δ 159.9, 156.4, 155.2, 133.5, 133.3, 132.8, 132.2, 130.7, 130.2, 129.9, 129.7, 129.6, 129.5, 128.9, 128.8, 128.2, 127.9, 127.5, 126.5, 125.8, 125.3, 123.1, 122.7, 108.7, 80.4, 77.4, 70.6, 58.5, 57.3, 52.3, 27.8. HRMS (ESI) calcd for $\text{C}_{37}\text{H}_{29}\text{N}_4\text{O}_5^+$ (MH^+) 609.2132, found 609.2144.



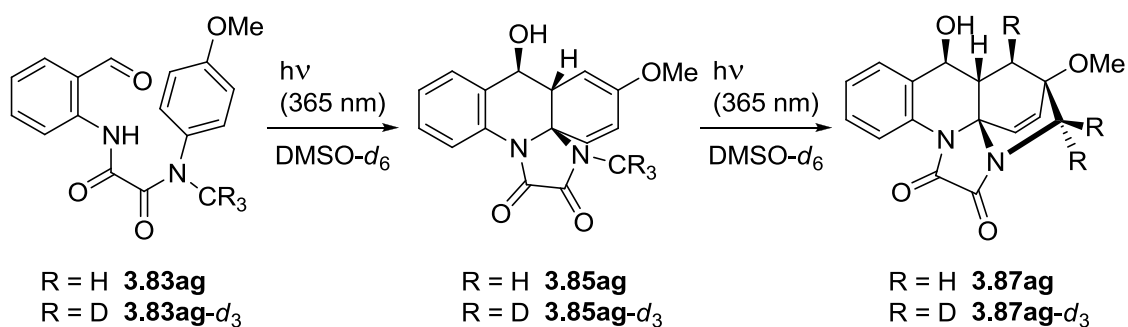
(±)-(1*R*,3*R*,4*S*,16*S*,20*S*,21*R*)-17-Bromo-4-hydroxy-1-methoxy-21-phenyl-19-oxa-11,14,18-triazahexacyclo[12.6.1.0^{3,15}.0^{5,10}.0^{11,15}.0^{16,20}]henicosa-5(10),6,8,17-tetraene-12,13-dione (**3.108**).

Photoprecursor **3.83ah** (0.241 g, 0.620 mmol) was dissolved in anhydrous DMF (25 mL), and the solution was degassed by bubbling argon for 1 h. The mixture was irradiated with UV LED-based illuminator (seven 2.9 W @ 365 nm LED Engin chips) with reaction progress monitored by ^1H NMR. After completion (reaction time = 10 h), the solution was treated with dibromoformaldoxime (**3.107**; 0.509 g, 2.51 mmol) and potassium bicarbonate (0.501 g, 5.01 mmol). The mixture was stirred at ambient temperature for 1 day, and then DMF was evaporated under high vacuum (50 °C/0.15 Torr). The residue was redissolved in ethyl acetate (100 mL) and washed

with water (20 mL). The aqueous layer was extracted with ethyl acetate (3×30 mL). The combined organic layers were washed with water (3×25 mL) and sat. aq. NaCl (2×25 mL), dried over anhydrous Na₂SO₄, and the solvent was removed *in vacuo*. Further purification by flash chromatography on silica gel (gradient elution: chloroform → chloroform–methanol 95:5) afforded 0.092 g (29% after two steps) of the title compound. ¹H NMR (500 MHz, DMSO) δ 8.17 (dd, *J* = 8.2, 1.1 Hz, 1H), 7.71 (dt, *J* = 8.2, 1.2 Hz, 1H), 7.49 (ddd, *J* = 8.7, 7.7, 1.9 Hz, 1H), 7.36 (m, 6H), 6.15 (d, *J* = 6.6 Hz, 1H), 5.48 (d, *J* = 11.7 Hz, 1H), 5.19 (s, 1H), 4.66 (dd, *J* = 9.8, 6.3 Hz, 1H), 4.50 (d, *J* = 11.7 Hz, 1H), 3.24 (s, 3H), 2.77 (td, *J* = 10.6, 5.7 Hz, 1H), 1.87 (ddd, *J* = 14.1, 5.7, 1.7 Hz, 1H), 1.76 (dd, *J* = 13.9, 10.9 Hz, 1H). ¹³C NMR (126 MHz, DMSO) δ 155.7, 154.2, 135.8, 132.7, 131.3, 130.1, 128.5, 128.5, 128.2, 128.0, 128.0, 125.9, 119.3, 79.8, 75.3, 68.9, 67.3, 55.9, 53.9, 51.3, 40.9, 25.8. HRMS (ESI) calcd for C₂₄H₂₁BrN₃O₅⁺ (MH⁺) 510.0659, found 510.0658.

Kinetic Isotope Effect Measurements

Experiment 1



0.01 M solutions of **3.83ag** and **3.83ag-d₃** in DMSO-*d*₆ (0.40 mL) with 0.75 mg (0.0037 mmol) of DSS (4,4-dimethyl-4-silapentane-1-sulfonic acid) as an internal

standard were degassed by bubbling nitrogen and irradiated in a carousel UV LED photoreactor (seven 2.9 W @ 365 nm LED Engin chips) with reaction progress monitored by ^1H NMR. Spectra were acquired at five time points:

- 0 min, 15 min, 20 min, 25 min and 37 min for **3.83ag**;
- 0 min, 37 min, 55 min, 114 min and 193 min for **3.83ag- d_3** .

The experiment was carried out two times. In the obtained spectra, the following signals were integrated:

- *In all spectra*: a peak from the internal standard at 0.80 ppm (integration was set to 1.00);
- *Only in the “0 min” spectrum*: peaks from photoprecursor (**3.83ag/3.83ag- d_3**) at 7.63 ppm (1H), 6.93 ppm (2H);
- *In all spectra, except “0 min”*: peaks from the primary photoproduct (**3.85ag/3.85ag- d_3**) at 6.20 ppm (1H), 5.57 ppm (1H; in some cases, skipped due to overlapping signals), 5.31 ppm (1H);
- *In all spectra, except “0 min”*: peaks from the secondary photoproduct (**3.87ag/3.87ag- d_3**) at 8.12 ppm (1H; skipped for **3.87ag- d_3** due to overlapping signals), 6.77 ppm (1H), 6.29 ppm (1H).

Integration values that correspond to the same compound were averaged. Then, the numbers obtained for **3.87ag** and **3.87ag- d_3** were normalized (the photoprecursors' integrations in the “0 min” spectra were set to 100%) and used to plot “conversion vs. time” graphs (**Figures 4.1, 4.2**). Based on the data from two experiments, linear trendlines were found for each secondary product; their slopes (“X Variable 1”) represent

relative rates of formation for **3.87ag** and **3.87ag-d₃**, and therefore were used to calculate KIE.

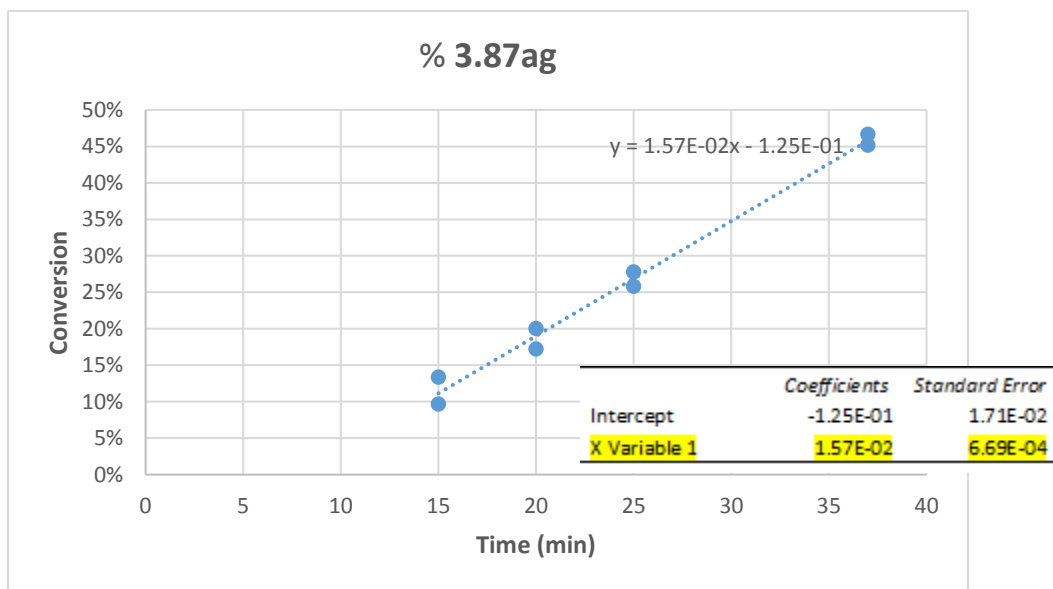


Figure 4.1: “Conversion vs. time” plot for **3.87ag**.

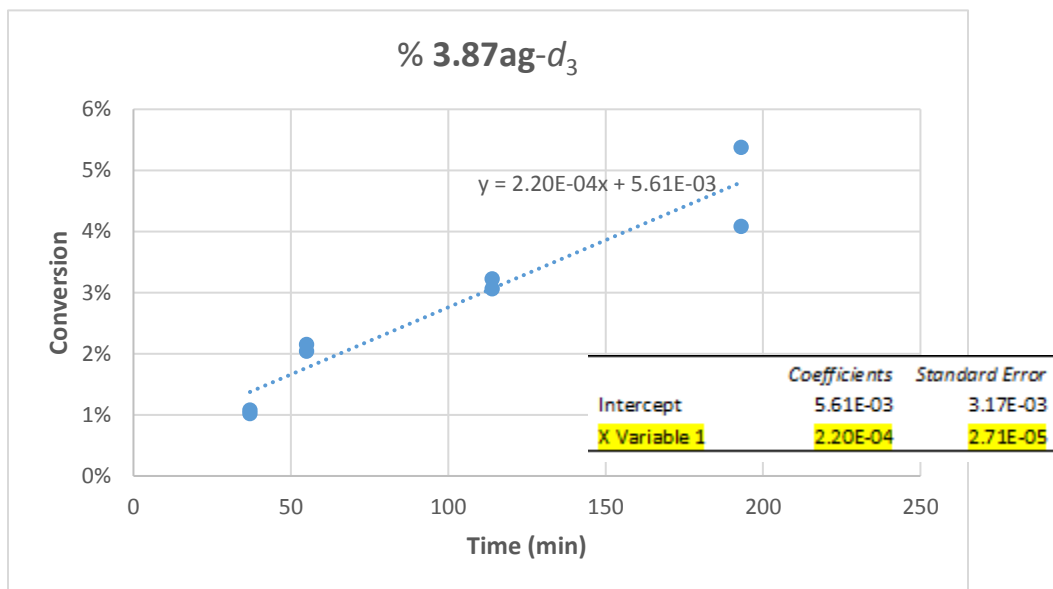
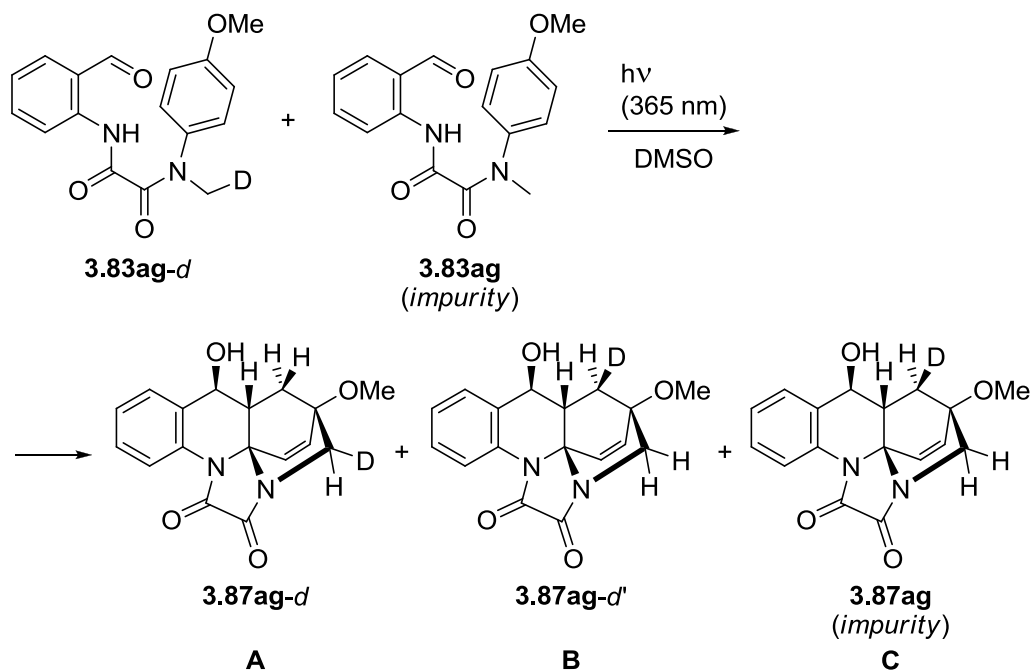


Figure 4.2: “Conversion vs. time” plot for **3.87ag-d₃**.

$$\begin{aligned}
 KIE(app) &= \frac{X \text{ Var. 1 (3.87ag)}}{X \text{ Var. 1 (3.87ag-d}_3)} = \frac{1.6 \times 10^{-2} \pm 6.7 \times 10^{-4}}{2.2 \times 10^{-4} \pm 2.7 \times 10^{-5}} \\
 &= 72 \pm 72 \times \left(\frac{6.7 \times 10^{-4}}{1.6 \times 10^{-2}} + \frac{2.7 \times 10^{-5}}{2.2 \times 10^{-4}} \right) = 72 \pm 12
 \end{aligned}$$

Experiment 2



0.237 g (0.756 mmol) of **3.83ag-d** was irradiated according to general procedure **F**.

The product (which is a mixture of **A**, **B** and **C**) was purified by flash chromatography on silica gel (gradient elution: DCM \rightarrow DCM–methanol 98:2) and analyzed by ^1H NMR (**Figure 4.3**).

The compound **A** was distinguished from two other components (**B** and **C**) based on the presence/absence of D in the methylene group at the α -position to the amide nitrogen (signal from another CH_2 group appeared to be non-first order and therefore was hard to analyze). By integrating the methylene signals, contents of **A** and **B** + **C** in the product were obtained.

Important notes:

- N-CHD proton in **A** gives two signals in the spectrum (3.59 and 3.53 ppm), because half of these protons are oriented “up” relative to the configuration of all other stereocenters, whereas another half has “down” orientation (assuming equal distribution of epimers);
- N-CH₂ group signals in **B** and **C** are expected to be split with large $^2J = 11$ Hz (see ¹H NMR data for **3.87ag**); given that this SSCC is not observed, it is conceivable that half of these signals overlap with N-CHD peaks from **A**.

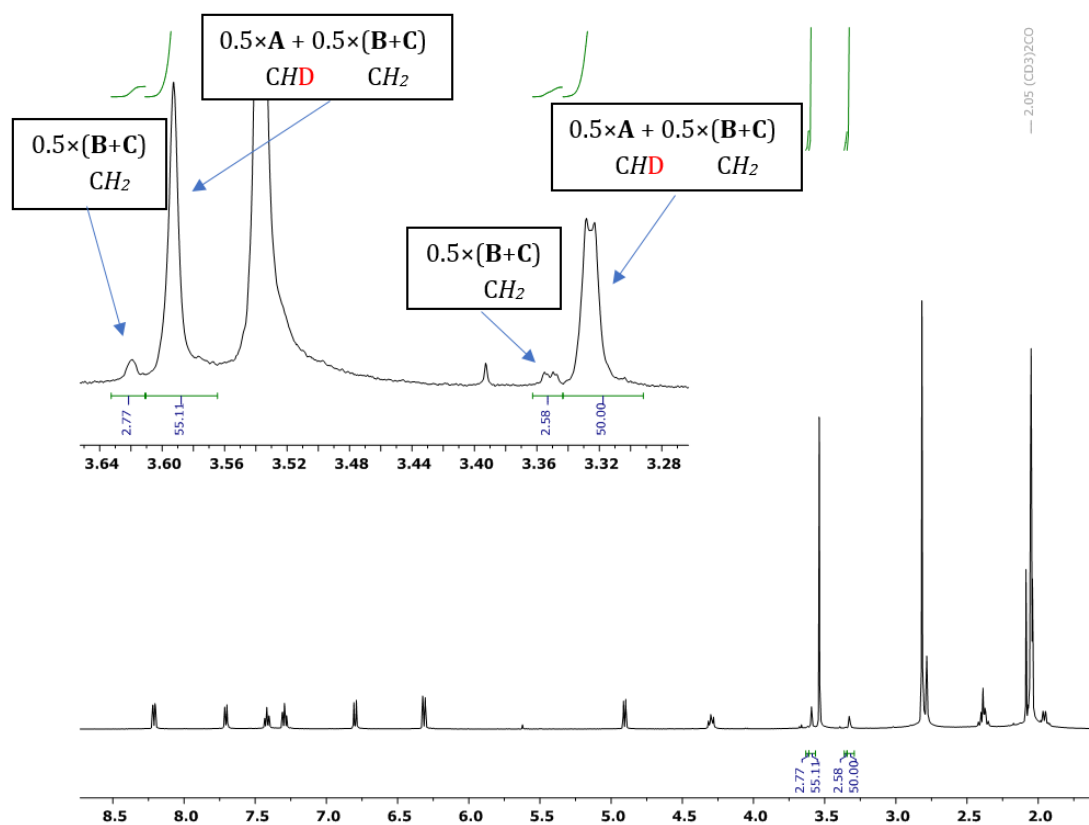


Figure 4.3: ¹H NMR spectrum of the product obtained by irradiation of **3.83ag-d**.

$$0.5 \times \mathbf{A} + 0.5 \times (\mathbf{B} + \mathbf{C}) = 52.6 \pm 6.9\% = 52.6 \pm 3.6$$

$$0.5 \times (\mathbf{B} + \mathbf{C}) = 2.7 \pm 5.0\% = 2.7 \pm 0.14$$

$$A = (52.6 \pm 3.6) \times 2 - (2.7 \pm 0.14) \times 2 = (49.9 \pm 3.74) \times 2 = 99.8 \pm$$

$$99.8 \times (3.74/49.9) = 99.8 \pm 7.48 \approx 94.8 \pm 7.11 \text{ (normalized)}$$

$$B + C = (2.7 \pm 0.14) \times 2 = 5.4 \pm 5.4 \times (0.14/2.7) = 5.4 \pm 0.28 \approx 5.1 \pm$$

$$0.26 \text{ (normalized)}$$

It was assumed that all non-deuterated product (**C**) originated from the protic precursor **3.83ag**, an impurity in **3.83ag-d**. Therefore, the content of **C** in the product should be equal to the percentage of **3.83ag** in the photoprecursor, which was calculated from the ^1H NMR spectrum of **3.83ag-d** by integrating CH_3 and CH_2D signals (**Figure 4.4**).

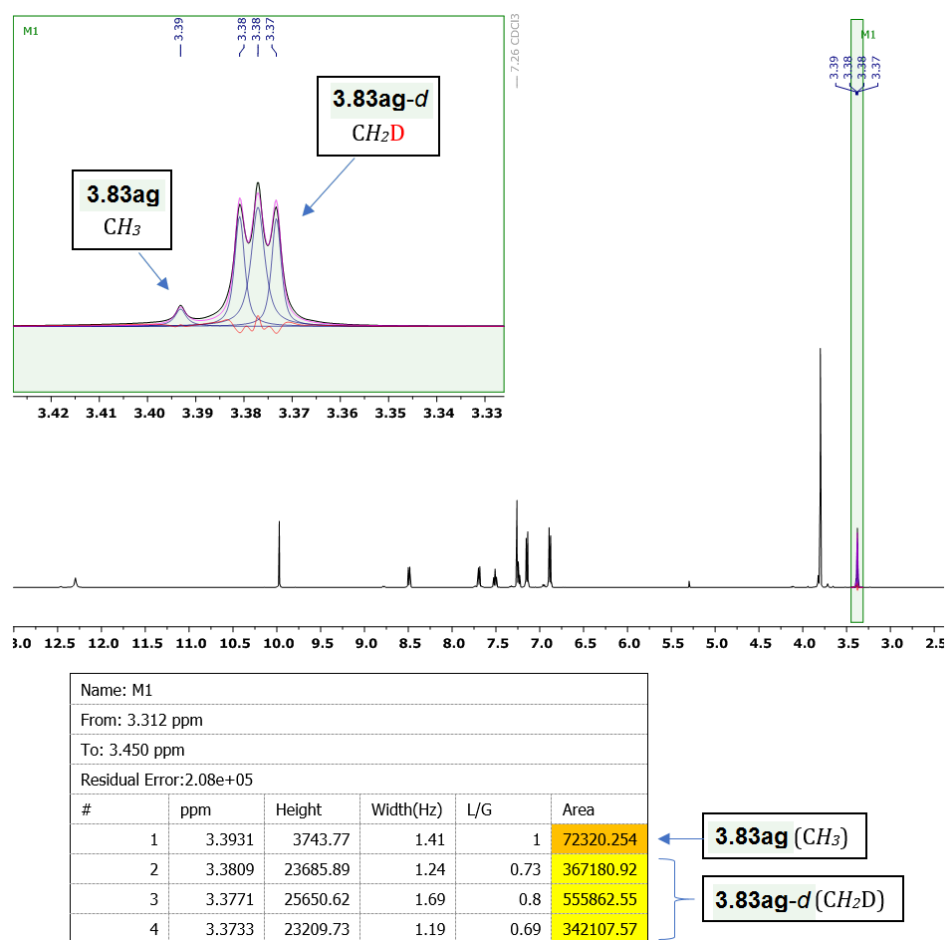


Figure 4.4: ^1H NMR spectrum of **3.83ag-d**.

$$\mathbf{C} = \mathbf{1a} = \frac{72320.254/3}{72320.254/3 + (367180.916 + 555862.554 + 342107.573)/2} \times 100$$

$$= 3.7 \pm 5\% = 3.7 \pm 0.19 \text{ (normalized)}$$

With the known content of **C**, percentage of **B** and then KIE were calculated:

$$\mathbf{B} = (\mathbf{B} + \mathbf{C}) - \mathbf{C} = (5.1 \pm 0.26) - (3.7 \pm 0.19) = 1.4 \pm 0.45$$

$$KIE = \frac{\mathbf{A}/2}{\mathbf{B}} = \frac{(94.8 \pm 7.11)/2}{1.4 \pm 0.45} = \frac{47.4 \pm 47.4 \times (7.11/94.8)}{1.4 \pm 0.45} = \frac{47.4 \pm 3.56}{1.4 \pm 0.45}$$

$$= 34 \pm 34 \times \left(\frac{3.56}{47.4} + \frac{0.45}{1.4} \right) = 34 \pm 14$$

Chapter Five: Conclusions

In this work, four new photoassisted synthetic methodologies have been presented. All of them take advantage of the light-induced process called excited-state intramolecular proton transfer (ESIPT), which generates a reactive *o*-azaxylylene species from readily available *o*-amido-substituted benzaldehydes and aromatic ketones by tautomerization. These reactive intermediates dearomatize tethered aromatic moieties and thereby lead to complex structures enriched with sp³ carbon atoms. Furthermore, the photoproducts contain functional groups suitable for a multitude of post-photochemical modifications, which add another layer of complexity to the final compounds.

Specifically, we have demonstrated the following:

- Epoxide-outfitted 2,5-diketopiperazino-quinolinols, which result from the diastereoselective intramolecular [4+4] reaction between *o*-azaxylylenes and 1,3,4-oxadiazoles with subsequent dinitrogen extrusion, can be engaged in various modifications providing access to diverse molecular scaffolds. These transformations include epoxide ring-openings and extensive rearrangements under Schmidt reaction conditions.
- Amino-*o*-azaxylylenes participate in diastereoselective [4+2] cycloadditions to tethered pyrrole units in enantiopure photoprecursors, which are quickly accessed from chiral amino acids. Reactive enamine double bonds present in

the photoproducts serve as entry points for subsequent modifications, such as 1,3-dipolar cycloaddition and intramolecular Friedel–Crafts reaction.

- Previously undocumented [2+4] topology of photoinduced benzene dearomatization can be achieved through the intramolecular cycloaddition to ESIPT-generated *o*-azaxylylenes. This process affords products with electron-rich 1,3-cyclohexadiene fragments modifiable by cyclic ketal formation, hydrolysis to enones and hetero-Diels–Alder reactions.
- Incorporation of the multifunctional oxalyl linker into precursor systems enables the unprecedented photocascade reaction, where the primary *o*-azaxylylene–aniline [2+4] cycloadducts undergo the subsequent secondary photoprocess sensitized by α -dicarbonyl fragment, furnishing complex architectures with azabicyclo[2.2.2]octene cores. Various functionalities in the photoproducts can be utilized for further transformations, such as acid-promoted cyclizations, epoxidations, and 1,3-dipolar cycloadditions.

A subset of the compounds obtained during this work (**Figure 5.1**) clearly demonstrates the diversity and complexity of the structures that can be accessed by the methodologies described herein. An important aspect of our chemistry is that the synthesis of the required photoprecursors is achieved in a modular fashion from simple starting materials and involves robust chemical transformations, creating opportunities for further diversification of the product library.

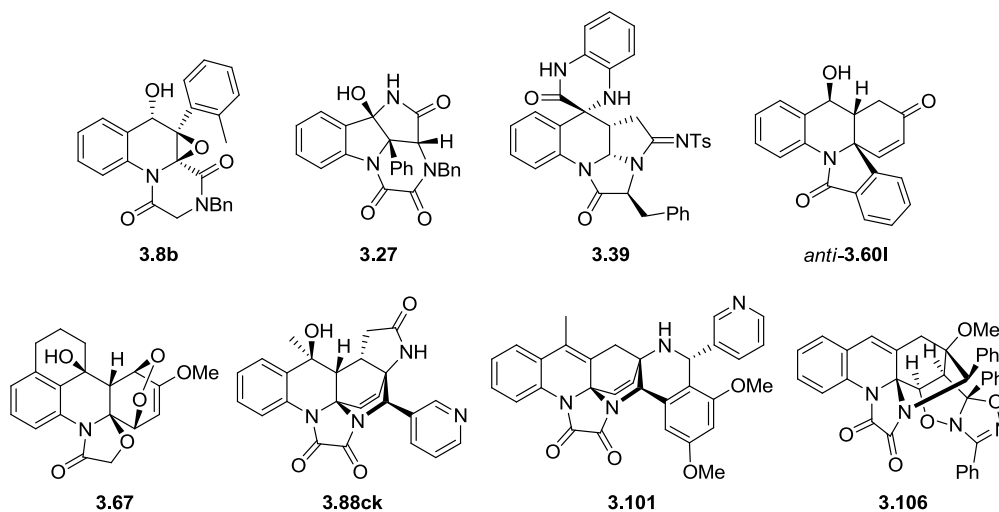


Figure 5.1: Selected products prepared by the photoassisted methods developed in this work.

To illustrate high levels of diversity and complexity of the molecules produced by our photochemistry-based methods, we ran calculations using the DataWarrior software developed by Actelion Pharmaceuticals Ltd. [183, 184]. For the array containing eight of our compounds (**Figure 5.1**) and three natural products (for comparison), we computed four types of *molecular descriptors* – abstract “fingerprints” containing information about certain structural features. By applying principal component analysis (PCA), the obtained data were converted into a three-dimensional plot visualizing the distribution of the molecules in the descriptor-defined chemical space (**Figure 5.2**). This 3D representation illustrates that our photoproducts are spread across a considerable area of chemical space, supporting the idea about the diversity of generated scaffolds.

In addition, we calculated molecular complexity indices (**Table 5.1**). The numbers show that our methodology is capable of producing structures being as complex as paclitaxel – a molecule that is regarded as one of the most challenging targets for total synthesis.

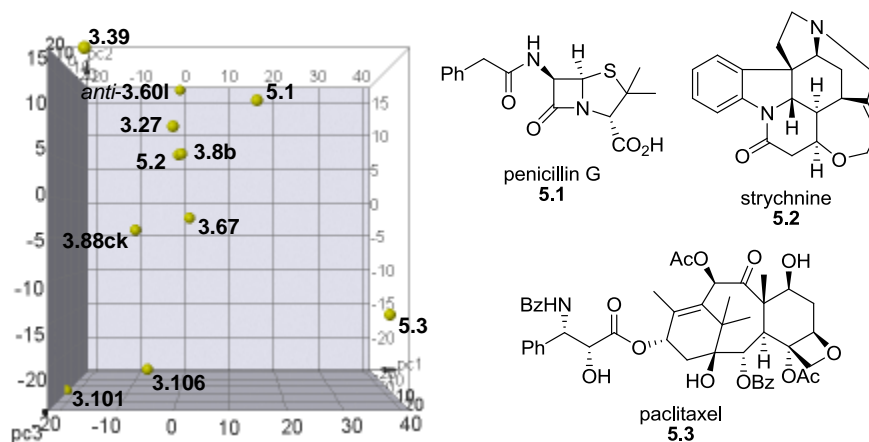


Figure 5.2: PCA-calculated distribution of the selected photoproducts (**Figure 5.1**) and natural products (**5.1–5.3**) in the chemical space defined by four types of descriptors.

Table 5.1: Molecular Complexity Indices for the Selected Photoproducts and Natural Products

Compound	Molecular Complexity (low < 0.5 < high)
3.8b	1.06
3.27	1.10
3.39	1.09
<i>anti-3.601</i>	1.02
3.67	1.09
3.88ck	1.13
3.101	1.13
3.106	1.18
5.1 (penicillin G)	0.88
5.2 (strychnine)	1.07
5.3 (paclitaxel)	1.10

Taking everything into account, we believe that our synthetic methods allow for probing large regions of unexplored chemical space, and therefore, are suitable for DOS-based strategy in the drug discovery. For that reason, we have started sending selected photoproducts to the National Cancer Institute, where they are evaluated for anti-cancer activities. We hope that our efforts in developing new chemical tools for creating small molecules can contribute to the discovery of novel therapies.

References

1. Jarvis, L. M. *Chem. Eng. News* **2019**, *97*, 11.
2. Woleben, J.; Young, D. US FDA shatters drug approval records in 2018.
<https://www.spglobal.com/marketintelligence/en/news-insights/trending/2t9lHb1VQaDxUOg2fMBLLA2> (accessed Jun 16, 2019).
3. Schreiber, S. L. *Science* **2000**, *287*, 1964–1969.
4. Haggarty, S. J. *Curr. Opin. Chem. Biol.* **2005**, *9*, 296–303.
5. Lipinski, C.; Hopkins, A. *Nature* **2004**, *432*, 855–861.
6. Prier, C. K.; Rankic, D. A.; MacMillan, D. W. C. *Chem. Rev.* **2013**, *113*, 5322–5363.
7. Mukhina, O. A.; Bhuvan Kumar, N. N.; Arisco, T. M.; Valiulin, R. A.; Metzler, G. A.; Kutateladze, A. G. *Angew. Chem. Int. Ed.* **2011**, *50*, 9423–9428.
8. Mukhina, O. A.; Kumar, N. N. B.; Cowger, T. M.; Kutateladze, A. G. *J. Org. Chem.* **2014**, *79*, 10956–10971.
9. Umstead, W. J.; Mukhina, O. A.; Kutateladze, A. G. *J. Photochem. Photobiol., A* **2016**, *329*, 182–188.
10. Cronk, W. C.; Mukhina, O. A.; Kutateladze, A. G. *Org. Lett.* **2016**, *18*, 3750–3753.
11. Hoffmann, N. *Photochem. Photobiol. Sci.* **2012**, *11*, 1613–1641.
12. Lovering, F.; Bikker, J.; Humblet, C. *J. Med. Chem.* **2009**, *52*, 6752–6756.
13. Ormson, S. M.; Brown, R. G. *Prog. React. Kinet.* **1994**, *19*, 45–91.
14. Weller, A. *Naturwissenschaften* **1955**, *42*, 175–176.
15. Sedgwick, A. C.; Wu, L.; Han, H.; Bull, S. D.; He, X.; James, T. D.; Sessler, J. L.; Tang, B. Z.; Tian, H.; Yoon, J. *Chem. Soc. Rev.* **2018**, *47*, 8842–8880.
16. Le Gourrierec, D.; Ormson, S. M.; Brown, R. G. *Prog. React. Kinet.* **1994**, *19*, 211–275.
17. Zhao, J.; Ji, S.; Chen, Y.; Guo, H.; Yang, P. *Phys. Chem. Chem. Phys.* **2012**, *14*, 8803–8817.

18. Chen, C.; Chen, Y.; Demchenko, A. P.; Chou, P. *Nat. Rev. Chem.* **2018**, *2*, 131–143.
19. Smith, T. P.; Zaklika, K. A.; Thakur, K.; Walker, G. C.; Tominaga, K.; Barbara, P. F. *J. Phys. Chem.* **1991**, *95*, 10465–10475.
20. Nagaoka, S.; Yamamoto, S.; Mukai, K. *J. Photochem. Photobiol., A* **1997**, *105*, 29–33.
21. Schmidtke, S. J.; Underwood, D. F.; Blank, D. A. *J. Phys. Chem. A* **2005**, *109*, 7033–7045.
22. Sasaki, S.; Drummen, G. P. C.; Konishi, G. *J. Mater. Chem. C* **2016**, *4*, 2731–2743.
23. Cantrell, A.; McGarvey, D. J.; Truscott, T. G. *Compr. Ser. Photosci.* **2001**, *3*, 495–519.
24. Tseng, H.; Liu, J.; Chen, Y.; Chao, C.; Liu, K.; Chen, C.; Lin, T.; Hung, C.; Chou, Y.; Lin, T.; Wang, T.; Chou, P. *J. Phys. Chem. Lett.* **2015**, *6*, 1477–1486.
25. Stasyuk, A. J.; Chen, Y.; Chen, C.; Wu, P.; Chou, P. *Phys. Chem. Chem. Phys.* **2016**, *18*, 24428–24436.
26. Santra, S.; Krishnamoorthy, G.; Dogra, S. K. *Chem. Phys. Lett.* **1999**, *311*, 55–61.
27. Isaks, M.; Yates, K.; Kalanderopoulos, P. *J. Am. Chem. Soc.* **1984**, *106*, 2728–2730.
28. Doria, F.; Percivalle, C.; Freccero, M. *J. Org. Chem.* **2012**, *77*, 3615–3619.
29. Kalanderopoulos, P.; Yates, K. *J. Am. Chem. Soc.* **1986**, *108*, 6290–6295.
30. Delgado, J.; Espinós, A.; Jiménez, M. C.; Miranda, M. A. *Chem. Commun.* **2002**, 2636–2637.
31. Leo, E. A.; Delgado, J.; Domingo, L. R.; Espinós, A.; Miranda, M. A.; Tormos, R. *J. Org. Chem.* **2003**, *68*, 9643–9647.
32. Lukeman, M.; Wan, P. *J. Am. Chem. Soc.* **2003**, *125*, 1164–1165.
33. Wang, Y.; Wan, P. *Photochem. Photobiol. Sci.* **2013**, *12*, 1571–1588.
34. Kostikov, A. P.; Popik, V. V. *J. Org. Chem.* **2007**, *72*, 9190–9194.
35. Kostikov, A. P.; Popik, V. V. *Org. Lett.* **2008**, *10*, 5277–5280.

36. Basarić, N.; Cindro, N.; Hou, Y.; Žabčić, I.; Mlinarić-Majerski, K.; Wan, P. *Can. J. Chem.* **2011**, *89*, 221–234.
37. Veljković, J.; Uzelac, L.; Molčanov, K.; Mlinarić-Majerski, K.; Kralj, M.; Wan, P.; Basarić, N. *J. Org. Chem.* **2012**, *77*, 4596–4610.
38. Kamboj, R. C.; Berar, S.; Berar, U.; Gupta, S. C. *J. Indian Chem. Soc.* **2011**, *88*, 879–885.
39. Gerard, B.; Jones, G.; Porco Jr., J. A. *J. Am. Chem. Soc.* **2004**, *126*, 13620–13621.
40. Gerard, B.; Sangji, S.; O'Leary, D. J.; Porco Jr., J. A. *J. Am. Chem. Soc.* **2006**, *128*, 7754–7755.
41. Gerard, B.; Cencic, R.; Pelletier, J.; Porco Jr., J. A. *Angew. Chem. Int. Ed.* **2007**, *46*, 7831–7834.
42. Roche, S. P.; Cencic, R.; Pelletier, J.; Porco Jr., J. A. *Angew. Chem. Int. Ed.* **2010**, *49*, 6533–6538.
43. Wang, W.; Clay, A.; Krishnan, R.; Lajkiewicz, N. J.; Brown, L. E.; Sivaguru, J.; Porco Jr., J. A. *Angew. Chem. Int. Ed.* **2017**, *56*, 14479–14482.
44. Bacher, M.; Hofer, O.; Brader, G.; Vajrodaya, S.; Greger, H. *Phytochemistry* **1999**, *52*, 253–263.
45. Proksch, P.; Edrada, R.; Ebel, R.; Bohnenstengel, F. I.; Nugroho, B. W. *Curr. Org. Chem.* **2001**, *5*, 923–938.
46. Xia, B.; Gerard, B.; Solano, D. M.; Wan, J.; Jones, G.; Porco Jr., J. A. *Org. Lett.* **2011**, *13*, 1346–1349.
47. Wang, W.; Cencic, R.; Whitesell, L.; Pelletier, J.; Porco Jr., J. A. *Chem. Eur. J.* **2016**, *22*, 12006–12010.
48. Nandurkar, N. S.; Kumar, N. N. B.; Mukhina, O. A.; Kutateladze, A. G. *ACS Comb. Sci.* **2013**, *15*, 73–76.
49. Kumar, N. N. B.; Mukhina, O. A.; Kutateladze, A. G. *J. Am. Chem. Soc.* **2013**, *135*, 9608–9611.
50. Mukhina, O. A.; Kutateladze, A. G. *J. Am. Chem. Soc.* **2016**, *138*, 2110–2113.
51. Shimada, H.; Nakamura, A.; Yoshihara, T.; Tobita, S. *Photochem. Photobiol. Sci.* **2005**, *4*, 367–375.

52. Mukhina, O. A.; Cronk, W. C.; Kumar, N. N. B.; Sekhar, M. C.; Samanta, A.; Kutateladze, A. G. *J. Phys. Chem. A* **2014**, *118*, 10487–10496.
53. Crimmins, M. T.; Pace, J. M.; Nantermet, P. G.; Kim-Meade, A.; Thomas, J. B.; Watterson, S. H.; Wagman, A. S. *J. Am. Chem. Soc.* **2000**, *122*, 8453–8463.
54. Chen, P.; Carroll, P. J.; Sieburth, S. M. *Org. Lett.* **2010**, *12*, 4510–4512.
55. Mucsi, Z.; Viskolcz, B.; Csizmadia, I. G. *J. Phys. Chem. A* **2007**, *111*, 1123–1132.
56. Bryce-Smith, D.; Gilbert, A.; Orger, B. H. *Chem. Commun. (London)* **1966**, 512–514.
57. Wilzbach, K. E.; Kaplan, L. *J. Am. Chem. Soc.* **1966**, *88*, 2066–2067.
58. Cornelisse, J. *Chem. Rev.* **1993**, *93*, 615–669.
59. Chappell, D.; Russell, A. T. *Org. Biomol. Chem.* **2006**, *4*, 4409–4430.
60. Wender, P. A.; Howbert, J. J. *J. Am. Chem. Soc.* **1981**, *103*, 688–690.
61. Wender, P. A.; Dreyer, G. B. *Tetrahedron* **1981**, *37*, 4445–4450.
62. Wender, P. A.; Ternansky, R. J. *Tetrahedron Lett.* **1985**, *26*, 2625–2628.
63. Gaich, T.; Mulzer, J. *J. Am. Chem. Soc.* **2009**, *131*, 452–453.
64. Wegmann, M.; Bach, T. *J. Org. Chem.* **2015**, *80*, 2017–2023.
65. Ayer, D. E.; Buchi, G. H. US2805242, 1957.
66. Ohashi, M.; Tanaka, Y.; Yamada, S. *Tetrahedron Lett.* **1977**, 3629–3632.
67. Wagner, P. J. *Acc. Chem. Res.* **2001**, *34*, 1–8.
68. Hoffmann, N.; Pete, J. *Synthesis* **2001**, *112*, 1236–1242.
69. Zech, A.; Bach, T. *J. Org. Chem.* **2018**, *83*, 3069–3077.
70. Wagner, P. J.; Sakamoto, M.; Madkour, A. E. *J. Am. Chem. Soc.* **1992**, *114*, 7298–7299.
71. Wagner, P. J.; McMahon, K. *J. Am. Chem. Soc.* **1994**, *116*, 10827–10828.
72. Kishikawa, K.; Akimoto, S.; Kohmoto, S.; Yamamoto, M.; Yamada, K. *J. Chem. Soc., Perkin Trans. 1* **1997**, 77–84.

73. Birbaum, F.; Neels, A.; Bochet, C. G. *Org. Lett.* **2008**, *10*, 3175–3178.
74. Streit, U.; Birbaum, F.; Quattropiani, A.; Bochet, C. G. *J. Org. Chem.* **2013**, *78*, 6890–6910.
75. Okumura, M.; Sarlah, D. *Synlett* **2018**, *29*, 845–855.
76. Kjell, D. P.; Sheridan, R. S. *J. Photochem.* **1985**, *28*, 205–214.
77. Southgate, E. H.; Pospesch, J.; Fu, J.; Holycross, D. R.; Sarlah, D. *Nat. Chem.* **2016**, *8*, 922–928.
78. Okumura, M.; Nakamata Huynh, S. M.; Pospesch, J.; Sarlah, D. *Angew. Chem. Int. Ed.* **2016**, *55*, 15910–15914.
79. Hernandez, L. W.; Pospesch, J.; Klöckner, U.; Bingham, T. W.; Sarlah, D. *J. Am. Chem. Soc.* **2017**, *139*, 15656–15659.
80. Okumura, M.; Shved, A. S.; Sarlah, D. *J. Am. Chem. Soc.* **2017**, *139*, 17787–17790.
81. Okumura, K.; Takamuku, S.; Sakurai, H. *Kogyo Kagaku Zasshi* **1969**, *72*, 200–203.
82. Gilbert, A.; Griffiths, O. *J. Chem. Soc., Perkin Trans. I* **1993**, 1379–1384.
83. Khatri, B. B.; Vrubliauskas, D.; Sieburth, S. M. *Tetrahedron Lett.* **2015**, *56*, 4520–4522.
84. Roux, M. V.; Temprado, M.; Chickos, J. S.; Nagano, Y. *J. Phys. Chem. Ref. Data* **2008**, *37*, 1855–1996.
85. Chirico, R. D.; Steele, W. V. *J. Chem. Thermodyn.* **2008**, *40*, 806–817.
86. Kimura, M.; Sagara, S.; Morosawa, S. *J. Org. Chem.* **1982**, *47*, 4344–4347.
87. Albin, A.; Fasani, E.; Giavarini, F. *J. Org. Chem.* **1988**, *53*, 5601–5607.
88. Noh, T.; Kim, D. *Tetrahedron Lett.* **1996**, *37*, 9329–9332.
89. Kohmoto, S.; Masu, H.; Tatsuno, C.; Kishikawa, K.; Yamamoto, M.; Yamaguchi, K. *J. Chem. Soc., Perkin Trans. I* **2000**, 4464–4468.
90. Hoffmann, N. *Tetrahedron* **2002**, *58*, 7933–7941.
91. Kalena, G. P.; Pradhan, P.; Puranik, V. S.; Banerji, A. *Tetrahedron Lett.* **2003**, *44*, 2011–2013.

92. Khatri, B. B.; Kulyk, S.; Sieburth, S. M. *Org. Chem. Front.* **2014**, *1*, 961–964.
93. Yang, C.; Nakamura, A.; Wada, T.; Inoue, Y. *Org. Lett.* **2006**, *8*, 3005–3008.
94. Yang, C.; Mori, T.; Inoue, Y. *J. Org. Chem.* **2008**, *73*, 5786–5794.
95. Kohmoto, S.; Hisamatsu, S.; Mitsuhashi, H.; Takahashi, M.; Masu, H.; Azumaya, I.; Yamaguchi, K.; Kishikawa, K. *Org. Biomol. Chem.* **2010**, *8*, 2174–2179.
96. Rabideau, P. W.; Marcinow, Z. *Org. React. (N. Y.)* **1992**, *42*, 1–334.
97. Stanislaus, A.; Cooper, B. H. *Catal. Rev. – Sci. Eng.* **1994**, *36*, 75–123.
98. Foubelo, F.; Yus, M. Reduction/Hydrogenation of Aromatic Rings. In *Arene Chemistry*; Mortier, J., Ed.; 2015; pp 337–364.
99. Dohi, T.; Kita, Y. *Chem. Commun.* **2009**, 2073–2085.
100. Pouysegu, L.; Deffieux, D.; Quideau, S. *Tetrahedron* **2010**, *66*, 2235–2261.
101. Ding, Q.; Ye, Y.; Fan, R. *Synthesis* **2012**, *45*, 1–16.
102. Harned, A. M. *Tetrahedron Lett.* **2014**, *55*, 4681–4689.
103. Pape, A. R.; Kaliappan, K. P.; Kündig, E. P. *Chem. Rev.* **2000**, *100*, 2917–2940.
104. Smith, P. L.; Chordia, M. D.; Dean Harman, W. *Tetrahedron* **2001**, *57*, 8203–8225.
105. Keane, J. M.; Harman, W. D. *Organometallics* **2005**, *24*, 1786–1798.
106. Zhuo, C.; Zheng, C.; You, S. *Acc. Chem. Res.* **2014**, *47*, 2558–2573.
107. Roche, S. P.; Porco Jr., J. A. *Angew. Chem. Int. Ed.* **2011**, *50*, 4068–4093.
108. Kumar, N. N. B.; Kuznetsov, D. M.; Kutateladze, A. G. *Org. Lett.* **2015**, *17*, 438–441.
109. Adam, W.; Finzel, R. *Tetrahedron Lett.* **1990**, *31*, 863–866.
110. Chiba, T.; Okimoto, M. *J. Org. Chem.* **1992**, *57*, 1375–1379.
111. Békhazi, M.; Warkentin, J. *Can. J. Chem.* **1983**, *61*, 619–624.
112. Klys, A.; Czardybon, W.; Warkentin, J.; Werstiuk, N. H. *Can. J. Chem.* **2004**, *82*, 1769–1773.

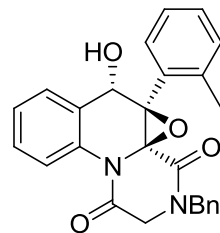
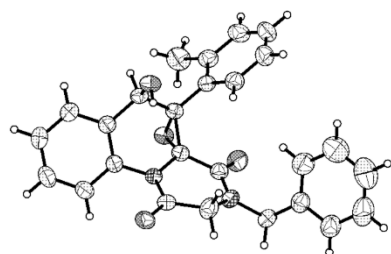
113. Xie, J.; Wolfe, A. L.; Boger, D. L. *Org. Lett.* **2013**, *15*, 868–870.
114. Lee, K.; Boger, D. L. *J. Am. Chem. Soc.* **2014**, *136*, 3312–3317.
115. Lee, K.; Boger, D. L. *Tetrahedron* **2015**, *71*, 3741–3746.
116. Leung, D.; Du, W.; Hardouin, C.; Cheng, H.; Hwang, I.; Cravatt, B. F.; Boger, D. L. *Bioorg. Med. Chem. Lett.* **2005**, *15*, 1423–1428.
117. Bordwell, F. G. *Acc. Chem. Res.* **1988**, *21*, 456–463.
118. MacFarlane, D. R.; Forsyth, S. A. Acids and Bases in Ionic Liquids. In *Ionic Liquids as Green Solvents*; Rogers, R. D., Seddon, K. R., Eds.; American Chemical Society: 2003; Vol. 856, pp 264–276.
119. Mukhina, O. A.; Kuznetsov, D. M.; Cowger, T. M.; Kutateladze, A. G. *Angew. Chem. Int. Ed.* **2015**, *54*, 11516–11520.
120. Weïwer, M.; Spoonamore, J.; Wei, J.; Guichard, B.; Ross, N. T.; Masson, K.; Silkworth, W.; Dandapani, S.; Palmer, M.; Scherer, C. A.; Stern, A. M.; Schreiber, S. L.; Munoz, B. *ACS Med. Chem. Lett.* **2012**, *3*, 1034–1038.
121. Kuznetsov, D. M.; Mukhina, O. A.; Kutateladze, A. G. *Angew. Chem. Int. Ed.* **2016**, *55*, 6988–6991.
122. Streit, U.; Bochet, C. G. *Beilstein J. Org. Chem.* **2011**, *7*, 525–542.
123. Kutateladze, A. G.; Mukhina, O. A. *J. Org. Chem.* **2014**, *79*, 8397–8406.
124. Kutateladze, A. G.; Mukhina, O. A. *J. Org. Chem.* **2015**, *80*, 5218–5225.
125. Karplus, M. *J. Am. Chem. Soc.* **1963**, *85*, 2870–2871.
126. Boger, D. L.; Patel, M. *J. Org. Chem.* **1984**, *49*, 4098–4099.
127. Ghogare, A. A.; Greer, A. *Chem. Rev.* **2016**, *116*, 9994–10034.
128. Casteel, D. A. *Nat. Prod. Rep.* **1999**, *16*, 55–73.
129. Dembitsky, V. M. *Eur. J. Med. Chem.* **2008**, *43*, 223–251.
130. Kuznetsov, D. M.; Kutateladze, A. G. *J. Am. Chem. Soc.* **2017**, *139*, 16584–16590.
131. Burke, M. D.; Schreiber, S. L. *Angew. Chem. Int. Ed.* **2004**, *43*, 46–58.

132. Newhouse, T.; Baran, P. S.; Hoffmann, R. W. *Chem. Soc. Rev.* **2009**, *38*, 3010–3021.
133. Wagner, P. J. *J. Am. Chem. Soc.* **1967**, *89*, 5715–5717.
134. Wagner, P. J.; Kochevar, I. *J. Am. Chem. Soc.* **1968**, *90*, 2232–2238.
135. Dalton, J. C.; Turro, N. J. *Annu. Rev. Phys. Chem.* **1970**, *21*, 499–560.
136. Wagner, P. J. *Acc. Chem. Res.* **1971**, *4*, 168–177.
137. Barltrop, J. A.; Carless, H. A. J. *J. Am. Chem. Soc.* **1971**, *93*, 4794–4801.
138. Barltrop, J. A.; Carless, H. A. J. *J. Am. Chem. Soc.* **1972**, *94*, 8761–8768.
139. Lamola, A. A.; Hammond, G. S. *J. Chem. Phys.* **1965**, *43*, 2129–2135.
140. Zhao, J.; Wu, W.; Sun, J.; Guo, S. *Chem. Soc. Rev.* **2013**, *42*, 5323–5351.
141. Guan, J.; Wang, X.; Smith, K.; Ager, A.; Gettayacamin, M.; Kyle, D. E.; Milhous, W. K.; Kozar, M. P.; Magill, A. J.; Lin, A. J. *J. Med. Chem.* **2007**, *50*, 6226–6231.
142. Abou-Seri, S.; Farag, N. A.; Hassan, G. S. *Chem. Pharm. Bull.* **2011**, *59*, 1124–1132.
143. Xia, G.; Benmohamed, R.; Kim, J.; Arvanites, A. C.; Morimoto, R. I.; Ferrante, R. J.; Kirsch, D. R.; Silverman, R. B. *J. Med. Chem.* **2011**, *54*, 2409–2421.
144. Rajabi, M.; Mansell, D.; Freeman, S.; Bryce, R. A. *Eur. J. Med. Chem.* **2011**, *46*, 1165–1171.
145. Arafa, R. K.; Nour, M. S.; El-Sayed, N. *Eur. J. Med. Chem.* **2013**, *69*, 498–507.
146. Ghorai, M. K.; Nanaji, Y. *J. Org. Chem.* **2013**, *78*, 3867–3878.
147. Lerchner, A.; Carreira, E. M. *J. Am. Chem. Soc.* **2002**, *124*, 14826–14827.
148. Kutateladze, A. G.; Mukhina, O. A. *J. Org. Chem.* **2015**, *80*, 10838–10848.
149. Kutateladze, A. G.; Reddy, D. S. *J. Org. Chem.* **2017**, *82*, 3368–3381.
150. Jackman, L. M.; Sternhell, S. Long-Range Interproton Coupling. *Application of Nuclear Magnetic Resonance Spectroscopy in Organic Chemistry*; Pergamon, 1969; pp 312–344.
151. Anslyn, E. V.; Dougherty, D. A. *Modern physical organic chemistry*; University Science: Sausalito, CA, 2006.

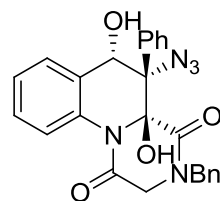
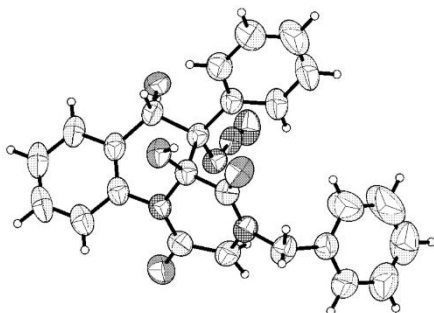
152. Truhlar, D. G.; Gao, J.; Alhambra, C.; Garcia-Viloca, M.; Corchado, J.; Sánchez, M. L.; Villà, J. *Acc. Chem. Res.* **2002**, *35*, 341–349.
153. Garcia-Garibay, M.; Gamarnik, A.; Pang, L.; Jenks, W. S. *J. Am. Chem. Soc.* **1994**, *116*, 12095–12096.
154. Garcia-Garibay, M.; Gamarnik, A.; Bise, R.; Pang, L.; Jenks, W. S. *J. Am. Chem. Soc.* **1995**, *117*, 10264–10275.
155. Johnson, B. A.; Gamarnik, A.; Garcia-Garibay, M. *J. Phys. Chem.* **1996**, *100*, 4697–4700.
156. Gamarnik, A.; Johnson, B. A.; Garcia-Garibay, M. *J. Phys. Chem. A* **1998**, *102*, 5491–5498.
157. Johnson, B. A.; Kleinman, M. H.; Turro, N. J.; Garcia-Garibay, M. *J. Org. Chem.* **2002**, *67*, 6944–6953.
158. Newcomb, M. Radical Kinetics and Clocks. In *Encyclopedia of Radicals in Chemistry, Biology and Materials*; John Wiley & Sons, 2012.
159. Choi, S.; Horner, J. H.; Newcomb, M. *J. Org. Chem.* **2000**, *65*, 4447–4449.
160. Bowry, V. W.; Lusztyk, J.; Ingold, K. U. *J. Am. Chem. Soc.* **1991**, *113*, 5687–5698.
161. Vatsadze, S. Z.; Loginova, Y. D.; dos Passos Gomes, G.; Alabugin, I. V. *Chem. Eur. J.* **2017**, *23*, 3225–3245.
162. González-Bobes, F.; Kopp, N.; Li, L.; Deerberg, J.; Sharma, P.; Leung, S.; Davies, M.; Bush, J.; Hamm, J.; Hrytsak, M. *Org. Process Res. Dev.* **2012**, *16*, 2051–2057.
163. Peet, N. P.; Weintraub, P. M. *Chem. Eng. News* **1993**, *71*, 4.
164. Conrow, R. E.; Dean, W. D. *Org. Process Res. Dev.* **2008**, *12*, 1285–1286.
165. Manley, D. W.; Mills, A.; O'Rourke, C.; Slawin, A. M. Z.; Walton, J. C. *Chem. Eur. J.* **2014**, *20*, 5492–5500.
166. Bolli, M. H.; Marfurt, J.; Grisostomi, C.; Boss, C.; Binkert, C.; Hess, P.; Treiber, A.; Thorin, E.; Morrison, K.; Buchmann, S.; Bur, D.; Ramuz, H.; Clozel, M.; Fischli, W.; Weller, T. *J. Med. Chem.* **2004**, *47*, 2776–2795.
167. Bahl, A.; Perry, M.; Springthorpe, B. GB2373186, 2002.

168. Nguyen, P.; Corpuz, E.; Heidelbaugh, T. M.; Chow, K.; Garst, M. E. *J. Org. Chem.* **2003**, *68*, 10195–10198.
169. Höke, T.; Herdtweck, E.; Bach, T. *Chem. Commun.* **2013**, *49*, 8009–8011.
170. Zhang, H.; Hay, E. B.; Geib, S. J.; Curran, D. P. *Beilstein J. Org. Chem.* **2015**, *11*, 1649–1655.
171. Gangjee, A.; Zaware, N.; Devambatla, R. K. V.; Raghavan, S.; Westbrook, C. D.; Dybdal-Hargreaves, N.; Hamel, E.; Mooberry, S. L. *Bioorg. Med. Chem.* **2013**, *21*, 891–902.
172. Peng, Y.; Liu, H.; Tang, M.; Cai, L.; Pike, V. *Chin. J. Chem.* **2009**, *27*, 1339–1344.
173. Reznichenko, A. L.; Hultsch, K. C. *J. Am. Chem. Soc.* **2012**, *134*, 3300–3311.
174. Yang, C.; Fu, Y.; Huang, Y.; Yi, J.; Guo, Q.; Liu, L. *Angew. Chem. Int. Ed.* **2009**, *48*, 7398–7401.
175. Tait, M. B.; Ottersbach, P. A.; Tetlow, D. J.; Clayden, J. *Org. Process Res. Dev.* **2014**, *18*, 1245–1252.
176. Betou, M.; Male, L.; Steed, J. W.; Grainger, R. S. *Chem. Eur. J.* **2014**, *20*, 6505–6517.
177. Jeong, J. U.; Tao, B.; Sagasser, I.; Henniges, H.; Sharpless, K. B. *J. Am. Chem. Soc.* **1998**, *120*, 6844–6845.
178. Levesque, P.; Fournier, P. *J. Org. Chem.* **2010**, *75*, 7033–7036.
179. Nicolaou, K. C.; Li, A.; Edmonds, D. J.; Tria, G. S.; Ellery, S. P. *J. Am. Chem. Soc.* **2009**, *131*, 16905–16918.
180. Moody, C. J.; Miah, S.; Slawin, A. M. Z.; Mansfield, D. J.; Richards, I. C. *Tetrahedron* **1998**, *54*, 9689–9700.
181. Lichter, R. L.; Wasylishen, R. E. *J. Am. Chem. Soc.* **1975**, *97*, 1808–1813.
182. Dubrovskiy, A. V.; Larock, R. C. *Org. Lett.* **2010**, *12*, 1180–1183.
183. Sander, T. DataWarrior – A Free Cheminformatics Program for Data Visualization and Analysis. <http://openmolecules.org/datawarrior/> (accessed Jun 18, 2019).
184. Sander, T.; Freyss, J.; von Korff, M.; Rufener, C. *J. Chem. Inf. Model.* **2015**, *55*, 460–473.

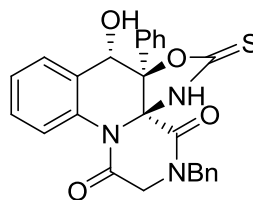
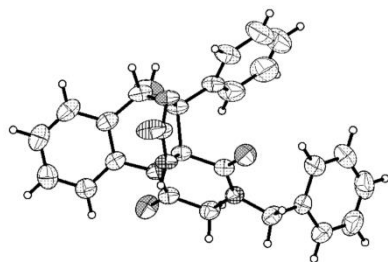
Appendix A: X-Ray Structures



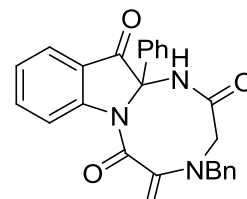
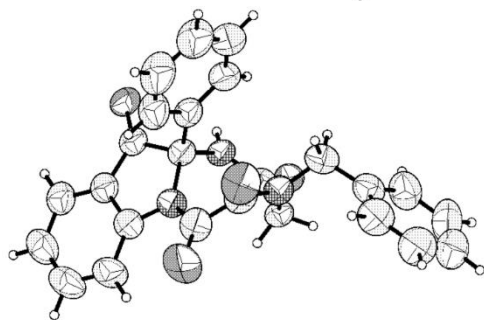
3.8b



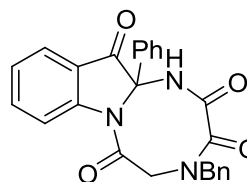
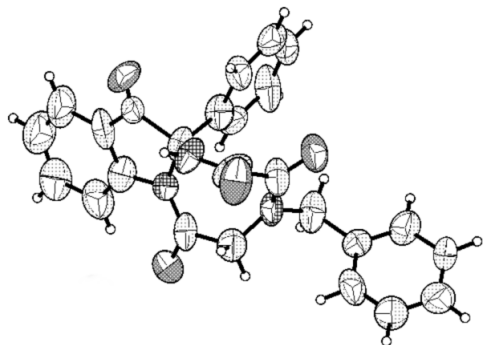
3.17



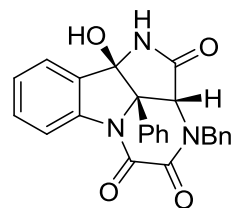
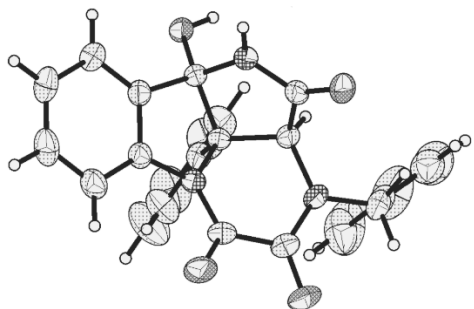
3.18



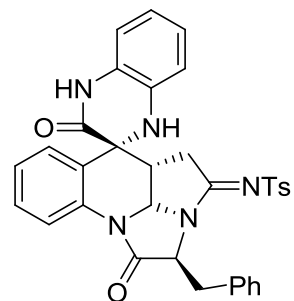
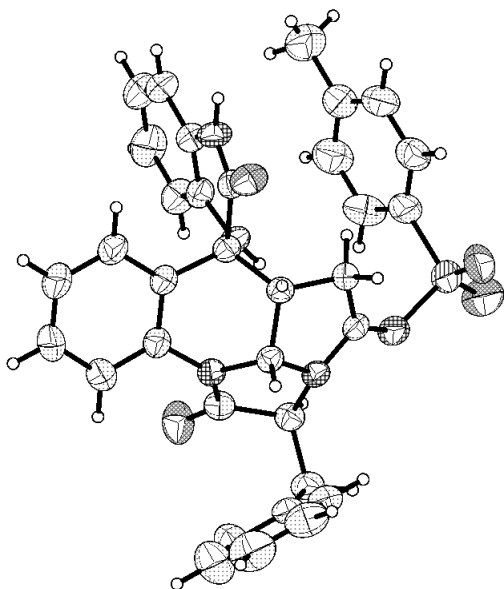
3.22



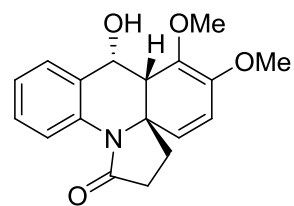
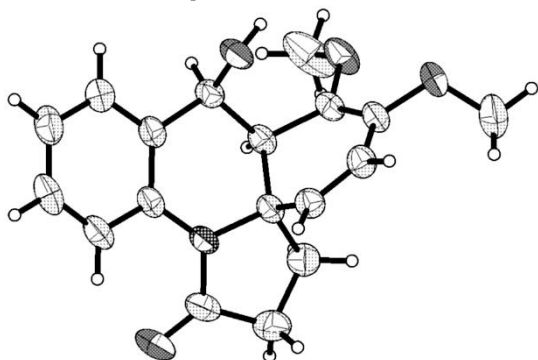
3.23



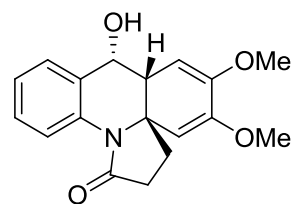
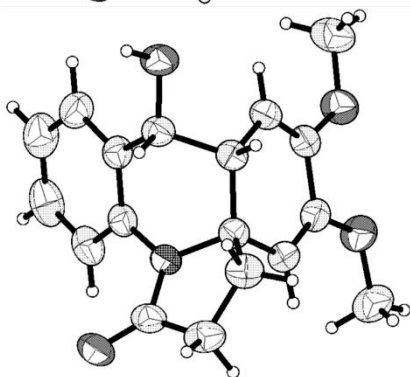
3.27



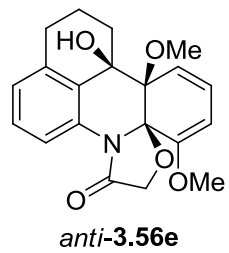
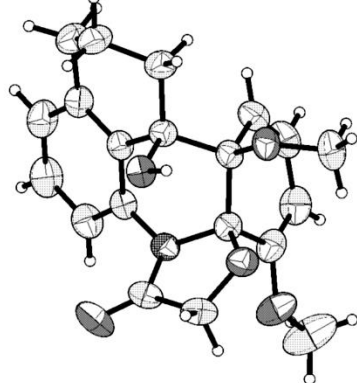
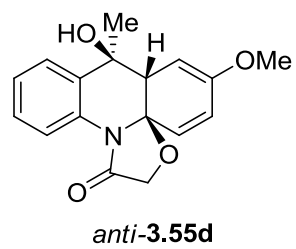
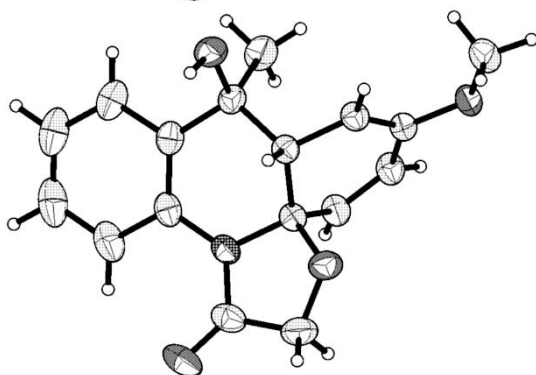
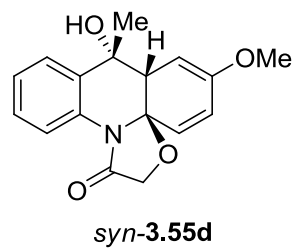
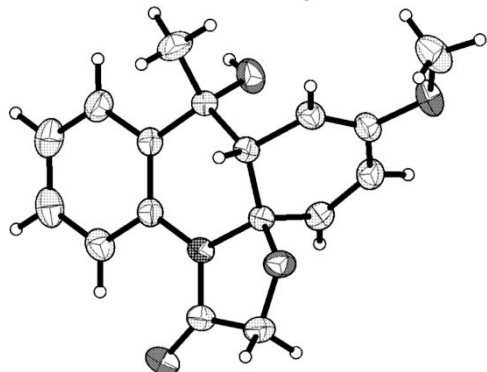
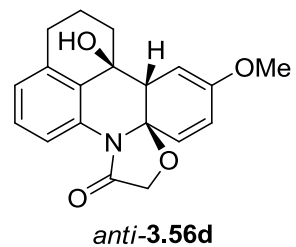
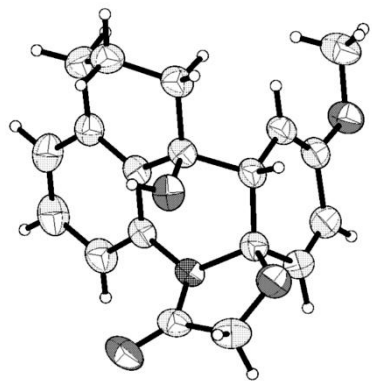
3.39

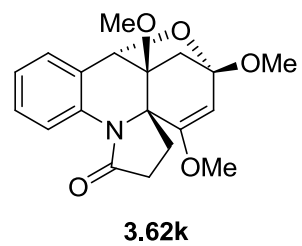
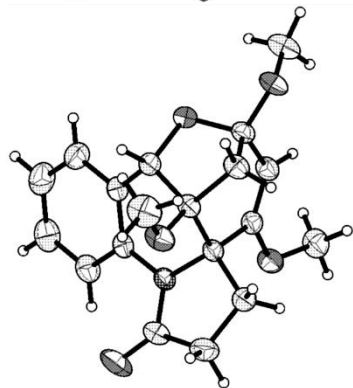
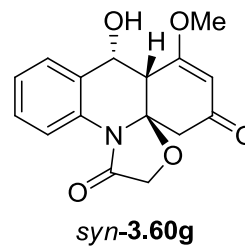
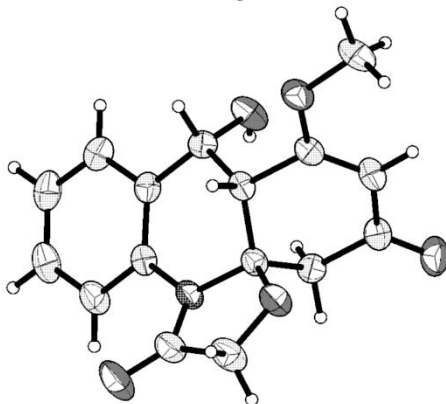
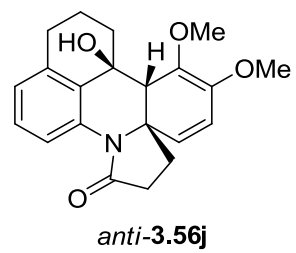
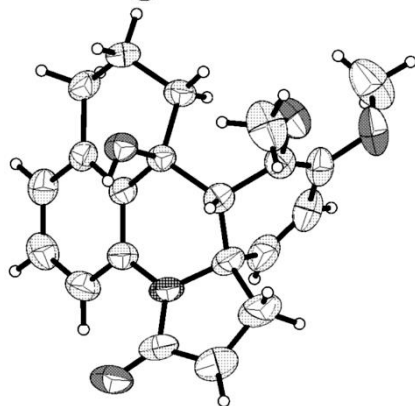
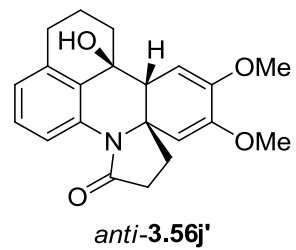
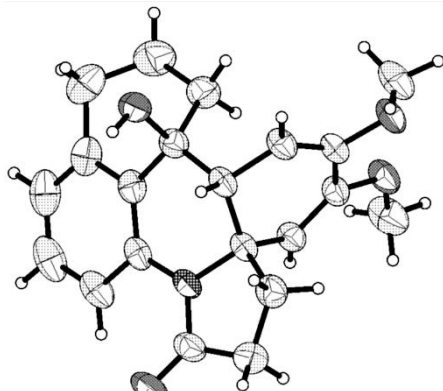


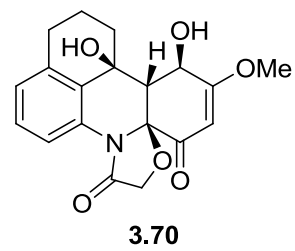
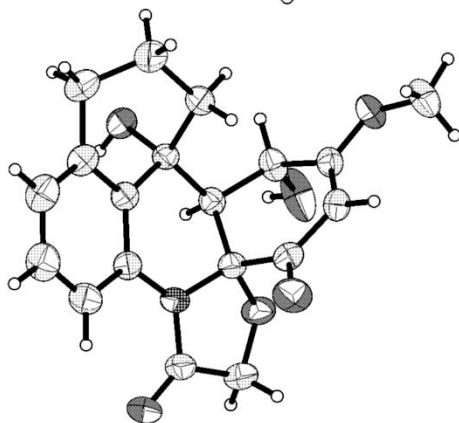
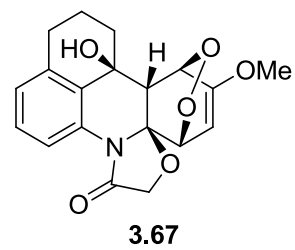
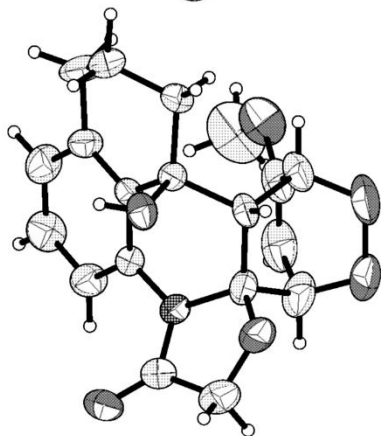
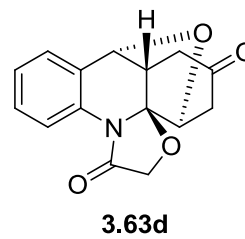
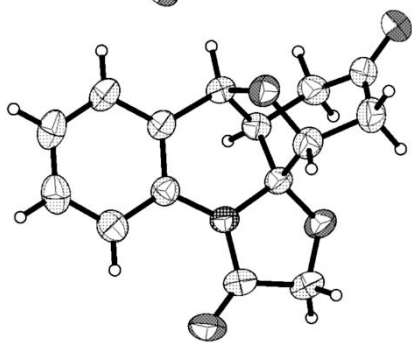
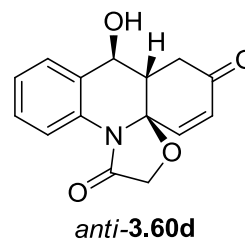
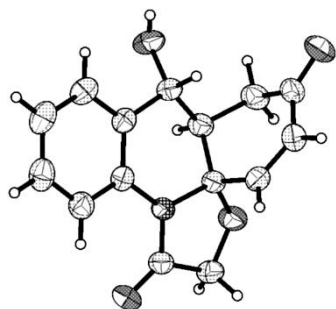
syn-**3.54j**

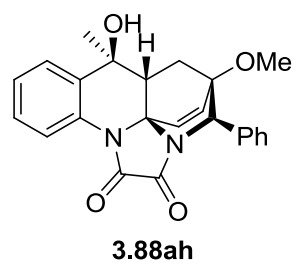
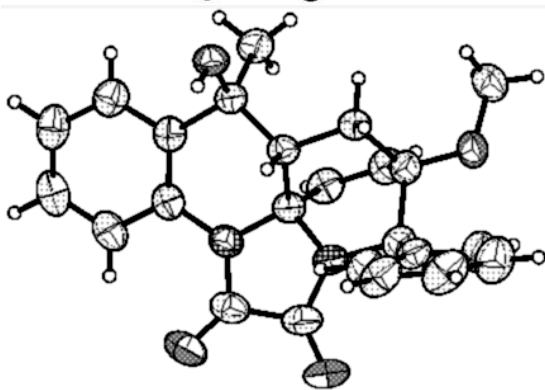
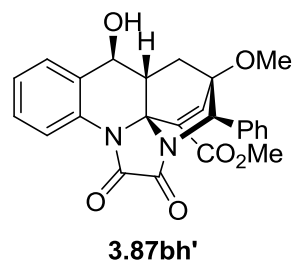
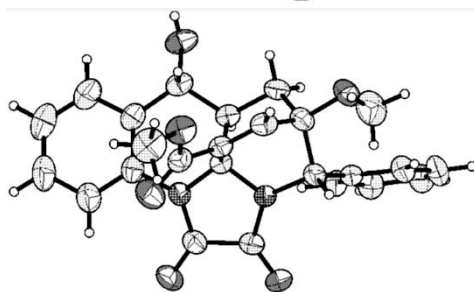
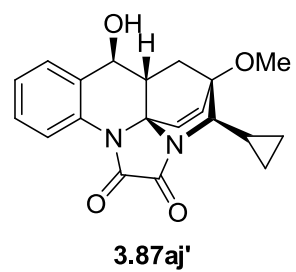
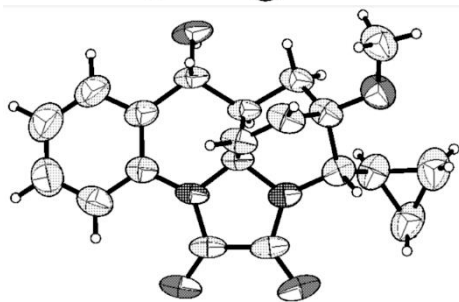
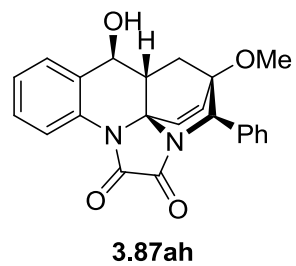
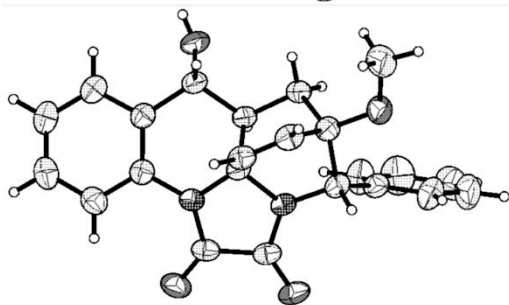
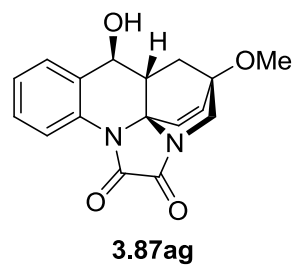
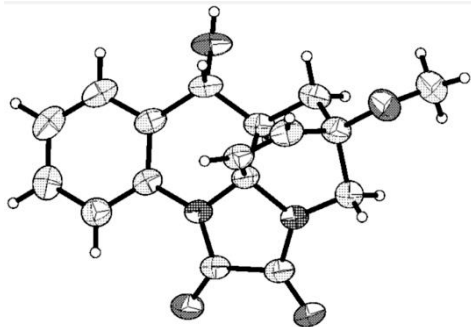


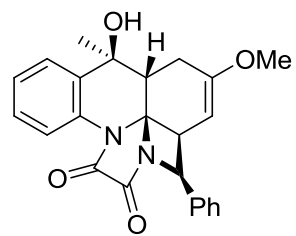
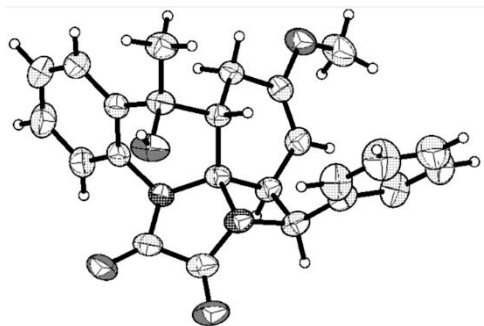
syn-**3.54j'**



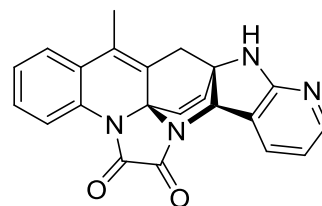
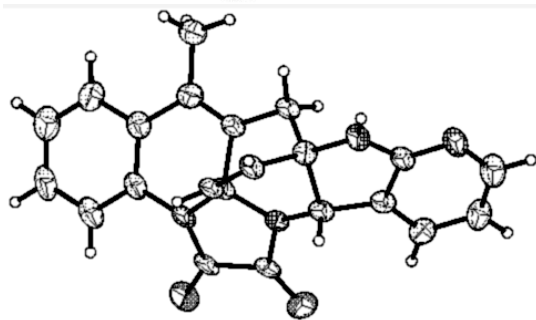




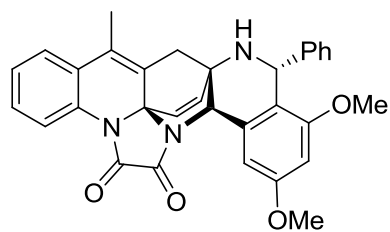
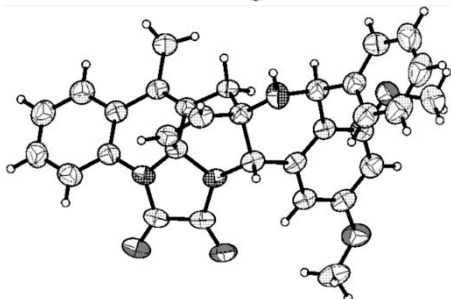




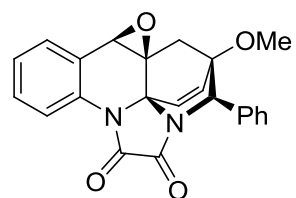
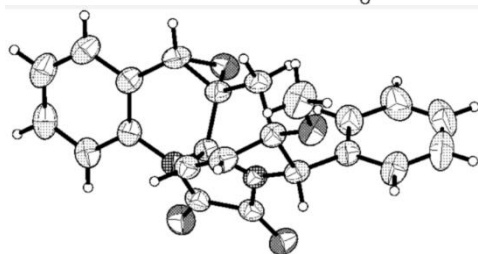
3.88ah'



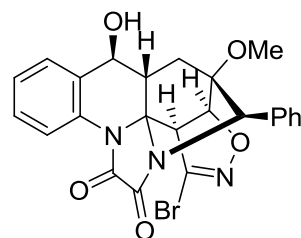
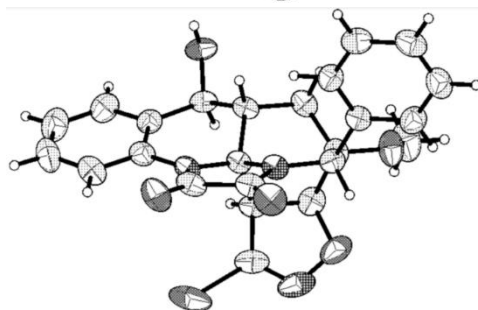
3.96



3.100



3.103



3.108

Appendix B: List of Abbreviations and Acronyms

ABT	2-(2'-aminophenyl)benzothiazole
Ac	acetyl
AIBN	azobisisobutyronitrile
app	apparent
aq.	aqueous
Ar	aryl
2-BAPBI	2-(2'-benzamidophenyl)benzimidazole
BINAP	(2,2'-bis(diphenylphosphino)-1,1'-binaphthyl)
Bn	benzyl
Boc	<i>tert</i> -butyloxycarbonyl
BPT	back proton transfer
BR	biradical
ⁿ Bu	<i>normal</i> -butyl
^t Bu	<i>tert</i> -butyl
Bz	benzoyl
CAAQ	1-(chloroacetylamino)anthraquinone
calcd	calculated
cat.	catalyst (or catalytic amount)
ccw	counterclockwise
comb.	combined
CT	charge transfer
cw	clockwise

DCAQ	1-(dichloroacetylamino)anthraquinone
DCE	1,2-dichloroethane
DCM	dichloromethane
de	diastereoisomeric excess
DFT	density functional theory
DIPEA	<i>N,N</i> -diisopropylethylamine
DMAP	4-(<i>N,N</i> -dimethylamino)pyridine
DMBP	4,4'-dimethoxybenzophenone
DMF	<i>N,N</i> -dimethylformamide
DMP	Dess–Martin periodinane
DMSO	dimethyl sulfoxide
DNA	deoxyribonucleic acid
DOS	diversity-oriented synthesis
dppb	1,4-bis(diphenylphosphino)butane
DR	diradical
DSS	4,4-dimethyl-4-silapentane-1-sulfonic acid
EDC	<i>N</i> -(3-dimethylaminopropyl)- <i>N'</i> -ethylcarbodiimide
ee	enantiomeric excess
er	enantiomeric ratio
ESI	electrospray ionization
ESICT	excited-state intramolecular charge transfer
ESIPT	excited-state intramolecular proton transfer
Et	ethyl

FDA	Food and Drug Administration
GP	general procedure
h	hour
HAT	hydrogen atom transfer
HATU	(1-[bis(dimethylamino)methylene]-1 <i>H</i> -1,2,3-triazolo[4,5- <i>b</i>]pyridinium 3-oxid hexafluorophosphate
HMPA	hexamethylphosphoramide
HOAt	1-hydroxy-7-azabenzotriazole
HPAQ	1-(heptanoylamino)anthraquinone
HPLC	high-performance liquid chromatography
HRMS	high-resolution mass spectrum
hν	light (irradiation)
int.	intermediate
IPA	2-(imidazo[1,2- <i>a</i>]pyridin-2-yl)aniline
ISC	intersystem crossing
KIE	kinetic isotope effect
LDA	lithium diisopropylamide
LED	light-emitting diode
LWA	long-wavelength absorption
LWE	long-wavelength emission
<i>m</i> CPBA	<i>meta</i> -chloroperbenzoic acid
Me	methyl
min	minute

N	normal or enol from
NBS	<i>N</i> -bromosuccinimide
Ni(cod) ₂	bis(1,5-cyclooctadiene)nickel(0)
NMO	<i>N</i> -methylmorpholine <i>N</i> -oxide
NMR	nuclear magnetic resonance
PBT	2-phenylbenzothiazole
PCA	principal component analysis
Pd(dba) ₂	bis(dibenzylideneacetone)palladium(0)
PET	photoinduced electron transfer
Ph	phenyl
Phth	phthalimide
PIP	2-phenylimidazo[1,2- <i>a</i>]pyridine
ⁱ Pr	<i>iso</i> -propyl
PTSA	<i>p</i> -toluenesulfonic acid monohydrate
Py	pyridine (or pyridyl)
QY	quantum yield
ref.	reference
RFF	relativistic force field
rfx	reflux
RNA	ribonucleic acid
rt	room temperature
S ₀	ground state
S ₁	first singlet excited state

sat.	saturated
SSCC	spin-spin coupling constant
Sulf	sulfonyl
SWA	short-wavelength absorption
SWE	short-wavelength emission
T	tautomeric or keto form
T ₁ (T ₂)	first (second) triplet excited state
TADDOL	$\alpha,\alpha,\alpha',\alpha'$ -tetraaryl-2,2-disubstituted 1,3-dioxolane-4,5-dimethanol
TCSPC	time-correlated single-photon counting
TEA	triethylamine
TES	triethylsilyl
TFA	trifluoroacetic acid
TFAQ	1-(trifluoroacetylamino)anthraquinone
TFE	2,2,2-trifluoroethanol
THF	tetrahydrofuran
TICT	twisted internal charge transfer
TMS	tetramethylsilane
Ts	<i>para</i> -toluenesulfonyl
U.S.	United States
UV	ultraviolet
Var.	variable
vis.	visible
vol	volume

Appendix C: List of Publications Based on this Dissertation

1. Kumar, N. N. B.; Kuznetsov, D. M.; Kutateladze, A. G. *Org. Lett.* **2015**, *17*, 438–441.
2. Mukhina, O. A.; Kuznetsov, D. M.; Cowger, T. M.; Kutateladze, A. G. *Angew. Chem. Int. Ed.* **2015**, *54*, 11516–11520.
3. Kuznetsov, D. M.; Mukhina, O. A.; Kutateladze, A. G. *Angew. Chem. Int. Ed.* **2016**, *55*, 6988–6991.
4. Kuznetsov, D. M.; Kutateladze, A. G. *J. Am. Chem. Soc.* **2017**, *139*, 16584–16590.